Endosomolytic arginine-rich peptides for therapeutic siRNA delivery

by

Wen Xu

A thesis
presented to the University of Waterloo
in fulfillment of the
thesis requirement for the degree of
Doctor of Philosophy
in
Chemical Engineering

Waterloo, Ontario, Canada, 2014

AUTHOR'S DECLARATION

I hereby declare that I am the sole author of this thesis. This is a true copy of the thesis, including any required final revisions, as accepted by my examiners. I understand that my thesis may be made electronically available to the public.

Abstract

At the forefront of revolutionizing medicine, gene therapy provides an effective way to treat a range of diseases by regulating defective genes at the root of the disease. Short interfering RNA (siRNA) holds great promise as therapeutic agents in this domain. The siRNAs are a class of 20 to 25 nucleotide-long double-stranded RNA molecules that play an important role in the RNA interference (RNAi) pathway. RNA interference is a post transcriptional process triggered by siRNA, which inhibits the expression of a specific gene by the degradation of its complementary messenger RNA (mRNA). Despite its potential value, intracellular delivery remains a major obstacle to clinical applications of therapeutic siRNAs. Its large size and negative charge prevent siRNA molecules from crossing cellular membranes while the sensitivity of naked siRNA to endogenous enzymes makes it vulnerable in serum. To address these problems, several novel strategies are created to achieve an effective and safe mode of delivery. Among them, peptide based drug/gene carriers are emerging as one promising delivery system for safer *in vitro* and *in vivo* applications.

This thesis focuses on the design, characterization and utilization of novel endosomolytic peptides for siRNA delivery. The studies include the following: (i) the design of new peptide sequences, and modification of existing sequences; (ii) the physicochemical characterization of peptides, and the interaction between peptides and siRNA molecules; (iii) the evaluation of the silencing efficiency, and toxicity of

peptides/siRNA complexes in cultured cells and *in vivo*; (iv) the study of their intracellular pathway, and endosomal release mechanism; (v) the *in vitro* biocompatibility study of the peptides/siRNA nanocomplexes, and (vi) the co-delivery of anti-cancer drugs and siRNA into cancer cells.

The peptide C6, a 18-mer peptide, was first evaluated as an siRNA carrier. C6 contains three types of amino acids: positively charged arginine, hydrophobic leucine and tryptophan. C6 would bind to negatively charged siRNA molecules through electrostatic interaction, whereby a peptide/siRNA molar ratio above 10/1 is needed to neutralize all the negative charges of siRNA molecules, indicated by the agarose gel shift assay. Fluorescence microscopy shows a punctuated distribution of peptide/siRNA complexes. Despite the great intracellular uptake, the silencing efficiency of siRNA delivered by C6 is very low, probably due to the entrapment in the endocytic vesicles.

Therefore, modifications by including pore-formation or pH-sensitive moiety to the sequence have been applied to enhance the endosomal escape capability of C6/siRNA complexes. Based on these strategies, a peptide library was generated by modifying prototype peptide C6. All the modifications improved the transfection efficiency of C6 to some degree. After completing the pre-screening for the activity, several promising candidates were used for further evaluations. Aromatic tryptophan residues were used to substitute some leucine residues in the sequence, since tryptophan rich motif is found abundantly in the pore-forming toxins of bacteria. The resulting peptide C6M1 shows increased endosomal membrane disruption ability in acidic environment. In addition, certain residues in C6 were replaced by histidine in the hope that they will facilitate the endosomal escape of peptide/siRNA complexes through the “proton sponge effect.”

Selected peptides C6M1, C6M3, and C6M6 could form stable complexes with siRNA. Formed nanoscale complexes are able to deliver siRNA into different cells and induce specific gene knockdown. Effective *in vivo* RNAi was achieved in a mouse model bearing a subcutaneous tumor. Intratumoral injection of the complexes resulted in a marked reduction of tumor growth through downregulation of antiapoptotic Bcl-2 protein in mice. Furthermore, these complexes were proven safe at transfection concentration by the cytotoxicity, the complement activation, and the cytokines activation assays. These results demonstrate that the C6 family peptides are a potent system for efficient gene delivery *in vitro* and *in vivo*.

As positive charges and endosomal escape ability both play an important role in promoting the transfection efficiency of siRNA, next the structure-activity relationship of efficient peptide-based siRNA carriers were explored. Here, oligoarginine peptides, prominent members in cell-penetrating peptide family, are rationally modified with oligohistidine and stearyl moieties (STR-). It is found that when the ratio of histidine/arginine in a stearylated peptide sequence is >1.5, pronounced GAPDH gene silencing is induced in a range of cell lines. Among these peptides, STR-HnR8 (n>12) showed high knockdown efficiency, which was rarely reported before. The main endosomal escape mechenism of stearylated and oligohistidylated oligoarginine/siRNA complexes is determined to be the “proton-sponge” effect. This peptide could also stabilize hydrophobic EPT/HCPT hybrid NPs in water. Co-delivery of EPT/HCPT hybrid NPs and Bcl-2 siRNA into cancer cells achieved a triple synergistic effect by greatly inhibiting cancer cells proliferation. Together, this work suggests a new strategy for the improvement and optimization of CPP-based siRNA delivery systems.

Acknowledgements

I would like to express my gratitude to all those who gave me the possibility to complete this thesis. I want to thank the University of Waterloo Chemical Engineering department and Waterloo Institute for Nanotechnology for giving me permission to commence my study in the first place, to do my research work and to use departmental resources. This thesis is the result of several years of intense work, whereby I have been accompanied, supported and tremendously helped by many people. I would take this opportunity to express my heartfelt thanks to all of them.

The first person I would like to thank is my supervisor, Dr. Pu Chen, who has provided me this invaluable opportunity to do innovative research in this cutting edge field. He gave me unlimited support, valuable advisory and critical guidance during my PhD study in his lab. His guidance helped me through difficulties in the research and his enthusiasm will inspire me to continue the exploration in nano-bioengineering. In addition, his excellent skills, scientific vision and keen attitude sets up a lively model for my future life and career.

I would like to express my gratitude to my PhD examination committee members who monitored my work and took effort in reading and providing me with valuable comments on this thesis: Professors William A. Anderson and Christine Moresoli from

Chemical Engineering department, Juewen Liu from Chemistry department, Wankei Wan from University of Western Ontario.

My next acknowledgements go to the following individuals who have contributed to the experiments and suggestions on my PhD research projects. Mishi Savulescu from Biology department and Cameron Postnikoff from Systems Design Engineering have carried out many flow cytometry analysis experiments for me. Professor Yongfang Yuan at the Shanghai Jiao Tong University School of Medicine and her students have collaborated with us on the *in vivo* studies, which are still going on. We have frequent tele-conferences to exchange ideas and discuss results on the animal study. Professor J. David Spafford in the Biology department kindly allowed us to use the fluorescence microscope in his lab and provided training. The TEM research described in this paper was performed by Chris Butcher at the Canadian Centre for Electron Microscopy at McMaster University.

I also want to extend my special thanks to our current and previous group members as well as lab managers. During my PhD study, I have received great help from all of you. I am so grateful that I learned the most valuable cell culture and qRT-PCR skills from Tatiana Sheinin. She is not only a wonderful colleague, but also a dear friend to me. Xiaoxia Han and Nita Modi are very appreciated for their help on western blot experiment and organizing the group. I would like to give my special thanks to siRNA delivery subgroup. Dafeng Chu has collaborated with me on several projects. I am deeply grateful to his invaluable experience and helpful suggestions to my research. I benefit a lot from our discussion. Moreover, I received great help from Ran Pan, Mousa Jafari, Baoling Chen, Dallas Willms and Yazan Bdour in my research project. Also I would like

to thank Yong Ding, Danyang Zhao, Sheng Lu, Parisa Sadatmousavi, Zizhen Wan, Ali Sheikholeslam, Lei Zhang in drug delivery group and all the members in Energy and Integrative Research.

I am deeply grateful to the financial support from the Natural Sciences and Engineering Research Council of Canada (NSERC), the Canada Research Chairs (CRC) Program and Waterloo Institute for Nanotechnology Nanofellowship.

Lastly, and also most importantly, I would like to thank my families and all my dear friends for give me boundless love, unlimited support and enormous encouragement to follow the dream I choose. Without them, none of my achievements would be possible. This thesis, a product of my PhD study, is dedicated to all of them.

Table of Contents

List of Figures

List of Tables

List of Abbreviations

Acronym	Full name
ATCC	American Type Culture Collection
AMD	age-related macular degeneration
Baf A1	bafilomycin A1
CQ	Chloroquine
CHO-K1	Chinese hamster ovary
CLSM	confocal laser scanning microscopy
CPP	cell-penetrating peptide
DLS	dynamic light scattering
DMEM	Dulbecco's Modified Eagle Medium
dsRNA	double-stranded RNA
EDTA	ethylenediaminetetraacetic acid
EMEM	Eagle's Minimum Essential Medium
ELISA	enzyme-linked immunosorbent assay
FACS	fluorescence-activated cell sorting
FBS	fetal bovine serum
FDA	Food and Drug Administration
GAPDH	glyceraldehyde 3-phosphate dehydrogenase
HBV	hepatitis B virus
IL	interleukin
LDH	lactate dehydrogenase
LNPs	lipid nanoparticles
LPS	lipopolysaccharide
MR	Molar Ratio

NPs	nanoparticles
PBS	phosphate-bufferred saline
PCR	polymerase chain reaction
PDI	polydispersity index
PEI	polyethyleneimine
PFA	paraformaldehyde
PTGS	post-transcriptional gene silencing
RISC	RNA-induced silencing complex
RNAi	RNA interference
RSV	respiratory syncytial virus
RT-PCR	reverse transcriptase PCR
SC5b-9	S-protein-bound C terminal complex
shRNA	short hairpin RNA
siRNA	small interfering RNA
SNALP	stable nucleic-acid-lipid particle
TCC	Terminal Complement Complex
TNF	tumor necrosis factor

Chapter 1

Introduction

1.1 Overview

The discovery of RNA interference (RNAi) is considered to be the most important and exciting breakthrough of the past decade by many biologists [1]. RNA interference is a highly efficient regulatory process in most eukaryotic cells by which double-stranded RNA (dsRNA) is able to cleave complementary mRNA and causes posttranscriptional gene silencing [2–4]. The high significance and transformative values of this discovery gained its inventors the award of Nobel Prize in Physiology or Medicine in 2006.

In general, long dsRNAs derived from either convergent transcription or hairpin-structured RNAs are the precursor of the short interfering RNA (siRNA) that can trigger RNAi [5]. When introduced into cells, dsRNA will be processively cleaved by the RNase III like enzyme, dicer, into short duplexed RNAs, i.e. siRNAs [6]. These newly formed 21-23nt long nucleotides will then be loaded onto an RNA-induced silencing complex (RISC). Argonaute 2 (Ago-2) is the catalytic core of RISC. Upon binding to siRNA, it will release one strand from the siRNA, resulting in an activated form of RISC containing a single-strand RNA (guide strand) that directs the specific recognition of complementary mRNA [7–10]. Ago-2 then cleaves the target mRNA, thereby preventing specific genes from expression of proteins [11]. Tuschl and his colleagues found that instead of using long dsRNA, the introduction of chemically synthesized siRNA into mammalian cells

can also efficiently silence specific genes [4]. Figure 1.1 shows the entire RNA interference pathway [12].

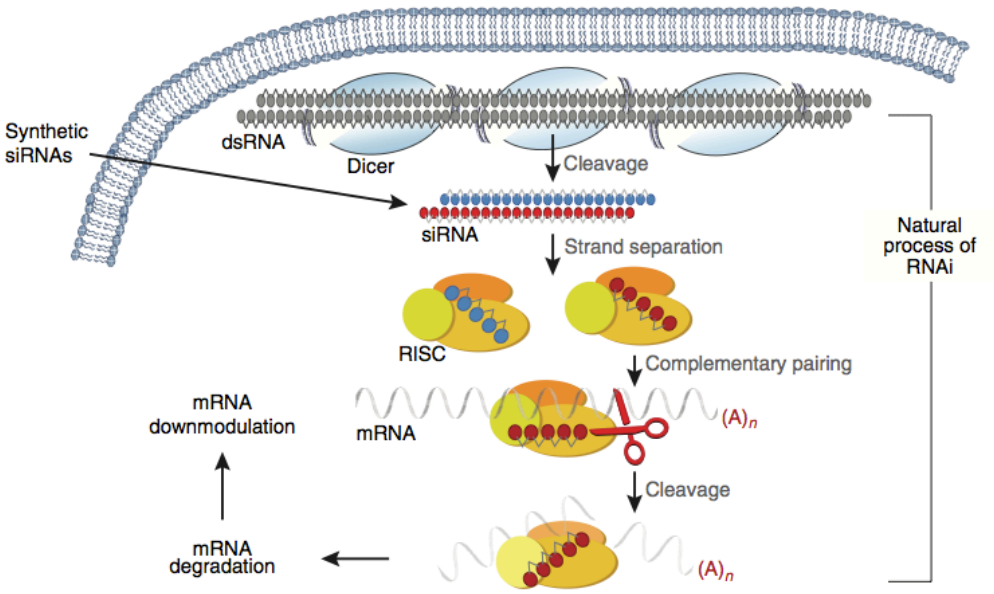

Figure 1.1 Schematic representation of siRNA mediated gene silencing

RNA interference has been widely used in basic biological research and clinical applications. Short interfering RNA therapy is becoming an important means for functional genomics study and the development of gene-specific drugs [13,14]. In biology, one of the most effective ways to determine the biological function of a protein or a pathway is to examine the phenotype of organisms that lack of or contain mutations in its encoding gene [15]. Thus, molecules that can specifically silence the expression of certain genes are powerful tools. The high efficiency and diversity in source of siRNA has made it one of the latest additions to gene-silencing reagents. RNA interference has also stimulated considerable interest in the pharmaceutical field as a potential therapeutic agent. Turning off problematic genes with RNA interference shows tremendous promise

for a huge number of human diseases. The first clinical trial with short interfering RNA (siRNA) in patients suffering from age-related macular degeneration (AMD) started in 2004 [16]. The relatively low safety concerns of siRNA in humans have led to its clinical evaluation in other genetic and viral diseases [17]. Moreover, the rapid development of RNA interference technology opens the path to powerful gene therapy for cancer treatment where traditional surgery, radiation and chemotherapy cause deleterious side effects due to their non-specificity to the tumor cells [18]. Some in vivo experiments have already demonstrated that siRNA could significantly inhibit tumor cell growth in a xenograft mouse model [19–23].

However, despite abundant promise, a number of problems and hurdles remain in the way for siRNA-based therapeutics. The most important concern is the effective delivery of siRNA to its site of action in the cytoplasm. Some unfavorable physicochemical properties, including their large molecule weight, negatively charged surface, hydrophilicity, sensitivity to nuclease degradation and instability with plasma half-lives of less than ten minutes [24] impede the uptake of siRNA into the cells, especially after systemic administration [25]. Therefore, the application of siRNA as a potential therapeutic agent requires efficient and safe delivery that will retain their biological functions. An ideal delivery system should bear following properties: (1) siRNA carriers should protect siRNA from serum degradation (2) increase the retention time of siRNA in the circulatory system by reducing clearance rate in the human body (3) ensure effective biodistribution (4) facilitate siRNA delivery to specific cell types (5) promote cellular uptake and release siRNA to the cytoplasm after internalization (6) be made from

biocompatible, well characterized and easily prepared material, showing minimized toxicity to the human body.

Many non-viral carriers have been developed to deliver siRNAs, including liposome [26], polymeric complexes [27], dendrimers [28] and gold nanoparticles [29]. They all have achieved varying degrees of success. Among the siRNA carriers, liposomes or lipidic carriers represent a mature technology. Cationic lipids have been used to encapsulate negatively charged siRNA molecules and deliver them into cells. Although satisfactory in certain *in vitro* systems, there are still difficulties with the lipidic strategies. The relatively large amount of the lipids required for siRNA transfection can often cause severe toxicity [30]. It has been reported that cationic lipids can modify cellular signaling pathways and stimulate specific immune or anti-inflammatory responses [31]. These toxic/immunogenic features limit the use of lipidic carriers *in vivo*. A clinical trial of liposomal siRNA delivery for hypercholesterolemia was terminated recently because of the potential for immune stimulation to interfere with further dose escalation [32]. Although new approaches have addressed some of the toxicity and targeting issues, long term *in vivo* safety and efficacy of this strategy remain in question.

Synthetic and natural polymers, consisting of repeated units of covalently bonded monomers, are another class of carrier systems for siRNA therapeutics. The structural and chemical properties of the polymers are well established, and cationic polymers bind to siRNAs through electrostatic interactions. A number of polymers, including poly (ethyleneimine) (PEI), poly (L-lysine) (PLL), chitosan, gelatin, poly-D, L-lactide-co-glycolide (PLGA), poly (dimethylaminoethylmethacry-late) (PDMAEMA), and poly (trimethylamino-ethylmethacrylate) (PTMAEMA) have been investigated as siRNA

carriers. Like lipidic carriers, polymeric delivery systems also suffer from cellular toxicity and immunogenicity [33]. So their *in vivo* applications have been hindered thus far.

In light of the safety concerns and efficacy issues with current drug delivery systems, peptide-based carriers are emerging as an alternative for safer *in vitro* and *in vivo* delivery. They can traverse cellular membrane and deliver a variety of cargos including small molecule pharmaceuticals, proteins and oligonucleotides into cells with efficiency and specificity. Particularly, these cell penetrating peptides can deliver active substances to area of the body that are not easily accessible, the blood-brain barrier for instance. Our lab has been studying a class of peptides, the self-assembling/co-assembling peptides, which can be used as drug or gene delivery vehicles [34]. These peptides have been successfully used to encapsulate a model anticancer drug and deliver it across the cell membrane in a controlled manner. Encouraged by these results, we generated libraries of peptides that have potential to deliver siRNAs into cells. After high-throughput screening, several peptides with high transfection efficiency were selected for further study. Physicochemical characterizations were first applied to study the formed peptide/siRNA complexes, which include the interaction between peptides and siRNAs; the size and zeta potential; the morphology of the complexes. Then, the peptide/siRNA complexes with certain combinations of peptide and siRNA concentrations were further tested on their cellular uptake, cytotoxicity and their *in vitro* therapeutic effect on several cell lines. Potential immune side effects of these peptides in terms of complement activation and cytokine activation were also addressed. Their intracellular trafficking mechanism was systematically studied to explore a rational design strategy for peptides

as siRNA carriers. This information will be critical to the next phase of *in vivo* studies. In the next step, human tumor xenografts in a nude mice model were used to conduct *in vivo* efficacy and toxicity evaluation of potential gene therapy for cancer treatment. The simultaneous delivery of two anticancer drugs and therapeutic siRNA was investigated in A549 cancer cells. Based on the results reported in this work, strategies could be developed to design efficient peptides to construct functional nanocarriers for *in vitro* siRNA delivery and cancer gene therapy.

1.2 Research Objectives

The goal of this research is to develop an efficient and safe peptide based delivery system for *in vitro* and *in vivo* siRNA delivery. To achieve this goal, several promising peptides selected from designed peptide libraries were studied for their siRNA binding ability, silencing efficiency and toxicity on cultured cells and a mouse model. The specific objectives of this thesis are listed in the following:

(1) Design of peptide libraries that consist of novel peptides and structurally modified analogues of existing peptides to achieve high siRNA transfection efficiency and low cytotoxicity.

(2) Characterization of peptide/siRNA complexes; This will give us a general understanding of their binding mode at different molar ratios, thereby providing information for formulating desirable siRNA/peptide complexes.

(3) Investigation of the therapeutic efficacy, toxicity and biocompatibility of the complexes *in vitro* with several cell lines.

(4) Evaluation of the antitumor activity of complexes *in vivo* on a mouse xenograft tumor model.

(5) Study of the intracellular traffic mechanism of the complexes, providing insight into the design of efficient peptide based siRNA delivery system.

(6) Exploration of the possibility to co-deliver anticancer drugs and siRNA into cancer cells.

1.3 Outline of the Thesis

The thesis consists of eight chapters. The scope of each chapter is listed as follows:

Chapter 1 gives an overview of the thesis, including a brief introduction to RNA interference and mechanism, its potential clinical applications, existing gene delivery materials and the promising future of peptide based delivery system. The objectives and the scope of the thesis are also given in this chapter.

Chapter 2 provides a review of the advantages of RNAi as potential new pharmaceutical drugs, therapeutical applications of siRNAs and current siRNA delivery systems. Uptake pathways and subsequent intracellular trafficking of these cell-penetrating peptides as siRNA delivery vector are also reviewed.

Chapter 3 presents a new amphiphilic cell-penetrating peptide C6. Physicochemical characterizations were conducted. Of particular interest is that this peptide could deliver large amounts of siRNA into cells, yet the knockdown efficiency is very low, probably due to poor endosomal escape ability.

In order to improve the endosomolytic ability of peptide C6, thus enhancing transfection efficiency, different strategies were applied to modify C6 sequence. In Chapter 4, we designed a new peptide C6M1 by substituting some leucine residues in C6 with tryptophan. In chapter 5, peptides were generated by adding pH-responsive histidine

residues to the sequence. Both modifications, though working through different endosomal escape pathways, greatly improve the knockdown efficiency of peptide/siRNA complexes. *In vivo* antitumor activity of therapeutic siRNA delivered by these peptides was investigated in a tumor xenograft mouse model.

To further explore the structure-activity relationship of cell-penetrating peptides, in Chapter 6, oligoarginine peptides, prominent members in CPPs, were rationally modified with oligohistidine and stearyl moieties (STR-). The optimal histidine/arginine ratio for efficient gene knockdown was determined.

Chapter 7 studies the possibility of simultaneous delivery the anticancer drugs and therapeutic siRNA into cancer cells by promising peptide. The importance of peptide to stabilize hydrophobic anticancer drugs hybrid nanoparticles in water was also described.

Chapter 8 presents the conclusions of studies in the thesis, contributions of this research and recommendations for future work.

Chapter 2

Literature Review

2.1 RNAi as a potential new class of pharmaceutical drugs

2.1.1 Comparison of siRNA therapy with traditional drugs

Most approved drugs share important features like relatively small in size (molecular weight< 500 Da), apolar and function by binding to proteins or altering protein function [35]. Although much is known about designing traditional drugs and how to modify them to improve their *in vivo* efficacy, the development of small molecule drugs is often marked by failure in preclinical and clinical trials even with this vast experience [36]. siRNA drugs are not quite similar to traditional drugs. "Traditional drug discovery was done by trial and error—applying materials to cells until the desired phenotype is obtained. Drugs discovered in this method usually are nonspecific and have extensive side effects. With siRNA, it's possible to identify the reason a phenotype develops, validate your identification, and attack the exact location in the cell that's responsible for disease with minimal side effects. RNAi's sequence specificity allows the kind of specific treatment you would demand from a next-generation drug," says Sharon Engel, director of genomic data at Compugen Ltd., Tel Aviv, Israel. As an alternative therapeutic approach, RNAi may provide solutions to the major disadvantages of traditional pharmaceutical drugs. Figure 2.1 compares the key features between RNAi as a therapeutic approach and the two major classes of traditional pharmaceutical drugs--

small molecules and proteins & antibodies [12]. One principle advantage of RNAi over other drugs is that all targets, including "non druggable" targets for traditional therapy, can be inhibited with RNAi and the corresponding siRNA can be rapidly identified and synthesized. The identification of highly selective and potent compounds for small molecule drugs is a difficult and time-consuming process, and can be unsuccessful sometimes. For RNAi, the identification of highly selective and potent target gene is

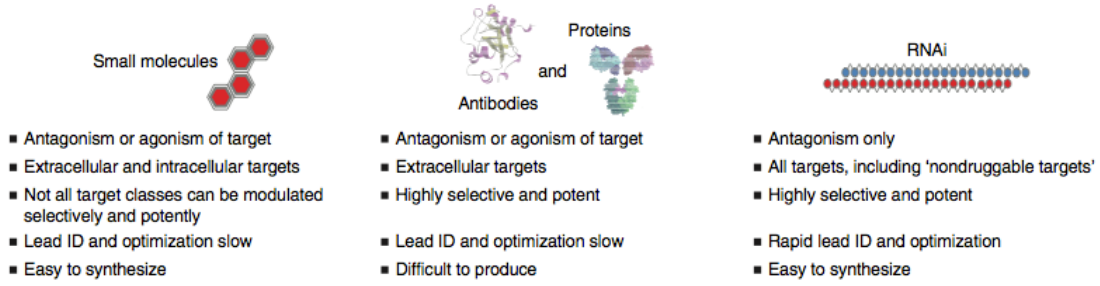

Figure 2.1 Comparison of the key features between RNAi as a therapeutic approach and the two major classes of traditional pharmaceutical drugs-- small molecules and proteins & antibodies.

rapid and has been demonstrated with numerous molecular targets. With protein and antibody drugs, the major technical challenge is production. Acceptable cellular production levels are difficult to achieve for protein drugs, while the aggregation problems continue to be a major issue for biologics. In contrast, siRNA molecules are easy to produce with respect to chemical synthesis process. One shortcoming of RNAi therapy is that they only have antagonism effect to the specific targets, whereas the other two classes of drugs provide agonism as well as antagonism effect. Overall, RNA holds

great promise as a pharmaceutical drug that will fill in a significant gap in modern medicine.

2.1.2 Therapeutic applications of RNAi

RNAi based therapeutics has significant advantages including broad applicability, therapeutic precision and selectivity avoiding side effects. Recent advances in RNAi therapy have broadened the scope of its application for a variety of human diseases. A number of studies have been reported demonstrating the silencing of disease genes by administration of siRNAs. Figure 2.2 shows the organs in the human body for which RNAi proof of concept has been demonstrated [12]. Direct RNAi means local delivery of siRNA molecules. This has been carried out successfully to specific tissues and organs like eye, lung, skin, nose, the nervous system and the digestive system. Systemic RNAi means intravenous delivery of siRNA molecules into lung, tumors, liver and joint.

Several different types of diseases that are very common and widely studied will be discussed here.

Infectious disease

Diseases caused by bacteria and viruses continue to be one major cause of death around the world. The emergence of resistant strains raises increasing concerns worldwide. The prominent examples are AIDS, influenza and hepatitis for virus infection and pneumonia and sepsis for bacterial infections [37]. Cell culture studies clearly demonstrated that RNAi was able to inhibit the cellular uptake or replication of infectious agents. Many studies have shown that siRNAs could knock down the expression of HBV gene [38,39].

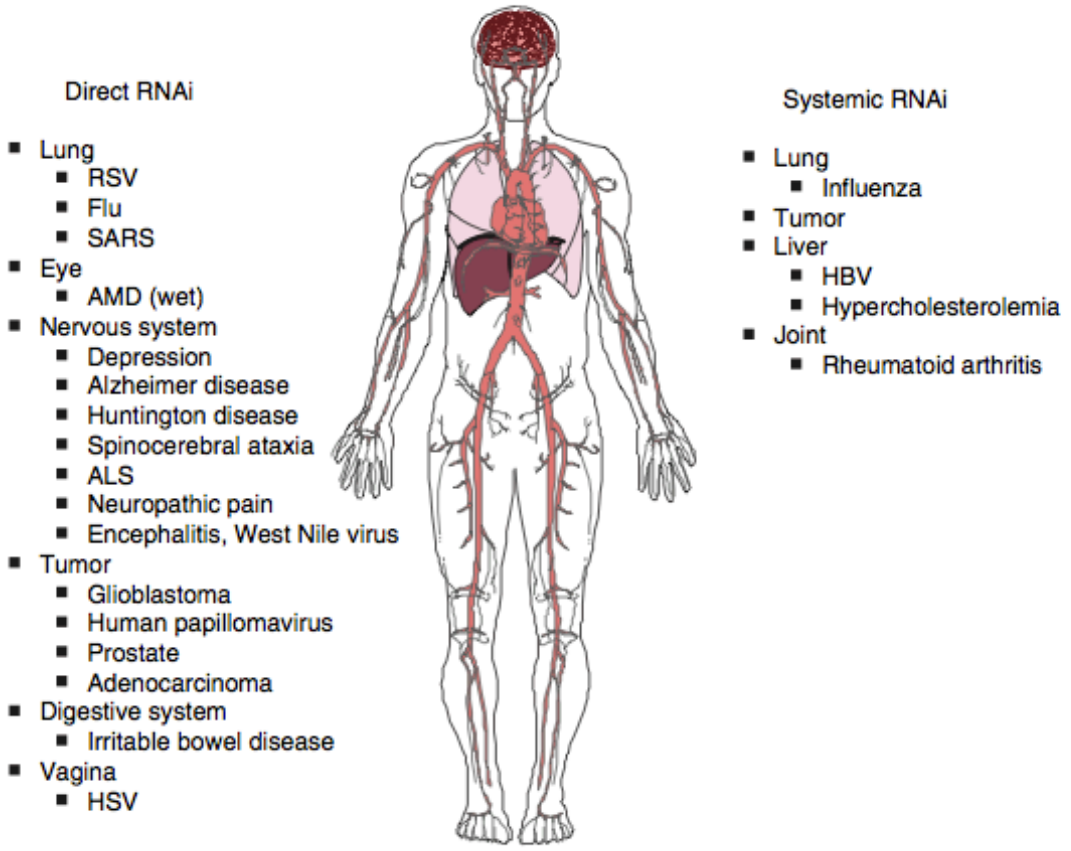

Figure 2.2 Organs and diseases for which the effect of RNAi has been proved [12].

HBV is a DNA virus, its DNA replicates through a genomic RNA intermediate and uses a virally encoded reverse transcriptase during replication. It is found that the distinct RNAi targeting sequences on specific gene on virus exhibited various efficacies on inhibition of the viral DNA replication and gene expression [40–42]. Morrissey *et al.* reported a reduced serum HBV DNA concentration in mice by intravenous injections of a stable nucleic-acid-lipid particle (SNALP) [40]. McCaffrey *et al.* injected a large volume of plasmids encoding the HBC gene along with HBV specific shRNAs (small heparin RNA) into mouse liver. The HBV specific shRNAs significantly reduced viral mRNAs

and protein expression, thus inhibiting HBV replication in infected mice [43]. More examples of siRNA treatment for HBV are shown in Table 2.1.

Table 2.1 Examples of siRNAs targeting HBV

Gene	Host	Transfection/Delivery	Results
S, C	HepG2.2.15 cells	Liposomes	Reduction in HBsAg secretion by 80% in cell culture
C	Mice	Tail vein injection	Significant reduction in HBsAg and HBeAg expression
S	Mice	Hydrodynamic injection	Three daily intravenous injections of 3 mg/kg day reduced serum
P, C, S	HepG2.2.15 cells	oligofectamine	HBeAg expression decreased by 73.8% and 72.8% after siRNAs targeting Pre C region
C	HuH7 and HepG2 cells	oligofectamine	HBeAg levels in the cell culture medium decreased to 4.6 fold and 4.9 fold
NA	HepG2.2.15 cells	DOTAP liposomes	Inhibition rate is approximately 80-90% in treated cells

Abbreviation: C, core antigen; S, surface antigen; P, polymerase; S, X protein; NA, not report; DOTAP, 1,2-dioleoyl-3-trimethylammonium propane

HIV was the first infectious agent targeted by RNAi, as the pattern and lifecycle of gene expression of HIV is well known. A number of studies have been carried out using siRNAs and shRNAs targeting HIV genome regions such as tat, rev, gag, pol, nef, vif, env, vpr, and the long terminal repeat (LTR) in infected cells and showed promising results to inhibit viral production [44]. Despite several successful cases, targeting the virus directly encounters a substantial challenge for clinical application, because the high viral mutant rate may lead to mutants that escape from being targeted [45]. Thus, RNAi mediated knockdown of cofactors associated with virus infection has become an alternative approach. Qin *et al.* successfully constructed a lentivirus-based vector to

deliver siRNAs against the HIV-1 co-receptor CCR5, into human peripheral blood T lymphocytes [46]. This resulted in up to 10-fold inhibition of CCR5 expression on the cell surface over two weeks, which therefore provided a substantial protection for the lymphocyte populations from HIV-1 virus infection, dropping infected cells by 3-7 fold. Kumar *et al.* conjugated a CD7 specific single-chain antibody to oligo-9-arginine peptide for T cell specific siRNA delivery in mice or $CD43^+$ hematopoietic stem cells [47]. This treatment controlled viral replication and prevented the disease-associated CD4 T cell loss. Surabhi and Gaynor [48] addressed that siRNAs directed against NF-κB p65 subunit could significantly decrease the levels of the protein and thus inhibiting HIV-1 replication. Multiplexing shRNAs or siRNAs targeting several sites in the HIV is an option that should be fully explored and carefully examined for efficacy, inhibition of viral mutants, and potential toxicity. One example of a potent combination of shRNAs with mixtures of non-shRNA antivirals is shown in Figure 2.3 [49]. However, the delivery of siRNAs to HIV infected cells is also problematic sometimes. The systemic delivery of siRNAs to T cells is probably not feasible owing to the immense number of target cells, which are primarily T lymphocytes, monocytes and macrophages. Therefore, the preferred method is to isolate T cells from patients. These cells are then transfected, expanded and reinfused into the same patients.

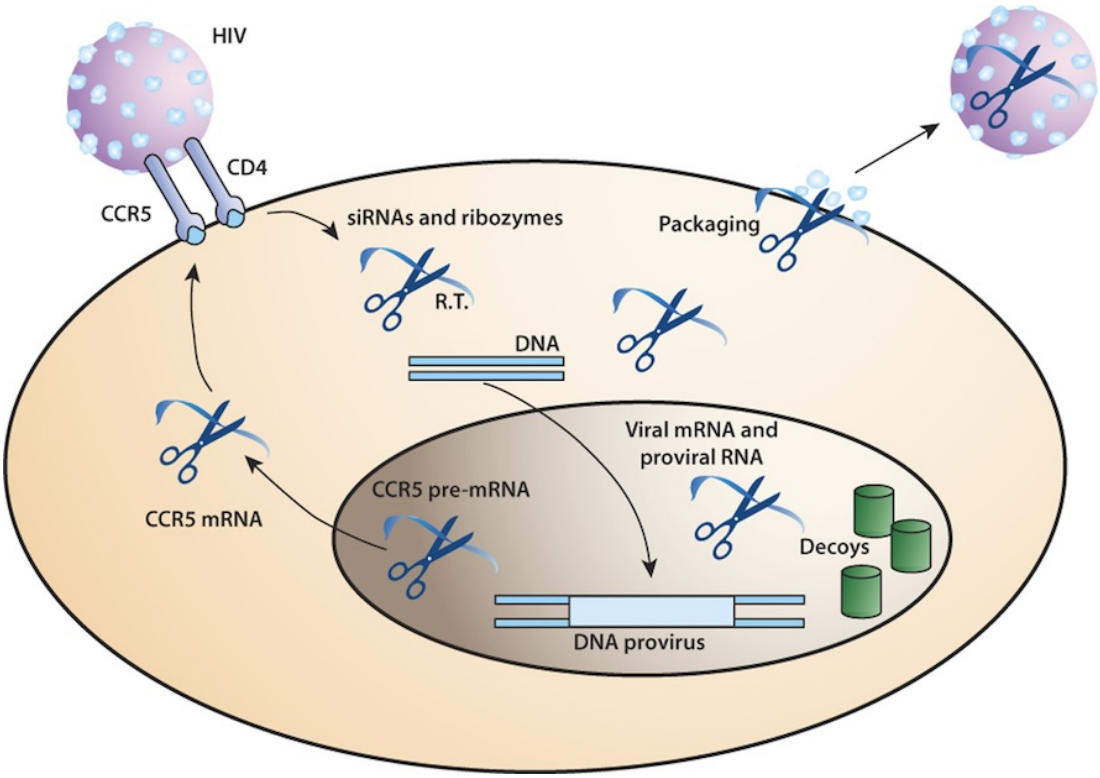

Figure 2.3 Proposed multiplexing RNA interference (RNAi) with ribozymes and decoys for the treatment of HIV infection. Different stages of HIV replication can be targeted using siRNA and combinations of other RNA based inhibitors. CD4 receptor and CCR5 co-receptor are binding site for HIV-1. The proviral RNA is reverse transcribed into DNA, which will integrate randomly into the host chromosomes. The scissors represent targeting site for siRNA or ribozymes. The decoy for binding viral Tat or Rev is depicted as a barrel in the nucleus. The virus may be attacked by siRNA or ribozymes at the preintegration step to block proviral DNA formation and integration. While at postintegration step, siRNAs can target all classes of HIV transcripts.

Neurodegenerative diseases

For many neurodegenerative disorders, a causative therapy is unavailable. Designing an inhibitor for any neurodegenerative disease that effectively suppresses the pathogenicity

of the disease is yet to be achieved. The challenge lies in crossing the blood-brain barrier (BBB) and blood-cerebrospinal fluid barrier (BCSFB) to reach the catalytic sites of the enzyme/protein involved in the molecular mechanism of the disease process [50]. siRNA holds a promising option for the development of novel therapeutic strategies for this kind of disease. Alzheimer's disease, Amyotrophic Lateral Sclerosis (ALS), Parkinson's disease, Huntington's disease are examples of relatively common age-related neurodegenerative disorders, each of which is characterized by the dysfunction and death of specific populations of neurons: Hippocampal and cortical neurons involved in learning and memory processes in Alzheimer's disease, dopamine- producing neurons in the substantia nigra controlling body movements in Parkinson's disease and spinal cord motor neurons in ALS [37]. Specific genetic mutations are responsible for a small percentage of cases of Alzheimer's disease, Parkinson's disease and ALS [51], where all cases of Huntington's disease result from mutations in the Huntington protein [52]. These neurodegenerative disorders share some biochemical cascades that result in neuronal cell death, including increased oxidative stress, irregulation of cellular calcium, homeostasis and apoptosis. Therefore, two different strategies were proposed for preventative and therapeutic treatment in these diseases. One is to silence the disease-causing genes that are believed to initiate the neurodegenerative process. The other is to target downstream events in the neurodegenerative cascade. Wang *et al.* used siRNA directed against the huntington gene to repress its transgenic mutant expression in an HD mouse model [53]. Results showed that intraventricular injection of siRNAs at an early postnatal period inhibited transgenic Huntington gene expression in brain neurons and induced a decrease in the numbers and sizes of intranuclear inclusions in striatal neurons. Treated model

mice showed significantly prolonged longevity, improved motor function and slowed down in the loss of body weight. In Alzheimer's disease, increased beta-secretase (BACE1) activity is associated with neurodegeneration and accumulation of amyloid precursor protein (APP) products. Therefore, the inhibition of BACE1 could be important in the treatment of Alzheimer's disease. Singer *et al.* found that decreasing BACE1 levels by using lentiviral vectors with siRNAs targeting BACE1 gene reduced amyloid production and the neurodegenerative and behavioral deficits in mice model with Alzheimer's disease [54]. In summary, *in vitro* cell culture experiments and *in vivo* animal studies have shown that siRNA is a highly effective tool to downregulate different target genes involved in the pathogenesis of neurodegenerative diseases.

Cancer

Cancer is one of the primary causes of death around the world and it is estimated to cause 13.1 million human casualties in 2030 [55]. Cancer is a chronic disease that causes growing burden to the patients, families and society. Thus, effective and safe treatments are urgently needed. Current available and common cancer treatment—surgery, chemotherapy and radiation have made tremendous progress, but they have ample of limitations. Recent understanding of the genetic causes of the disease provides the prospective for gene therapy as an alternative approach. The antigene approaches include ribozymes [56], antigene oligonucleotides [57], peptide nucleic acids (PNAs) and antisense oligonucleotides. In contrast to antisense technology, siRNA applies a post-transcriptional gene silencing (PTGS) mechanism. siRNAs are much better in silencing the target gene compared to the antisense RNA alone as the transcript of the gene is

rapidly degraded without accumulation. Table 2.2 compares the pros and cons of different gene silencing strategies [18].

In cancer cells, proto-oncogenes have frequently been activated by various mechanisms. Cancer cells are different from normal cells in that they exhibit abnormality in cell cycle resulting in uncontrolled growth; they are resistant to death as a result of the dysfunction of the proteins that mediate cell apoptosis; they gradually acquire resistance to many anti-cancer drugs. Therefore, the approach for siRNA in the treatment of cancer is downregulation of genes that contribute to tumor progression, e.g. the expression of the oncogenes in cell cycle and/or an anti-apoptotic gene in cancer cells. The other genes involved in tumor formation were also widely studied—vascular growth factor involved in cancer metastasis, mutated genes that contributed to the development of drug-resistant cancer cells.

This high-throughput screening technique has paved the way for loss-of-function studies, thus numerous genes involved in tumor formation have been identified. This has indeed led to a recent acceleration in the development of siRNA-based strategies for cancer therapy. Figure 2.4 shows different target genes and pathways for which *in vivo* animal studies have been conducted successfully [58].

Table 2.2 Advantages and disadvantages of different gene-silencing strategies

Strategy	Advantages	Disadvantages
Low-molecular-weight agents	Easy to administrate	Often nonspecific
	Often inexpensive	May not be available
		Off-target effects
Antisense ODNs	Easy to synthesize	Only exogenous delivery
	Inexpensive	Protein binding
	Modification to improve selectivity and efficacy	Off-target effects
		Induction of interferon response
Ribozymes	Simple catalytic domain	Requirement of specific cleavage triplets
	Delivery as free molecules and by expression vectors	Protein binding
	Tissue-specific delivery if vector established	
	Administration to subcellular compartments	
DNAzymes	Inexpensive	Only exogenous delivery
	Good catalytic properties	Off-target effects
	Modification for systemic delivery	
RNAi	Highly effective at low concentrations	Off-target effects
	Delivery as free siRNA molecules and by short hairpin RNA expression vector	Induction of interferon response
	Tissue-specific delivery if vector established	Expensiveness of siRNAs

ODN: Oligodeoxynucleotide; siRNA: Short interfering RNA

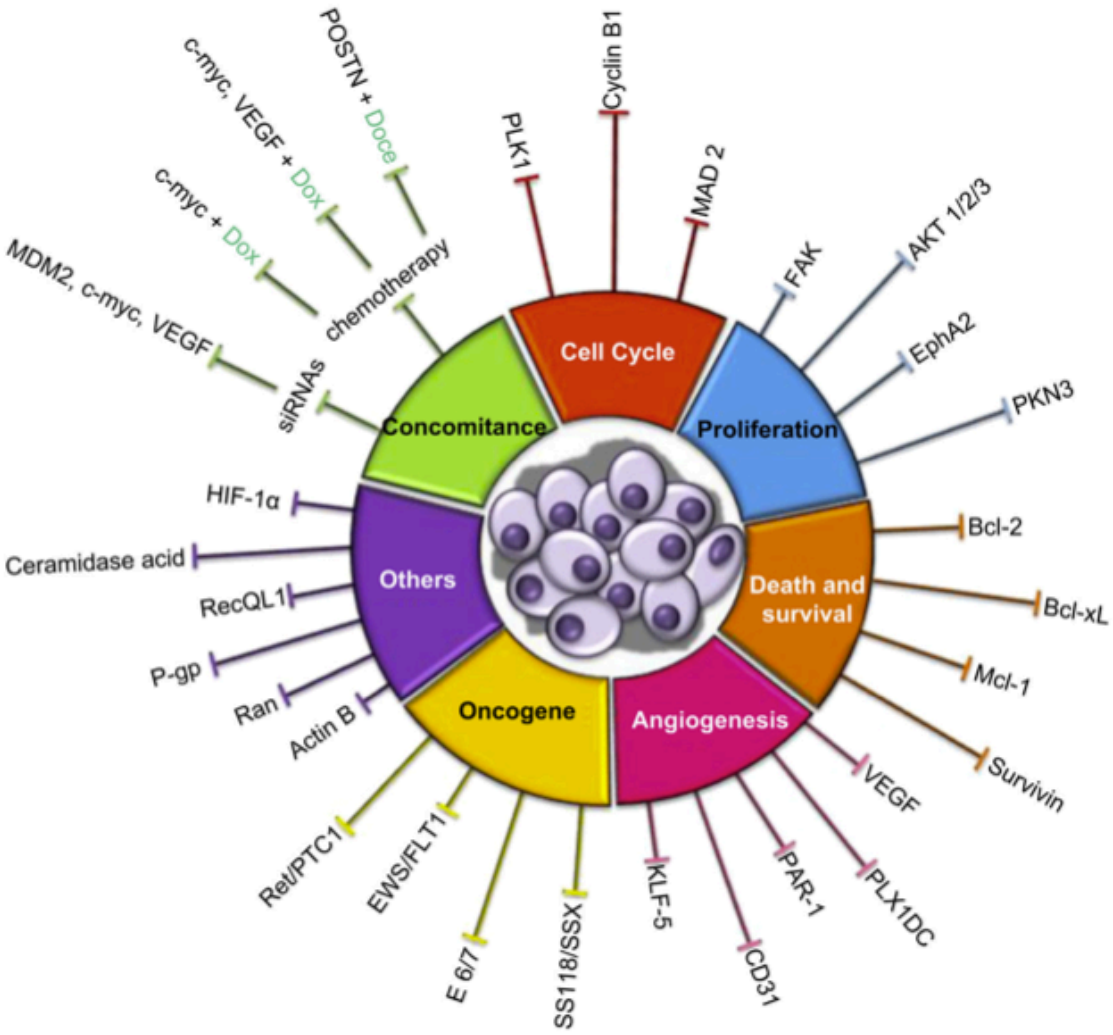

Figure 2.4 Pathway targeting by siRNA delivery systems in cancer. Representation of siRNA targeted molecules used in preclinical studies to develop an anti-cancer treatment. Dox: doxorubicin; Doce: docetaxel. Plk1: polo-like kinase1; MAD2: mitotic-arrest deficient 2; EphA2: receptor of ephrins; AKT 1/2/3: KLFisoforme of serinethreonin kinase; PKN3: protein kinase N3; FAK: focal adhesion kinase; Bcl: B-cell lymphoma; Mcl-1: myeloid cell leukemia; VEGF: vascular endothelium growth factor; PAR-1: protease activated receptor 1; KLF-5: Kruppel-like factor 5; PLX1DC: plexin domain

containing 1; HIF-1a: hypoxia inducible factor 1a; CA: ceramidase acid; MDM2: murine double minute 2; POSTN: periostin.

Many studies have confirmed the therapeutic potential of RNAi *in vivo* by demonstrating the anticipated tumor inhibition effect. Table 2.3 summarizes these studies with detailed information [58].

Table 2.3 Studies based on siRNA delivery in cancer therapy

Pathway	**siRNA target**	**Cancer model**	**Injection route**	**Inhibition of tumor volume**	**Other effects**
Cell cycle	Cyclin B	Prostate	s.c	70%-92%	50% long survivial
	PLK1	Breast	s.c	70%	Caspase 3 activation
	MAD2	Colon	s.c	35%	Increased apoptosis
Proliferation	EphA2	Ovarian	i.p	55%	/
	AKT1	Prostate	s.c	66%	/
	AKT2	Prostate	s.c	89%	/
	AKT3	Prostate	s.c	57%	/
	PKN3	Prostate	Orthotopic	60%	75% for metastasis
	FAK	Ovarian	i.p	60%	/
Cell death and Survival	Bcl-2	Prostate	s.c	65%	/
	Mcl-1	Breast	s.c	75%	no toxicity for max dose
	Survivin	Prostate	s.c	30%	/

Angiogenesis	VEGF	Prostate	s.c	87%	No toxicity
	PAR-1	Melanoma	s.c	77%	/
		Melanoma meta	i.v	/	Decreased metastase number 81%
	CD31	Prostate	Orthotopic	65%	/
	KLF-5	Lung carcinoma	s.c	60%	/
		Prostate	s.c	48%	Prolonged survival median
	PLX1DC	Ovarian	i.p	87%	Increased apoptosis 35%
Oncogene protein	E6/7	Renal	s.c	55%	No synergic effect with cisplatin
	ret/PTC1	Fibroblast	s.c	90%	/
	EWS-FLI1	Ewing sarcoma	i.v	80%	No inflammatory response
	SS18-SSX	Synovial sarcoma	s.c	83%	/
Hypoxy	HIF-1a	Glioblastoma	s.c	50%	/
Metabolism	CA	BT474	s.c	75%	Increased apoptosis,non-immunogenic
DNA repair	RecQL1	Colorectal meta	Spleen	43%	/
		Pancreatic meta	Spleen	31%	/
		Lung	s.c	46%	/
Nuclear transport	Ran	Neuroblasto-ma	s.c	49%	Increased apoptotic cell

Resistance	P-gp	Breast	s.c	60%	/
Migration	Actine B	HT-1080	s.c	65%	No inflammatory response
siRNA concomitance	MDM2, c-myc, VEGF	Melanoma	i.v	30%	No inflammatory response
Chemotherapy Concomitance	c-myc	Colon	s.c	60%	Increased apoptosis
	c-myc, VEGF	Ovarian	s.c	57%-60%	Increased apoptosis, no inflammatory response
	POSTN	Ovarian	i.p	90%	Increased apoptosis 45%, decreased proliferation 60%

Plk1: Polo-like kinase1; MAD2: mitotic-arrest deficient 2; EphA2: receptor of ephrins; AKT 1/2/3: KLFisoforme of serinethreonin kinase; PKN3: protein kinase N3; FAK: focal adhesion kinase; Bcl: B-cell lymphoma; Mcl-1: myeloid cell leukemia; VEGF: vascular endothelium growth factor; PAR-1: protease activated receptor 1; KLF-5: Kruppel-like factor 5; PLX1DC: plexin domain containing 1; HIF-1a: hypoxia inducible factor 1a; CA: ceramidase acid; MDM2: murine double minute 2; POSTN: periostin. s.c: sub-cutaneous injection, i.p: intraperitoneal injection, i.v: intravenous injection.

However, to avoid the side effects often inccurred in traditional treatment, we should selectively eliminate cancer cells without damaging normal cells. To do so, the siRNA would be targeted to a gene specifically involved in the growth or survival of cancer cells, or the siRNAs would be selectively delivered into the cancer cells.

2.1.3 siRNA therapeutics in clinical trials

RNAi has rapidly advanced from research discovery to clinical trials. Large amounts of money and effort have been invested in bringing siRNA technology to drug market. Initial trials have focused on well validated therapeutic targets, such as the VEGF pathway for the wet form of AMD, a leading cause of blindness and on the RSV genome, for the treatment of RSV infection, the leading cause of pediatric hospitalizations [59]. Phase I trials for above studies have already been completed without untoward toxicity. A total of 14 RNAi therapeutic programs have been reported to enter clinical trials in 2010 [60]. Till 2013, this number has increased to 22, as shown in Table 2.4, and many more are still in the development pipeline [61]. However, few publications detailing these clinical practices have emerged currently, we can only acquire following information from company press releases or the US National Institutes of Health hosted database of ongoing and completed clinical trials.

Table 2.4 siRNA based drugs in clinical trials

Drug	Target	Disease	Phase	Company
ALN-VSP02	KSP and VEGF	Solid tumors	I	Alynylam Pharmaceuticals
siRNA-EphA2-DOPC	EphA2	Advanced cancers	I	MD Anderson Cancer Center
Atu027	PKN3	Solid tumors	I	Silence Therapeutics
TKM-080301	PLK1	Cancer	I	Tekmira Pharmaceutical
TKM-100201	VP24, VP35, Zaire Ebola,	Ebola-virus infection	I	Tekmira Pharmaceutical

ALN-RSV01	RSV nucleocapsid	Respiratory syncytial virus infections	II	Alynylam Pharmaceuticals
PRO-040201	ApoB	Hypercholesterolaemia	I	Tekmira Pharmaceutical
ALN-PCS02	PCSK9	Hypercholesterolaemia	I	Alynylam Pharmaceuticals
ALN-TTR02	TTR	Transthyretin-mediated amyloidosis	II	Alynylam Pharmaceuticals
CAKAA-01	RRM2	Solid tumors	I	Calando Pharmaceuticals
TD101	K6a (N171K mutation)	Pachyonychia congenita	I	Pachyonychia Congenita Project
AGN211745	VEGFR1	Age-related macular degeneration, choroidal neovascularization	II	Allergan
QPI-1007	CASP2	Optic atrophy, non-arteritic anterior ischaemic optic neuropathy	I	Quark Pharmaceuticals
I5NP	p53	Kidney injury, acute renal failure	I	Quark Pharmaceuticals
PF-655	RTP801	Choroidal neovascularization, diabetic retinopathy,diabetic macular oedema	II	Quark Pharmaceuticals
siG12D LODER	KRAS	Pancreatic cancer	II	Silenseed
Bevasiranib	VEGF	Diabetic macular oedema,macular degeneration	II	Opko Health
SYL1001	TRPV1	Ocular pain, dry-eye syndrome	I, II	Sylentis
SYL040012	ADRB2	Ocular hypertension, open-angle glaucoma	II	Sylentis

CEQ508	CTNNB1	Familial adenomatous polyposis	I, II	Marina Biotech
Rxi-109	CTGF	Cicatrix scar prevention	I	Rxi Pharmaceuticals
ALN-TTRsc	TTR	Transthyretin-mediated amyloidosis	I	Alynylam Pharmaceuticals
ARC-520	Conserved regions of HBV	HBV	I	Arrowhead Research

As these and other trials advance through the clinic in the near future, the exciting potential of siRNAs may be demonstrated. Despite the obvious promise, there are several extracellular and intracellular challenges that currently limit the use of RNAi in the clinic. Important considerations for therapeutic RNAi include that gene silencing approaches rarely remove 100% of the mRNA, that off-target silencing can occur and that each target organ and tissues sometimes requires unique treatment. In some cases, the goal is to target every cell in the tissue, in other instances certain cell type in an organ is the objective. siRNA can also induce potential unwanted effects by activating the innate immune response, shutting off defense systems usually needed to fight against viruses.

2.2 Current delivery systems

siRNA molecules must be delivered to the target cells to activate the RNAi pathway. Many reports have described the direct delivery of naked siRNA to tissues *in vivo* such as eye, lung and central nervous system [59]. It is still not understood why certain cells, other than the rest, can directly take up siRNA into cytoplasm. But in most cases, as siRNAs are too large and hydrophilic to pass through cell membranes by themselves, a delivery strategy is required to assist their uptake and protect them from degradation. Figure 2.5 lists the barriers the delivery system may encounter *in vivo* [62]. Many types of delivery strategy have been created therefore to solve these issues. These include some physical internalization method, such as hydrodynamic injection [63,64], which rapidly inject large volume of siRNA solution into a mouse via the tail vein; particle bombardment and electroporation [63,64]. Physical delivery methods have not been studied as extensively as chemical delivery systems, though these approaches may avoid possible immune system stimulations that often arise in normal chemical based delivery systems. Viral vectors are still the most powerful transfection tools used currently with respect to their high efficiency. However, viral vectors are difficult to produce in a large scale and more important, their inflammatory and immunogenic nature prevents them from clinical administration. To overcome these limitations, non-viral vectors have been investigated as an alternative safer way for siRNA delivery. These non-viral nanoparticles are preferred to viral carrier due to their relatively low immunogenicity and high biocompatibility. Three major types of siRNA delivery system will be discussed here.

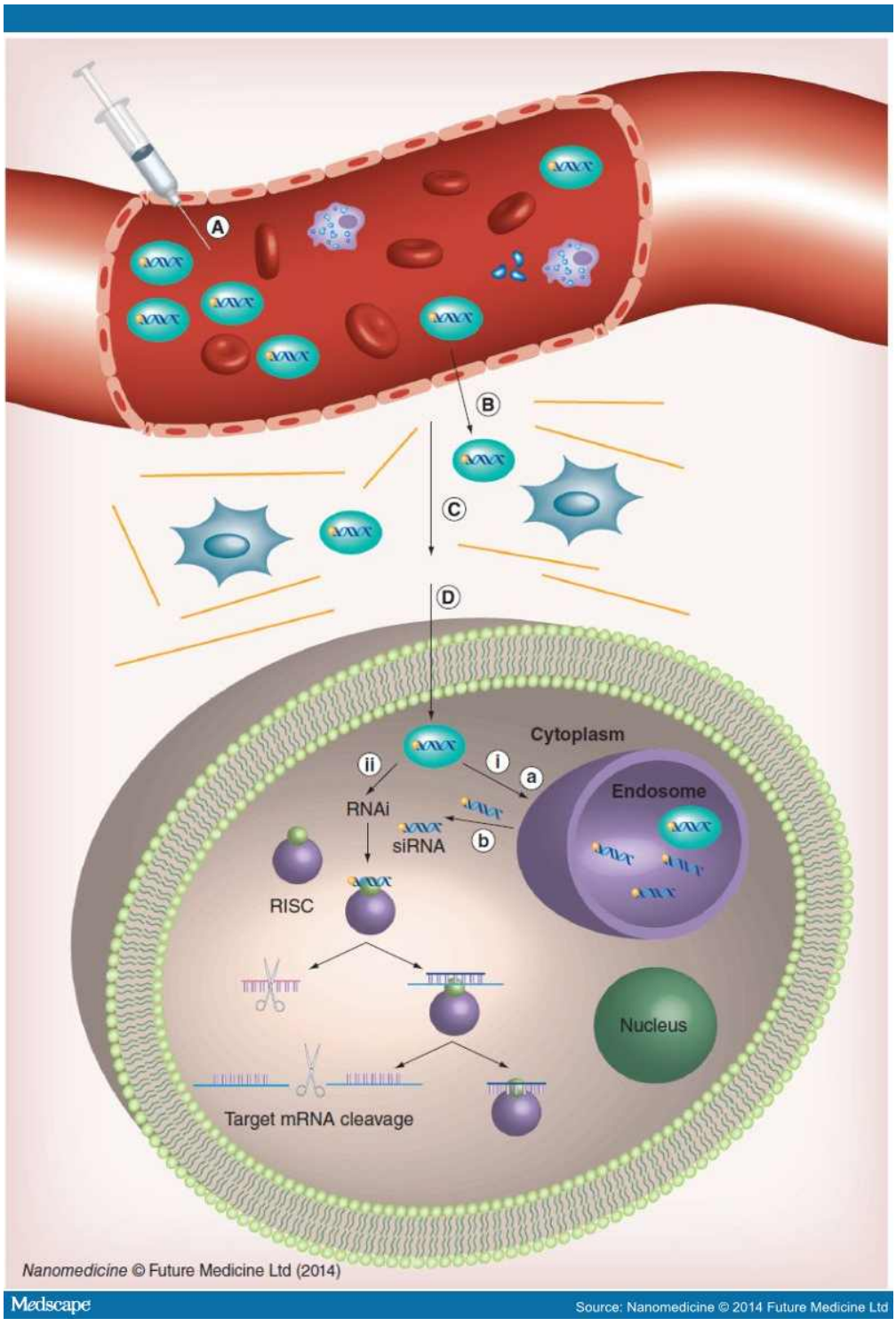

Figure 2.6 *In vivo* siRNA systemic delivery barriers. (A) Stability in the blood stream; (B) transport across the vascular endothelial barrier; (C) diffusion through the extracellular matrix; (D) delivery into the cytoplasm by (Di) endosomal escape and (Dii)

direct cytosolic delivery. (Dia) The siRNAs or siRNA nanoparticles were trapped in the endosome and (Dib) the siRNAs were released from the endosome into the cytoplasm.

2.2.1 Lipid based siRNA delivery system

Since the first discovery and active research of lipid carriers in 1965, the field has attracted enormous interest among scientists around the world [65]. Liposomes are considered the most versatile supramolecular assemblies with respect to size variety, composition and capacity to capsulate a variety of compounds. Liposome technology has made significant progress in the pharmaceutical industry, especially in drug and gene delivery. Several liposomes have been proved efficient and safe to deliver small molecule drugs in patients. Doxorubicin liposome (Doxil; Orthobiotech) has received FDA approval for treatment of breast cancer, ovarian cancer and other solid tumors [66].

The ideal liposomes for siRNA delivery will encapsulate siRNA with high efficiency, protect siRNA from enzymatic degradation in serum, and form a narrow size distribution of less than 200 nm to be able to access extravascular regions. A number of different lipid and lipid-like formulation methods have been developed, generating a variety of LNPs including liposomes, micelles, microemulsions and solid lipid nanoparticles [67]. Among these synthetic carriers, cationic liposomes and lipoplexes emerged as the most promising vehicles. Liposomes usually consist of an aqueous core enclosed in a phospholipid bilayer with hydrophilic drug entrapped in the aqueous phase. In contrast, lipoplexes are spontaneously formed through static interaction [68]. The interaction of lipid with siRNA is based on the electrostatic interaction between the positive charges of the cationic lipid and the negatively charged phosphate backbone of

the siRNA. Upon mixing of the two species in solution, the siRNA is condensed with lipid in order to neutralize negative charge. The structure of the lipid/siRNA complex depends on the composition of lipid, the properties of solution and the molar ratio of them. The structure of the cationic lipids is known to influence the transfection efficiency and toxicity of the lipid based delivery system [69]. Thus, the ratio of lipid and siRNA should be optimized before experiment to facilitate its interaction with the cell membrane and cellular internalization.

Lipid-based carriers have been successfully used to deliver siRNA into cells. Lipofectamine, RNAifect, Oligofectamine are commercial lipid-based delivery system that are routinely used in the laboratory [70]. For instance, siRNA targeting CD31 and Tie2 genes complexed with a mixture of cationic and fusogenic lipids can downregulate the corresponding mRNA and protein levels *in vivo* after intravenous injection [71]. Intraperitoneal injection of anti-TNF-α siRNA complexed with cationic liposomes DOTAP can inhibit LPS induced anti-TNF-α gene expression in mice [72].

Although satisfactory results were obtained for lipid based siRNA delivery system, there are still inherent difficulties exist. The amount of lipid required for efficient siRNA delivery in vivo is often accompanied by severe toxicity problems [73]. Besides, lipid can rapidly adsorb to serum proteins and trigger immune system response in the body. Thus, limited successful use of lipid was reported *in vivo*.

2.2.2 Polymers and dendrimer based siRNA delivery system

Linear or branched cationic polymers, made up of repeated units of covalently bonded monomers is another class of widely studied siRNA delivery system. The positively

charged polymers bind to siRNA through electrostatic interaction [74]. Figure 2.7 illustrates the schematic structures of siRNA nanocarriers formed by polymers [75].

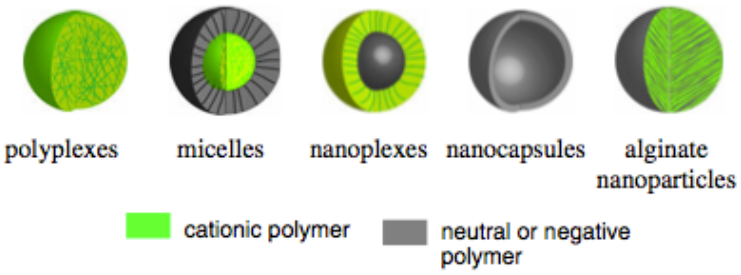

Figure 2.7 Schematic structure of various polymer based nanocarrier for siRNA delivery

A variety of polymers including poly(ethyleneimine)(PEI), poly-(L-lysine)(PLL) [76], chitosan [77], gelatin [78], poly-D,L-lactide-co-glycolide (PLGA) [79], poly (dimethylaminoethylme-thacrylate) (PDMAEMA) [80,81] and poly (trimethylamino-ehylmethacrylate) (PTMAEMA) were investigated. PEI is the most widely used polymer for siRNA delivery. In general, a branched structure of PEI offers higher transfection efficiency and a high molecular weight complex leads to increased toxicity. Non-covalently complexed PEI/siRNA could be internalized by the cells and achieve significant silencing effect. The systemic application of HER-2-specific gene complexed with PEI inhibited the growth of established tumors [82]. The intrathecal injection of PEI-siRNA complex targeting the pain receptor NR2B subunit decreased the mRNA level and its associated protein expression [83]. Dendrimers are synthetic macromolecules with highly branched peripheral chain ends. Although the investigation of dendrimers as siRNA delivery vector is still in its infancy, there are several reported advantages, which make it a promising versatile carrier. A novel surface neutral

dendrimers generated from poly(amidoamine) (QPAMAM) [84] was reported to show low cytotoxicity and highly organized compact ability because of its neutral surface and cationic inside structure.

2.2.3 Cell-penetrating peptide based siRNA delivery system

Cell penetrating peptides are defined by their ability to reach the cytoplasmic and/or other cellular compartments after internalization [85,86]. The initial discovery of cell penetrating peptide goes back about twenty years when the HIV-1 transactivating protein Tat was found to be taken up by mammalian cells [87,88]. And the following discovery of the homeodomain of *Drosophila melanogaster* transcription factor Antennapedia demonstrated that some "non-nature" peptides also share this property [89]. Mutation and deletion analyses have shown that in fact small domains within these proteins are responsible for the cellular uptake instead of the full-length peptide. These small peptide sequences are now referred to as CPPs or protein transduction domains (PTDs). Some of the CPPs, like Tat and penetratin, are small domains obtained from nature sequences, while some others are artificial designed constructs containing the critical feature of already known CPPs [90,91]. These CPPs share some common properties such as amphipathic and net positively charged at physiological pH [92]. Sometimes, siRNAs are linked to CPPs by expression as a fusion or by chemical coupling. Less peptide is required for this method. This is extremely important if peptide shows high toxicity to the cells. Recently, a more popular way to construct siRNA/peptide complex is allow them to bind each other non-covalently through mainly ionic interactions. The advantage of the later approach is that it does not require chemical modification of siRNAs, which maintain the nature structure of RNAs and reduces the purification procedures [93].

Some positively charged amino acid such as arginine, lysine and histidine are often included in the peptide sequence for this purpose.

MPG, which is derived from the fusion peptide domain of HIV-1 gp41 protein and the nuclear localization sequence (NLS) of SV 40 T antigen, is the first peptide non-covalently complexed with siRNA [94]. Luciferase activity was decreased by 80% after transfection with the complex. The derivatives MPGΔ^{NLS} and MPGα shows enhanced transfection efficiency and increased siRNA binding ability [95]. Further variations in the hydrophobic part of MPG led to pep-family [96,97]. In addition, more information on the recent discovered CPPs can be found in a variety of reviews [98–103].

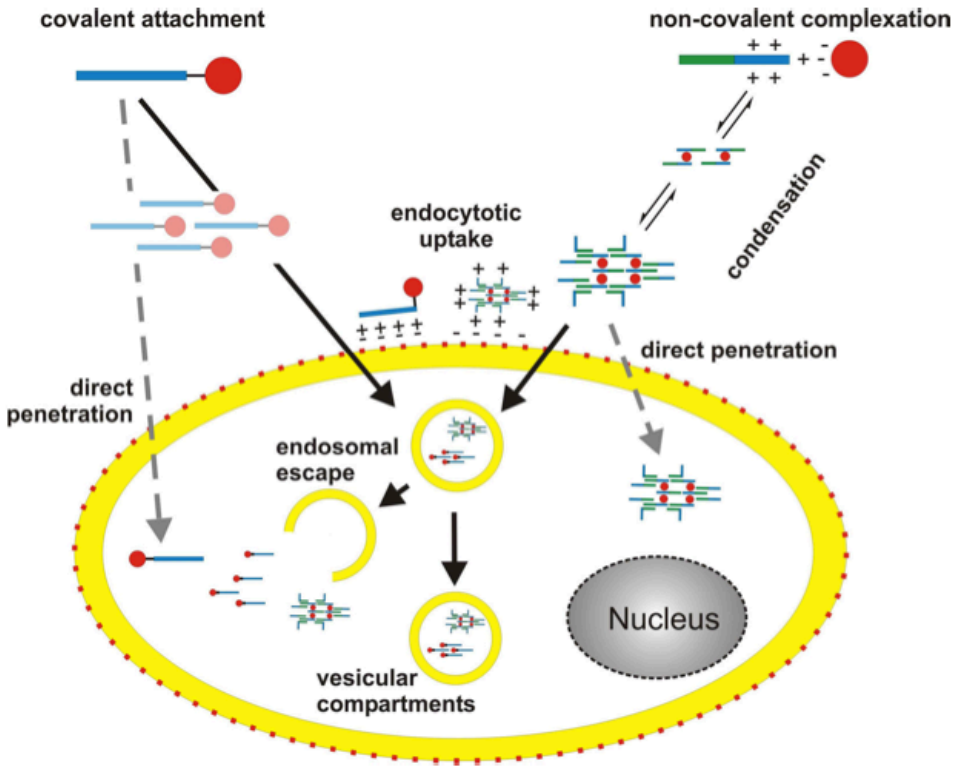

Figure 2.8 Principles of peptide mediated siRNA delivery [104]

2.3 Uptake pathways and subsequent intracellular trafficking of cell-penetrating peptides as siRNA delivery vector

2.3.1 Internalization mechanism of CPP/siRNA complexes

Despite the intensive study in cell penetrating peptide, the uptake mechanisms are still elusive and remain a major controversy. In general, positively charged CPPs will attach to membrane surface through ionic interactions with negatively charged membrane components, i.e. heparin sulfate proteoglycans [105–107]. Subsequently, the complexes are internalized to cells by directly penetrating or endocytosis, depending on the uptake mechanism. Early study on labeled siRNA with fluorescence microscopy and flow cytometry showed that these peptides seemed to be internalized very rapidly within minutes even at 4°C, suggesting an energy-independent mechanism [108]. The secondary structure of peptides possibly plays an important role in cell membrane penetrating process. The peptides would form secondary structures as α-helix or β-sheet depending on the sequences and solvent. These structures would help the complex to translocate the cell membrane [109,110]. However, some peptides such as oligoarginine can translocate through cell membranes in a random coil, suggesting secondary structure is not the only factor that decides the uptake mechanism [111]. The recent studies that the uptake mechanism of CPPs also can be influenced by the kind of cargo it carries make the situation more complicated. For example, a Tat-GFP fusion protein was involved in caveolae/lipid raft-dependent process [112] while a fusion construct of Tat and Cre recombinase went through a macropinocytotic uptake pathway [113]. In a word, the mechanism of internalization strongly depends on the properties of both CPP and cargo as well as on the cell lines, transfection condition and even complex concentration [114].

CPPs can cross the membrane bilayer directly in a non-endocytic, energy independent manner [115]. This occurs when the peptide are compatible with the membrane or can sufficiently disturb the structural integrity of the membrane. The process will be influenced if there are changes in membrane properties, such as fluidity and membrane potential. MPG and Pep-1 are reported to deliver siRNA into cells efficiently in an endosomal independent pathway [116,117].

Endocytosis is a process by which cells use to internalize solutes and fluids from the extracellular matrix [118]. It comprises of phagocytosis and pinocytosis. Phagocytosis relates to the uptake of large particles and exists in special cell types, where pinocytosis occurs in all cells and can be further divided into four mechanistically different pathways: macropinocytosis, clathrin-mediated endocytosis (CME), caveolae-/lipid-raft mediated endocytosis and clathrin and caveolin-independent endocytosis [119]. Figure 2.9 lists the uptake pathways for CPP/siRNA complexes. Extracellular molecules will be encapsulated in a lipid vesicle after internalization. Whether they can reach RISC in cytosol depends on their ability to escape the endosome before they are delivered back to the cell membrane for recycling or degraded by enzymes in lysosomes. Evidences have shown that the release of CPP-siRNA complex into the cytoplasm is a bottleneck for many peptide-mediated siRNA delivery systems.

To determine which uptake pathway the complex applys, some biological tools are used. These tools are usually various endocytosis pathways inhibitors, which will block the specific uptake of labeled complex. Tracer molecules for labeling endocytic pathway

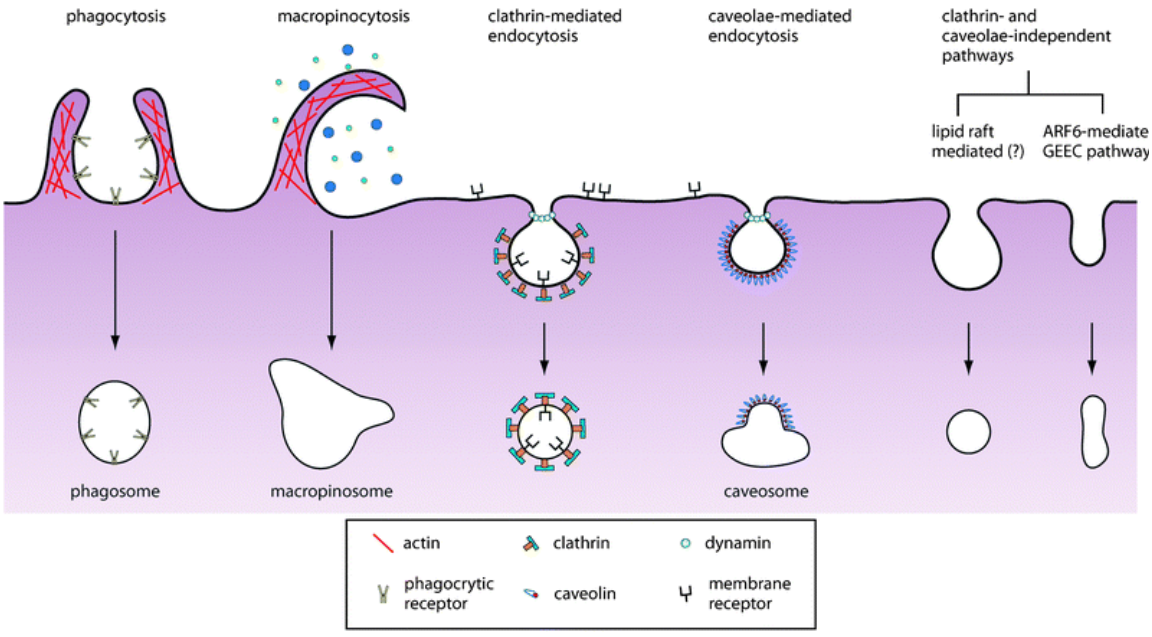

Figure 2.9 Uptake pathways of CPP/siRNA complexes

compartments can be use to investigate uptake mode as well [120]. Based on experimental results, widespread opinions favor endocytosis as major pathway for most CPPs while direct membrane penetration is also regarded as possible for individual CPPs.

2.3.2 Endosomal escape strategy

For now, the most widely used delivery strategy for macromolecules including siRNA is to take advantage of the endocytosis pathway. After internalized via endocytosis, the internalized complexes exist in endosomes with no access to the cytosol. Therefore, endocytosed siRNA will need to escape from the endosome to reach the cytoplasm where the RISC locates. The endosomal entrapment and subsequent enzymatic degradation in lysosome contribute to the low transfection efficiency and is a major impediment for most non-viral carriers. Therefore, a variety of strategies have been used to facilitate

endosome escape, these include the addition of pore formation or fusion in the endosomal membrane, pH-buffering effect (the proton sponge effect), and photosensitizers [121].

Liposomes represent a mature delivery system as mentioned above. The mechanism by which cationic lipids escape from the endosome was proposed by Xu and Szoka [122]. The cationic lipids can interact with negatively charged membrane lipids in early endosome by formation of ion-pair. The electrostatic interaction could further promote the formation of the inverted hexagonal phase [123]. This will lead to the fusion of the liposome with endosome membrane, triggering the release of siRNA into cytoplasm.

For many cell penetrating peptides[124], the most troublesome problem is the entrapment in endosome after uptake, rather than the internalization itself. Thus, these CPPs can be further modified to promote endosomal escape, preventing degradation and allowing the siRNA to reach targets in cytosol. Endosomolytic reagents that are able to disturb endosome membrane can be used in combination with CPPs to enhance the release of complex. Chemical reagent chloroquine is thought to disrupt endosomes by inhibiting the acidification process of the endosome [98]. Some studies have demonstrated that an enhancement of the silencing effect was obtained by adding chloroquine with CPP-siRNA complex [95,113,125]. However, chloroquine is not suitable for *in vivo* therapeutic administration.

As alternatives, some peptides, known as fusogenic or endosomolytic peptides can be utilized to destabilize the endosomal membrane. The majority of viruses such as the influenza and adeno virus have single integral membrane peptides that will induce endosomal disruption or fusion upon acidic pH of endosomes. These peptides will go

through conformational changes in response to acidification of the endosome [126]. HA2 peptide, derived from influenza virus hemagglutinin [127] is the most widely used fusogenic peptide. Protonation of the acidic residues of HA2 when endosome acidification happens results in a sided α-helix with a hydrophobic and a hydrophilic face. The hydrophobic face will strongly interact with the endosomal membrane, thus destabilizing it and cause the cargo molecules released [128]. In a study, the silencing ability of cell-penetrating peptide penetratin fused with HA2 was examined. The results indicated that the fusion of HA2 to penetratin significantly improve the transfection efficiency of penetratin alone [129]. Similarly, the biological activity of another CPP Tat was also enhanced by the fusion of HA2 to it, or by the administration of HA2-Tat protein with Tat at the same time [127]. Covalently linking the fusogenic peptide to the CPP directly increases the endosomolytic property of CPP, in contrast to adding chemical endosomolytic reagent.

Photostimulation strategy can also be applied to release endocytosed molecules in a biologically active form from endosomal vesicles. The photosensitizer reagents used here can be small molecules like $TPPS_{2a}$ and $AlPcS_{2a}$ [130] or fluorescent dye [131,132]. After internalization, the photosensitizers are mainly localized in the endosome with trapped CPP/siRNA complex. The cells or tissues are then exposed to light at a wavelength close to the excitation of the photosensitizers. This photostimulation will trigger the generation of highly reactive singlet oxygen ($^1O_2$), which result in disruption of endosomal membranes and the release of contents into the cytosol [98]. Some experiments have proved that this photostimulation strategy could greatly improve siRNA silencing efficiency [133,134]. This photoinduced endosomal escape strategy has potential use in

therapeutics as a targeting method without inducing extensive cell death and with maintenance of the biological activity of the released cargos.

The “proton sponge ” effect is mediated by agents with high buffering ability and the flexibility to swell when protonated. In this approach, proton absorbance by buffering agents prevents acidification of endosomes, thereby increasing the ATPase-mediated influx of protons, as well as counter ions, which enter endosomes to balance the proton flux. Increased ion concentrations inside endosomes will lead to osmotic swelling, endosomal membrane rupture and eventually leakage of the contents into cytosol [135]. Figure 2.10 demonstrates the endosomal escape process via “proton sponge” effect [136].

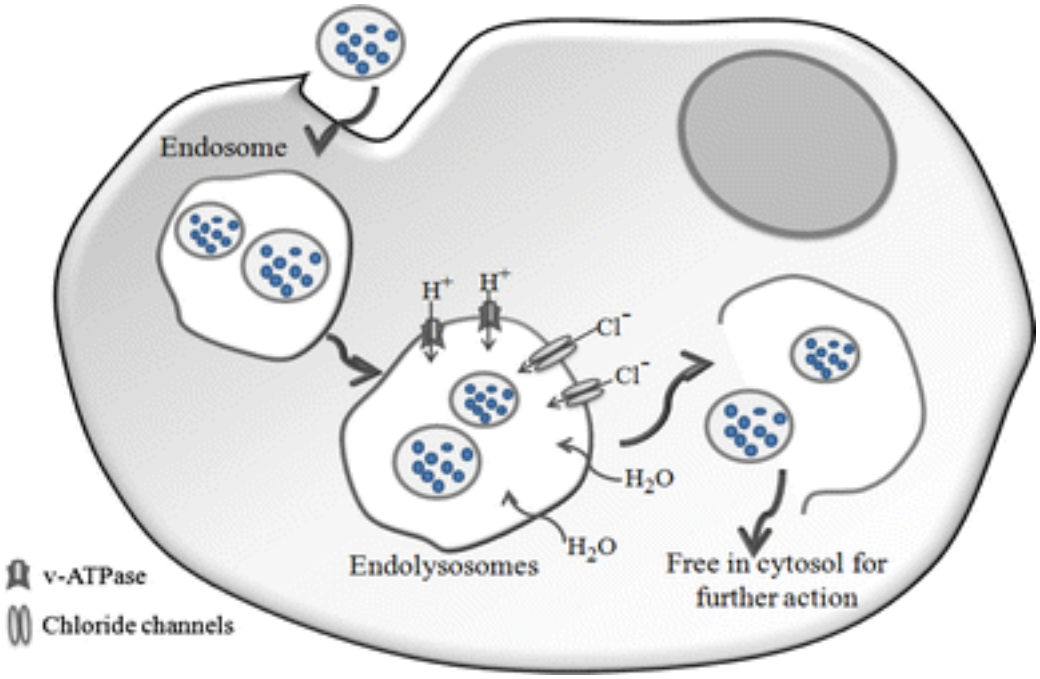

Figure 2.10 Endosomal escape process via “proton sponge” effect

With the aim to increase the endosomal escape of siRNAs after peptide-mediated delivery, we can rationally include some agents with buffering effect when we design the cell-penetrating peptide, such as histidine residues. The imidazole group of histidine has a pK_a of around six and can absorb protons in the acidic environment (pH5-6.5) of the endosome, leading to osmotic swelling, membrane disruption and eventually cargos escape [137]. Lundberg has reported a new peptide EB1 derived from penetratin by replacing two basic amino acids with histidines and the N-terminal addition of six amino acids [129]. This peptide will undergo a pH-dependent conformational change to a higher degree of helicity. The followed transfection experiment demonstrated that this modified peptide had better silencing effect than penetratin. Other examples of histidine containing peptide improving the transfection efficiency of peptide are also reported in literatures [138,139].

Chapter 3

A New Amphipathic Peptide as siRNA Delivery Carrier: Physicochemical Characterization and Cellular Uptake*

3.1 Introduction

The recent discovery of RNA interference (RNAi) is considered to be the most important and exciting discovery of the past multiple decades [140]. RNAi is a natural regulatory process where small, double-stranded RNA molecules (typically 21-25 nucleotides) turn off specific genes in a biological cell [4]. Because RNAi is highly specific and efficient, it has become a widely used tool to dissect signaling pathways, discover important genes to embryonic development, and elucidate the function of novel genes in various fundamental biological processes—functional genomics [1,141]. However, the real payoff of RNAi lies in new therapies—short interfering RNAs (siRNAs)—which could yield more efficient drugs to fight cancer, HIV, influenza, and other diseases where conventional therapies fail. Rather than blocking the effects of specific proteins, which is what most conventional drugs do, an RNAi-based therapy could, in theory, stop the proteins from being made in the first place.

---

* This chapter is based on a paper M. Jafari, W. Xu, S. Naahidi, B. Chen, P. Chen, A new amphipathic, amino-acid-pairing (AAP) peptide as siRNA delivery carrier: physicochemical characterization and in *vitro* uptake, J. Phys. Chem. B. 116 (2012) 13183–13191. M. Jafari and W. Xu contribute equally to this paper.

However, despite abundant promise, the translation of RNAi to realistic therapeutics has faced serious obstacles. The large size and polyanionic nature of free siRNAs prevent them from translocating across the negatively charged cell membrane. Moreover, without protection, siRNAs are subject to enzymatic degradation under physiological conditions. These highlight the importance of developing an efficient siRNA delivery system. In light of the safety concerns and efficacy issues with current drug delivery systems, cell-penetrating peptides (CPPs), net positively charged peptides with fewer than 30 amino acids, have been widely applied to deliver cargos into cells. We have been studying a class of peptides, the self-assembling/co-assembling peptides, which can be used as drug or gene delivery vehicles [34]. These peptides have been successfully used to encapsulate a model anticancer drug and deliver it across the cell membrane in a controlled manner [142]. Encouraged by these results, we generated libraries of peptides that have potential to deliver siRNAs into cells. After high throughput screening from the first library of designed peptide [143], we have discovered a promising peptide C6 that is able to form stable non-covalent complexes with siRNA and deliver into cells efficiently. Considering the amphiphilic nature of the cell membrane, most CPPs possess both hydrophilic and hydrophobic moieties. C6 is amphiphilic, as the hydrophilic side interacts with the hydrophilic drugs/gene through electrostatic interaction, whereas the hydrophobic side is anchored in the hydrophobic core of the bilayer, triggering the endocytosis pathways or assisting the direct translocation of peptide-cargo to the cytosol. The amphiphilicity of the peptides may evolve from their primary structure, for example, MPG [144], or secondary structure, for example, penetratin, where the peptide needs to adapt a helical

structure to organize hydrophilic and hydrophobic moieties at different sides of the peptide.

Three types of amino acids were incorporated in the design of C6 peptide (Ac-RLLRLLLRLWRRLLRLLR-NH2): (1) seven arginine residues were incorporated to interact with siRNA and cell membrane. Positively charged arginine residues can interact with the negatively charged phosphate groups on the siRNA backbone via ionic interactions. These basic residues also interact with negatively charged cell surface proteoglycans to initiate their cellular uptake [145]. CPPs with six to nine arginine residues have been reported to have the highest translocation efficiency [146]. (2) Ten leucine residues were incorporated to induce the amphiphilicity and helicity to the peptide structure. These hydrophobic residues are found abundantly in the helical regions of proteins [147]. They also interact with hydrophobic tails of lipid bilayer and facilitate the translocation of peptide [148]. (3) An aromatic tryptophan residue in the middle of the sequence was incorporated to use as an intrinsic fluorescence probe to study the structural change of peptide upon changing the environment or interaction with siRNA.

Because each turn of a peptide helix includes 3.6 residues, arginine residues were distributed along the peptide sequence in three or four residue intervals, so when a helical structure was formed, they all faced the same side of the helix (Figure 3.1). This induces amphiphilicity to the peptide structure as polar (R) and nonpolar (L, W) residues face opposite sides when peptide adopts a helical structure. The presence of all arginine residues on hydrophilic face of the helix facilitates ionic interaction of positively charged residues with siRNA backbone, maximizing the loading capacity of the peptide.

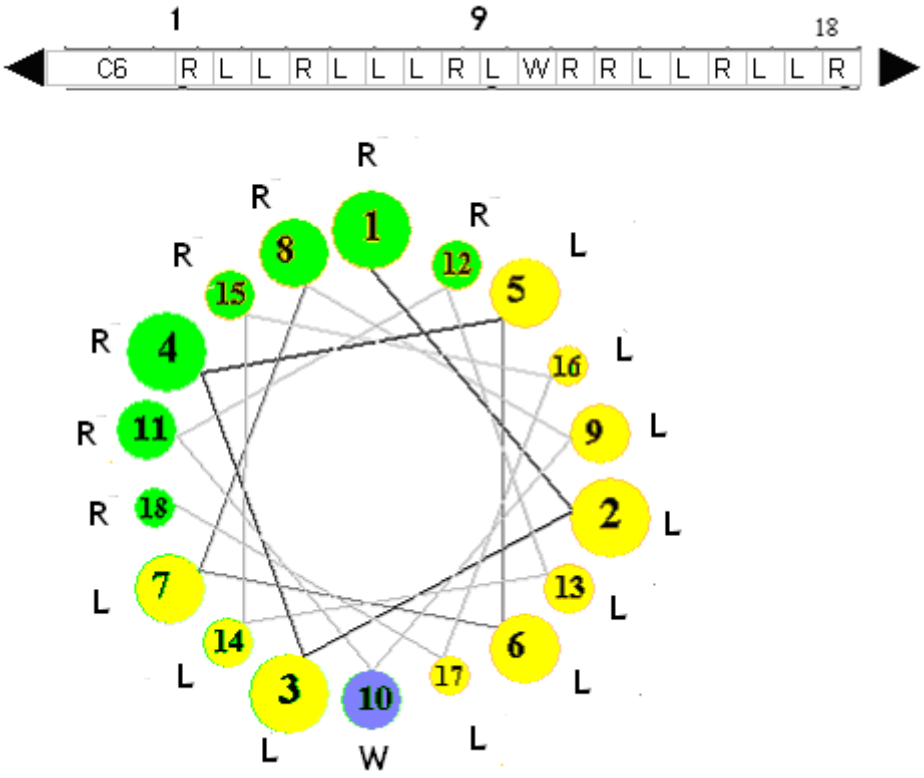

Figure 3.1 Helical wheel projection of peptide C6. A downward cross-sectional view of the α helix axis, orthogonal to the paper plane, is shown. The bigger the circle is, the upper turn the residue is located at, when viewing from the top. R (green), L (yellow), and W (blue) represent arginine, leucine and tryptophan residues, respectively.

The chapter will be focused on physicochemical characterization of C6 and its coassembly/complex with siRNA as well as C6-mediated cellular uptake of siRNA using several biophysical, spectroscopy, and microscopy approaches.

3.2 Materials and Methods

3.2.1 Peptide and siRNA

The C6 peptide (Ac-RLLRLLLRLWRRLLRLLR-NH2, MW 2470.2 g/mol) was purchased from CanPeptide (Montreal, Canada). High performance liquid chromatography (HPLC) analysis indicated that the synthetic peptide was at least 98% pure. Silencer^{TM} GAPDH siRNA (Life Technologies, Carlsbad, USA) was used as siRNA targeting the glyceraldehyde 3-phosphate dehydrogenase (GAPDH) gene. The Silencer^{TM} Cy3-labeled GAPDH siRNA (Life Technologies, Carlsbad, USA) was used in fluorescence microscopy and Fluorescence Activated Cell Sorting (FACS). The siRNA used in agarose gel electrophoresis and fluorescence spectroscopy is eGFP siRNA, which was purchased from Dharmacon with an extinction coefficient of 362408 L/mol cm. The sense sequence is GACGUAAACGG CCACAAG UUC and antisense sequence is ACUUGUGGCCGU UUACGUCGC. The negative control siRNA (Life Technologies, Carlsbad, USA) used in the experiment was siRNA with scrambled sequence.

3.2.2 Cell Culture

CHO-K1 (Chinese hamster ovary) cells were purchased from American Type Culture Collection (ATCC, Manassas, USA). Cells were cultured in F-12K medium (Thermo scientific, Ottawa, Canada) supplemented with 10% fetal bovine serum (FBS) (Sigma, Oakville, Canada). All of the cells were incubated at 37°C in a humidified atmosphere containing 5% CO2.

3.2.3 Preparation of Peptide/siRNA Coassembly/Complex

The C6 peptide was prepared by dissolving peptide powder in RNase-free water. A stock solution of 1 mM was made and diluted at desirable concentrations for various experiments. The solution was vortexed for 10 s and sonicated for 10 min in a tabletop ultrasonic cleaner (Branson, model 2510, Danbury, USA). siRNA was diluted in RNase-free water to a concentration of 50 μM. Peptide/siRNA complexes were formed by adding peptide solution into siRNA in proportion according to the designed experiment. The complexes were incubated for 20 min at room temperature before each experiment.

3.2.4 Atomic Force Microscopy (AFM)

The nanostructures of peptide C6 (40 μM) and C6/siRNA (molar ratio of 40/1) complexes were characterized by AFM. The sample solution (10 μL) was placed on a freshly cleaved mica surface, fixed on a glass slide, and incubated for 30 min at room temperature to allow the sample to adhere onto the mica surface. The mica was then rinsed five times with Milli-Q water to remove any unattached particles, followed by air-drying overnight. The mica surface was analyzed by a PicoScan AFM (Molecular Imaging, Phoenix, USA) at room temperature using the tapping mode with silicon single-crystal tips (NCL type, Molecular Imaging, Ann Arbor, USA), with a typical tip radius of 10 nm and resonance frequency of <170 kHz. A scanner with the maximum scan size of 5 μm × 5 μm was used. All AFM images were obtained at a resolution of 512 × 512 pixels on a scale of 2 μm × 2 μm.

3.2.5 Agarose Gel-Shift Assay and Heparin Competition Assay

The ability of C6 to coassemble with siRNA was investigated by agarose gel (1.2 wt %/

vol) shift assay. siRNA was incubated for 30 min at 37 °C in RNase-free water with different concentrations of C6 to obtain peptide/ siRNA molar ratios ranging from 1/1 to 80/1. The samples (10 μL containing 0.3 μg of siRNA per well) and loading dye were loaded to each well, and electrophoresis was carried out at a constant voltage of 55 V for 1.5 h in TBE buffer (4.45 mM Tris−base, 1 mM sodium EDTA, 4.45 mM boric acid, pH 8.3) containing 0.5 μg/mL ethidium bromide.

In the case of heparin competition assay, different amounts of heparin corresponding to final concentrations from 0.5 to 10 μg heparin per 10 μL of complex were added to C6/siRNA complexes at molar ratios of 15/1, 40/1, 60/1, and 80/1. Ten microliters of each sample, corresponding to 50 pmol of siRNA, was then analyzed by electrophoresis on agarose gel (1.2 wt %/vol) stained with ethidium bromide.

3.2.6 Peptide mediated siRNA transfection in cultured cells

CHO-K1 cells were seeded in F-12K medium with 10% FBS without antibacterial agents in a 24 well plate, 24 hrs before transfection. Overlay the cells with 100 ul of preformed complexes after rinse the cells with PBS, incubate for 3–5 minutes, and then 200 μl of Opti-MEM (Life Technologies, Carlsbad, USA) were added. After 4 hours of incubation in 37°C, 300ul of media containing 20% FBS was added to obtain a final FBS concentration of 10%. For siRNA uptake experiment, cells were harvested after 3 hours while for knockdown experiments, cells were collected after 48 hours.

3.2.7 Fluorescence-Activated Cell Sorting (FACS)

The amount of Cy-3 labeled siRNA uptaken by the cells was studied by Flow Cytometry (type BD Biosciences, BD FACSVantage SE Cell Sorter, Franklin Lakes, USA).

Approximately 50000 CHO-K1 cells were seeded in a 24-well cell culture plate 24 h before treatment. Cy3-labeled GAPDH siRNA was complexed with C6 peptide at molar ratios of 15/1, 25/1, and 40/1 and incubated at room temperature for 20 m. Lipofectamine 2000 (Life Technologies, Carlsbad, USA) was complexed with labeled siRNA according to manufacturer's protocol and used as a positive control. The complexes were added to cells with a final siRNA concentration of 50 nM per well and incubated at 37 °C for 3 h in Opti-MEM. The medium was removed by aspiration, and the wells were washed with heparin (10 U/mL, three times total for 1 h at 37 °C). After washing, the cells were detached from the plate by adding trypsin-EDTA and resuspended in fresh 4% paraformaldehyde (PFA) in phosphate-bufferred saline (PBS) and collected in FACS tubes for analysis.

3.2.8 mRNA level measurement

Approximately $4x10^4$ CHO cells were plated in a 24-well cell culture plate. 24 h later, the medium was replaced by Opti-MEM. GAPDH siRNA or scrambled siRNA complexed with C6 at different molar ratios were prepared in Opti-MEM medium and added to the cells. Three hours later, growth medium with 20% FBS was added, followed by 48 h incubation at 37 °C in a 5% CO_2 atmosphere. The cultures were then washed with PBS. Total RNA was extracted from the cells with TRIzol reagent (Life Technology, Carlsbad, USA), then treated with chloroform (Sigma, Oakville, Canada) and 2-propanol (Sigma, Oakville, Canada) as recommended by the manufacturer. RNA concentrations were measured by Nanodrop spectrophotometer ND-1000 (Thermo scientific, Ottawa, Canada). All RNAs were reverse transcribed with Bio-Rad iScript cDNA synthesis kit. The cDNA synthesis was primed with a unique blend of oligo (dT) and random primers.

The following pairs of primers were used for PCR: 5′-TTGCTGTTGAAGT-CGCAGGAG-3′, 5′-TGTGTCCGTCGTGGATCTGA-3′ (Sigma, Oakville, Canada). Here, the housekeeping gene cyclophilin was chosen as an internal control to normalize the GAPDH gene. The normalization was performed by the amplification of mouse/rat cyclophilin mRNA with the following primers: 5′-AGGGTTTCTCCACTTCGATCT-TGC-3′ and 5’-AGATGGCACAGGAGGAAAGAGCAT-3′ (Sigma, Oakville, Canada). PCR reaction was performed with Brilliant II Fast SYBR Green QPCR Master Mix (Agilent Technologies, Wilmington, USA) on an Mx3005P™ Real-Time PCR System (Agilent Technologies, Wilmington, USA).

3.3 Results and Discussion

3.3.1 Morphology of C6/siRNA complex

The particle size and charge significantly affect its circulation in the bloodstream, biodistribution, and uptake by the cells. The particle size ranging from 100 to 500 nm would be ideal for passive targeting to solid tumors through the enhanced permeability and retention (EPR) effect [149]. Therefore, engineering the nanoparticle to obtain appropriate physical properties could significantly enhance its therapeutic effect. The particle size and zeta potential of C6/siRNA complex were first studied by dynamic light scattering and zeta potential. As reported [150], the majority of C6/siRNA coassemblies at molar ratios of 10/1 to 20/1 had an average size of ~50 nm. However some larger particles (~200 nm) were also observed. The size of complexes was increased by adding more peptides, because the extra peptides added layers to the initially formed peptide/RNA cores. This finding was in agreement with AFM images (Figure 3.2b),

which show high population of small nanoparticles (~50 nm) as well as the presence of larger complexes (~100−200 nm). At molar ratio of 40/1, the complex became more uniform as the intensity and number-based DLS results showed the average size between 150 and 250 nm. The peptide only sample formed globular structures with an average diameter of ~45 nm, eventually organized to form a network of strings of nanospheres, shown in Figure 3.2b. The formation of these globular structures was derived by hydrophobic attraction between leucine residues, distributed along the peptide sequence.

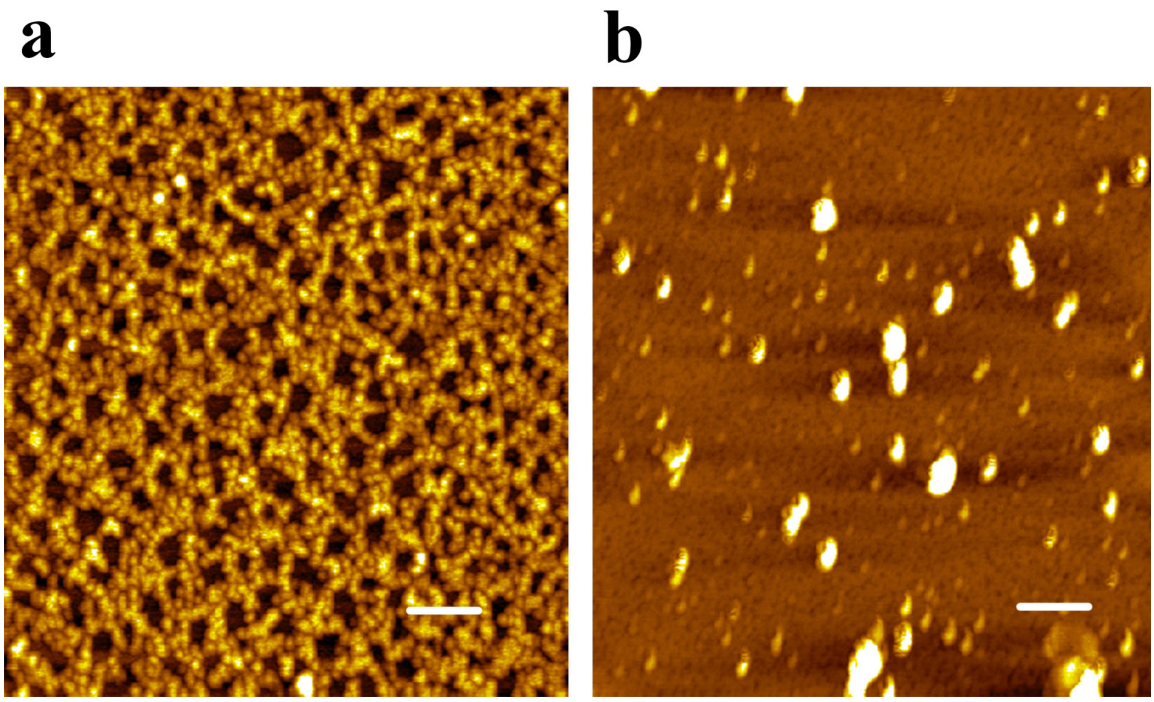

Figure 3.2 AFM images of (a) C6 peptide aggregates/assemblies (40 μM) and (b) C6/siRNA complex (MR = 40/1). The sample solution (10 μL) was placed on the mica surface and incubated for 30 min at room temperature. The mica was then rinsed five times with Milli-Q water, followed by air-drying overnight. The scan size of the images is 2 × 2 μm^2. The scale bar denotes 200 nm.

Because there was not such a template for nanoparticles in solution in DLS experiment to form the network, they aggregated, instead, as larger particles to minimize the interaction of hydrophobic residues and water molecules. This self-assembly/aggregation process is thermodynamically favored by minimizing Gibbs free energy through limiting the exposure of hydrophobic residues to the aqueous environment and having mostly charged arginine residues on the surface of globules.

The surface charge of C6/siRNA complex at molar ratio of 10/1 was slightly negative, which implies that siRNA molecules were not fully saturated by peptides. Considering seven positively charged arginine groups of the peptide C6 and 21 pairs of negatively charged nucleotides in a siRNA molecule, it was theoretically expected to neutralize the negative charge of siRNA at molar ratio of 6/1; however, at a higher molar ratio, that is, 15/1, the zeta potential of the complex jumped to +30 mV, indicating that peptides fully covered the surface of the complex. With the increasing concentration of peptide at the same siRNA concentration, the positive value of the surface charge of the complexes increased from +30 (MR = 15/1) to +60 mV (MR = 40/1) due to the increase in the number of positively charged arginine residues. The net positive charge of the particles is crucial because it inhibits particle aggregation and enhances electrostatic interaction with the negatively charged phospholipids of the cell membrane upon siRNA delivery.

The helical structure of C6 was also confirmed by CD spectroscopy. C6 in water showed a small content of a random coil conformation with a minimum at 203 nm. By adding a small amount of siRNA (MR of 40/1), a clear shift in the spectrum minimum from 203 to 208 along with a maximum around 190 nm was observed, which represents a

typical helical conformation. The absolute values of the minima at 208 and 222 nm and the maximum at 190 nm were increased by adding more siRNAs to MR of 10/1, which indicates the increase in helical content in secondary structure of the peptide at a higher concentration of siRNA. Adding further siRNA beyond the MR of 10/1 did not significantly change the secondary structure of the peptide. Considering the nature of C6 and siRNA interaction, that is, ionic interaction, the charge neutralization of seven arginine residues in the peptide sequence may decrease the repulsion between them, which eventually facilitated the peptide adoption to a helical conformation.

3.3.2 Agarose gel-shift assay and heparin competition assay

Agarose gel shift assay was used to detect the interaction between siRNA and peptide molecules and the stability of the formed complex in the presence of heparin. Peptide can interact with siRNA through noncovalent interactions such as Coulombic forces and hydrogen bonding. In particular, basic amino acids such as lysine, arginine, or histidine can interact with the negatively charged phosphate groups on the siRNA sugar rings through electrostatic interactions. Free siRNA molecules could move toward the positive electrode when the voltage is applied, whereas the inability of peptide/siRNA complexes to enter the agarose gel suggests the formation of stable complex with no free siRNAs to be shown in siRNA bands. As shown in Figure 3.3a, the effective formation of the C6/siRNA complex started at molar ratio of as low as 5/1 because the band was less bright than that of siRNA only. At the molar ratio of 10/1, siRNA molecules were almost completely associated with peptide C6 because a very small amount of free siRNA was observed on siRNA band. This band completely disappeared at the molar ratio of 15/1.

This finding suggests that excess peptide molecules are needed to obtain stable peptide/RNA complexes, as six molecules of peptides are theoretically required to neutralize electrostatically one molecule of siRNA. Further experiments showed that the excess peptide molecules could provide a shield to protect siRNA molecules against degradation and also interact with cell membrane to initiate the peptide/siRNA cellular uptake.

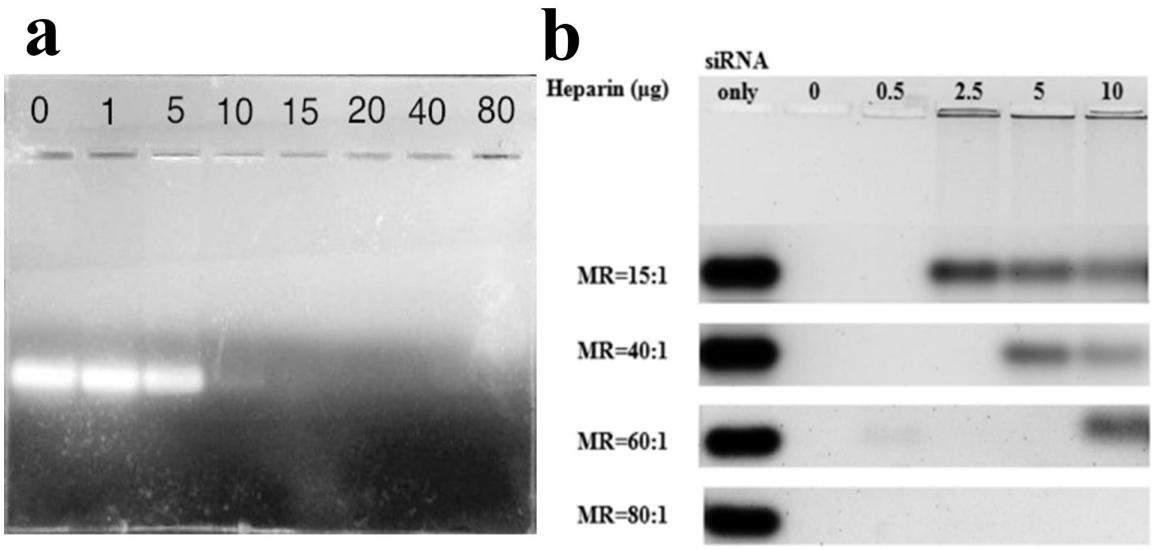

Figure 3.3 (a) Formation of C6/siRNA complexes at different molar ratios, indicated by agarose gel. siRNA was incubated with different concentrations of C6 corresponding to a molar ratio ranging from 1/1 to 80/1. Lane 1 refers to siRNA control in the absence of C6, and lanes 2−8 refer to different molar ratios. (b) Stability of C6/siRNA complex indicated by heparin competition assay. Different amounts of heparin corresponding to final concentrations of 0.5 to 10 μg heparin per 10 μL of complex were added to C6/siRNA complexes at different molar ratios. The stability of complexes was analyzed by electrophoresis on agarose gel (1.2 wt %/vol) stained with ethidium bromide. For better comparison, the siRNA bands of four independent gels were put in the same image.

The stability of C6/siRNA complexes at different molar ratios in the presence of heparin was also analyzed by gel electrophoresis. As shown in Figure 3.3b, C6/siRNA complexes were stable in the absence of heparin (second well from left), and no free siRNA was shown in siRNA bands at all MRs. The complex at MR of 15/1 was stable at very low concentration of heparin, that is, 0.5 μg per 10 μL of sample, but dissociated at higher heparin concentration. The minimum concentration of heparin required for dissociation of the complex increased by increasing the MR up to 60/1. However, the complex at the molar ratio of 80/1 was completely stable even at high heparin concentration (10 μg in 10 μL of loaded sample).

3.3.3 Subcellular distribution of C6/Cy-3 siRNA

To study the cellular uptake, distribution, and localization of siRNA complexed with C6, we transfected CHO cells with Cy3-labeled siRNA alone or in complex with C6 or lipofectamine 2000. CHO cells were incubated with or without complexes for 3 h and observed under a fluorescence microscope (Figure 3.4).

As expected, Cy-3 siRNA alone was not able to enter the cells by itself due to the negative charge and lack of an appropriate delivery vector (Figure 3.4b). siRNA internalization happened within 3 h of incubation at the presence of transfection reagent, Lipofectamine 2000, as shown as small red dots in the cytosol of most of the cells (Figure 3.4d). In the cells treated with C6/siRNA complexes (Figure 3.4e, f), siRNA was localized to regions in close proximity to the nuclear membrane. siRNAs delivered by C6

showed a punctual nonhomogeneous distribution pattern around the periphery of the nucleus inside the cell, which indicated the possibility of endocytosis pathways [95].

C6/siRNA complexes at high molar ratios 40/1 may form high-molecular-weight complexes or aggregate, as previously documented for other CPPs. These large complexes may be internalized through the macropinocytosis pathway, which can include all pinosomes larger than 200 nm. However the uptake of large aggregates by fluid phase endocytosis may not result in the effective release of siRNA into the cytoplasm and eventually significant gene knockdown. Thus, precautions should be taken into account when increasing the molar ratio because the large aggregates might have problems dissociating and releasing siRNA in the cells, eventually decreasing the knockdown efficiency of the complex.

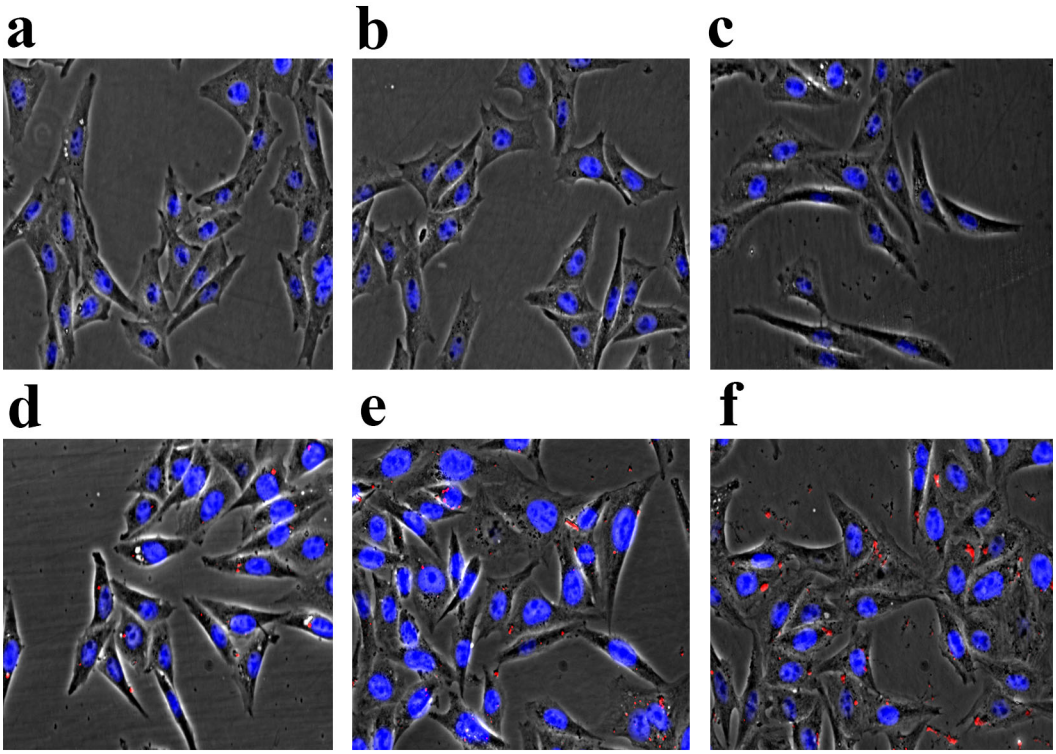

Figure 3.4 Subcellular distribution pattern of Cy3-labeled siRNA 3 h post-treatment. Cy3-labeled GAPDH siRNA (red) was transfected to CHO-K1 cells with positive control reagent and different molar ratio of C6 at a siRNA concentration of 50 nM. Cells were analyzed by fluorescence microscopy 3 h after transfection (magnification, 40×). Nuclei were stained with DAPI (blue). (a) Nontreated cells and (b) cells treated with 50 nM siRNA only, (c) with C6 peptide only, (d) with Lipofectamine 2000 as positive control, and (e) with siRNA complexed with C6 at molar ratio of 15/1 and (f) molar ratio of 40/1.

3.3.4 Cellular uptake of peptide/siRNA complex

The efficiency of C6 to deliver siRNA into CHO-K1 cells was evaluated using FACS. As shown in Figure 3.5, cellular uptake efficiency of siRNA was correlated to the molar ratio of C6/siRNA. Even though a 15/1 molar ratio was sufficient to deliver an even higher amount of siRNA into cells compared with Lipofectamine 2000, the intracellular fluorescence intensity increased with increasing molar ratio (MR 25/1 and MR 40/1).

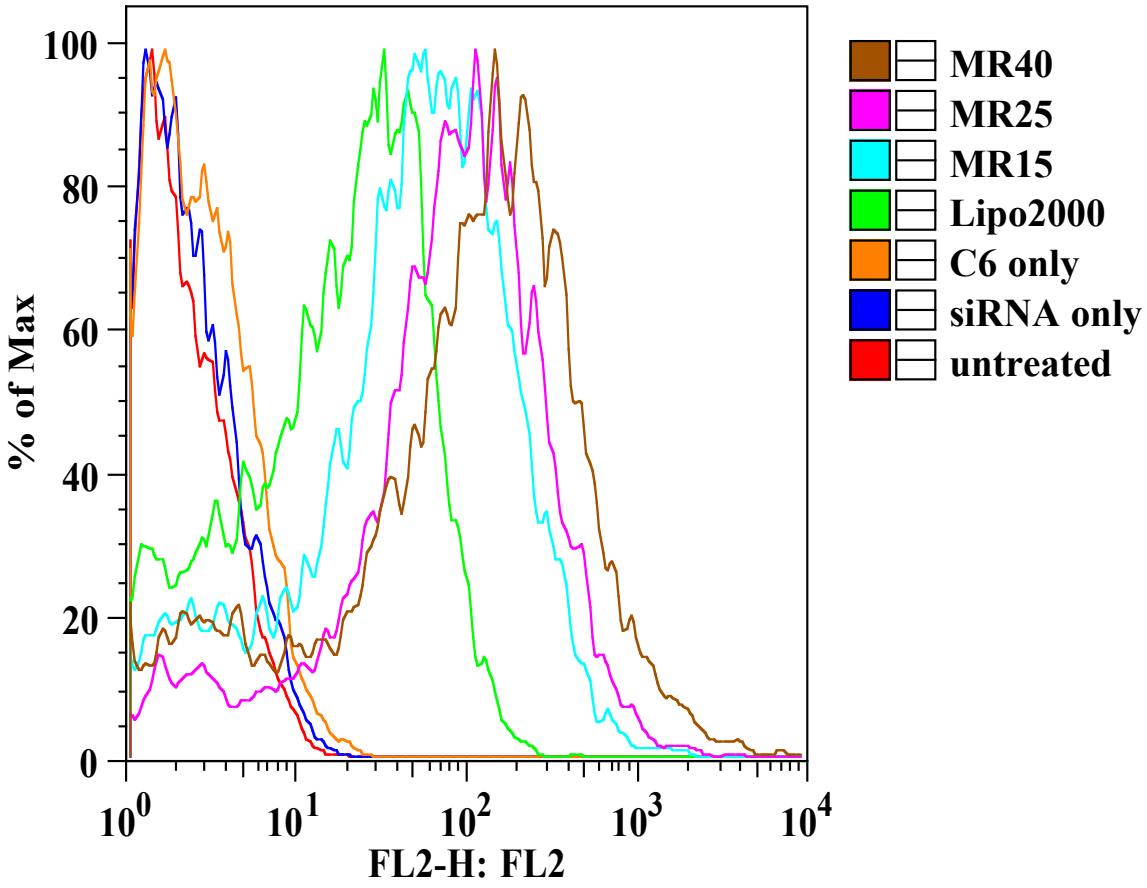

Figure 3.5 Flow cytometry results for Cy3-labeled siRNA delivered by Lipofectamine 2000 and C6 at different molar ratios (MRs).

3.3.5 Gene silencing efficiency of C6/siRNA complexes

As GAPDH siRNA can be effectively delivered to CHO-K1 cells, next we want to see whether this delivered siRNA is able to perform RNAi and decrease the expression level of GAPDH mRNA. As shown in Figure 3.6, the positive control Lipo2000/siRNA complex demonstrates around 80% knockdown efficiency of GAPDH mRNA.

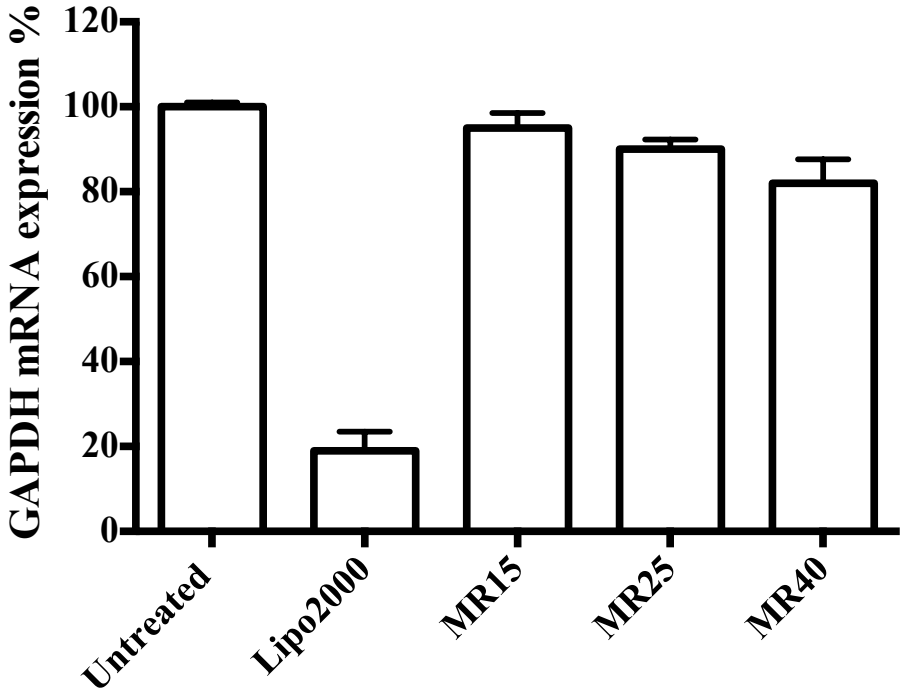

Figure 3.6 Gene silencing efficiency of C6/siRNA complex on CHO-K1 cells. Relative GAPDH mRNA level in CHO-K1 cells after transfected with C6/GAPDH siRNA complexes was measured by qRT-PCR method. All the data were normalized to another house keeping gene cyclophilin and compared to scrambled siRNA control. The results correspond to an average of at least three separate experiments.

We expected that C6/siRNA complex would show similar transfection efficiency as Lipo2000, since the internalization efficiency is similar. However, C6/siRNA complexes only showed 20% knockdown efficiency at most with MR 40/1. This great discrepancy was very likely caused by the entrapment of C6/siRNA complexes in the endosomes after internalization. In order to increase the silencing efficiency of peptide/siRNA complexes, we should improve the endosomolytic ability of peptide C6 itself.

3.4 Conclusions

C6, an amphipathic peptide, was introduced as a safe and efficient carrier for siRNA delivery *in vitro*. The noncovalent interaction/coassembly between C6 and siRNA and the physicochemical properties of the resulting coassemblies were studied. C6 alone showed a random coil secondary structure in water but adopted a helical conformation upon binding to siRNA. The gel electrophoresis and AFM results confirmed stable C6/siRNA complex formation in the molar ratios from 10/1 to 40/1. The flow cytometry data and fluorescence microscopy images also indicated the high cellular uptake and cytoplasmic localization of siRNA delivered by C6. However, in contrast to the high uptake efficiency, the silencing efficiency of C6/siRNA is very low at various molar ratios, probably due to endosome entrapment of this complex after being internalized into cells through endocytosis pathway. Thus, in the following experiments, we try to improve the silencing efficiency of C6/siRNA complex by modifying C6 sequence with the addition of endosomolytic moiety.

Chapter 4

In vitro and *in vivo* therapeutic siRNA delivery induced by a tryptophan-rich endosomolytic peptide

---

4.1 Introduction

RNA interference (RNAi) is considered one of the most important and exciting discoveries in biology of the past decade [151]. Only over ten years following its discovery, RNAi has already become a widely used tool in biology and medicine, and is poised to catalyze development of the next major class of pharmaceutical drugs. Rather than blocking the effects of faulty proteins, which is what most conventional drugs do, an RNAi-based therapy would, in theory, stop the proteins from being made in the first place. Despite abundant promise, several sizable challenges remain in the way of siRNA-based therapeutics. The most important concern is the effective delivery of siRNA to its site of action in the cytoplasm. Some unfavorable physicochemical properties impede the uptake of siRNA into the cells, particularly following systemic administration [25], including: a relatively large molecular weight, negatively charged surface, hydrophilicity, sensitivity to nuclease degradation, and instability (plasma half-life of less than ten minutes) [24]. The application of therapeutic siRNA for the targeted silencing of specific genes to most tissues and organs requires clinically suitable, efficient and safe delivery systems.

Although demonstrated to have high transfection efficiency *in vitro*, the application of some lipids (e.g., Lipofectamine 2000) and polymers (e.g., PEI) [21] as siRNA vectors *in vivo* is limited due in large part to high toxicity [73] and a tendency to induce the immune response [32,33]. Among non-viral delivery systems, cell-penetrating peptides (CPPs) are emerging as one of the most promising to facilitate cellular uptake of various biomolecules, including siRNA. By comparison, CPPs mediated internalization is highly efficient and often harmless to the cell in therapeutic dosages, avoiding severe cell membrane destabilization [152]. Most well characterized cell penetrating peptides to date are derived from known transduction domains of proteins that interact with cell membranes, e.g., TAT(-YGRKKRRQRRR-) from HIV-1 TAT protein [153], penetratin from the homeodomain of the Antennapedia protein of Drosophila [154], and CADY from fusion peptide JTS1 [155]. These peptides usually consist of 30 or less amino acids and share some common characteristics, such as amphipathicity and a positive charge at physiological pH.

In previous chapter, we have reported a new cell penetrating peptide C6 (RLLRLLLRLWR RLLRLLR) that can form stable complexes with siRNA and deliver them into cells in a highly efficient manner [156]. However, the knockdown efficiency of the complex is low, probably due to the poor endosome escape ability. siRNA that remains entrapped within endosomes cannot display biological activity, as it can not reach cytoplasm where RNAi happens. In order to optimize delivery, we modified the C6 sequence by replacing some amino acids to increase its endosomolytic property. Among derivatives, C6M1 is one of the peptides showing potent therapeutic siRNA delivery ability. This new peptide, C6M1 (Ac-RLWRLLWRLWRRLWRLLR-NH_2) maintains the

seven arginine residues in C6, in accordance with reports that peptides with six to nine arginine residues have the highest translocation efficiencies [146]. These positively charged arginine residues can interact with the negatively charged phosphate groups on the siRNA sugar rings through electrostatic interaction and increase the affinity of the complex with negatively charged head groups of plasma membrane [157]. Some of the leucine residues were kept from C6, as leucine is the strongest structure forming residue found abundantly in the helical regions of proteins [158]. Hydrophobic residue leucine, as well as other hydrophobic residues, may facilitate the translocation of the peptide by interacting with the hydrophobic tails in the lipid bilayer [148]. To improve endosomal escape, we use aromatic tryptophan to substitute some leucine residues in the sequence, since tryptophan rich motif is found abundantly in the pore-forming toxins of bacteria [159,160]. Meanwhile, tryptophan is able to interact with lipids/cholesterols within the cell membrane and have therefore been shown to play an essential role in the cellular uptake of many cell-penetrating peptides [109,154]. We arrange the amino acid residues in alternating order in the sequence that if the peptide adopts α-helical structure, it has an amphiphilic helical structure with one side of the helix contains mainly hydrophilic amino acid residues, while the other side contains mainly hydrophobic ones. This amphiphilic helical structure is widely found in antimicrobial peptides [161,162], which have high affinity for cell membrane. Viewed from the top, C6M1 displayed an α-helical secondary structure with three distinct sections, see Figure 4.1a. When folded, the ordered segregation of polar (R) and nonpolar (L, W) amino acids on different sides of the helix constitutes a secondary amphiphilic structure.

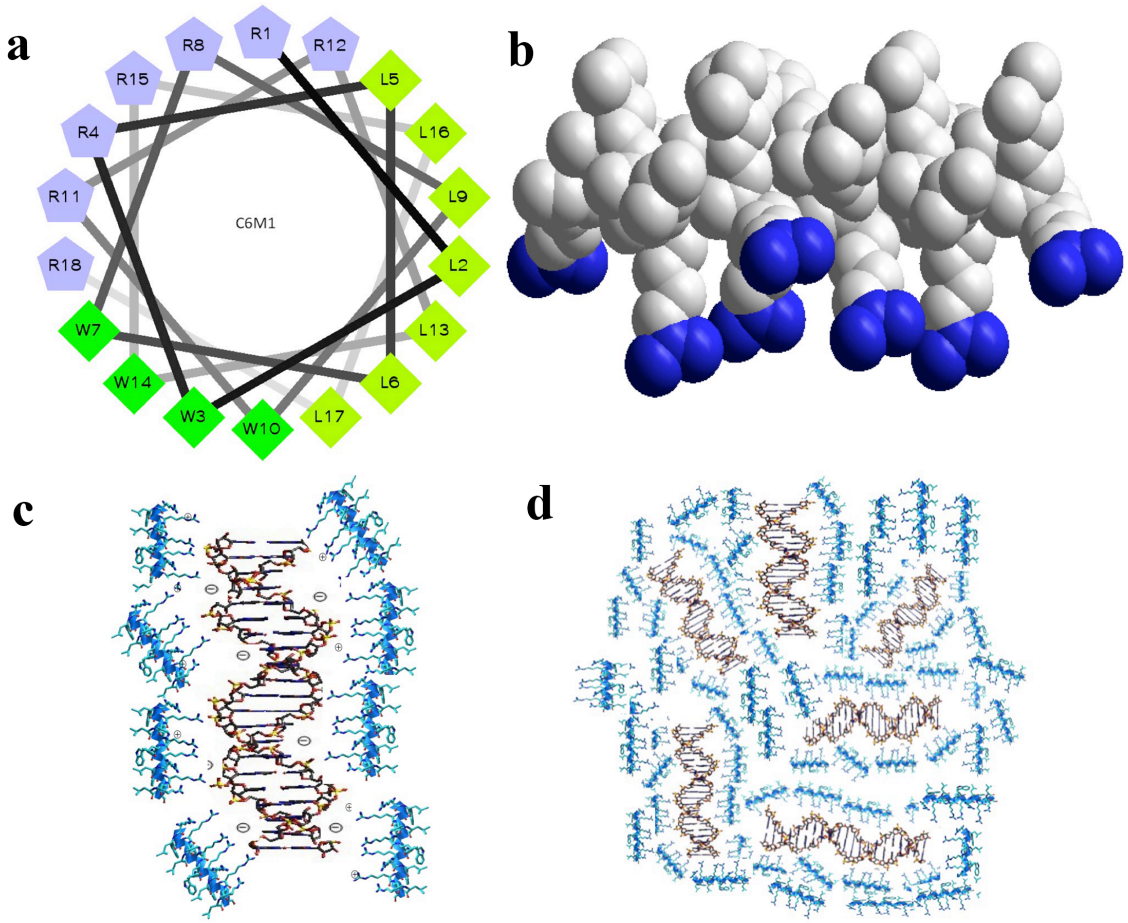

Figure 4.1 Predicted helical structure of peptide C6M1. (a) Helical wheel projection of C6M1 peptide. R represents arginine, L represents leucine, W represents tryptophan. (b) 3D molecular structure of C6M1. Positively charged functional groups are denoted in blue. (c) Formulation strategy for siRNA and C6M1 molecules. Double helix represents siRNA. (d) The final nanocomplex of siRNA and peptides. The figures b-d were generated using Hyperchem (Hypercube, Inc.)

The hydrogen bonding between C=O and N-H groups in the backbone of the peptide is involved in the formation of the helical structure. Also, the role of electrostatic, π-π stacking, hydrogen bonding, and hydrophobic interactions between side chains in stabilizing the helices has also been reported [163,164]. The unique arrangement of amino acids in C6M1 helical structure facilitates hydrophobic interaction between leucine residues, π-π stacking between tryptophan residues, and hydrogen bonding between arginine residues, which eventually stabilize the helical conformation of the peptide. By concentrating the positive charge on one side of the helix (see Figure 4.1b), the loading capacity of the peptide may be maximized, enabling it to more easily neutralize siRNA molecules, which may subsequently reduce the dose required for effective delivery, Figure 4.1c. Theoretically, around 10 molecules (7 being minimum) of the peptide are needed to neutralize one siRNA molecule in the formation of peptide-siRNA complexes. These monomers will then further aggregate to form nanocomplex that can be internalized by cells, see Figure 4.1d.

Here, we characterized this peptide-siRNA complex/nanocomplex and determined the optimal transfection condition. The amount of the complexes taken up by cells was determined by flow cytometry. Quantitative RT-PCR was applied to measure the mRNA level of cells treated with C6 and C6M1. Our results show that the substitution of tryptophan for leucine in C6 sequence significantly increases transfection efficiency. In addition, the complex could significantly inhibit tumor growth in a xenograft mouse tumor model without causing toxicity effect, suggesting potential therapeutic application.

4.2 Materials and Methods

4.2.1 Materials

Peptide and siRNA: The C6 and C6M1 peptides were synthesized in bulk by CanPeptide Inc (Montreal, Canada). High performance liquid chromatography (HPLC) analysis indicated that the synthetic peptide was at least 95% pure. Silencer^{TM} GAPDH siRNA (Life Technologies, Carlsbad, USA) was used as siRNA targeting the glyceraldehyde 3-phosphate dehydrogenase (GAPDH) gene. The Silencer^{TM} Cy3-labeled GAPDH siRNA (Life Technologies, Carlsbad, USA) was used in fluorescence microscopy and Fluorescence Activated Cell Sorting (FACS). For experiments involving A549 cells, siRNA targeting Bcl-2 oncogene (Sigma, Oakville, Canada) was used, with a sense sequence of GUGAAGUCAACAUGCCUGCdTdT and antisense sequence of GCAGGCAUGUUGACUUCACdTdT. The negative control siRNA (Life Technologies, Carlsbad, USA) used in the experiment was siRNA with scrambled sequence.

4.2.2 Cell culture

CHO-K1 (Chinese hamster ovary) cells were purchased from American Type Culture Collection (ATCC, Manassas, USA). Cells were cultured in F-12K medium (Thermo scientific, Ottawa, Canada) supplemented with 10% fetal bovine serum (FBS) (Sigma, Oakville, Canada). The non-small lung carcinoma A549 cells were obtained from American Type Culture Collection (ATCC, Manassas, USA), and cultured in Dulbecco's Modified Eagle Media-high glucose (Life Technologies, Carlsbad, USA) with 10% heat-inactivated FBS. All of the cells were incubated at 37°C in a humidified atmosphere containing 5% CO_2.

4.2.3 Preparation of peptide/siRNA complex

The peptides were prepared by dissolving peptide powders in RNase free water. The solution was vortexed for 5 sec and sonicated for 10 min in a tabletop ultrasonic cleaner (Branson, model 2510, USA). siRNA was diluted with RNase free water. Peptide/siRNA complexes were formed by adding peptide solution into siRNA in proportion according to the designed experiment. The complexes were incubated for 20 min at room temperature before characterization and transfection.

4.2.4 Agarose gel-shift assay

siRNA was incubated for 30 min at 37°C in RNase free water with different concentrations of C6M1 corresponding to a peptide/siRNA molar ratio ranging between 1/1 and 80/1. Each well contains 300 ng of siRNA. The preformed complexes were then analyzed by electrophoresis in agarose gel (1.2% wt/vol) stained with ethidium bromide.

4.2.5 Particle size and zeta potential

The hydrodynamic diameter of C6M1/siRNA complexes were measured on a Zetasizer Nano ZS (Malvern Instruments, Malvern, UK) equipped with a 4 mW He-Ne laser operating at 633 nm. Samples at molar ratios of 40/1 with final siRNA concentrations of 100 nM were prepared as mentioned above. A quartz microcell (45 μL) with a 3 mm light path was used and the scattered light intensities were collected at an angle of 173°. Zeta potential measurements were also performed on the same machine using clear disposable zeta cells. Three measurements were performed to generate the intensity-based size and zeta potential plot reported herein.

4.2.6 Circular Dichroism (CD*)*

Spectra from 190 to 250 nm with spectral resolution and pitch of 1 nm and scan speed of 200 nm/min were recorded by a J-810 spectropolarimeter (Jasco Europe, Cremella, Italy). A 40 μM C6M1 sample was measured in a 1 mm long quartz cell and maintained at 25°C. Spectra reported herein are the averages of three replicates. The raw CD ellipticity (in millidegrees) was converted to residue molar ellipticity ($deg.cm^2.dmol^{-1}.residue^{-1}$).

4.2.7 Transmission electron microscopy (TEM)

An electron micrograph of the C6M1/siRNA complex was acquired using a transmission electron microscope. A 10 ul sample of 300 nM siRNA at a peptide/siRNA ratio of 40/1 was applied to a 400 mesh Formva coated copper grid (Canemco-Marivac, Canton de Gore, Canada) for 3-5 min. The sample was then washed using 5 successive wash steps (RNase free water) and dried overnight. The complex was stained with uranyl acetate (Electron Microscopy Sciences, Hatfield, USA) and analyzed using TEM (Philips CM10 TEM, Amsterdam, the Netherlands).

4.2.8 Confocal and Fluorescence microscopy

Approximately 50,000 CHO cells were plated in a 24-well cell culture plate 24 h before transfection. Cy3-labeled GAPDH siRNA was mixed with C6M1 peptide at a peptide/siRNA molar ratio of 40/1 for 20 min. The complexes were added to cells to reach a final siRNA concentration of 50 nM per well. Treated cells were incubated at 37°C for 3 h with Opti-MEM medium. For endosome labeling, the cells were incubated with 50 nM Lysotracker Green (Life Technology, Carlsbad, USA) for 30 min before

fixing. The wells were then washed with heparin (15 U/ml, a total of three times for one hour at 37°C) and fixed with 500 ul/well of fresh 4% Paraformaldehyde (PFA) in phosphate buffer saline (PBS) at 37°C for 30 min. The fixation agent was aspirated, and the cells were washed twice with PBS before they were covered with Fluoroshield with DAPI mounting medium (Sigma, Oakville, Canada). Carl Zeiss LSM 700 Confocal laser scanning microscopy (Zeiss, Jena, Germany) was used to visualize the cells. The microscope was equipped with Plan-Apochromat 60x/1.4 NA oil immersion objective lens. The images were analyzed with LSM Zen 2009 software. For fluorescence microscope, the samples were visualized on a Zeiss Observer Z1 microscope with a 40x objective lens. Images were analyzed using AxioVision software.

4.2.9 Fluorescence-activated cell sorting (FACS)

Cellular uptake of Cy-3 labeled siRNA was studied using Flow Cytometry (type BD Biosciences, BD FACSVantage SE Cell Sorter, Franklin Lakes, USA). Cells were transfected with peptide/siRNA complexes according to the protocol listed above. Untreated cells and naked siRNA served as a negative control. Lipofectamine 2000, a commercial transfection reagent, was used as a positive control. After 3 h incubation, the culture medium was discarded and cells were washed with PBS, Trypsin-EDTA was then added to detach the cells from the plate; cells were suspended in 4% PFA solution and collected.

4.2.10 mRNA level measurement

Approximately 40,000 CHO cells were plated in a 24-well cell culture plate. 24 h later, the medium was replaced by Opti-MEM. GAPDH siRNA or scrambled siRNA

complexed with C6M1 at different molar ratios were prepared in Opti-MEM medium and added to the cells. Three hours later, growth medium with 20% FBS was added, followed by 48 h incubation at 37 °C in a 5% CO_2 atmosphere. The cultures were then washed with PBS. Total RNA was extracted from the cells with TRIzol reagent (Life Technology, Carlsbad, USA), then treated with chloroform (Sigma, Oakville, Canada) and 2-propanol (Sigma, Oakville, Canada) as recommended by the manufacturer. RNA concentrations were measured by Nanodrop spectrophotometer ND-1000 (Thermo scientific, Ottawa, Canada). All RNAs were reverse transcribed with Bio-Rad iScript cDNA synthesis kit. The cDNA synthesis was primed with a unique blend of oligo (dT) and random primers. The following pairs of primers were used for PCR: 5′-TTGCTGTTGAAGT- CGCAGGAG-3′, 5′-TGTGTCCGTCGTGGATCTGA-3′ (Sigma, Oakville, Canada). Here, the housekeeping gene cyclophilin was chosen as an internal control to normalize the GAPDH gene. The normalization was performed by the amplification of mouse/rat cyclophilin mRNA with the following primers: 5′-AGGGTTTCTCCACTTCGATCTTGC-3′ and 5’-AGATGGCACAGGAGGAAAGAG CAT-3′ (Sigma, Oakville, Canada). PCR reaction was performed with Brilliant II Fast SYBR Green QPCR Master Mix (Agilent Technologies, Wilmington, USA) on an Mx3005P™ Real-Time PCR System (Agilent Technologies, Wilmington, USA). The Bcl-2 mRNA levels in A549 cells were also measured using the method described above. The primers for PCR were: 5′-GGATTGTGGCCTTCTTTGAG-3′ (sense), 5′-CCAAACTGAGCAGAGTCTTC-3′ (antisense).

4.2.11 pH dependent membrane disruption

8,000 CHO-K1 cells were plated on 96-well plates and incubated overnight in 200 μL of F-12K medium containing 10% FBS. The cell culture medium was removed and replaced by Opti-MEM medium with PH 7.4, PH 6.3 and PH 5.2, respectively. Peptides were then added accordingly. After incubation at 37 °C for 3 h, the plates were centrifuged. 50 μL of aliquots in each well were collected for the LDH assay. The LDH activity in these samples was determined using a CytoTox 96 Non-Radioactive Cytotoxicity Assay kit (Promega, Madison, USA) according to the manufacturer's protocol, which determined the LDH activity from the amount of produced red formazan product by a colorimetric assay. The amount of formazan produced was assessed by measuring the absorbance at 490 nm with a FLUOstar OPTIMA microplate reader (BMG Labtech, Ortenberg, Germany). Percentages of the LDH activity in each well were calculated from a raito of the obtained value to the control well containing 10 μL lysis buffer.

4.2.12 Cytotoxicity assay

CHO cells were plated in to 96-well plates (5,000/well) in F-12K medium with 10% FBS in the presence of the C6/siRNA and C6M1/siRNA complexes formed at different molar ratios: 20/1, 40/1, 60/1. After 48 h, MTT dissolved in PBS (5 mg/ml) was added to each well. Cells were incubated with MTT for 4 h, followed by the addition of 100 ul MTT solubilization solution (Sigma, Oakville, Canada). Cell viability was assessed by measuring the absorbance at 570 nm with a FLUOstar OPTIMA microplate reader (BMG Labtech, Ortenberg, Germany) and expressed as the ratio of the cells treated with C6M1/siRNA over the nontreated cells (negative control).

4.2.13 *In vivo* experiment *

Six-week-old male BALB/c nude mice were obtained from the B&K Universal Group Limited (Shanghai, China). The mice were maintained under a 12 h light/dark cycle at 25°C and a humidity of 60 ± 10%. In order to generate the xenograft tumor model, the mice were inoculated subcutaneously with 5×10^6 A549 cells at the right armpit. When the tumor volume reached 100-200 mm^3, Bcl-2 siRNA complexed with C6M1 at molar ratio 60:1 was injected directly into the tumor. Treatment was administered every 3 d for a total of nine treatments at the siRNA dose of 160 μg/kg. Mice were sacrificed on day 27. Tumor diameters were measured every day and the volume was calculated as follows: tumor volume=$0.5\times(\text{width})^2\times\text{length}$. Mouse body weight was also monitored. All the procedures and care administered to the animals have been approved by the institutional ethics committee, under a permit of animal use (Approval ID: (2012) 005) in No.3 People's Hospital affiliated to Shanghai Jiao Tong University School of Medicine, compliance with the Experimental Animal Regulation by the National Science and Technology Commission, China.

4.2.14 Western blot

Proteins were extracted using a total protein extraction kit (Kangchen Biotechnology, Shanghai, China) according to the manufacturer's instructions. The total protein was stored at -20°C until use. The antibodies used included Bcl-2 rabbit polyclonal IgG

---

* The *in vivo* experiments were designed by us and performed in NO.3 people's hospital affiliated to shanghai Jiao Tong University School of Medicine

(Santa Cruz Biotechnology, Dallas, USA), horseradish peroxidase (HRP) conjugated goat anti-rabbit IgG (Kangchen Biotechnology, Shanghai, China) and goat anti-glyceraldehyde-3-phosphate dehydrogenase (GAPDH) (Kangchen Biotechnology, Shanghai, China). Protein samples were separated by 12% SDS-PAGE gels and then transferred to nitrocellulose (NC) membranes. After blocking with blocking buffer for 2 h, the membranes were incubated with polyclonal rabbit anti-Bcl-2 (1:1000, overnight at 4°C). HRP-goat anti-rabbit IgG (1:2000, 2 h) conjugate was used as a secondary antibody. The bound secondary antibody was detected by enhanced chemiluminescence (Pierce Biotechnology, Rockford, USA). The housekeeping gene, GAPDH, was used as an internal standard.

4.2.15 Statistical analysis

Results were expressed as mean values ± SD. Data were analyzed by two tailed T test and only p-values < 0.05 were considered statistically significant.

4.3 Results and Discussion

4.3.1 Characterization of C6M1/siRNA complexes

Circular Dichroism (CD) result confirmed the secondary structure of C6M1 peptide. As shown in Figure 4.2a, C6M1 showed a CD spectrum with two minima at 208 and 222 nm, confirming a typical helical structure.

Agarose gel shift assay was applied to detect the interaction between siRNA and C6M1 molecules. Basic amino acids such as lysine, arginine and histidine can interact

with the negatively charged phosphate groups on siRNA sugar rings through electrostatic interactions. C6M1 is designed to contain seven positively charged arginine residues so as to strongly bind siRNA molecules. Complex formation between siRNA and increasing amounts of peptide C6M1, from molar ratios 1/1 to 80/1, was followed by agarose gel electrophoresis of the mixture. Free siRNA will move toward the positive electrode when voltage is applied. Results shown in Figure 4.2b indicate that the formation of a stable peptide-siRNA complex began at a relatively low molar ratio, since the band produced by molar ratio 1/1 was less bright than band produced by siRNA alone. At molar ratios above 15/1, siRNA molecules complexed completely with C6M1, as no free siRNA was detected on the agarose gel at these ratios. This suggests that C6M1 at molar ratios higher than 15/1 is sufficient to neutralize and form a complex with siRNA.

The interaction was also confirmed by zeta potential measurements of C6M1/siRNA complexes at different molar ratios, Figure 4.2c. Naked siRNA alone in solution had a large negative zeta potential (-37 mV), reflecting the contribution from the negative charges on the phosphate group. Increasing the C6M1/siRNA molar ratio gradually neutralized the negative charge of siRNA. The increase in zeta potential was most pronounced when the molar ratio reached 15/1 (+51.67 mV); however, its value increased consistently as the peptide content increased. Thus, molar ratios above 15/1 can be used in the following transfection experiment. Resulting complexes were stable, as zeta potential obtained for molar ratios 15/1, 20/1, 40/1, and 80/1 were all around 50 mV. As a general rule, particles with zeta potentials more positive than +30 mV or more negative than -30 mV are normally considered stable [165].

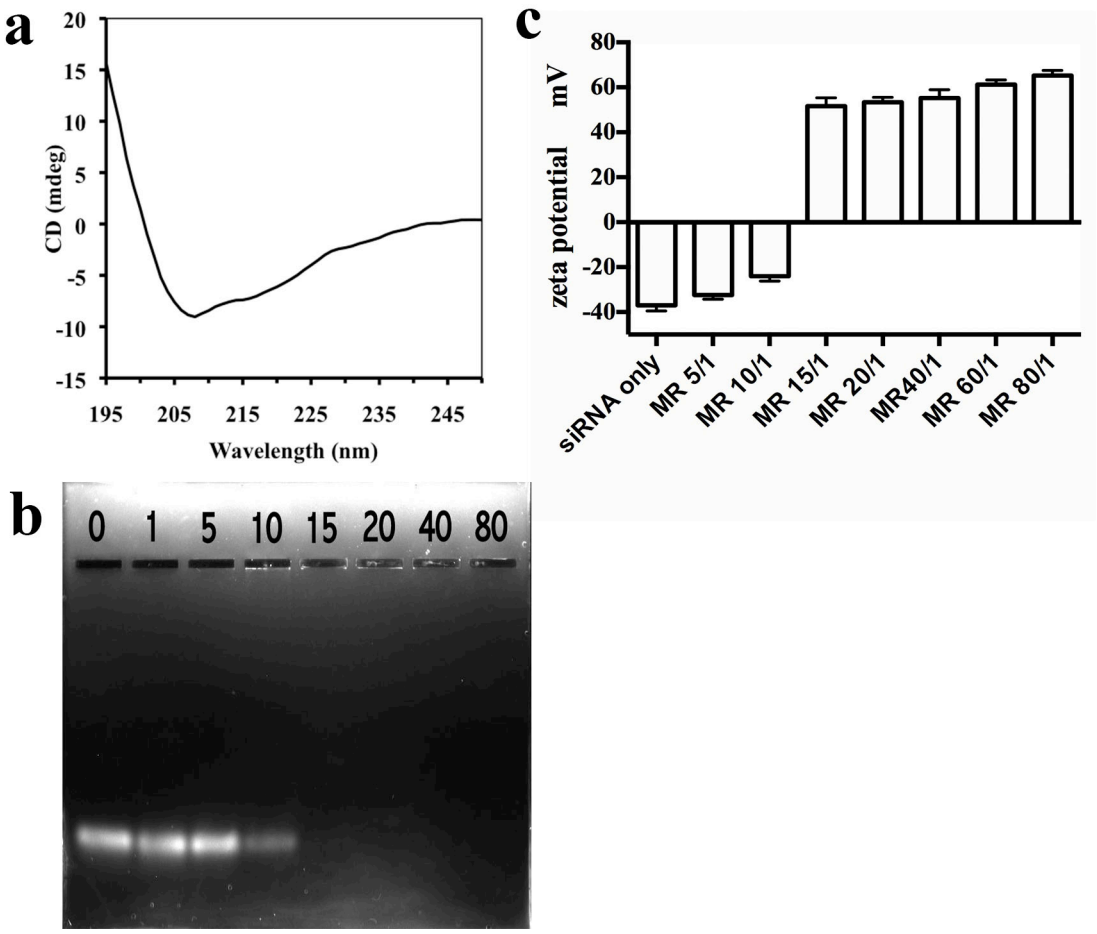

Figure 4.2 (a) Secondary structure of peptide C6M1 (40 μM) was obtained by far-UV CD spectroscopy. (b) The formation of siRNA-peptide complex indicated by agarose gel. The preformed C6M1/siRNA complexes were analyzed by electrophoresis on agarose gel (1.2% wt/vol) stained with ethidium bromide. The siRNA targeting eGFP gene was incubated with different concentrations of C6M1 corresponding to molar ratios ranging between 1/1 and 80/1. Lane 1 refers to siRNA only control in the absence of C6M1, and lanes 2–8 to molar ratios of 1/1, 5/1, 10/1, 15/1, 20/1, 40/1, and 80/1, respectively. 300 ng of siRNA per well was used here. (c) Zeta potential of C6M1/siRNA complexes at different molar ratios. Error bars represent the standard deviation from three replicates.

The size and morphology of the complex formed in transfection medium OPTI-MEM at a peptide to siRNA molar ratio of 40/1 was examined by transmission electron microscopy and dynamic light scattering, shown in Figure 4.3. The electron micrograph exhibited isolated particles of nanometric size and irregular shape, with an average diameter of about 100 – 200 nm (Figure 4.3a). This is the optimal size for cellular internalization through clathrin- and caveolae- mediated endocytosis [166]. Smaller complexes, depending on their surface properties, can directly penetrate the cell membrane, but are quickly removed from the blood [167]. Larger particles, on the other hand, can be easily recognized and removed by phagocytic cells [168]. The diameter of the complex, around 200 nm, was consistent with the DLS results shown in Figure 4.3b. Peptide C6M1 was able to condense siRNA into positively charged nanosized particles suitable for intracellular delivery.

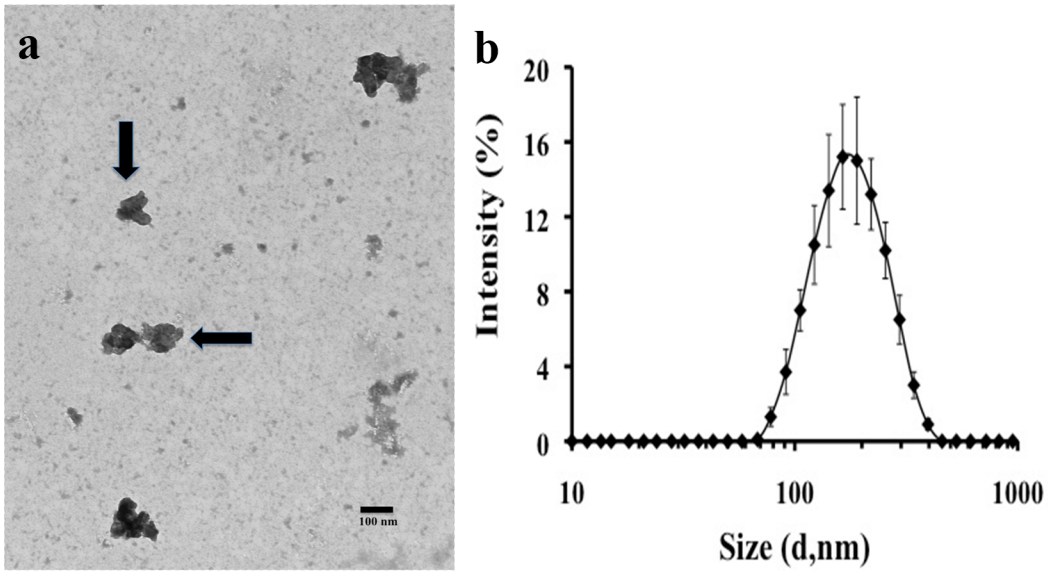

Figure 4.3 The complexes have a particle size suitable for transfection. (a) Transmission electron micrograph of C6M1/siRNA complexes (examples pointed by arrow) containing

300 nM siRNA at molar ratio 40/1 in OPTI-MEM medium. (b) Size distribution of C6M1-siRNA complex at molar ratio 40/1.

4.3.2 C6M1/siRNA complexes silence gene expression *in vitro*

It is widely accepted that the main prerequisite for an optimal siRNA delivery system is the ability to deliver siRNA into cells and then release it into the cytoplasm, where it can guide sequence specific mRNA degradation. We next used fluorescently labeled siRNA molecules to evaluate the efficacy of C6M1 to delivery siRNA molecules into cultured cells. Internalized siRNA is reported to selectively localize in the cytoplasm or translocate into the nucleus, depending on the target RNA residues [169]. To study cellular uptake, distribution, and localization of the C6M1/siRNA complex, we transfected the Chinese hamster ovary (CHO) cells with Cy3-labeled siRNA for visualization under fluorescent microscope and confocal microscope. CHO cells were treated with or without the complex for 3 hours and observed. To eliminate the effect of extracellular complexes on the image [170], cells were washed with 15 U/ml heparin in OPTI-MEM three times at 37°C to remove extracellularly bound complexes [95]. This ensures that the fluorescent siRNA we observed is indeed inside the cells and not attached to the cell membrane. Figure 4.4a and b show a typical fluorescence microscope image of CHO-K1 cells treated with siRNA alone and siRNA complexed with peptide C6M1, respectively. As expected, uncomplexed Cy3-labeled siRNA could not enter the cells. siRNA internalization occurred within three hours of incubation, and only in the

presence of peptide C6M1. The red fluorescence signal can be found in almost every cell.

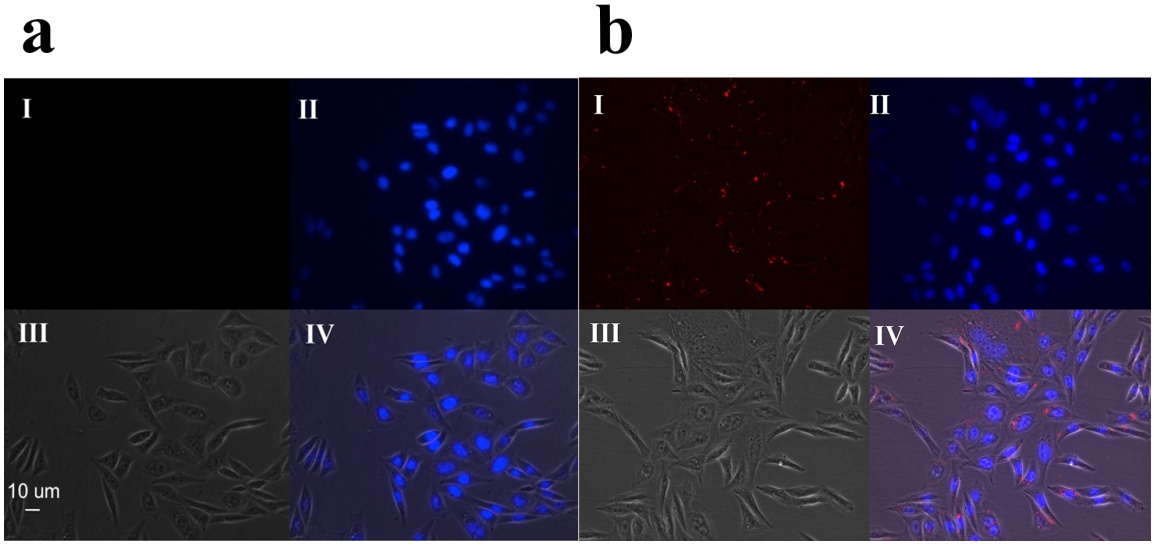

Figure 4.4 Uptake of C6M1/siRNA complexes in CHO cells. Fluorescent microscopy analysis of CHO cells 3 h after transfection with Cy-3 labeled GAPDH siRNA alone (a) or Cy-3 siRNA/C6M1 complexes (b), respectively. Panel i. Cy3-labeled siRNA (red); Panel ii. Nuclei were stained with DAPI (blue); Panel iii. Differential interference contrast (DIC); Panel iv. Merged image. Scale bar stands for 10 um.

To visualize subcellular localization, we applied peptide/siRNA complexes to CHO-K1 cells and visualized intracellular trafficking via confocal microscopy. As can be seen in Figure 4.5, siRNA delivered by C6 and C6M1 were localized to regions in close proximity to the nuclear membrane, but not in the nucleus. Labeled siRNA was delivered only to the cytosol, where it will bind to RNA-induced silencing complex (RISC) and then initiate RNA interference.

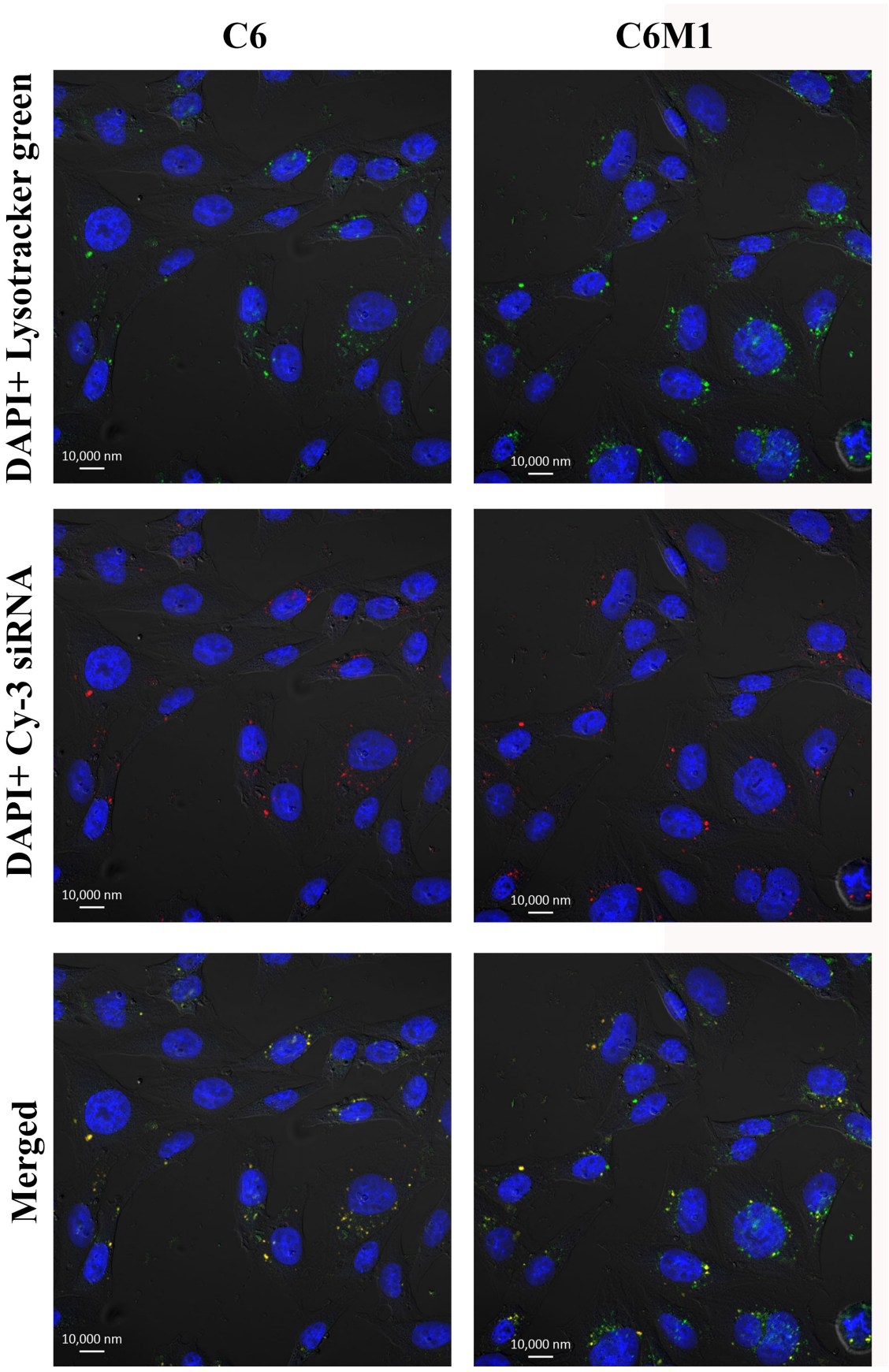
C6
C6M1
DAPI+ Lysotracker green
DAPI+ Cy-3 siRNA
Merged
10,000 nm
10,000 nm
10,000 nm
10,000 nm
10,000 nm
10,000 nm

Figure 4.5 Intracellular trafficking of C6/siRNA and C6M1/siRNA nanocomplexes. CHO-K1 cells were transfected with peptides carrying 50nM Cy-3 labeled siRNA for 3 h and subsequently incubated with LysoTracker Green. Images were pseudocolored for visualization: blue = DAPI; red = Cy-3 siRNA; green = LysoTracker Green. Co-localization of siRNA with the endosomal/lysosomal marker is in yellow.

The siRNA delivered by peptides showed a punctual non-homogeneous distribution pattern around the periphery of the nucleus inside the cell, rather than a diffuse distribution, which indicated the possibility of an endocytosis pathway [95]. Meanwhile, the colocalization of Cy-3 labeled siRNA (red) with a marker of endosome (green) yielded yellow spots, suggesting that both C6/siRNA and C6M1/siRNA complexes enter the cells via endocytosis. Endosomal escape of Cy-3 labeled siRNA can be observed 9 hours after treatment, see Figure 4.6.

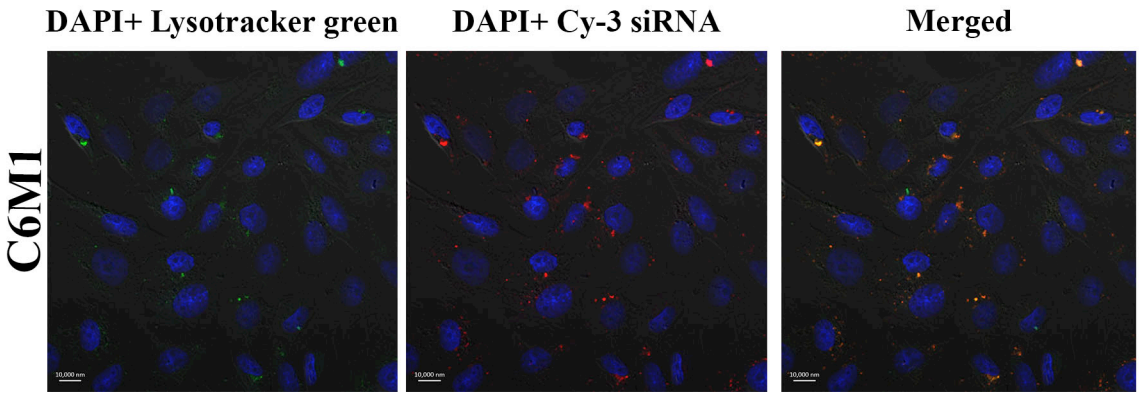

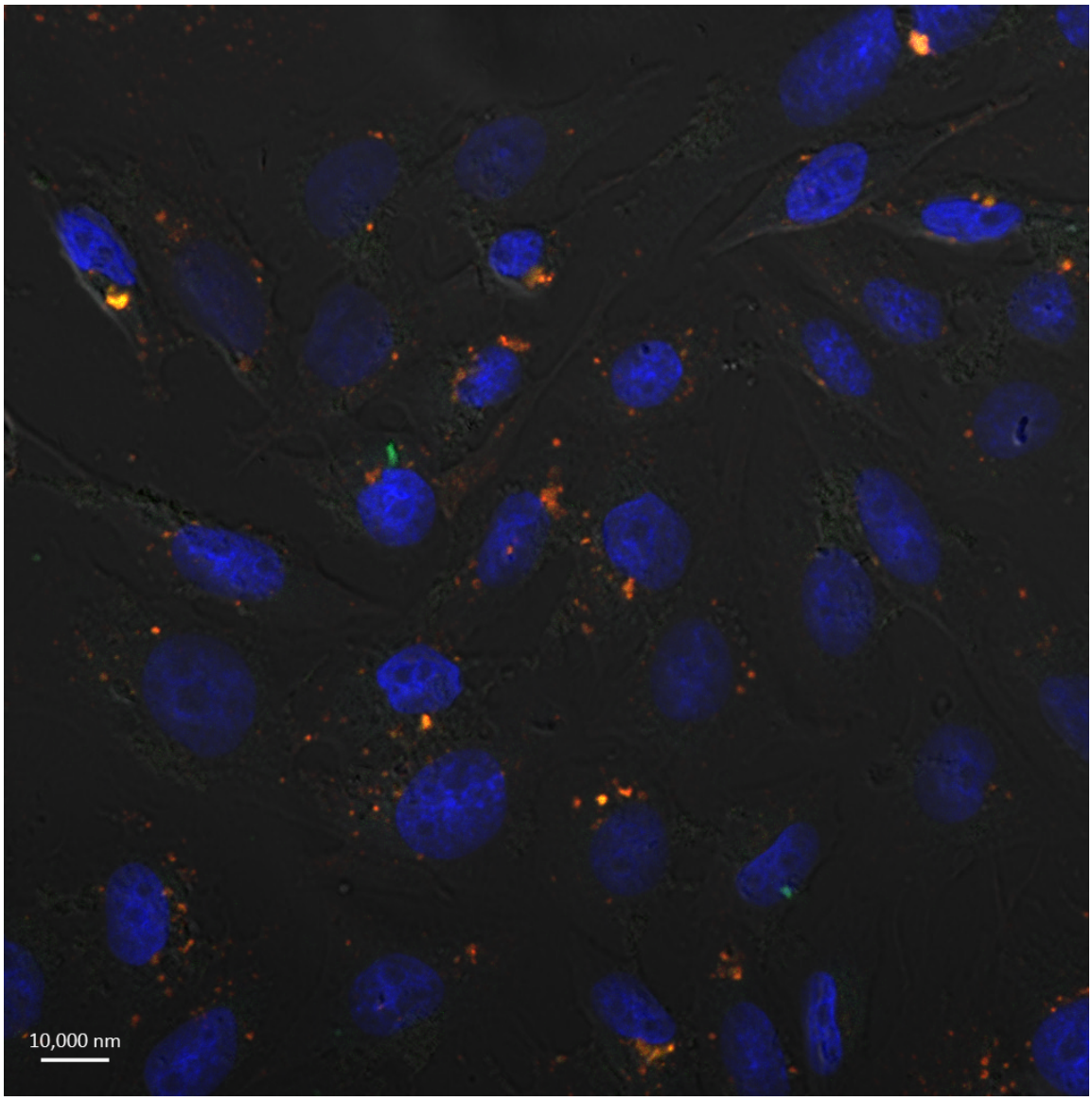

Figure 4.6 Confocal microscopy images of CHO-K1 cells treated with C6M1 peptide carrying 50 nM Cy-3 labeled siRNA. Images were taken 9 h after treatment. Images were pseudocolored for visualization: blue = DAPI; red = Cy-3 siRNA; green = LysoTracker Green. Co-localization of siRNA with the endosomal/lysosomal marker is in yellow. To clearly see the intracellular location of the complexes, the merged image was enlarged.

Cellular uptake of labeled siRNA was quantified using fluorescence-activated cell sorting (FACS). As shown in Figure 4.7, labeled siRNA alone was not internalized,

which is in good agreement with the fluorescence microscope results. Complexing with C6M1 will increase cellular uptake efficiency of siRNA accordingly, depending on the molar ratio of C6M1/siRNA. The intracellular fluorescence intensity of siRNA delivered by C6M1 is stronger than that of Lipofectamine 2000. The FACS data for peptide C6 has been reported previously [156], indicating high cellular uptake.

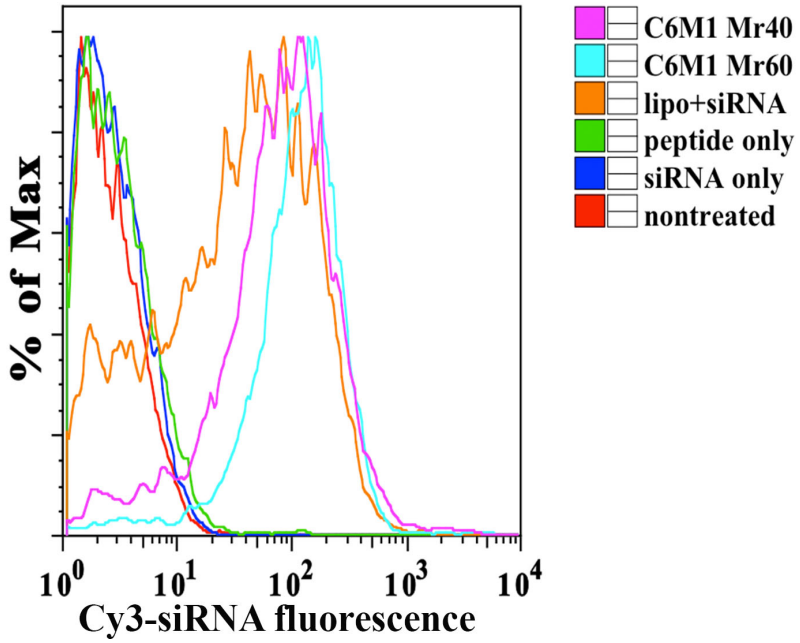

Figure 4.7 Cellular uptake of C6M1/siRNA complex in CHO-K1 cells. C6M1 delivered siRNA into cells in a molar ratio dependent manner. C6M1/siRNA complexes were formed at different molar ratios (40/1 and 60/1) and then added to CHO cells. Cells were then washed, trypsinized, and fixed. Fluorescent cells were counted by FACS.

In order to evaluate whether the amino acid change in sequence improved the biological effect of the delivered siRNA, RT-PCR measurement of GAPDH mRNA levels in the CHO-K1 cell line was used as a gene knockdown assay. The GAPDH

mRNA level in each sample was compared to the level measured in cells treated with a scrambled siRNA (negative control). Quantitative real-time PCR results revealed a spontaneous decrease in GAPDH mRNA levels in C6M1/siRNA transfected cells over the 48 h testing period, while steady state levels of another housekeeping gene, cyclophilin, remained relatively stable. As shown in Figure 4.8a, C6M1 mediated siRNA

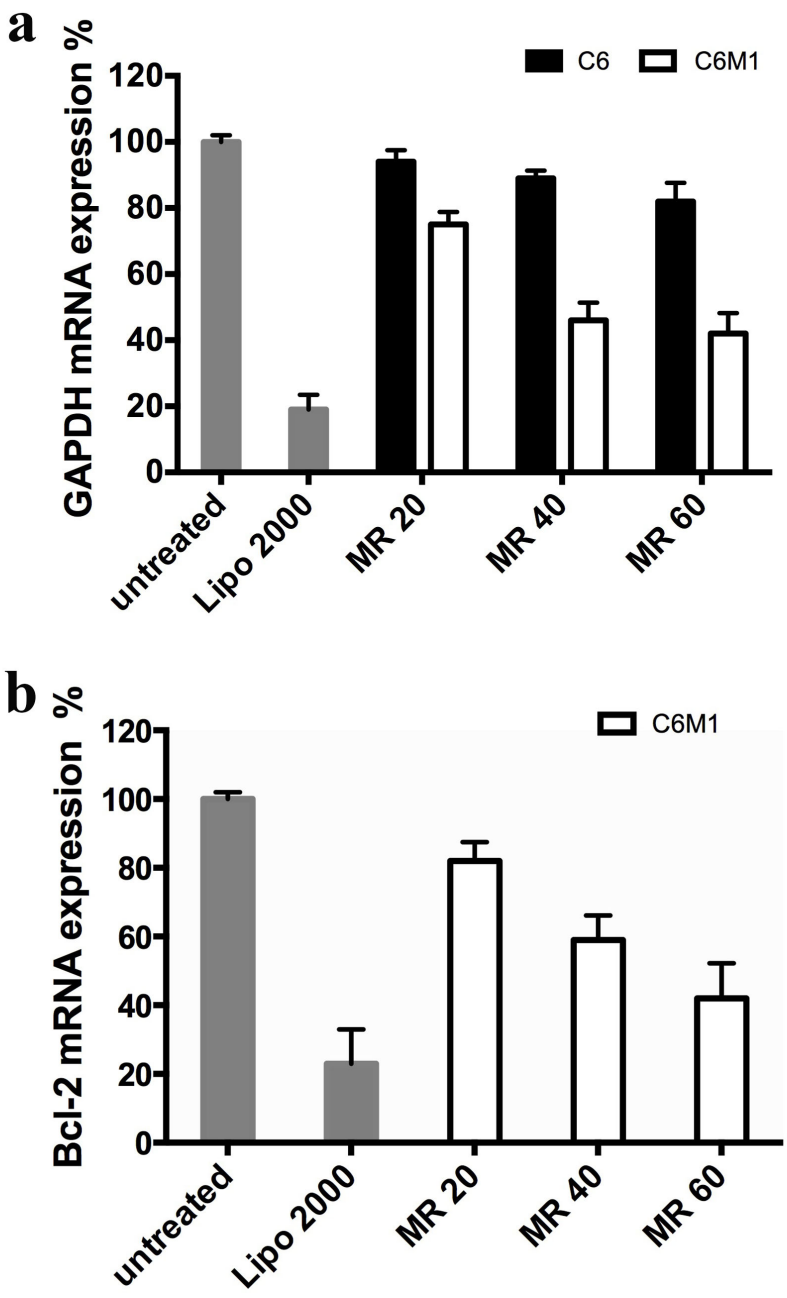

Figure 4.8 Gene silencing efficiency of C6/siRNA and C6M1/siRNA complexes in CHO-K1 cells. (a) Relative GAPDH mRNA level in CHO cells after transfected with peptides/GAPDH siRNA complexes. Black and white bar denote C6/siRNA and C6M1/siRNA complexes separately. (b) Silencing effect of C6M1/siRNA targeting Bcl-2 gene in A549 cells.

delivery resulted in a significant GAPDH mRNA decreases in a molar ratio dependent manner. A notable mRNA level reduction was initiated at a molar ratio of 20/1 at 50 nM siRNA concentration. Compared to untreated cells, C6M1/siRNA complexes at molar ratio 40/1 and 60/1 reduced mRNA levels by 54 ± 5.4% and 58 ± 6.2%, respectively, much higher than cells treated with C6/siRNA complexes, which only showed 20% knockdown. The knockdown efficiency of C6M1/siRNA complex was also evaluated on cultured A549 cancer cells before further *in vivo* study. The result showed similar silencing effect (Figure 4.8b).

MTT assay was performed to evaluate the cytotoxicity of 50 nM siRNA complexed with C6 and C6M1 at various concentrations. Lipofectamine 2000 was used as a control. As shown in Figure 4.9a, cell survival was not significantly impacted by the treatments of peptide C6M1. 48 h after transfection, CHO cells showed more than 85% viability even at the highest molar ratio, much higher than that of control Lipofectamine 2000, which achieved only 70% cell viability. Compared to C6, which showed slightly lower cell viability, the change in amino acid sequences also helped to improve the cytotoxicity.

The FACS data showed similar uptake amounts of C6/siRNA and C6M1/siRNA complexes. In direct contrast, quantitative PCR revealed a significant difference in

knockdown efficiency, indicating better release of siRNA delivery by C6M1. Therefore, the modification with tryptophan must have an impact on the endosomal membrane since both peptides are internalized via endocytosis. We next sought to directly evaluate the membrane disruption ability of peptides to CHO-K1 cells. This was realized through a colorimetric LDH assay, which estimate the membrane destabilizing capacity of peptides by measuring the activity of extracellular lactate dehydrogenases (LDH) liberated from disrupted cell membrane [171]. Medium with pH 7.4, 6.3 and 5.2 were used respectively to mimic the pH drops along the endocytic pathway, from extracellular pH 7.4 to pH 6.0-6.5 in early endosomes to pH 4.5-5.5 in late endosomes [172]. As clearly seen in Figure 4.9b, peptide C6M1 induced LDH release was critically enhanced by decreasing the environmental pH from neutral to acidic at both concentrations. These date suggested a strong capacity of C6M1 to destabilize cell membrane as well as endosomal membrane with the decrease of pH. Though peptide C6 also showed the trend to trigger cytosolic release of LDH when pH decreased, it is not so obvious compared to C6M1. Apparently, the increase in the membrane disruption ability under acidic condition corresponds to the enhanced transfection efficiency of C6M1. Therefore, the substitution of tryptophan for leucine indeed improves the endosomolytic property of the peptide. The role tryptophan played in the endosomolytic activity is not conclusive. Considering the absence of protonable residues in tryptophan at physiological pH, the "proton sponge" hypothesis [121] does not apply here. It is possible that tryptophan residues which are crucial for pore formation [173] disrupt the endosome membrane, causing endosomal/lysosomal leakage. The α-helical component of C6M1 may also play a crucial role in endosomal

membrane destabilization. The endosomolytic property of a series amphiphilic α-helical structural peptides such as HA2 and GALA have been reported [174].

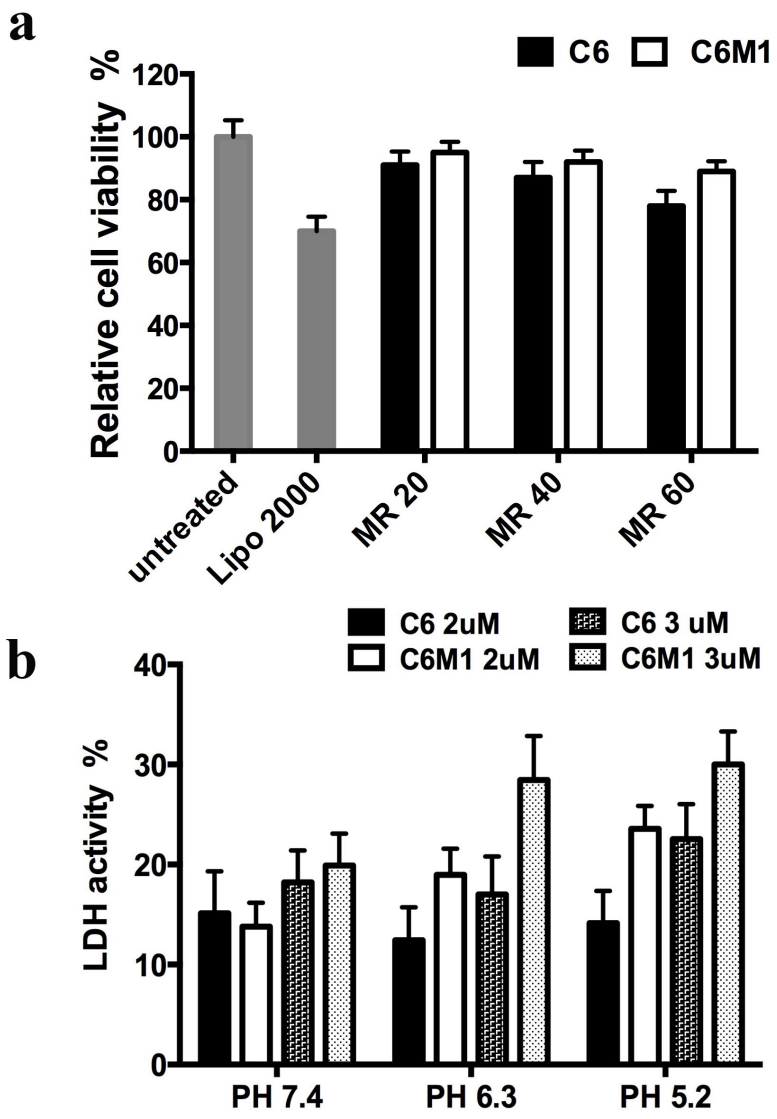

Figure 4.9 Cytotoxicity assay and pH dependent membrane disruption of C6/siRNA and C6M1/siRNA complexes in CHO cells. (a) Cytotoxicity of Lipofectamine 2000/siRNA and peptide/siRNA complex and at different molar ratios for CHO cells. Experiments were performed in quintuplicate each time. Results correspond to the average of three separate experiments and compared to untreated cells cultured in the same condition. (b) The activity of lactate dehydrogenase released from CHO cells upon interaction with peptides at different pH.

4.3.3 C6M1/siRNA complexes inhibit cancer cell proliferation *in vivo*

siRNA has widely been used to interfere with oncogene activity in mouse tumor models. In recent years, many studies have investigated the efficacy of liposomes as *in vivo* gene delivery agents [175–177], while the application of peptides in this area were rarely reported. Although some siRNA carriers can achieve high transfection efficiency *in vitro*, *in vivo* delivery presents unique challenges, such as the extracellular matrix barrier, serum degradation, and immune response, which limit their utility as clinical therapeutic agents. Thus, in an effort to demonstrate its clinical potential, we investigated the antitumor activity of the C6M1/siRNA complex in a mouse xenograft tumor model.

The Bcl-2 protein is an attractive target for gene therapy because it regulates the mitochondria-mediated apoptosis pathway [178]. A drug designed to reduce the level of this protein is expected to promote apoptosis and therefore inhibit tumor growth. The experimental results showed that Bcl-2 siRNA complexed with C6M1 at molar ratio 60/1 suppressed the tumor cell proliferation throughout the experimental period, even at low siRNA dose (160 μg/kg) (Figure 4.10a). After treatments, the tumor tissues were separated and weighed (Figure 4.10b). The average tumor volume was 1113 mm^3 in the control group and 459 mm^3 in the C6M1/siRNA group. The tumor weight of C6M1/siRNA group (0.5176 g) is significantly lower than that of untreated control (1.12 g) and saline treated control (1.24 g) groups, indicating a tumor inhibition rate of 53.7%. Reduced tumor volumes were due to decreased tumor cell proliferation. Moreover, the complexes showed minimal toxicity; all mice survived the 27 day treatment period without incurring severe side effects and none of the treatment groups demonstrated significant changes in body weight (Figure 4.10c), suggesting the complexes are

relatively safe to use.

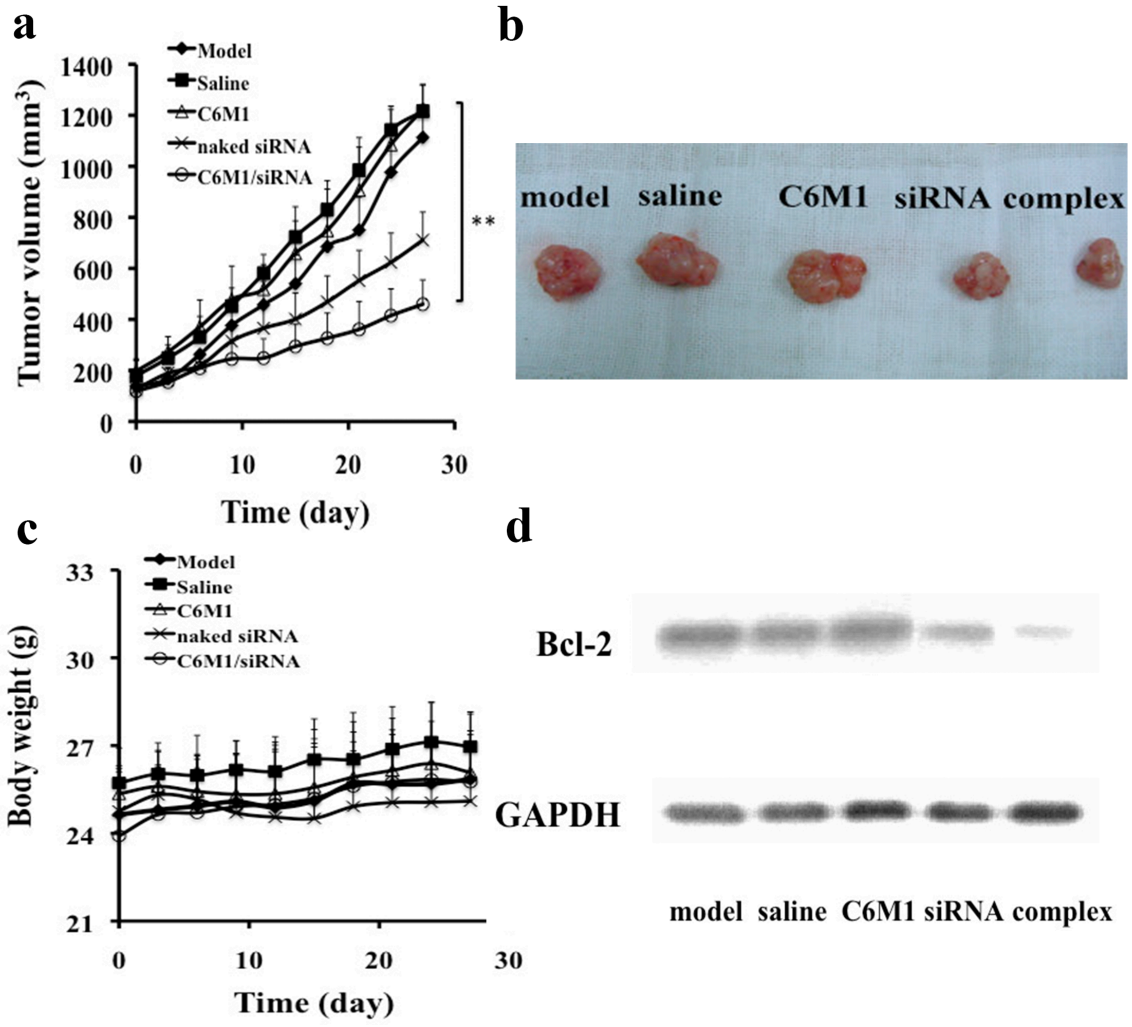

Figure 4.10 Local treatments with C6M1/siRNA complexes inhibit tumor growth in a mouse xenograft tumor model. (a) Antitumor activity of C6M1/siRNA complex in a mouse tumor model. The complexes were administered intratumorally in mice model bearing A549 cancer cells xenografted under the skin. The tumor sizes were measured everyday. Data shown is the mean value of eight mice in each group. S.D. of the data points is not shown for clarity. ** $p<0.01$ versus model group (n=8). (b) Dissected tumor tissues after treatment. Mice were killed by cervical dislocation on the 27th day. Tumors were then separated. Representatives of five treatment groups: model, saline, C6M1 peptide, naked Bcl-2 siRNA and C6M/siRNA complex. (c) The body weight of each group. Body weights of the mice were measured everyday during the treatment. Data shown is the mean value of eight mice in each group (n=8). (d) Inhibition of Bcl-2

protein expressions by C6M1/siRNA in CHO cells. Tumor tissues were dissected after treatment and total proteins were extracted. Bcl-2 levels in five treatment groups: model, saline, C6M1, naked siRNA, C6M1/siRNA were analyzed by western blot.

Western blot analysis was used to detect Bcl-2 protein expression in tumor tissue specimens. The analysis revealed specific downregulation of Bcl-2 protein in the C6M1/siRNA complex treated group and the housekeeping protein GAPDH remained unchanged. From Figure 4.10d, we conclude that, compared to untreated and saline control treated groups, the C6M1/siRNA complex can significantly inhibit Bcl-2 protein expression in cancer cells.

4.4 Conclusions

Peptide delivery systems have recently emerged as an alternative means to transport the therapeutic genes into targeted cells. Our study reported the silencing of an endogenous gene in tumor tissues using unmodified siRNA delivered by a novel peptide. C6M1 was rationally designed to improve the endosome escape ability of cell penetrating peptide C6. C6M1 adopts a helical structure that aligns all positive charges along one side. C6M1 demonstrated significant gene knockdown efficiency, both on CHO-K1 cells and A549 cells, compared to unmodified C6, though similar cellular uptakes were observed. We conclude that the enhanced membrane disruption of C6M1 at acidic pH improved the endosomal escape ability of the complexes, inducing obvious silencing effect. Our novel peptide delivery system is not only able to deliver siRNA into cultured cells, but also to

tumor cells via intratumoral injection in a xenograft mouse tumor model. *In vivo* results suggest that Bcl-2 siRNA complexed with peptide C6M1 specifically inhibited tumor growth, as treated animals showed a significant reduction in tumor size compared with untreated and saline control groups. The toxicological analysis showed that the treatment was well tolerated at therapeutic dosage both *in vitro* and *in vivo*. Results obtained here not only shed light on the development of a new peptide vector for siRNA delivery, but also on the new system as a practicable anticancer therapy strategy in clinical application.

Chapter 5

Design and evaluation of endosomolytic biocompatible peptides as carrier for siRNA delivery

---

5.1 Introduction

A new class of drugs that can silence specific gene expression, such as small interfering RNAs (siRNAs), has the potential to transform modern medicine [12]. In RNA interference (RNAi), which is induced by a particular siRNA, target mRNA is degraded by enzyme, leading to decreased expression of corresponding protein [179]. In principle, siRNA therapy could selectively downregulating pathological proteins, including those that are difficult to modulate with traditional drugs, with less extensive systemic toxicity [180]. Numerous research labs and pharmaceutical companies have already been developing siRNA drugs for age-related macular degeneration [181], cancer [67] and HIV infection [182], among other diseases. Although very promising, efficient *in vivo* siRNA delivery to the target site encounters many obstacles, including incapacity of highly negatively charged siRNA to cross cell membrane efficiently and vulnerability of siRNA to nuclease degradation in serum [183]. Therefore, an appropriate delivery formulation is required for siRNA treatment in order to transform the breakthrough science of RNAi into a new class of clinical therapy. Cationic liposomes [184] and polymers [27] are some of the more popular delivery method among non-viral carriers.

They facilitate delivery by encapsulating or condensing siRNA into nano-sized particles, which can be taken up by cells in a highly effective manner. Yet, when applied in *vivo* these approaches sometimes suffer from limitations such as cytotoxicity and immunogenicity [185–187].

Alternative strategies are necessary and one possibility is cell-penetrating peptides (CPPs). CPPs are a class of amphiphilic and positively charged short peptides that are able to penetrate cell membranes and translocate different cargoes [90]. The first discovery of CPPs dated back to 1988, when trans-activating transcriptional activator (TAT) [87] from human immunodeficiency virus 1 (HIV-1) was found to be taken up efficiently by various cells. After more CPPs were found in the following studies, they have been used to transport a wide range of cargoes into cells, including active proteins [188], quantum dots [189] and oligonucelotides [190]. With respect to siRNA delivery, TAT, penetratin and transportan [191] have been covalently linked to siRNA and successfully delivered them to various cell types. Other CPPs can form stable noncovalent complexes with siRNA. In this category, MPG [144], Pep-1 [96], as well as CADY [192], are among the best characterized. A well-designed CPP carrier should promote cellular uptake as well as intracellular release of the cargo. The endocytosis pathway is one major internalization mechanism for biological molecules [193]. These agents become entrapped in endosome and are degraded by enzymes in the lysosome if they are not able to escape in time. Thus, a key step in achieving effective biological function of siRNA is to facilitate the endosomal escape and ensure cargos reach cytosol where RNAi happens. The mechanisms by which siRNA carriers manage to escape endosome are extensively studied in recent years. In general, several mechanisms such as

pore formation in the endosomal membrane, pH-buffering effect of protonable groups (pH sponge effect) and fusion into the lipid bilayer of endosomes have been proposed [121].

In our laboratory, we focus on the study of cell penetrating peptides derived from peptide C6, a peptide that has been reported to delivery large amount of siRNA into cells but with low knockdown efficiency due to poor endosomal escape ability [150]. C6 consists of amino acids arginine, leucine and tryptophan. The seven positively charged arginine residues would interact with siRNA that carries negatively charged phosphate groups and provide extra charge for cell membrane interaction. These amino acids were arranged alternatively in the sequence so that when adopt a helical structure, polar (R) and nonpolar (L, W) residues would face opposite to form a secondary amphiphilicity structure [161]. However, for efficient siRNA delivery, we need to enhance the endosomolytic property of peptide C6. Thus, we first designed a peptide C6M1 by replacing certain hydrophobic leucine with tryptophan residues. The modified peptide showed significant membrane disruption ability with the decrease of pH, promoting the release of siRNA from endosome [194]. In this paper, an alternative modification applied to facilitate endosomal escape and ensure cytosolic delivery of siRNAs will be discussed. The incorporation of histidine residues is a common way to introduce protonable groups into peptide or polymer sequences [195]. The accumulation of histidine residues inside acidic endosomes causes influx of protons, which increases osmolarity, leading to swelling and hence disruption of the endosome membrane, according to proton sponges effect. Therefore, in the following design, peptides C6M2-C6M8 were obtained by substituting some residues in C6 and C6M1 with pH responsive histidine. From C6M6 to

C6M8, glycine was used as the first amino acid in N-terminal, as a number of cell-penetrating peptides have a glycine residue in the N-end, such as MPG [144], CADY [196], PPTG1[155] and Tat (48-60) [197]. Free N-terminal glycine was required by some CPPs for full membrane activity. The substitution of glycine with other amino acid would influence the stability and fusion activity of peptides [198]. In this study, we intended to elucidate whether our modifications were able to increase knockdown efficiency of C6 mediated siRNA delivery. The physiochemical properties of several peptides were characterized and compared followed by in vitro activity and toxicity measurements. Furthermore, the particular therapeutic significance of C6 family mediated siRNA delivery was demonstrated by the inhibition of cancer cell proliferation in a tumor xenograft mouse model. The immunogenicity of siRNA delivery systems has not been intensively studied in the past. As some reports appear in the literature concerning immune response elicited by liposomes in clinical trial, it is crucial to address possible immune side effects of these peptides. Hence, complement activation in human serum and cytokines activation in macrophages by peptide C6M3 and C6M6 were examined.

5.2 Materials and Methods

5.2.1 Materials

The C6 series peptides were synthesized in bulk (Pepscan, Lelystad, Netherland). High performance liquid chromatography (HPLC) analysis indicated that the synthetic peptide was at least 75% pure. Peptide sequences were shown in Table 5.1. Peptide C6, C6M3 and C6M6 for further characterization, *in vitro* and *in vivo* experiments were synthesized by CanPeptide Inc (Montreal, Canada) with at least 95% purity. Silencer^{TM} GAPDH

siRNA (Life Technologies, Burlington, Canada) was used as siRNA targeting the glyceraldehyde 3-phosphate dehydrogenase (GAPDH) gene. The Silencer^{TM} Cy3-labeled GAPDH siRNA (Life Technologies, Burlington, Canada) was used in fluorescence microscopy and Fluorescence Activated Cell Sorting (FACS). For experiments involving A549 cells, siRNA targeting Bcl-2 oncogene (Sigma, Oakville, Canada) was used, with a sense sequence of GUGAAGUCAACAUGCCUGCdTdT and antisense sequence of GCAGGCAUGUUGACUUCACdTdT. The negative control siRNA (Life Technologies, Burlington, Canada) used in the experiment was siRNA with scrambled sequence.

Table 5.1 Peptides sequences used in this study

Peptide	Sequence	M. W.	Net charge in neutral PH
C6	RLLRLLLRLWRRLLRLLR	2470.2	+7
C6M1	RLWRLLWRLWRRLWRLLR	2689.4	+7
C6M2	RLWRLLWHLWRHLWRLLR	2651.3	+5
C6M3	RLWHLLWRLWRRLHRLLR	2621.2	+6
C6M4	HLLRLLLRLWHRLLRLLR	2505.2	+5
C6M5	HLWHLLLRLWRRLLRLLR	2505.2	+5
C6M6	GLWHLLLHLWRRLLRLLR	2406	+4
C6M7	GLWHLLLHLWRRHHRHHR	2502	+4
C6M8	GLWHLHLHLWRRHHRLLR	2478	+4

Peptides were all modified by N terminal acetylation and C terminal amidation.

5.2.2 Cell culture

CHO-K1 (Chinese hamster ovary) cells and the non-small lung carcinoma A549 cells were purchased from American Type Culture Collection (ATCC, Washington DC, USA).

Cells were cultured in F-12K medium (Thermo scientific, Ottawa, Canada) supplemented with 10% fetal bovine serum (FBS) (Sigma, Oakville, Canada). All of the cells were incubated at 37°C in a humidified atmosphere containing 5% CO2.

5.2.3 Preparation of peptide/siRNA complex

siRNA was diluted in RNase free water. The final concentration was determined by Nanodrop 2000 Spectrophotometer (Thermo scientific, Ottawa, Canada). All peptide solutions (1 mM) were made by dissolving peptide powder in RNase free water. The solution was vortexed for 5 sec and sonicated for 10 min with a Microson XL2000 Sonicator (Qsonica, Newtown, USA). Peptide/siRNA complexes were made by mixing peptide and siRNA solution in a desired concentration. The complexes were then incubated for 20 min at room temperature before further experiments.

5.2.4 Particle size and zeta-potential

The hydrodynamic diameter of formed peptide/siRNA complexes were determined by dynamic light scattering on a Zetasizer Nano ZS (Malvern Instruments, Worcestershire, UK) equipped with a 4 mW He-Ne laser operating at 633 nm. Samples at molar ratio of 40/1 with final siRNA concentration 100nM were held in a quartz microcell (45 µl) with a 3 mm light path. The scattered light intensities of the samples at an angle of 173° were collected with appropriate viscosity and refractive index of water at 25 °C. Zeta potential measurements were also performed on the same machine using clear disposable zeta cells. Three measurements were performed to generate the intensity-based size and zeta potential plot reported herein.

5.2.5 Atomic Force Microscopy (AFM)

The nanostructure of peptide/siRNA complexes was imaged on AFM. The samples were prepared according to the following procedures: The peptide/siRNA complex solutions were prepared as mentioned in 2.3. 10 μl of the sample solution (1 μM siRNA with a peptide/siRNA molar ratio of 60:1) was put on a freshly cleaved mica surface. The sample was incubated for 10 min at room temperature to allow the complexes to adhere onto mica surface. Mica was then washed at least five times with RNase free water to remove unattached complexes. After air-drying, the mica surface was analyzed by a Dimension Icon AFM (Bruker, Santa Barbara, USA) at room temperature using the tapping mode with ScanAsyst-Air tips (Bruker, Santa Barbara, USA). All AFM images were obtained at a resolution of 512 × 512 pixels on a scale of 2 μm × 2 μm.

5.2.6 RiboGreen intercalation assay

RiboGreen assay was performed to quantify the encapsulation efficiency of siRNA with peptides. RiboGreen working solution was prepared by diluting Quant-it^{TM} RiboGreen RNA Assay Kit (Life Technologies Inc, Burlington, Canada) 1 to 32 in water. Initial siRNA concentration is 50 nM. Different volumes of peptide stock solution were added to the fixed siRNA concentration to obtain peptide/siRNA molar ratio from 1:1 to 80:1. Samples (60 μL) were mixed with 5 μl RiboGreen working solution and then transferred to a quartz cell (1 cm × 1 cm) and excited at 480 nm, The fluorescence was acquired on a Photon Technology International spectrafluorometer (Type LS-100, London, Canada) with a pulsed xenon lamp as the light source. Spectra were collected in the range of 500−600 nm. The amount of free siRNA after peptide addition was calculated by

subtracting the values of RiboGreen background fluorescence from the average intensities of sample at 528 nm, and expressed as a percentage of the control (naked siRNA only) with the following equation: Free siRNA percentage = Fluorescence intensity of complexes/Fluorescence intensity of naked siRNA x 100%

This percentage was then plotted versus peptide/siRNA molar ratios.

5.2.7 Fluorescence microscopy cell imaging

To investigate the distribution of the peptide/siRNA complexes in CHO-K1 cells, we used Cy-3 labeled GAPDH siRNA. Approximately 80,000 CHO cells were plated in a 24-well cell culture plate 1 d before transfection. Cy-3 labeled siRNA was mixed with different peptides at a peptide/siRNA molar ratio of 40/1 for 20 min. The cells were transfected with complexes (final siRNA concentration 50 μM) at 37°C for 3 h in Opti-MEM medium. The wells were washed with heparin in medium (15 U/ml, a total of three times for one hour at 37°C) to eliminate the effect of extracellular complexes and then fixed with 500 μl/well of fresh 4% Paraformaldehyde (PFA) for 30 min. After that, the fixation agent was aspirated, and the cells were washed twice with phosphate buffer saline (PBS) before they were subjected to Fluoroshield with DAPI (Sigma, Oakville, Canada) staining to visualize nuclei. The samples were monitored on a Zeiss Observer Z1 microscope with a 40x objective lens. Images were analyzed using AxioVision software.

5.2.8 Fluorescence-activated cell sorting (FACS)

The amount of Cy-3 labeled siRNA taken up by the cells via different peptide delivery vector was studied using Flow Cytometry (type BD Biosciences, BD FACSVantage SE Cell Sorter, USA). Cells were transfected with peptide/siRNA complexes according to

the protocol listed above. Untreated and naked siRNA only treated cells served as negative controls. Lipofectamine 2000 was used as a positive control. After 3 h incubation, cells were washed with PBS and trypsinized for 5 min, then resuspended in 4% PFA solution and collected. For each sample, data was acquired on 10,000 cells. The siRNA delivered to the cells was assessed using the FL-2 detection channel.

5.2.9 GAPDH enzyme activity measurement

CHO-K1 cells were seeded in a 96-well plate with 5,000 cells/well one day before transfection. 24 h later, the peptide/siRNA complexes containing GAPDH siRNA or negative control siRNA were prepared in Opti-MEM and added to each well in quintuplicate giving a final siRNA concentration of 50 nM. After 4 h of incubation at 37°C, equal volume of medium with 20% FBS were added to the cells. After 48 h, the GAPDH enzyme activity was detected using KDalert™ GAPDH assay kit (Life Technologies, Burlington, Canada) according to the manufacturer's protocol. The increase of fluorescence intensity was measured by a FLUOstar OPTIMA microplate reader (BMG Labtech, Ortenberg, Germany) with excitation wavelength at 560 nm and emission wavelength at 590 nm. The GAPDH gene knockdown efficiency was expressed as 100% - the fluorescence intensity of cells treated with GAPDH siRNA/ the cells treated with negative control siRNA.

5.2.10 qRT-PCR for GAPDH mRNA measurement

40,000 CHO-K1 cells were seeded in a 24-well plate 1 d before transfection. The transfection process was mentioned above. Gene knockdown efficiency was assessed 48 h later. Total RNA was isolated from the cells using TRIzol reagent (Invitrogen, Life

Technologies Inc, Burlington, Canada) according to the manufacturer's instructions. RNA concentration measurements and quality control were performed using Nanodrop spectrophotometer ND-1000. 0.5 µg of isolated RNA was reverse transcribed to cDNA with qScript™ cDNA SuperMix (Quanta Biosciences, Gaithersburg, USA). A quantitative PCR analysis was performed using PerfeCTa SYBR Green FastMix (Quanta Biosciences, Gaithersburg, USA) on an Mx3005P™ Real-Time PCR System (Agilent Technologies, Santa Clara, USA). The primers for mouse GAPDH were: 5′-TTGCTG-TTGAAGTCGCAGGAG-3′, 5′-TGTGTCCGTCGTGGATCTGA-3′. The housekeeping gene Cyclophilin was used as an internal control. Following primers were used: 5′-AGGGTTTCTCCACTTCGATCTTGC-3′ and 5'-AGATGGCACAGGAGGAAAGAG-CAT-3′. The PCR parameters consisted of an initial denaturation at 95°C for 30 s, followed by 40 cycles of PCR at 95°C for 5 s and 60°C for 30 s.

5.2.11 Cell viability assay

CHO-K1 cells (5,000 cells/well) in 200 µl F-12K medium with 10% FBS were seeded on 96-well plates and incubated. After 24 h, the cells were washed with PBS and transfected with peptide/negative control siRNA complexes formed at different molar ratios: 20/1, 40/1, 60/1. 4 h later, equal volume of medium with 20% FBS was added. After 48 h, MTT dissolved in PBS (5 mg/ml) was added to each well. Cells were incubated with MTT for 4 h, followed by the addition of 100 µl MTT solubilization solution (Sigma, Oakville, Canada). Cell viability was assessed by measuring the absorbance at 570 nm with a FLUOstar OPTIMA microplate reader. The absorbance of

control cells was set as 100% viability, and the viability of all other cells was expressed as a percentage relative to the absorbance of the control cells.

5.2.12 *In vitro* complement activation assay

The ELISA-based method for quantification of serum S-protein bound C terminal complex (SC5b-9) was performed. The test peptides C6M3, C6M6, at the concentration determined to be best in transfection experiment, and control compound Zymosan (Sigma, Oakville, Canada) were incubated with human serum (Quidel, San Diego, USA) for 1 h at 37°C. After that, the serum was diluted by specimen diluent (provided in the ELISA kits) at a 150-fold volume. Samples were tested for SC5b-9 levels using the MicroVue SC5b-9 plus (Quidel, San Diego, USA) kit following the manufacture's instruction. All reactions were tested in duplicates.

5.2.13 Cytokine activation in RAW 264.7 cells

$2.5x10^5$ RAW 264.7 cells were seeded in a 12-well plate 1 d before experiment. 24 h later, peptides/siRNA complexes at transfection concentration were added to the cells. 6 h post treatment, RNA was extracted with the method mentioned above. qRT-PCR were then performed with the primers in Table 5.2.

Table 5.2 Sequences of primers for qRT-PCR assay

Gene	Primer sequence
β-actin	(F) AGAGGGAAATCGTGCGTGAC
	(R) CAATAGTGATGACCTGGCCGT

iNOS	(F) CAGCTGGGCTGTACAAACCTT
	(R) CATTGGAAGTGAAGCGTTTCG
COX-2	(F) AGAAGGAAATGGCTGCAGAA
	(R) CTCAATACTGGAAGCCGAGC
IL1-β	(F) CCCAAGCAATACCCAAAGAA
	(R) GCTTGTGCTCTGCTTGTGAG
TNF-α	(F) AGACCCTCACACTCAGATCATCTTC
	(R) TTGCTACGACGTGGGCTACA
IL6	(F) AAGTGCATCATCGTTGTTCAT
	(R) GAGGATACCACTCCCAACAGA

5.2.14 *In vivo* experiment*

Tumor-bearing mice were prepared by subcutaneous injection of 5×10^6 A549 cells into the right armpit of six-week-old male BALB/c nude mice (B&K Universal Group Limited, Shanghai, China). Tumor diameters were measured every day and the tumor volume was calculated using the equation: tumor volume=$0.5\times(\text{width})^2\times\text{length}$. When the tumor volume reached 100-200 mm^3, Bcl-2 siRNA complexed with peptides at molar ratio 1/60 was injected directly into the tumor. Treatment was administered every 3 d at the dose of 4 μg siRNA per mouse. After the 9th injection the mice were sacrificed and tumors were excised. Mouse body weight was also monitored during the treatments.

*The *in vivo* experiments were designed by us and performed in
NO.3 people's hospital affiliated to shanghai Jiao Tong University School of Medicine

5.2.15 Western blot

Proteins were extracted using a total protein extraction kit (Kangchen Biotechnology, China) according to the manufacturer's instructions. The cell extracts containing 60 μg of protein samples were loaded into a 12% SDS-PAGE gels and electrophoresis was run. After that, they were transferred to a nitrocellulose (NC) membrane. After blocking with blocking buffer for 2 h, the membranes were incubated with polyclonal rabbit anti-Bcl-2 (1:1000, overnight at 4°C) (Santa Cruz Biotechnology, USA). HRP-goat anti-rabbit IgG (1:2000, 2 h) (Kangchen Biotechnology, Shanghai, China) conjugate was used as a secondary antibody. The bounded secondary antibody was detected by enhanced chemiluminescence (Pierce Biotechnology, Rockford, USA). In order to control protein loading, membranes were stripped and then incubated with goat anti-glyceraldehyde-3-phosphate dehydrogenase (GAPDH) antibody (Kangchen Biotechnology, Shanghai, China).

5.2.16 Statistical analysis

Results were expressed as mean values ± SD. Data were analyzed by two tailed T test and only p-values < 0.05 were considered statistically significant.

5.3 Results and Discussion

5.3.1. Peptide screening with KDalert™ GAPDH assay

To preliminarily determine the rank-order potency, all the peptides from C6 family were formulated with siRNA and tested by KDalert GAPDH assay kit. This kit relies on a

fluorescence-based assay to measure GAPDH enzyme activity in cell lysates, thus the amount of GAPDH protein activity was determined. By comparing GAPDH enzymatic activity in cells transfected with GAPDH siRNA to those transfected with a negative control siRNA, the level of gene silencing can be readily determined. Figure 5.1 shows the knockdown efficiency of GAPDH gene by GAPDH siRNA with C6 family peptides as carriers. Total nine peptides from C6 family were complexed with siRNA at molar ratio 20/1 and 40/1. The derivatives showed higher transfection efficiency than C6, indicating all the modifications improved the performance of their prototype C6 to some extent. The optimal peptides that produced an approximately 60% reduction in the GAPDH activity without being toxic to the cells were then selected. Apart from C6M1, two other peptides C6M3 and C6M6 achieved over 60% knockdown and therefore were chosen for further detailed study. Comparison of results obtained with C6 family shows that the transfection efficiency of the peptides seems not to be solely linked to the amount of histidine in the sequence, as peptides C6M2-C6M6 have the same number of histidine residues, but the efficiency varies. The location of histidine may also play an essential role in determining the transfection efficiency. It is reported that histidine residues have to be positioned in the core of peptide LAH4 and its derivatives to achieve high transfection efficiency [199].

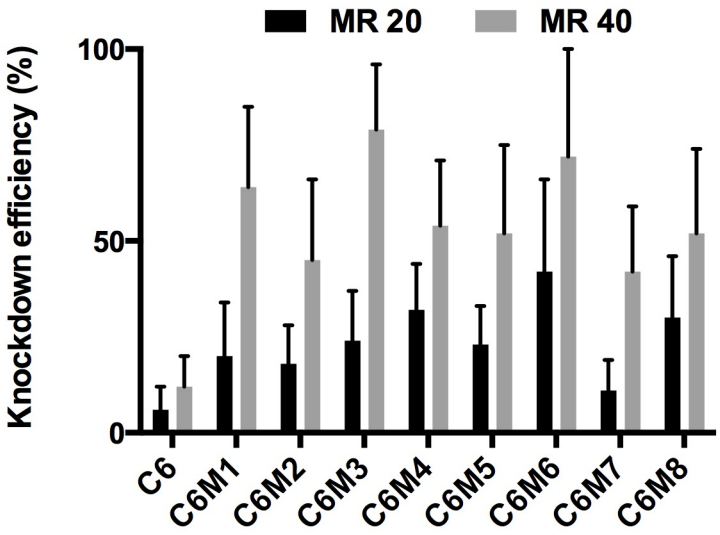

Figure 5.1 Percent knockdown of GAPDH protein levels after treatment. After 48 h of transfection, the cells were disrupted in lysis buffer before adding KDalert master mix. The fluorescence intensity was read on a plate reader at 590 nm. The knockdown efficiency was calculated as mentioned in the methods. Each sample was repeated by five times.

5.3.2 Insights into the characteristics and *in vitro* effect of peptides/siRNA complexes

The abilities of these peptides to bind to siRNA were studied using a RiboGreen intercalation assay. This reagent is a highly sensitive fluorescent nucleic acid stain for siRNA quantification [200]. Plot of decreased siRNA fluorescence intensity with increased peptides/siRNA molar ratios was shown in Figure 5.2. The siRNA encapsulation efficiency of all four peptides increased along with the increase of molar ratio of peptide/siRNA, reaching a plateau when the molar ratio was over 40/1 for peptides C6, C6M1, C6M3 and over 60/1 for C6M6. C6 and C6M1 showed similar siRNA binding ability, since they have the same overall charges contributed by seven

arginine residues. C6M3 and C6M6 have six and four arginine residues separately, in addition to two partially charged histidine at neutral pH. Therefore, their affinity for siRNA is weaker. It is obvious that at the molar ratio between 10/1 and 40/1, siRNA remaining free after complexed with C6M6 was significantly more than with other peptides, due to the less negative charges. However, this discrepancy became much smaller when the molar ratio is over 60/1, where siRNA was almost all saturated by peptides. To ensure better transfection efficiency, we will use molar ratio higher than 40/1 for all the peptides for *in vitro* and *in vivo* experiment.

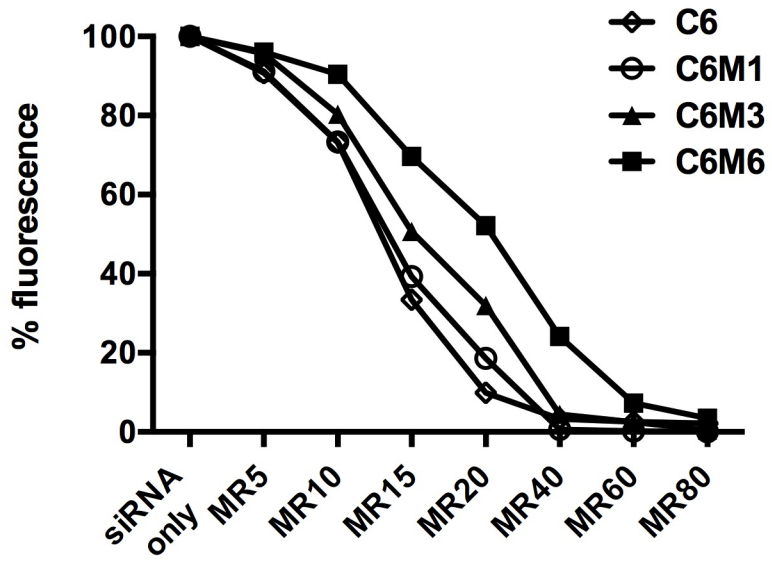

Figure 5.2 Evaluation of siRNA encapsulation efficiency. siRNA concentration was determined by a Quant-iT^{TM} RiboGreen RNA assay. Initial siRNA concentration is 50 nM. Different volumes of peptide stock solution were added to the fixed siRNA concentration to obtain peptide/siRNA molar ratio from 1/1 to 80/1.

Peptide/siRNA complexes at molar ratio 60/1 were imaged by AFM (Figure 5.3a and 5.3c). The morphology of siRNA complexes with C6 and C6M1 were reported earlier [150]. For C6M3 and C6M6 complexed siRNA, the height and amplitude scan of a 2 × 2 μm field revealing a scattered distribution of particles. The main particles were characterized by a width of 100 nm and a height around 30 nm, which were confirmed later by DLS results. Interestingly, different from the smooth edge of particles formed by other peptides, we can observe a granular morphology of C6M6/siRNA complexes (Figure 5.3c). A magnification of several complexes revealed that the particles were formed by association of smaller complex elements. C6M6 and siRNA may first form smaller particles, which will then aggregate to larger complexes. This shape is similar to another cell penetrating peptide CADY, which was reported to adopt a "raspberry" like structure when complexed with siRNA [201]. Zeta potential results obtained for C6M3/siRNA (Figure 5.3b) at molar ratio 20/1, 40/1 and 60/1 are positive, with values of 26 ± 4.1 mV, 32± 3.5 mV and 37± 4.4 mV. The complexes are stable at these molar ratios, with a value of +/- 25 mV has been proposed as the arbitrary line between stable and unstable particles [202]. Particles with a zeta potential above +25 mV or below-25 mV are considered electrically stable, while particles within the range tend to aggregate and coagulate. In contrast, C6M6/siRNA complexes at molar ratio 20/1 with a very low zeta potential of 15± 3.3 mV clearly indicates instability whereas a higher molar ratio of 40/1 and 60/1 suggest stable particles. This can be explained by the fewer overall positive charges in C6M6 than C6M3. Apparently at molar ratio 20/1, the arginine residues in C6M6 are just enough to neutralize all the negative charges of siRNA. A molar ratio above 20/1 is needed to form stable complexes.

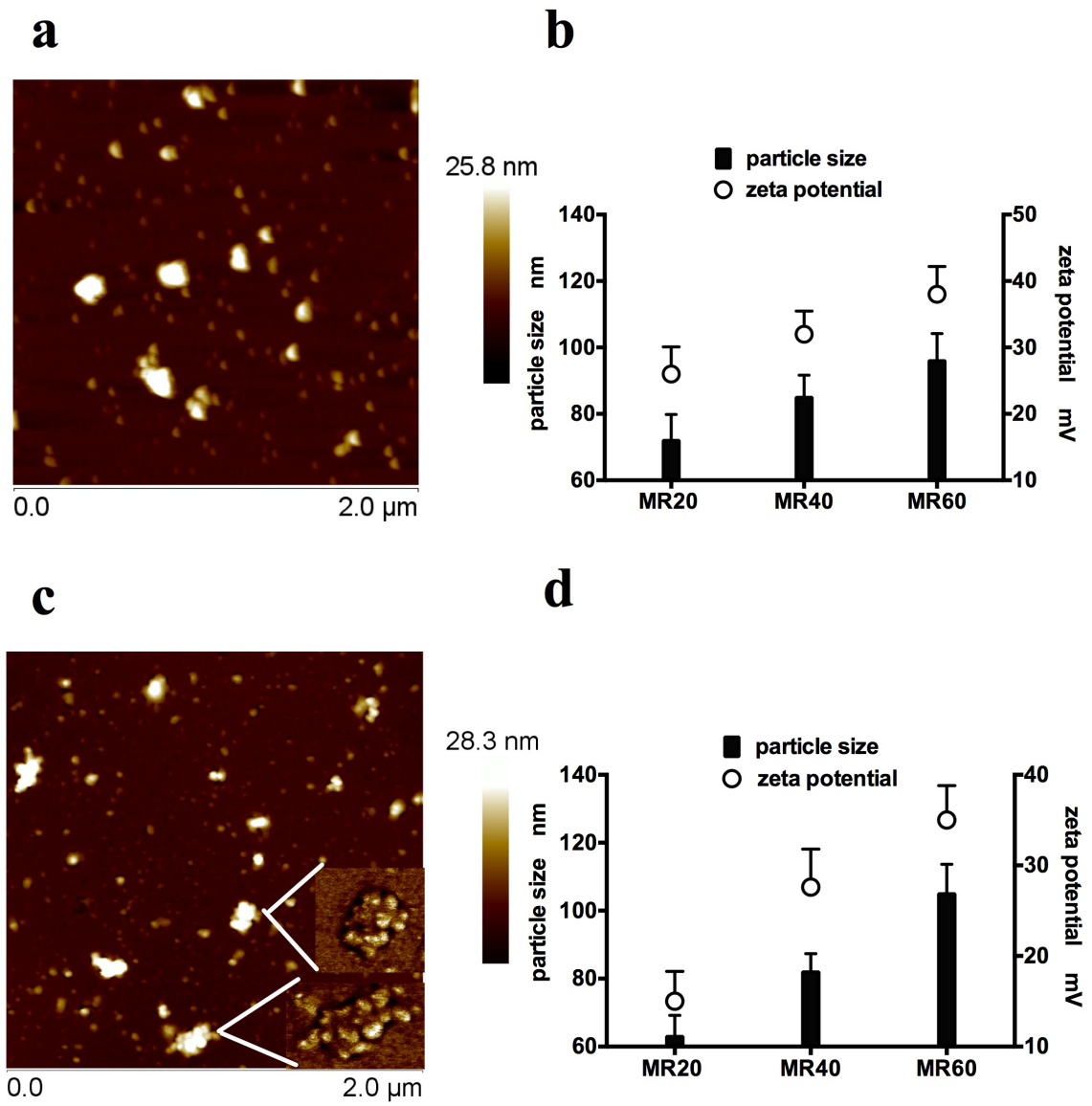

Figure 5.3 Representative AFM images and particle size of peptide/siRNA complexes. AFM images of 1 μM siRNA complexed with peptide C6M3 (a) and C6M6 (c) at molar ratio 40/1 and 60/1 respectively. Smaller images in (c) denotes enlarged AFM image of C6M6/siRNA complexes by DMT modulus. (b) (d) Particle size and zeta potential of C6M3/siRNA and C6M6/siRNA complexes at molar ratios 20/1, 40/1 and 60/1. Data are presented as the mean of three measurements.

The cellular uptake and intracellular localization of Cy-3 labeled siRNA was observed by fluorescence microscopy. Successful siRNA delivery to the cells is shown in Figure 5.4, which depicts fluorescence microscopy images of the Cy3 labeled siRNA transfected cells 3 h post-transfection. As expected, uncomplexed Cy3-labeled siRNA could not enter the cells. siRNA internalization occurred within three hours of incubation, and only in the presence of peptide C6M3 and C6M6. The red fluorescence signal can be found in almost every cell. As can been seen in the image, siRNA was localized to regions in close proximity to the nuclear membrane, but not in the nucleus. Labeled siRNA is delivered only to the cytosol, where it will bind to RNA-induced silencing complex (RISC) and then initiate RNA interference. The siRNA delivered by peptides C6M3 and C6M6 shows a punctual non-homogeneous distribution pattern around the periphery of the nucleus inside the cell, rather than a diffuse distribution, which indicated the possibility of an endocytosis pathway [95].

Effectiveness of carriers for siRNA delivery was determined by measuring the fluorescence intensity of cells after delivery of Cy-3 labeled GAPDH siRNA. Three peptides from the library were studied here. Fluorescence activated cell sorting (FACS) analysis of CHO-K1 cells, gated for live cells (Figure 5.5a) clearly showed comparable or higher siRNA delivery efficiency than a market leader Lipofectamine 2000. The mean fluorescence intensity of CHO cells (Figure 5.5b) after 3 h transfection with Cy-3 labeled siRNA complexed with peptides C6, C6M3, C6M6 at molar ratio 60/1 also shows a large amount of uptake.

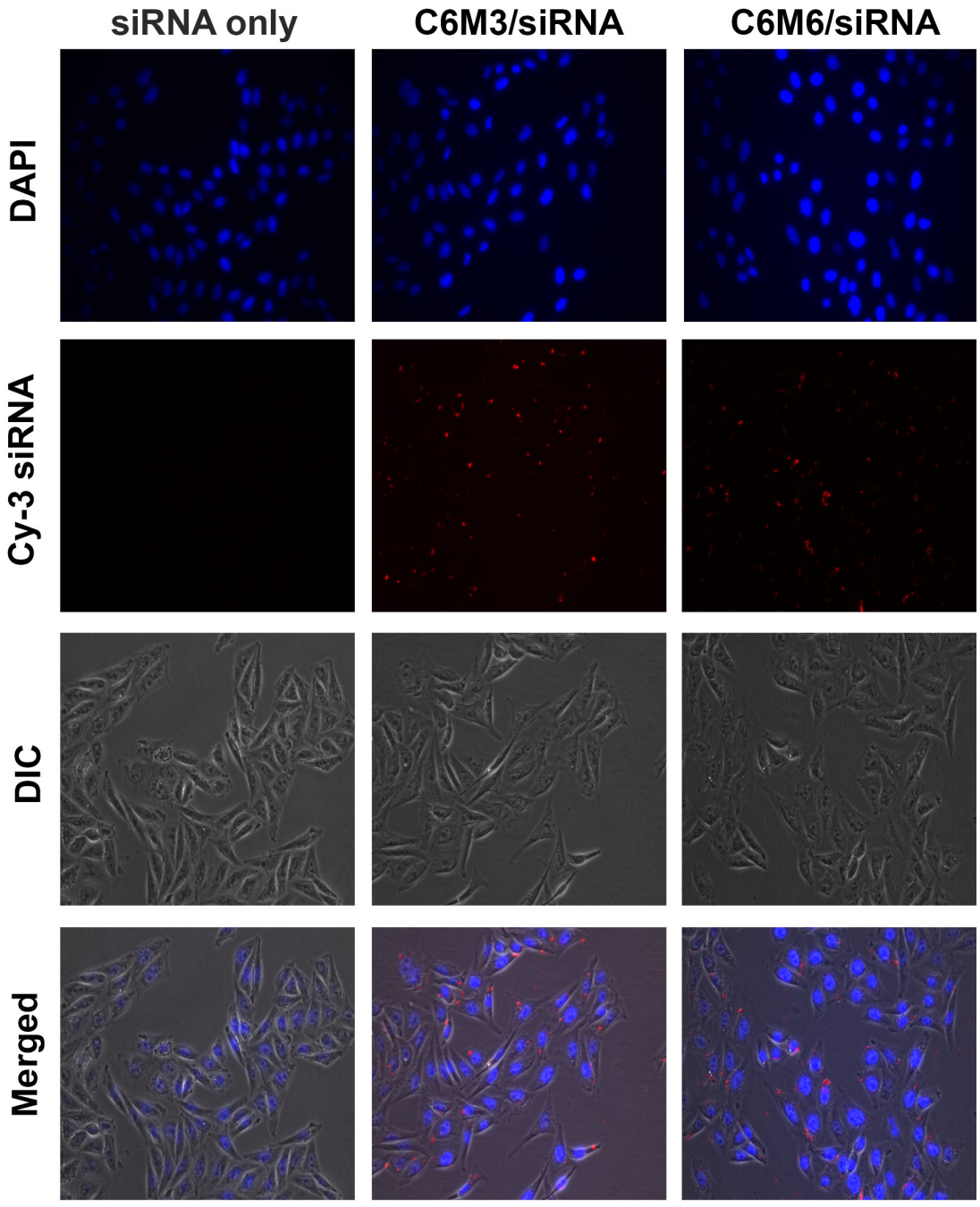

Figure 5.4 Uptake of peptides/siRNA complexes in CHO cells. Fluorescent microscopy analysis of CHO cells 3 h after transfection with Cy-3 siRNA only, C6M3/Cy-3 siRNA complexes and C6M6/Cy-3 siRNA complexes, respectively. Nuclei were visualized by DAPI (blue).

To confirm the delivered siRNA performed its function, quantitative RT-PCR was utilized to analyze GAPDH mRNA level in CHO-K1 cells. The cells were transfected with both the negative control siRNA (using siRNA with a nonsense / scrambled sequence) and GAPDH siRNA. The GAPDH mRNA level was first normalized to an internal control Cyclophilin mRNA and the ratio between GAPDH siRNA transfected samples and the corresponding negative control was used to calculate the relative GAPDH mRNA expression level. The result reveals that C6/siRNA complexes did not decrease GAPDH mRNA level at all tested molar ratios, as reported before. The modified peptides, C6M3 and C6M6 suppress GAPDH gene expression in a molar ratio dependent manner, Figure 5.5c. At molar ratio 60/1, C6M3/siRNA and C6M6/siRNA complexes demonstrate comparable gene knockdown efficiency, inhibiting GAPDH mRNA expression levels by 65% and 62%, respectively. This data was in accordance with KDalert results, but with smaller error bars. Given the fact that peptide C6 only shows 20% silencing efficiency at most, it is obviously that the replacement of some arginine residues with histidine improves transfection efficiency of the peptides remarkably. Histidine contains an imidazole ring, which is a weak base with pKa of 6 [203]. Studies have shown that the incorporation of histidine into polymeric and peptide gene delivery vehicles increases the endosomal buffering capacity, improving the efficiency of endosomal escape [204–207]. Proton sponge effect was attributed as the mechanism for the endosomolytic ability of histidine. Protonation of histidine residues in acidic endosomes will induce an extensive inflow of ions and water, subsequently leading to rupture of endosomal membrane and release of the entrapped components [121].

In addition, the toxicity of peptides based formulations was investigated using MTT assay. As reported in Figure 5.5d, almost no toxicity was detected for C6M3/siRNA complexes at various molar ratios tested. For C6/siRNA and C6M6/siRNA complexes, only 10–15% of cell death was observed at molar ratio 40/1 and less than 20% of cell death at molar ratio 60/1, still lower than Lipofectamine 2000, which caused around 30% of cell death.

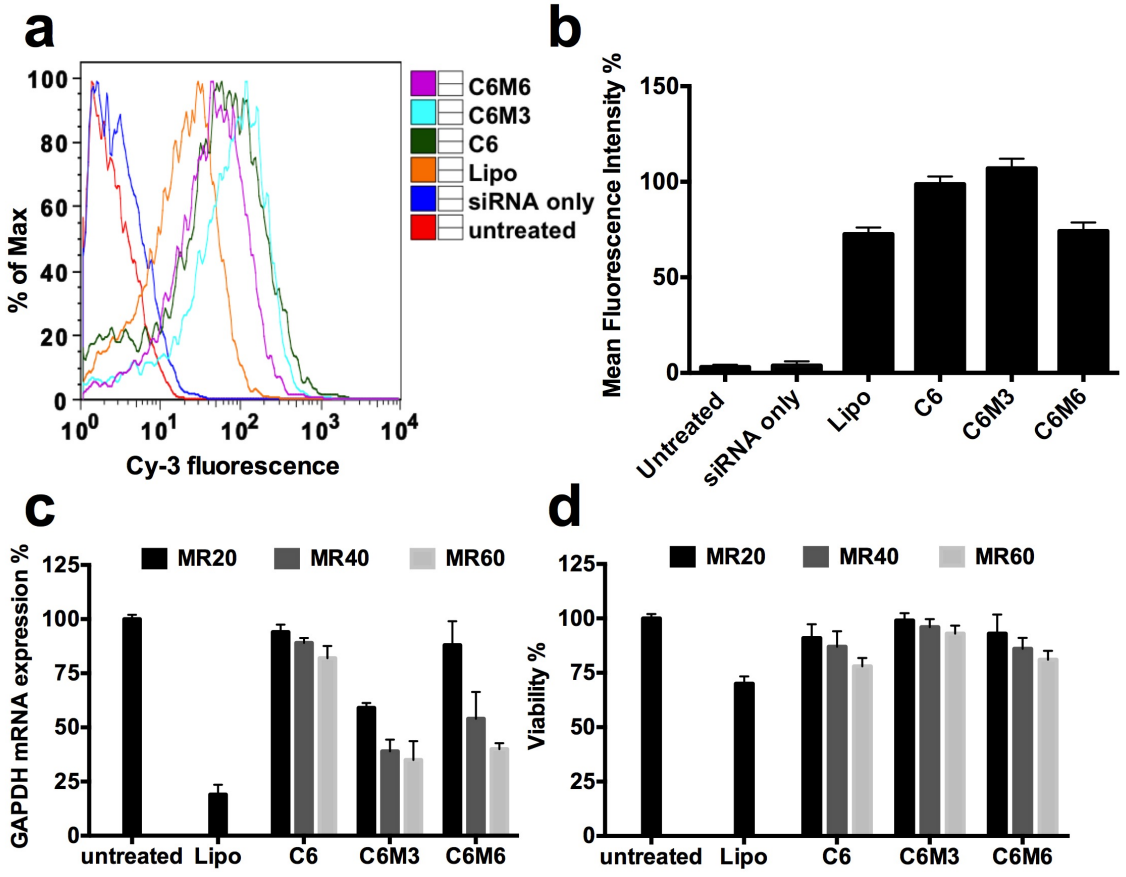

Figure 5.5 Peptide mediated delivery of siRNA into CHO-K1 cells. (a) Cellular uptake of peptide/siRNA complexes. CHO-K1 cells were incubated with the complexes of peptide/Cy-3 siRNA or Cy-3 siRNA alone for 3 h. The cells were then analyzed by fluorescence activated cell sorting (FACS) in the Cy-3 channel. (b) Mean fluorescence

intensity of Cy-3 siRNA in CHO cells treated with different peptides. (c) Relative GAPDH mRNA level in CHO-K1 cells after treatment. CHO-K1 cells were incubated with preformed complexes at different peptide/siRNA molar ratios (20/1, 40/1 and 60/1) for 3 h. 48 h later, total RNA was extracted and gene knockdown efficiency was determined by RT-PCR. All the data were normalized to another house keeping gene cyclophilin and compared to cells treated with corresponding peptide/scrambled siRNA control. (d) The toxicity of peptide/siRNA complexes was investigated by MTT assay. CHO-K1 cells were treated with increasing molar ratios of peptide/siRNA complexes ranging from 20/1 to 60/1 and cell viability was then evaluated 24 h after treatment. Scrambled siRNA was used here. Reported data are the average of three separate experiments.

5.3.3 *In vitro* complement and cytokine activation assay

The complement system is an important part of the innate immunity and serves as a first-line of defense after the invasion of a foreign object. The complement system can be activated via the classical, the lectin and the alternative pathway [208]. The Terminal Complement Complex (TCC, SC5b-9) is generated by the assembly of C5 through C9 as a consequence of activation of the complement system by either the classical, lectin or alternative pathway. The ELISA-based method for quantification measures concentration of serum S-protein-bound C terminal complex (SC5b-9), thereby giving an indication of the status of the level of complement activation in the specimen. High levels of complement activation have been demonstrated in a variety of disease states. In Figure 5.6a, positive control Zymosan caused significant elevation of SC5b-9 over baseline, compared to serum only sample. While peptides C6M3 and C6M6 at transfection

concentration did not exhibit SC5b-9 activation. To determine whether these complexes could induce pro-inflammatory cytokines, the mRNA levels of five types of cytokine in macrophage RAW 264.7 cells after treated with peptide/siRNA were measured by qRT-PCR, Figure 5.6b. The RAW 264.7 murine macrophages were incubated with either 0.1μg/ml bacterial endotoxin LPS or peptides/siRNA complexes. High induction of cytokines iNOS, COX-2, IL1-β, TNF-α and IL6 was observed 6 h post treatment with the positive control LPS. This induction of COX-2 expression was 3-fold higher than untreated cells and more than 100-fold higher for other cytokines. There was almost no significant cytokines induction from the peptide/siRNA complexes treatment in RAW 264.7 cells.

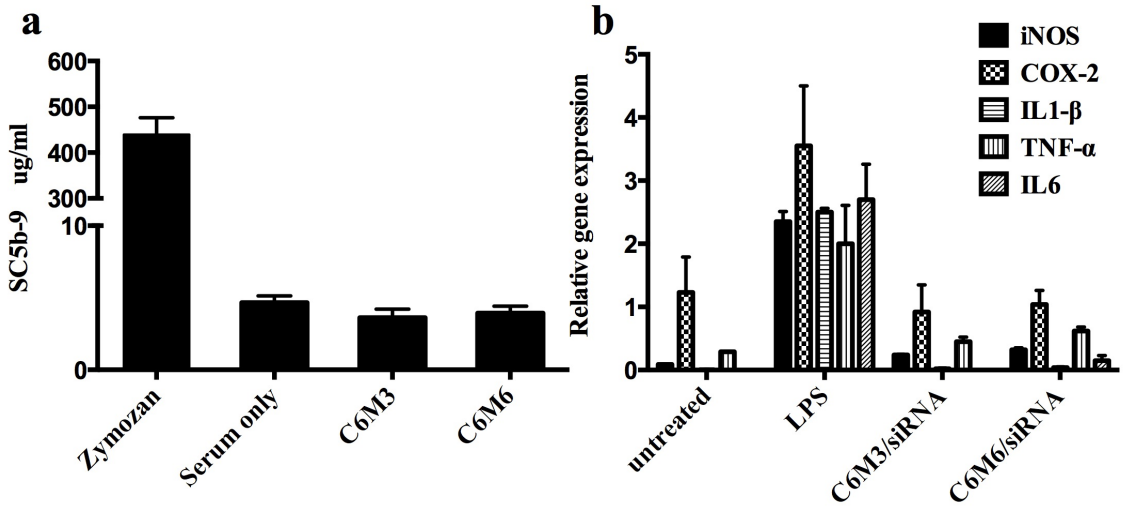

Figure 5.6 *In vitro* complement and cytokine activation assay. (a) SC5b-9 formation in human serum after incubation with peptides was quantified by ELISA assay. 5 ug/ml Zymosan was used as positive control. (b) Cytokine mRNA expressions in RAW 264.7 cells, measured 6 h after treatment with 0.1 μg/ml LPS, C6M3/siRNA and C6M6/siRNA complexes. Housekeeping gene β-actin was used as an internal control. All cytokine mRNA levels were normalized to β-actin mRNA.

5.3.4 Anti-tumor effect of peptide/siRNA complexes in mice bearing A549 derived tumors

Bcl-2 protein, encoded by the Bcl-2 gene, is the founding member of Bcl-2 family that regulate cell death [209]. The Bcl-2 family comprises antiapoptotic proteins (Bcl-2, Mcl-1, Bcl-w and A-1) and proapoptotic proteins (Bax, Bak, Bik, Bad, Bid, BMF, and PUMA) [210,211]. The Bcl-2 oncogene overexpression occurs in many cancer types and is associated with chemoresistance and radioresistance [212,213]. Inhibition of Bcl-2 will either restore normal apoptotic process in cancer cells or enhance the sensitivity of these cells to conventional chemotherapy. Thereby, Bcl-2 gene is an important therapeutic target in various human cancers. The potential of peptides C6M3 and C6M6 to deliver therapeutic siRNA *in vivo* was first evaluated on human non-small cell lung cancer A549-xenografted mice. The effect of local intra-tumoral administration of C6M3/ Bcl-2 siRNA and C6M6/ Bcl-2 siRNA complexes on the growth of established subcutaneous tumors was assessed. When tumor volume reaches 100-200 mm^3, four groups of mice were injected with saline, 4 μg (0.16 mg/kg) naked siRNA, peptide only and peptide/siRNA complexes at molar ratio 60/1, separately. The treatment was given every three days for a total of 9 times. Reduction of tumor size was observed in both C6M3/siRNA and C6M6/siRNA treatment group Figure 5.7a and 5.7b. In contrast, intra-tumoral administration of saline and peptide only did not significantly reduce tumor growth, compared to the model group. Surprisingly, we found that naked Bcl-2 siRNA treated group also showed decreased tumor size, which has also been reported by other researchers in A549 xenograft mice [214] and other types of cancer cells [215]. The

mechanisms for greater uptake of siRNA into tissue cells *in vivo*, compared with ineffectiveness in cultured cells are not known, but could involve serum proteins or components of the complex extracellular matrices in tissues [215]. However, peptide C6M3 and C6M6 as carrier for siRNA could promote the anti-tumor effect further and provide better protection against enzymatic degradation. On day 27, mice were sacrificed and tumor tissues were excised (Figure 5.7c and 5.7d). Tumor inhibition rate was calculated as tumor inhibition rate=(1- tumor weight of treatment group/tumor weight of model group)×100%. The tumor growth was reduced by 54.72% and 53.86% with 4 μg of Bcl-2 siRNA formulated with C6M3 and C6M6 respectively. The body weights of mice were monitored throughout treatment (Figure 5.7e and 5.7f). Mice exposed to peptide/siRNA complexes or peptide only did not suffer from weight loss for 27 days. Therefore, no toxicity was observed and the treatment was well tolerated. Next, we tried to validate that the Bcl-2 siRNA mediated inhibition of tumor growth was directly associated with a decrease in the level of Bcl-2 protein. Western blot analysis (Figure 5.7g and 5.7h) using lysates from A549 tumors collected at the end of treatment revealed that the reduction in tumor size was directly correlated to Bcl-2 protein level, as evidenced by significant reduction in Bcl-2 expression with decreased tumor size. These data suggest silencing Bcl-2 protein expression is an effective way for inhibiting tumor growth.

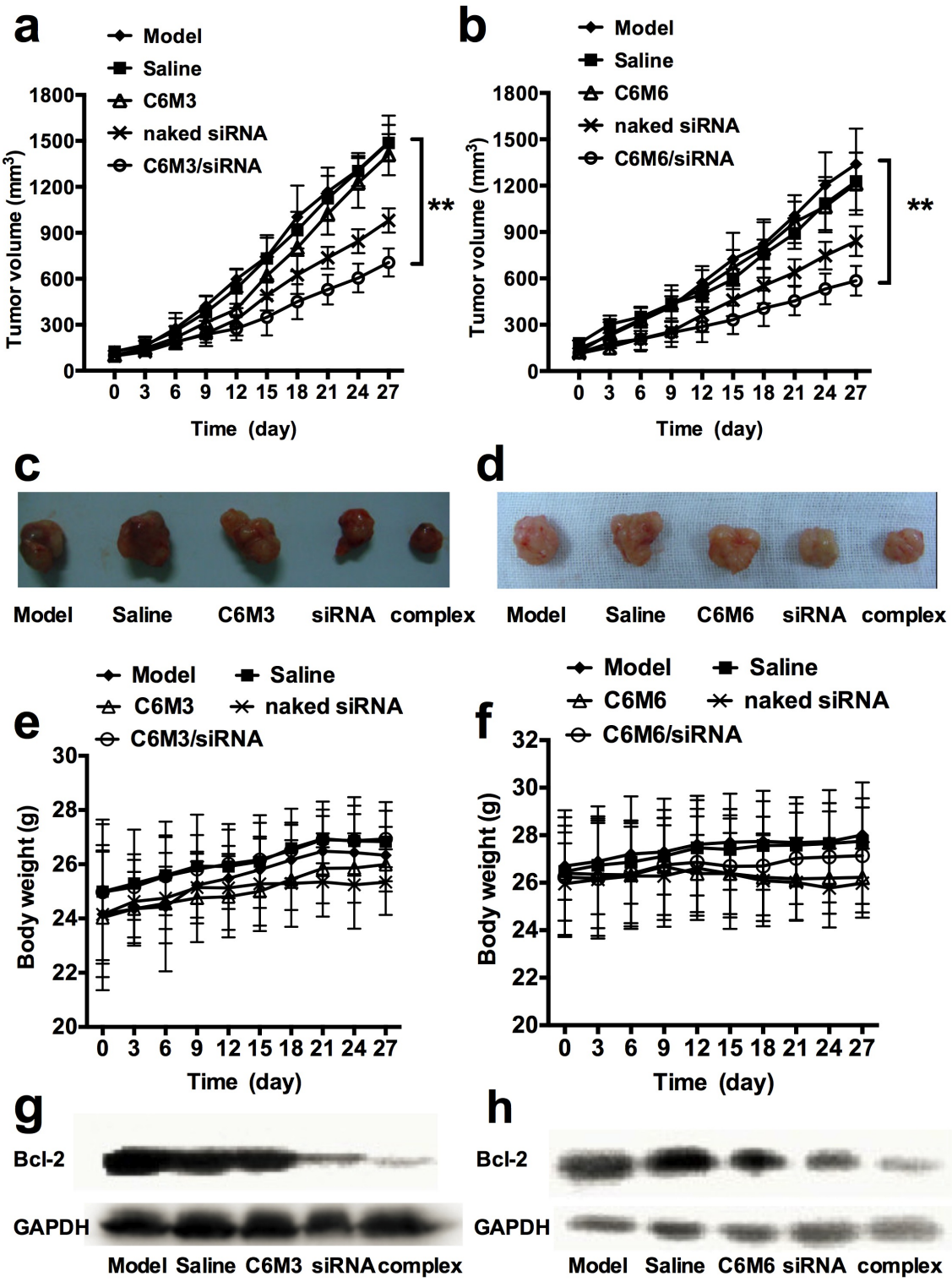

Figure 5.7 Suppression of tumor growth in a non-small cell lung cancer xenograft mouse model by peptide based delivery of Bcl-2 siRNA. BALB/c nude mice (N=8) were

injected subcutaneously with 5×10^6 A549. When the tumor volume reached 100-200 mm^3, animals were treated by intratumoral injection of 20 μl saline solution, free Bcl-2 siRNA (4 μg/mouse), peptide alone or Bcl-2 siRNA (4 μg/mouse) complexed with C6M3 or C6M6 at a 1/60 molar ratio, every three days. Curves show the mean value of each group. (a) (b) Tumor diameters were measured during treatment. The tumor volume was calculated as Tumor volume=$0.5\times(\text{width})^2\times\text{length}$. ** $P< 0.01$ versus nontreated control. (c)(d) Images of tumors excised from the tumor-bearing mice on day 27 after treatments. (e)(f) Body weight of each mouse was monitored during treatment to evaluate toxicity. (g)(h) Total proteins were extracted from tumor tissues. Bcl-2 protein expression was detected by western blot. House keeping protein GAPDH was used as control.

5.4 Conclusions

In the present work, various numbers of histidine residues were placed in a prototype peptide C6 in an effort to aid in the endosomal release of siRNA, thereby improving its intracellular delivery. Preliminary GAPDH protein assay reveals that all the modifications increased the biological activity of siRNA with varying degrees. The transfection efficiency seems not solely depend on the number of histidine residues in the sequence, as peptides with same histidine numbers vary by effect in silencing efficiency. Two peptides C6M3 and C6M6 achieving above 60% knockdown efficiency were selected for further in-depth study. These two peptides could saturate all the negative charges of siRNA molecules at molar ratio 40/1 and 60/1, assessed by RiboGreen intercalation assay. The formed complexes are around 100 nm at molar ratio 60/1, with a

more than 30 mV surface charge enough for stability. Subsequent experiments focused on the biological effect of peptide/siRNA complex reveals its strong uptake in CHO-K1 cell line and its ability to reduce GAPDH gene expression with low cytotoxicity. In addition, this peptide-based delivery system is biocompatible, as it has been shown that no complement or cytokines were stimulated after treatment with peptides in vitro. Furthermore, we tried to suppress tumor growth by regulating Bcl-2 protein level, which enhances the growth of tumors by suppressing apoptosis. The in vivo results show that the reduction in Bcl-2 protein level could inhibit tumor growth in a mouse xenograft tumor model. Collectively, in vitro and in vivo data suggest our new carriers based on peptides C6M3 and C6M6 promote the delivery of siRNA into tumor cells, and might have therapeutic utility in a variety of diseases.

Chapter 6

Rational modification of cell penetrating peptides for highly efficient siRNA delivery: structure-activity relationship and mechanism of intracellular trafficking of siRNA

6.1 Introduction

RNA interference (RNAi)-mediated silencing offers one of the most attractive methods of gene therapy for many diseases. Many types of diseases including viral infections and cancers have been demonstrated to be potential targets for RNAi based therapy [59,216,217]; however efficient delivery of short interfering RNAs (20~25 base pairs) (siRNAs), the molecules that mediate RNAi, is still a key challenge in realizing the full potential of RNAi therapeutics [218].

siRNAs must first enter target cells, typically by endocytosis, cross the endosomal membrane to be released into the cytosol, and finally get loaded onto the RNA-induced silencing complex (RISC) for silencing of the target gene [2,4]. However, passive diffusion of "naked" siRNAs across biological membranes is impeded by the physicochemical properties of the siRNA, including their high molecular weight, negative charge and hydrophilicity [219,220]. Thus, different systems have been developed for siRNA delivery by taking advantage of viral or nonviral vectors. Viral

vectors are highly efficient but they bear an inherent risk for the patient to encounter severe immunological responses or even develop cancer [221–223]. These problems in viral delivery have initiated an intense search for efficient non-viral delivery systems. Common non-viral siRNA delivery systems include cationic lipids and polymers. These vectors have various levels of efficiency and toxicity, but for most clinical indications still remain unsatisfactory [224–231]. Hence, the development of appropriate delivery systems is still an essential requirement to turn these molecules into medicine.

Recently, cell-penetrating peptides (CPPs), consisting of short cationic or amphipathic sequences of about 5-30 amino acids, have received much attention owing to their low toxicity, along with their ability to translocate through plasma membranes [85,232,233], which is a significant barrier for siRNA access to the intended targets in the cytoplasm. In most cases, however, the CPP/siRNA complexes were either internalized by the cells only in very low amounts, or the internalized CPP/siRNA complexes were trapped in endosomes, therefore inducing little or no gene silencing [98,234–236]. In terms of cellular uptake, stearyl modification of CPPs has significantly improved the internalization of siRNA by cells in comparison to the unmodified peptide [237]. For CPP/siRNA entrapments inside the endosomes, it is highly desirable to modify these complexes in order to facilitate their endosomal escape. Two main mechanisms are currently proposed to explain the escape of biologicals induced by peptides. The first is the “proton sponge” effect [238], that relies on protonable groups in the molecules with pKa values close to the endosomal/lysosomal pH. This will lead to a higher influx of protons, along with chloride ions and water, resulting in inevitable endosomal swelling and rupture. This release mechanism of contents to the cytosol has been established for

polyhistidine based delivery systems [238,239]. The second mechanism is pH-sensitive membrane disruption [240,241]. The hypothesis is that as endosomes acidify, endocytosed pH-sensitive peptides shift from an inactive state to an active, membrane-disruptive state. In line with this concept, a histidine-rich peptide [242] and a pentadecaarginine (R15)-PLGA-PEG polymer [243] with pH-sensitive membrane disruption capability have been developed.

In this study, by taking all this knowledge into account, we undertake a rational design of CPP derivatives aiming to provide highly efficient siRNA delivery. First, oligoarginine, one group of the most widely utilized CPPs for intracellular delivery of biologicals, is employed as a model carrier because it can bind to the cell surface with high affinity [244] and is additionally more effective at entering cells than oligolysine, oligoornithine and arginine-rich peptides [146,245]. Second, in order to overcome the lack of silencing activity induced by oligoarginine [236,246], we introduce stearic acid and various oligohistidine modifications that are found to significantly enhance cellular uptake and endosomal escape of siRNA. Moreover, we hypothesize that hydrophobic stearyl groups conjugated to a peptide sequence would improve the co-assembly of peptide with siRNA in forming nanoparticles (<200 nm) in aqueous solution due to their hydrophobic interaction. We explore in detail the relationship between structures and properties of the oligoarginine based molecules with their biological activities. Particularly, we demonstrate that the residue number ratio of histidine/arginine in a stearylated peptide sequence is important for inducing pronounced gene silencing, and use this knowledge to deliberately design stearylated and oligohistidylated oligoarginine based siRNA carriers that have significantly improved efficiency compared to the most

commonly used benchmark delivery systems, Lipofactamine 2000 (Lipo). Finally and most notably, we discover the mechanism of intracellular siRNA release mediated by the carrier. In culmination, not only do these newly developed, highly efficient carriers provide practical advancement in terms of siRNA delivery, the understanding surrounding oligoarginine-based siRNA delivery system developments reported herein will provide valuable guidance for future investigation of CPP-based siRNA vectors. Figure 6.1 demonstrates the whole process of peptide mediated siRNA delivery, from peptide-siRNA binding, internalization, intracellular trafficking, to endosomal release and RNA interference.

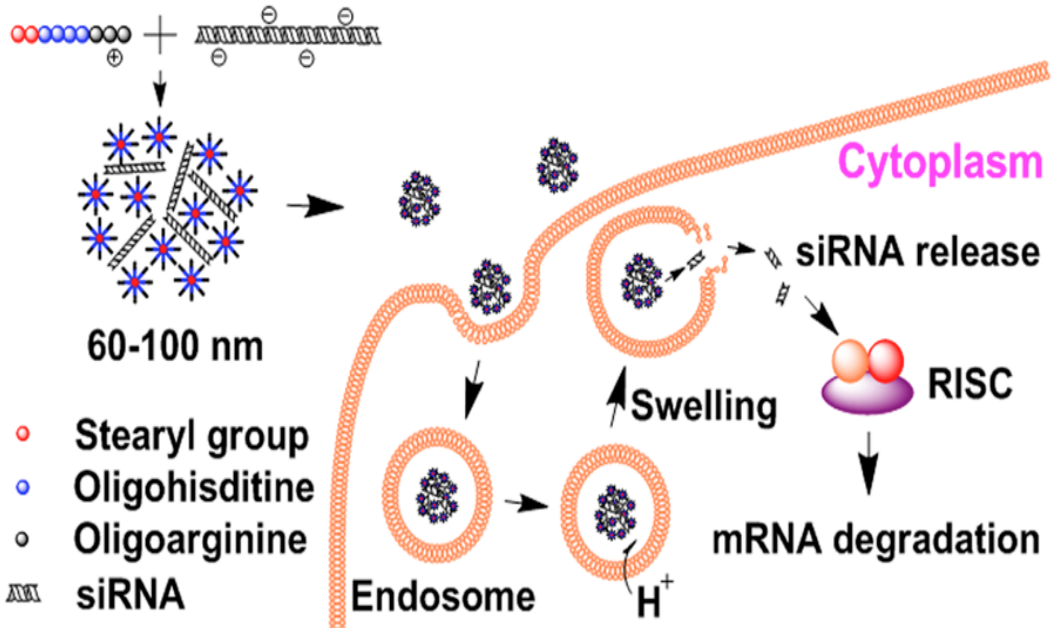

Figure 6.1 Schematic diagram depicting the application of stearylated and oligohistidylated oligoarginine based peptide as siRNA carriers.

6.2 Materials and Methods

6.2.1 Materials

Peptides, stearylated peptides and siRNA: The R8, R15, STR-R8 and STR-H12R8 were synthesized in bulk (CanPeptide Inc., Pointe-Claire, Canada). The H16R8, STR-H8R8, H8R15, STR-H8R15, STR-H16R8 and STR-H20R8 were synthesized in bulk by Pepscan (Lelystad, The Netherlands). Silencer^{TM} GAPDH siRNA (Life Technologies, Carlsbad, USA) was used to target the glyceraldehyde 3-phosphate dehydrogenase (GAPDH) gene. The sense sequence was 5'-GGU CAU CCA UGA CAA CUU Utt-3' and antisense sequence was 5'-AAA GUU GUC AUG GAU GAC Ctt-3'. The Silencer^{TM} Cy3-labeled GAPDH siRNA (Life Technologies, Carlsbad, USA) was used in confocal laser scanning microscopy (CLSM) and Fluorescence Activated Cell Sorting (FACS). The scrambled siRNA (Life Technologies, Carlsbad, USA) was used as negative control in the experiments.

6.2.2 Cell culture

CHO-K1 (Chinese hamster ovary) cells were purchased from American Type Culture Collection (ATCC CCL-61). Cells were cultured in F-12K (Thermo scientific, Ottawa, Canada) supplemented with 10% fetal bovine serum (FBS, Sigma-Aldrich, Oakville, Canada). The Hela cells were obtained from American Type Culture Collection (ATCC CCL-2), and cultured in Eagle's Minimum Essential Medium (Thermo scientific, Ottawa, Canada) with 10% heat-inactivated FBS. All of the cells were incubated at 37°C in a humidified atmosphere containing 5% CO_2.

6.2.3 Preparation of the complexes

Both of the powders of the modified or unmodified peptides and siRNA were dissolved in RNase free water, respectively. The complexes were formed by mixing the two solutions at various molar ratios of arginine residues in peptides to phosphate groups of siRNA (R/P ratio). Lipofactamine 2000 (Lipo) (Life Technologies, Carlsbad, USA), a commercial transfection reagent, was also diluted in RNase free water and mixed with the siRNA solution to form complexes with the final concentration of 20 μL Lipo/mL. The final siRNA concentration was 1μM for all the samples containing complexes, which were incubated for 20 minutes at room temperature before characterization and siRNA release study. The samples were diluted further to 10% of the original concentration in Opti-MEM medium (Life Technologies, Carlsbad, USA) before transfection.

6.2.4 Particle size and zeta potential

The hydrodynamic diameter of the complexes were measured on a Zetasizer Nano ZS (Malvern Instruments, Malvern, UK) equipped with a 4 mW He-Ne laser operating at 633 nm. A quartz microcell (45 μL) with a 3 mm light path was used and the scattered light intensities were collected at an angle of 173°. Zeta potential measurements were also performed on the same machine using clear disposable zeta cells. Three measurements were performed to generate the intensity-based size and zeta potential plot reported herein.

6.2.5 Atomic force microscopy (AFM)

The nanostructure of the complexes was imaged on AFM. 10 μL of the sample solution containing complexes of H16R8 or STR-H16R8/siRNA with an R/P ratio of 10:1 was put on a freshly cleaved mica surface. The sample was incubated for 10 min at room temperature to allow the complexes to adhere onto mica surface. Mica was then washed at least five times with RNase free water to remove unattached complexes. After air drying, the mica surface was analyzed by a Dimension Icon AFM (Bruker, Santa Barbara, USA) at room temperature using the tapping mode with ScanAsyst-Air tips (Bruker, Santa Barbara, USA). All AFM images were obtained at a resolution of 512 × 512 pixels on a scale of 5 μm × 5 μm and 2 μm × 2 μm.

6.2.6 Transmission electron microscopy (TEM)

10 μL of sample solution containing the complexes of STR-H16R8/siRNA at R/P 10 or STR-H16R8 only in the same concentration was applied to a 400 mesh Formvar coated copper grid (Canemco-Marivac, Canton de Gore, Canada) for 3-5 minutes. The sample was then washed using 5 successive wash steps and dried overnight. The complexes was stained with uranyl acetate and analyzed using a JEOL JEM 1200 EX TEMSCAN transmission electron microscope (JEOL, Peabody, USA) operating at an accelerating voltage of 80kV. The images were acquired with an AMT 4 megapixel digital camera (Advanced Microscopy Techniques, Woburn, USA).

6.2.7 siRNA loading efficiency

RiboGreen assay was used to determine the siRNA loading efficiency using the manufacturer's protocol (Life Technologies, Carlsbad, USA). This assay is based on the

strong fluorescence of riboGreen upon intercalation with siRNA. RiboGreen solution was diluted to 1/30 (v/v) and then added to the samples (1:12, v/v). After 5 min, the RiboGreen fluorescence was measured by a QM4-SE spectrofluorometer (Photon Technology International, London, Canada) at *excitation wavelength* of 480 nm and emission wavelength of 525 nm. Free siRNA concentrations were obtained from the fluorescence using a standard curve prepared with standard siRNA solution. Peptides or stearylated peptides only were used as controls. The results were obtained from three independent experiments (n = 3).

6.2.8 Gene silencing

CHO-K1 cells (40,000/well) were plated in a 24-well cell culture plate in F-12K medium with 10% FBS. 24 h later, the medium was removed and washed with PBS, and then 300 μL of the sample solution containing the complexes of the Peptides, stearylated peptides or Lipo/GAPDH siRNA or scrambled siRNA was added to the cells. 3 h later, 300 μL of F-12K with 20% FBS was added. In case of chloroquine and bafilomycin A1, both of them was dissolved in 300 μL of F-12K with 20% FBS, respectively, which was added to the cells 3 h after the cells were treated with the complexes. Afterwards, the cells were incubated for 48 hours at 37 °C in a 5% CO_2 atmosphere. The cultures were then washed with PBS. Total RNA was extracted from the cells with TRIzol reagent (Life Technologies, Carlsbad, USA), then treated with chloroform (Sigma, Oakville, Canada) and 2-propanol (Sigma-Aldrich, Oakville, Canada) as recommended by the manufacturer. RNA concentrations were measured by Nanodrop spectrophotometer ND-1000 (Thermo scientific, Ottawa, Canada). All RNAs were reverse transcribed with Bio-Rad iScript cDNA synthesis kit (Bio-Rad, Mississauga, Canada). The cDNA synthesis was primed

with a unique blend of oligo (dT) and random primers. The following pairs of primers were used for PCR: 5′-TTGCTGTTGAAGTCGCAGGAG-3′, 5′-TGTGTCCGT-CGTGGATCTGA-3′ (Sigma, Oakville, Canada). Here, the housekeeping gene cyclophilin was chosen as an internal control to normalize the GAPDH gene. The normalization was performed by the amplification of mouse/rat cyclophilin mRNA with the following primers: 5′-AGGGTTTCTCCACTTCGATCTTGC-3′ and 5'-AGATGGCACAGGAGGAAAGA- GCAT-3′ (Sigma, Oakville, Canada). PCR reaction was performed with Brilliant II Fast SYBR Green QPCR Master Mix (Agilent Technologies, Wilmington, USA) on an Mx3005P™ Real-Time PCR System (Agilent Technologies, Wilmington, USA).

6.2.9 Fluorescence-activated cell sorting (FACS)

Cellular uptake of Cy-3 labeled GAPDH siRNA was studied using BD FACSCalibur Flow Cytometry (BD Biosciences, Mississauga, Canada). CHO-K1 cells were transfected with the cationic molecules/Cy3-labeled GAPDH siRNA complexes according to the protocol listed above. nontreated cells and naked siRNA served as a negative control. After 3 h incubation, the culture medium was discarded and cells were washed with PBS, Trypsin-EDTA was then added to detach the cells from the plate; cells were suspended in 4% PFA solution and collected.

6.2.10 Confocal laser scanning microscopy (CLSM)

CHO-K1 cells (80,000/well) were plated in a Nunc Lab-Tek 4-well glass chamber slides (Thermo scientific, Ottawa, Canada) 24 h before transfection. CHO-K1 cells were also treated with the same protocol as described above. Treated cells were incubated at 37°C

for 3 h with Opti-MEM medium. For endosomal labeling, the cells were incubated with 50 nM Lysotracker Green (Life Technology, Carlsbad, USA) for 30 min before fixing. The wells were then washed with 15 U/mL heparin (Grade I-A, ≥180 USP U/mg, Sigma-Aldrich, Oakville, Canada) for three times in one hour at 37°C and fixed with 500 μL/well of fresh 4% paraformaldehyde (PFA) in phosphate buffered saline (PBS) at 37°C for 30 min. The fixation agent was aspirated, and the cells were washed twice with PBS before they were covered with Fluoroshield with DAPI mounting medium (Sigma-Aldrich, Oakville, Canada). Carl Zeiss LSM 700 Confocal laser scanning microscopy (Zeiss, Jena, Germany) was used to visualize the cells. The microscope was equipped with Plan-Apochromat 20x/0.8 NA objective lens. The images were analyzed with LSM Zen 2009 software.

6.2.11 Membrane integrity assay

CHO-K1 cells (8,000/well) were plated on 96-well plates and incubated overnight in 100 μL of F-12K medium containing 10% FBS. The cell culture medium was removed and washed with PBS. The modified and unmodified oligoarginine were dissolved in Opti-MEM medium with pH 7.4, pH 6.3 and pH 5.5, respectively. After stand for 5 min, the solution was added to the cells. After the incubation at 37°C for 3 h, the plates were centrifuged. 50 μL of aliquots in each well were collected for the LDH assay. The LDH activity in these samples was determined using a CytoTox 96 Non-Radioactive Cytotoxicity Assay kit (Promega, Madison, USA) according to the manufacturer's protocol, which determined the LDH activity from the amount of produced red formazan product by a colorimetric assay. The amount of formazan produced was assessed by measuring the absorbance at 490 nm with a FLUOstar OPTIMA microplate reader (BMG

Labtech, Ortenberg, Germany). Percentages of the LDH activity in each well were calculated from a ratio of the obtained value to the control well containing 10 μL lysis buffer.

6.2.12 pH-dependant siRNA release

The solutions containing the complexes at R/P 10 were diluted to 10% of the original concentration in a serial dilution of heparin in PBS, pH7.4 or 5.5, respectively. 15 min later, the released siRNA was determined by the RiboGreen method as described above in "siRNA loading efficiency".

6.2.13 Cytotoxicity assay

CHO cells were plated in to 96-well plates (8,000 cells/well) in F-12K medium with 10% FBS. 24 h later, the medium was removed and washed with PBS. The solutions containing carriers were prepared in RNase free water and diluted by Opti-MEM medium to 10% of the original concentration. After stand for 5 min, 60 μL of the solution was added to the cells. 3 h later, 60 μL F12-K medium with 20% FBS was added. After incubation for 24 hours at 37 °C in a 5% CO_2 atmosphere, the cultures were washed with PBS. 100 μL of Opti-MEM medium with CCK-8 reagent was then added to each well. Cell viability was assessed by measuring the absorbance at 570 nm with a FLUOstar OPTIMA microplate reader and expressed as the ratio of the cells treated with the carriers over the nontreated cells (negative control).

6.3 Results and Discussion

6.3.1 Modification of oligoarginine

It has been reported that oligoarginine uptake increases with increasing charge, peaking between octaarginine (R8) and pentadecaarginine (R15) [146,245]. For this reason, in our approach, ten peptides were designed and investigated including R8 and R15, along with their high purity derivatives obtained by modification with oligohistidine and a stearyl moiety synthesized by a solid-phase synthesis method and purified by HPLC (Table 6.1).

Table 6.1 Sequences of the unmodified and modified oligoarginine complexes along with their molecular weight and purity. These compounds were synthesized by a solid-phase synthesis method and purified by HPLC

Name	Sequences[1]	MW[2]	Purity[3]
R8	Acetyl-RRRRRRRR-NH2	1,308.6	98.8
STR-R8	Stearyl-RRRRRRRR-NH2	1.533.0	96.8
STR-H8R8	Stearyl-HHHHHHHHRRRRRRRR-NH2	2,630.2	94.0
R15	Acetyl-RRRRRRRRRRRRRRR-NH2	2,401.9	98.8
H8R15	Acetyl –HHHHHHHHRRRRRRRRRRRRRRR-NH2	3,499.1	99.4
STR-H8R15	Stearyl-HHHHHHHHRRRRRRRRRRRRRRR-NH2	3,723.6	92.4
STR-H12R8	Stearyl-HHHHHHHHHHHHRRRRRRRR-NH2	3,178.7	96.0
H16R8	Acetyl-HHHHHHHHHHHHHHHHRRRRRRRR-NH2	3,503.0	99.9
STR-H16R8	Stearyl-HHHHHHHHHHHHHHHHRRRRRRRR-NH2	3,727.4	98.3
STR-H20R8	Stearyl-HHHHHHHHHHHHHHHHHHHHRRRRRRRR-NH2	4276.0	98.7

[1] N-term acetylation or stearylation and C-term amidation
[2] Molecular weight of dalton by LC/MS
[3] by HPLC, %

6.3.2 Particle size and morphology of peptides/siRNA complexes

We first examined the ability of the ten peptides to form nano-sized complexes with siRNA. For all the non-stearylated and stearylated peptides only, no diameters were detected, which indicated that these molecules were not self-assembled, but freely dissolved in water. This highlights that hydrophilicity as well as the positive charges of the peptides impeded the aggregation of hydrophobic stearyl moieties. Ideally, cationic carrier/siRNA complexes should be smaller than 200 nm to: (i) ensure optimal diffusion through tumor tissues by the enhanced permeation retention effect (EPR) [247]; and (ii) reduce the recognition and removal by phagocytic cells *in vivo*. At various molar ratios of arginine residues in peptides to phosphate groups of siRNA (R/P ratio), un-stearylated peptides of R8, R15, H8R15 and H16R8 failed to condense the siRNA into nanoparticles (<200 nm). This was especially apparent for H8R15 and H16R8, which can only form complexes with siRNA having particle sizes > 1 μm and polydispersity index (PDI) > 0.5. Conversely, peptides with stearic acid modification—STR-R8, STR-H8R8, STR-H8R15, STR-H12R8, STR-H16R8 and STR-H20R8 showed particle sizes of less than 200 nm at various R/P ratios (Table 6.2), indicating the stearic acid moiety was able to assist peptides to condense siRNA into small complexes suitable for transfection.

Table 6.2 Particle Size of the unmodified and modified oligoarginine/siRNA complexes, determined by dynamic light scattering (DLS) measurements. The complexes were formed by mixing the solutions of cationic carriers and siRNA with the final siRNA concentration of 1μM at various molar ratios of arginine residues in peptides versus phosphate groups of siRNA (R/P ratio).

Name	R/P[1] 2.5 (nm)	PDI[2]	R/P 5 (nm)	PDI	R/P 10 (nm)	PDI
R8	415±154	0.48±0.17	288±13	0.18±0.03	364±19	0.39±0.1
STR-R8	120±35	0.31±0.06	89±15	0.29±0.04	73±14	0.24±0.04
STR-H8R8	65±16	0.22±0.02	71±9	0.27±0.01	78±7	0.29±0.03
R15	257±27	0.35±0.09	> 1μm	> 0.5	> 1μm	> 0.5
H8R15	> 1μm	> 0.5	> 1μm	> 0.5	> 1μm	> 0.5
STR-H8R15	64±8	0.31±0.05	78±5	0.29±0.05	77±8	0.28±0.04
STR-H12R8	88±2	0.31±0.01	95±3	0.28±0.03	89±2	0.27±0.01
H16R8	> 1μm	> 0.5	> 1μm	> 0.5	> 1μm	> 0.5
STR-H16R8	79±11	0.22±0.03	88±12	0.3±0.03	75±9	0.31±0.03
STR-H20R8	89±13	0.29±0.05	95±7	0.32±0.04	92±7	0.29±0.04

[1] R/P: Molar ratio of arginine residues in peptides versus phosphate groups of siRNA

[2] PDI: Polydispersity index

AFM and TEM imaging also supported the DLS size measurements, showing no regular nanoparticles for H16R8/siRNA and peptide STR-H16R8 only (Figure 6.2a and 6.2b).

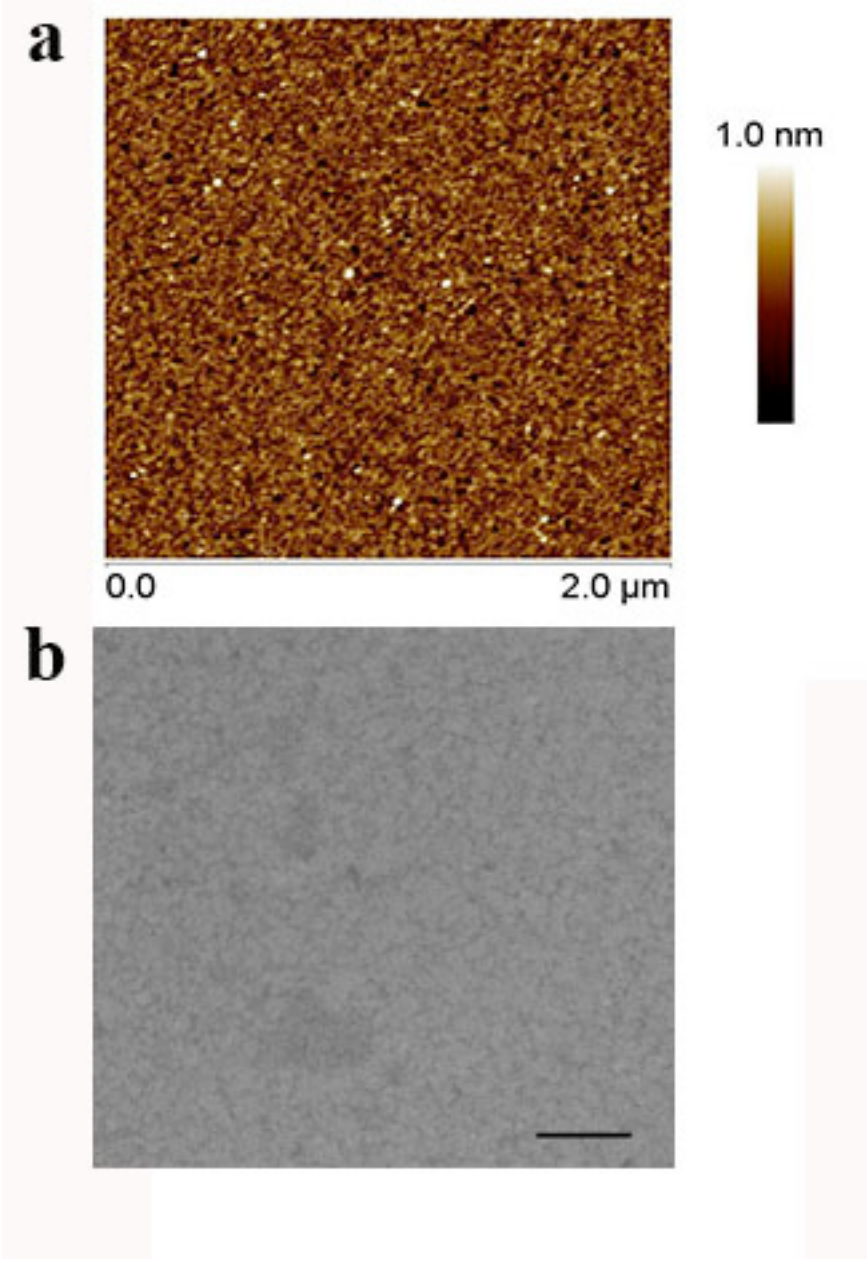

Figure 6.2 (a) AFM image of H16R8/siRNA complexes does not reveal the formation of regular nanoparticles with 1μM siRNA concentration at R/P 10. (b) TEM image of STR-H16R8 only shows no nanoparticles. The concentration of STR-H16R8 is in accordance with that at R/P 10. Scale bar is 100 nm.

AFM images depict the presence of distinct nanoparticles with an average diameter of 70 nm for STR-H16R8/siRNA complexes (Figure 6.3). The larger height (2.6 nm, Figure 6.3b) of STR-H16R8/siRNA complexes than that from H16R8/siRNA (1.1 nm) also suggested the formation of nanoparticles between peptide STR-H16R8 and siRNA. TEM image of STR-H16R8/siRNA (Figure 6.4a) also confirm the formation of uniform sized particles. These indicated that the hydrophobic stearyl moiety could significantly improve the formation of the nano-scaled complexes between siRNA and the cationic carriers, even with the addition of oligohistidine. The reason would be that the negative charge on siRNA molecules neutralizes the positive charge of the peptides, leading to a reduced intermolecular repulsion from arginine residues, and consequently improving the hydrophobic interaction of stearyl groups.

The zeta potentials of R8/siRNA complexes at R/P 2.5 and 5 were 15.2 and 19.2 mV, but increased to 22.4 mV at R/P 10. We only measured the zeta potential of R15/siRNA complexes at R/P 2.5 to be 19.8 mV, because the particle size can be detected only at this R/P ratio (Table 2). The zeta potentials of stearylated peptides/siRNA complexes at R/P 2.5 to 10 were all in the range of 20~30 mV, which is suitable for gene transfection (Figure 6.4b).

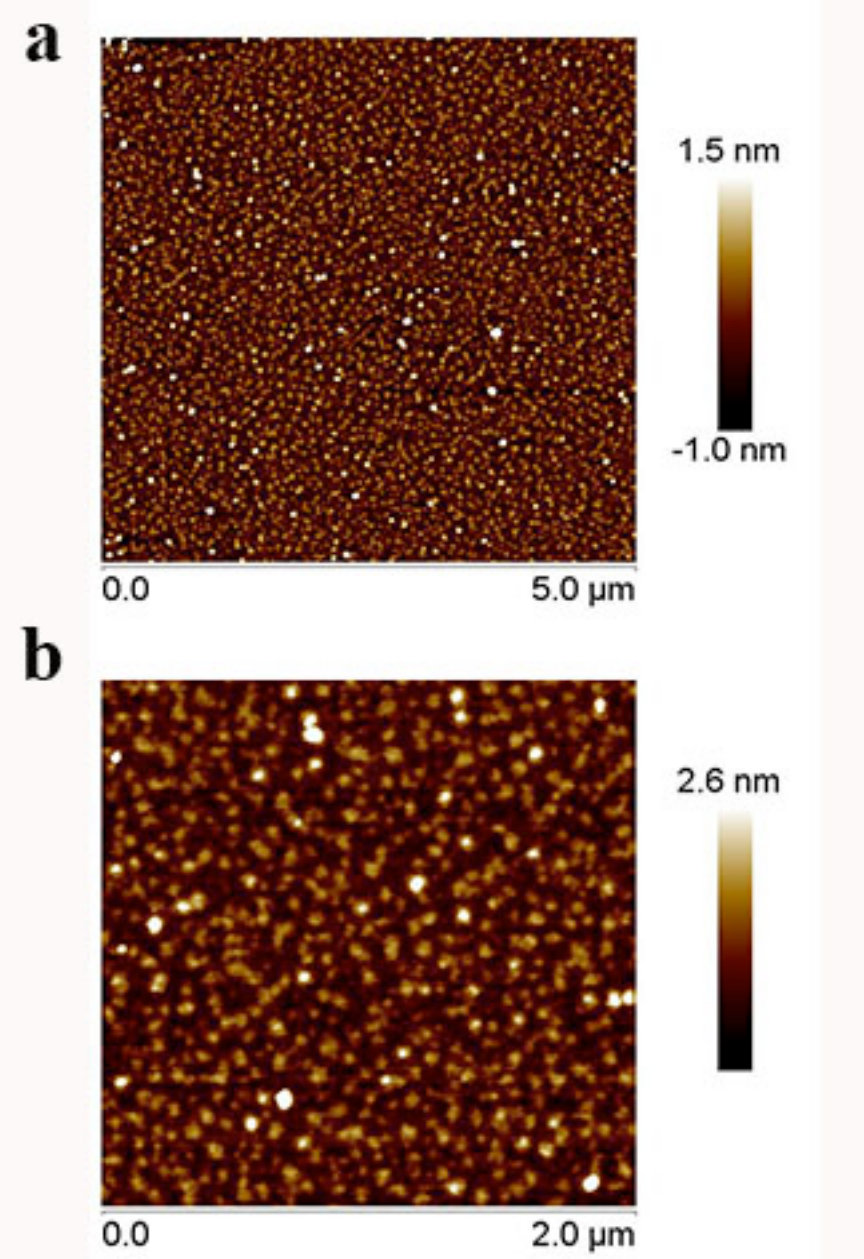

Figure 6.3 AFM images of STR-H16R8/siRNA complexes at a 5 µm × 5 µm scale and 2 µm × 2 µm scale. AFM image reveals an average particle size of 70 ± 8 nm (n = 96).

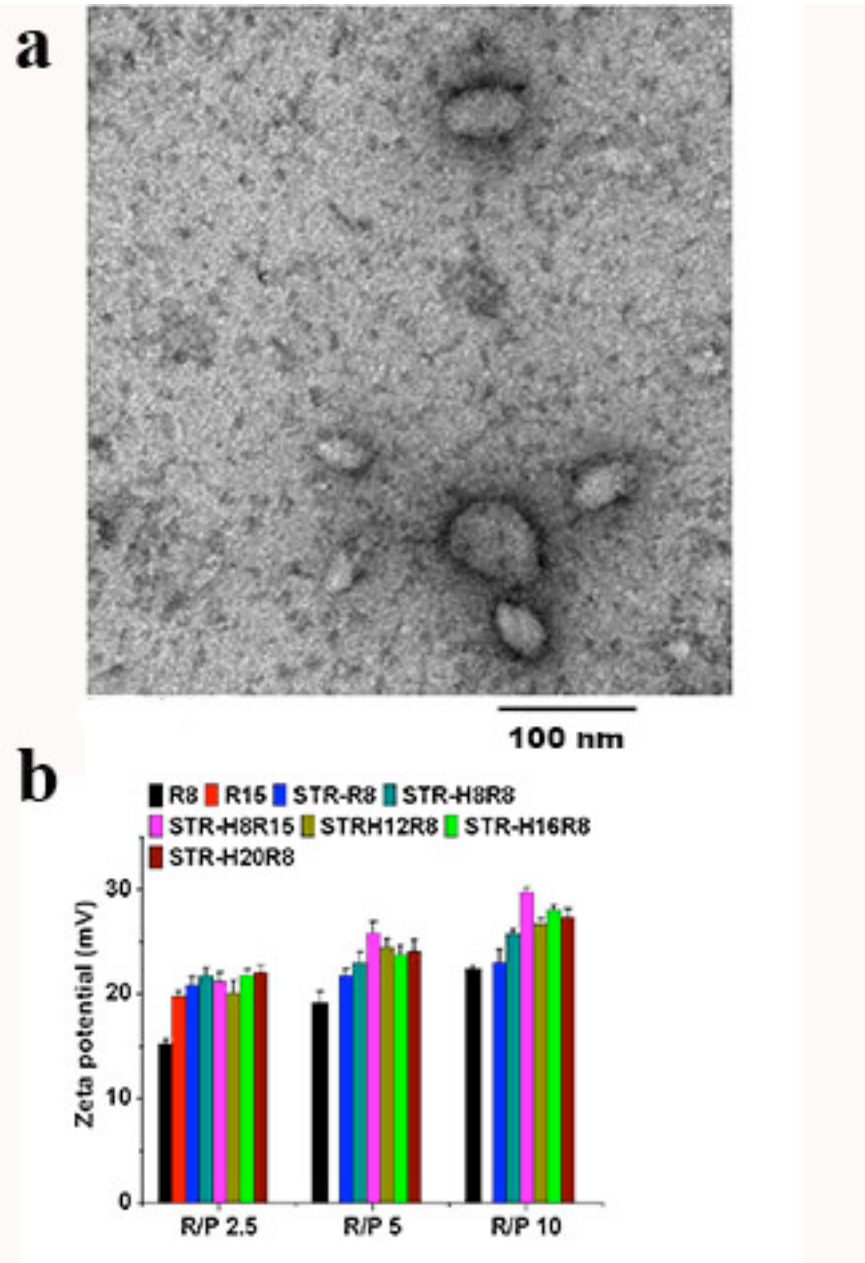

Figure 6.4 (a) TEM image of STR-H16R8/siRNA complexes with siRNA concentration of 1μM at R/P 10. (b) Zeta potential of the oligoarginine based peptides/siRNA complexes at R/P ratios of 2.5, 5 and 10. The concentrations of the complexes were the same as that of the particle size measurement. The results indicated that stearylation modification on oligoarginine increased the surface charges of the complexes.

6.3.3 siRNA binding capacity of peptides

To gain deeper insight into the interactions occurring between these oligoarginine-based molecules and siRNA, siRNA loading capacities were determined by RiboGreen assay. This assay was based on the strong fluorescence of RiboGreen upon intercalation with free siRNA. In this assay, H16R8 and H8R15 were not included as they were difficult to form nanoparticles with siRNA at various R/P ratios.

Generally, R8, R15, STR-R15 and STR-(H)nR8 (n=0, 8, 12, 16 or 20) showed significant fluorescence quenching above an R/P ratio of 2.5, meaning these molecules could condense siRNA efficiently above this ratio (Figure 6.5). For an R/P ratio of < 2.5, R8 exhibits less siRNA binding capacity than the corresponding stearylated R8. This confirmed that the stearyl moiety could help condense siRNA more efficiently to form smaller complexes as shown in Table 2. Interestingly, after the conjugation of oligohistidine, fluorescence quenching was clearly increased with extended chain length of oligohistidine in the order of STR-H20R8 > STR-H16R8 > STR-H12R8 > STR-H8R8 > STR-R8. We assumed that a portion of histidine (pKa of the side chain is 6.0) residues in the stearyl-oligohistidine-oligoarginine were positively charged in aqueous solutions and interact with siRNA as well, so that they can show a more pronounced binding effect. In the case of STR-H8R15 however, this assumption is not suitable, since at the same R/P ratio, the number ratio of histidine/arginine in the sequence was only 0.53, far lower than that of STR-H8R8 and STR-H12R8 with the histidine/arginine ratio of 1 and 1.5, respectively. However, the binding capacity of STR-H8R15 is higher than those of STR-H8R8 and STR-H12R8. This phenomenon suggested that the extended chain length of oligoarginine improved the condensing of siRNA significantly, which surpassed the

contributions made by histidine residues to the siRNA binding. In terms of unmodified oligoarginine peptides, R15 also showed a higher siRNA binding capacity than that of R8, verifying that longer oligoarginine had greater capability to condense siRNA compared with the short one.

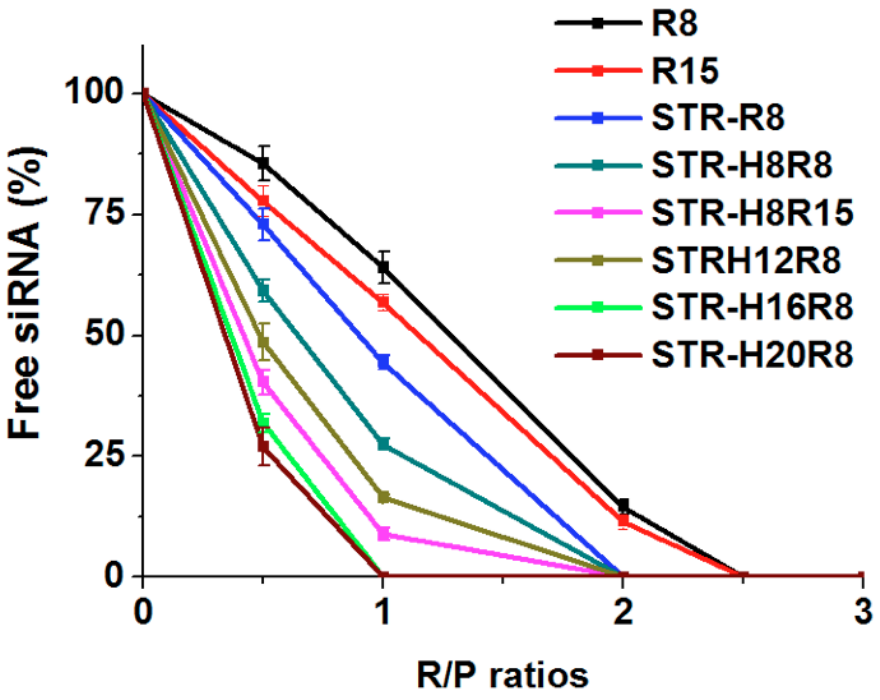

Figure 6.5 siRNA binding capacity of the unmodified and modified oligoarginine peptides was measured by RiboGreen intercalation assay. Initial siRNA concentration is 100 nM. Different volumes of peptide stock solution were added to the fixed siRNA concentration to obtain peptide/siRNA charge ratios from 1 to 3.

6.3.4 Gene silencing efficiency and cytotoxicity of peptide/siRNA complexes on cultured cells

The gene silencing efficacy of siRNA delivered by the individual oligoarginine-based carriers was examined using a GAPDH gene knockdown assay. The mRNA levels in CHO-K1 cells after treatment were measured by quantitative real-time PCR. As shown in Figure 6.6a, R8, R15 and STR-R8 did not induce GAPDH mRNA knockdown at various R/P ratios. The STR-H8R8/siRNA formulations showed 16 and 26% lower mRNA levels than that of nontreated cells at R/P 5 and 10, respectively. However, STR-H8R15/siRNA formulations revealed decreased mRNA levels by 17% at R/P 10, lower than that of STR-H8R8. This implied that increased chain length of oligoarginine could not improve the efficacy of siRNA delivery. Furthermore, with an increased chain length of oligohistidine, STR-H12R8 induced gene silencing with the knockdown efficiency of 31% at R/P 5 and 59% at R/P 10. Taking the positive correlation between the ratios of histidine/arginine in stearylated oligoarginine derivatives and knockdown efficiency into consideration as well, we assumed that histidine residues would play an important role in the cellular delivery of siRNA. Following this finding, we extended the chain length of oligohistidine further in stearylated and oligohistidylated R8 molecules, and STR-H16R8 and STR-H20R8 were evaluated in gene silencing assays. STR-H16R8 showed significant gene knockdown levels of 50% at R/P 5 and 88% at R/P 10. The latter value was similar to that of a benchmark, Lipofactamine 2000 (Lipo), which is the most commonly utilized and efficient transfection reagent to introduce siRNA into cells, inducing 84% gene silencing in this assay. Moreover, the knockdown efficiency was improved further to 92% by STR-H20R8, which verified the established theory very well.

When these oligoarginine-based peptides are used as siRNA delivery agents, a low cytotoxicity is critical. The followed investigation therefore was evaluation of the cytotoxicity of these cationic molecules. The viability of cells treated with R8, R15 and modified R8 was almost the same as that in nontreated cells. However, Lipo showed slight cytotoxicity with only 87% of the cells surviving (Figure 6.6b). The STR-H8R15 showed 80% cell viability at R/P 10, though the molar concentration of it was much lower than those of the molecules containing R8 at the same R/P ratio, which would be due to that both the longer chain length of oligoarginine and stearyl group improved the interaction between it and cell membrane. Hela cells were also employed for the mRNA knockdown study, which showed a similarly higher silencing efficiency induced by STR-H16R8 than that of Lipo (Figure 6.7a). STR-H16R8 did not show any cytotoxicity up to R/P 10 in Hela cells as well (Figure 6.7b).

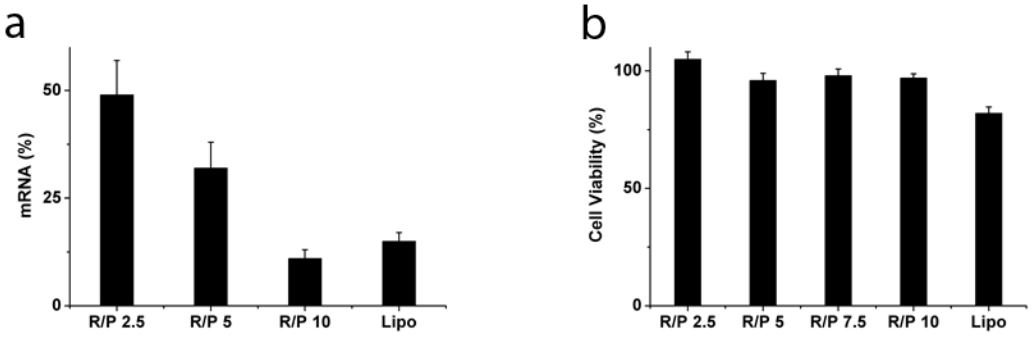

Figure 6.7 (a) Gene knockdown efficiency and (b) cytotoxicity of STR-H16R8/siRNA complexes on Hela cells. In gene knockdown assay, GAPDH siRNA was used and in cytotoxicity assay negative control siRNA was used.

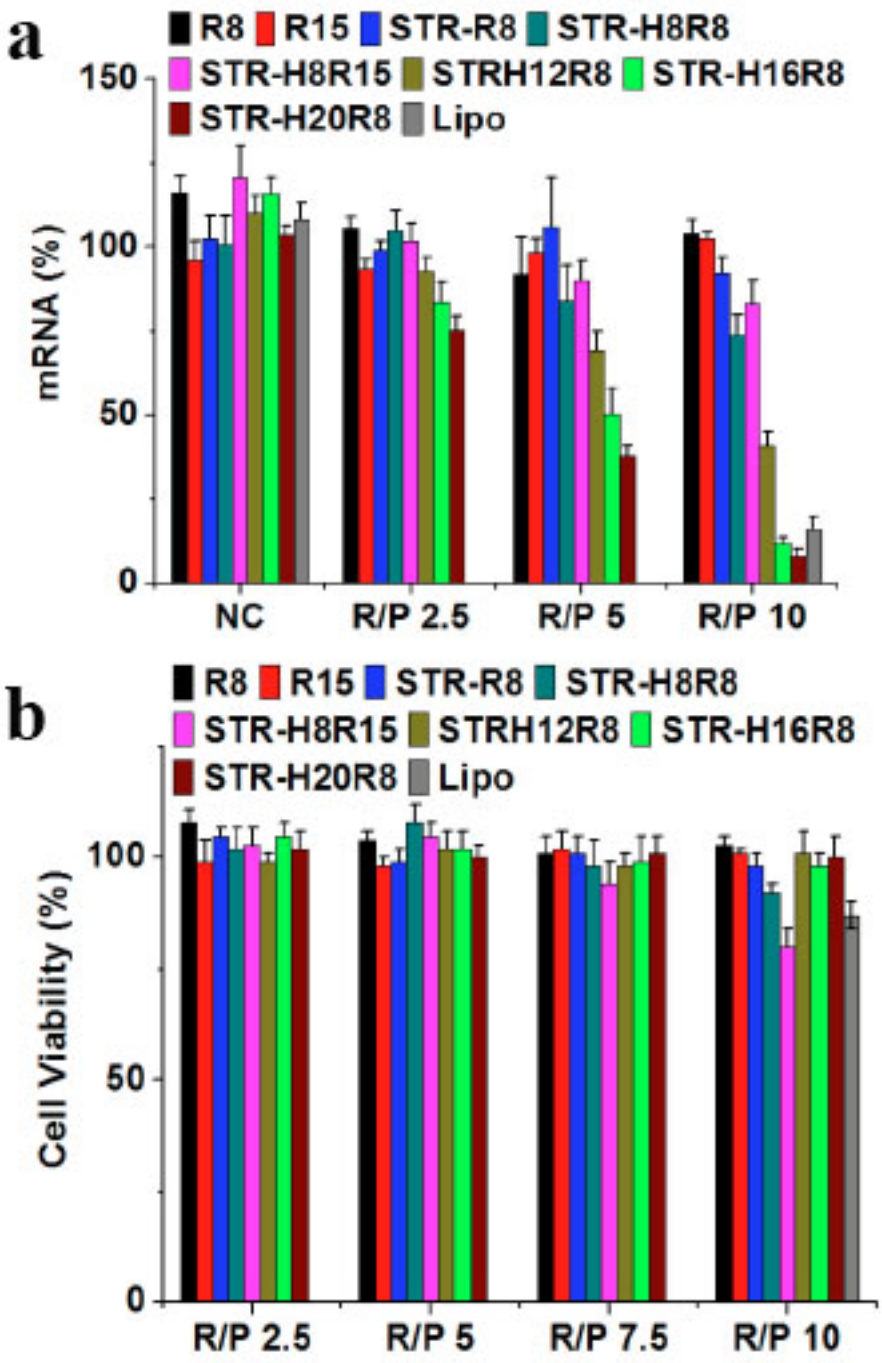

Figure 6.6 (a) Gene knockdown efficiency and (b) cytotoxicity of STR-H16R8/siRNA complexes on CHO-K1 cells. In gene knockdown assay, GAPDH siRNA was used and in cytotoxicity assay negative control siRNA was used.

6.3.5 Cellular uptake

Cellular uptake of Cy-3 labeled siRNA formulated with the carriers at R/P 10 was measured by fluorescence activated cell sorting (FACS). As shown in Figure 6.8a, in comparison to the other modified peptides R8 and R15 mediated a markedly lower internalization of siRNA, which would be one main reason for its ineffectiveness in gene silencing. In terms of stearylated peptides, STR-R8 had the highest mean fluorescence intensity of 260, with STR-H8R8, STR-H8R15, STR-H12R8, STR-H16R8 and STR-H20R8 inducing mean fluorescence intensities of 160, 195, 187, 220 and 211, respectively. These intensities were all much greater than that of Lipo, inducing a mean fluorescence intensity of 59 (Figure 6.8b). Based on these observations, we can conclude that stearylated peptides with various chain lengths of oligoarginine and oligohistidine resulted in similar cellular uptakes of the complexes. These findings were directly in accordance with the excellent ability of them to condense siRNA. Furthermore, significant differences in the efficacy of the stearylated peptide/siRNA complexes would not be attributed to the internalization of the complexes, which were only slightly different, but rather to the varying degrees of released siRNA into the cytosol, where siRNAs have to reach and then get loaded onto the RNA-induced silencing complex (RISC) for gene silencing.

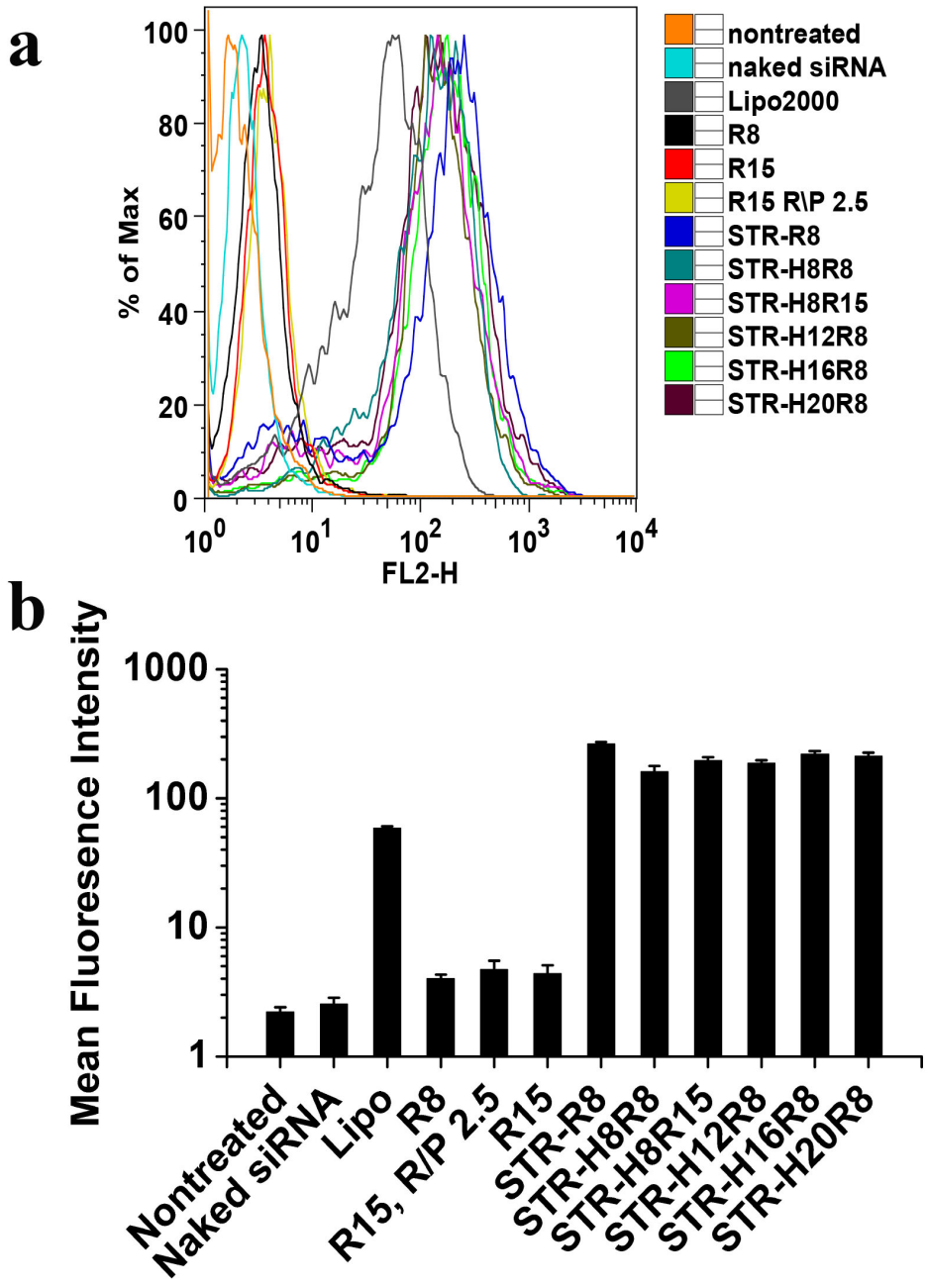

Figure 6.8 Cellular uptake of Cy3-siRNA complexes formed with the modified and unmodified oligoarginine at 3 h after the treatment in CHO-K1 cells. The same procedure as that involved in gene silencing assay was used to prepare the complexes with the final siRNA concentration of 100 nM at R/P 10 for all cationic molecules and at R/P 2.5 for

R15, only where nanoparticles can be detected. Flow cytometry and reveals the stearylated oligoarginine with or without oligohistidine segments deliver similar amounts of Cy3-labeled siRNA into cells, which were much higher than these induced by the unmodified oligoarginine.

6.3.6 Subcellular localization of peptides/Cy-3 siRNA complexes

The sub-cellular localization of the complexes was imaged using confocal laser scanning microscopy (CLSM). Particularly, DAPI was used to stain nuclei, and Lysotracker Green was used to stain endolysosomal vesicles. Figure 6.9 shows that the cells treated with the Lysotracker Green revealed a punctuate pattern of endolysosomes in the cytosol. The Cy3-labeled GAPDH siRNA with red fluorescence delivered by the two typical cationic molecules, STR-R8 and STR-H16R8, also showed a punctuate distribution pattern in the cytosol. The majority of Cy-3 fluorescence-labeled siRNA appeared to be trapped in endosomal/lysosomal vesicles as demonstrated by its extensive colocalization with the LysoTracker Green marker, visualized as yellow punctuate fluorescence. This suggested that the uptake of the complexes followed an endocytosis pathway. Moreover, for the STR-H16R8/siRNA complexes inducing high gene silencing, a small amount of the Cy3 labelled siRNA can be observed distributed in the cytosol at 6h (Figure 6.10). A zoomed in image for the co-localization of STR-H15R8/Cy-3 siRNA and lysosomes/endosomes was shown in Figure 6.11.

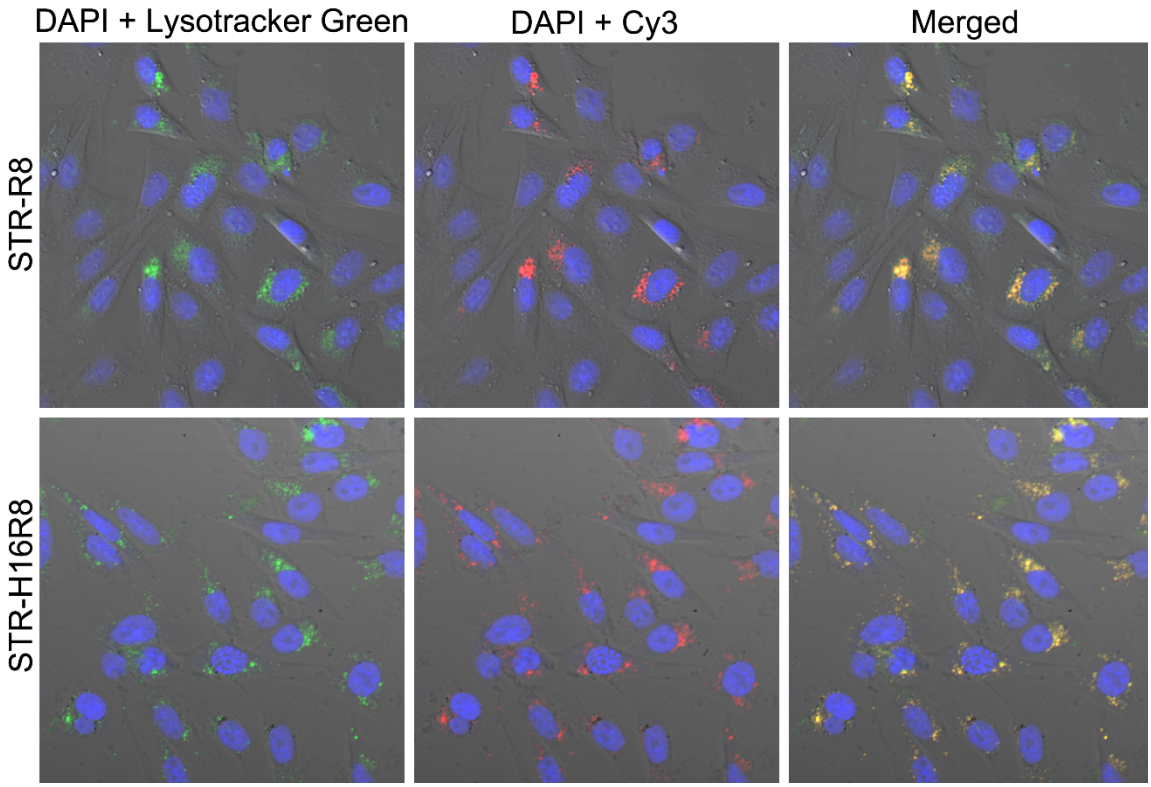

Figure 6.9 Intracellular localization of Cy-3 siRNA in CHO-K1 cells at 3 h after the treatment with STR-R8 or STR-H16R8/Cy3-labeled siRNA (red) complexes at R/P 10 with 100 nM of siRNA in Opti-MEM medium determined by confocal laser scanning microscopy. Nucleic was stained with DAPI (blue). Endosomes/lysosomes were stained with LysoTracker Green (green). Full co-localization of siRNA with endosomes/lysosomes was observed in punctuate pattern with yellow fluorescence in merged images suggesting the complexes were taken up by endocytosis. Both length and width are 160 μm for every picture. Plan-Apochromat 20x/0.8 NA objective lens was used to obtain these images.

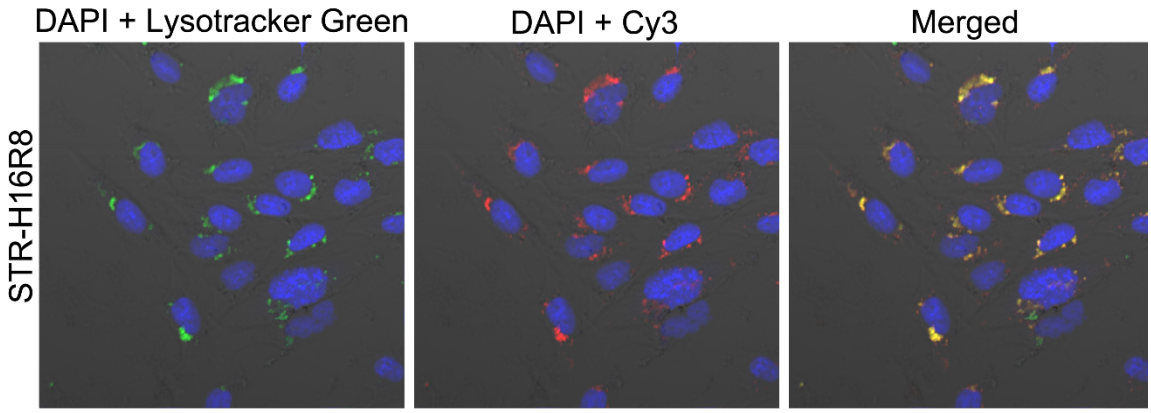

Figure 6.10 Intracellular localization of siRNA in CHO-K1 cells at 6 h after the treatment with STR-H16R8/Cy3-labeled siRNA (red) complexes at R/P 10 with 100 nM of siRNA in Opti-MEM medium determined by confocal microscopy. Nucleic is stained with DAPI (blue). Endosomes/lysosomes are stained with LysoTracker Green (green). Most of the siRNA is localized in endosome/lysosome and a small amount of siRNA can be found distributing in cytosol (red dots). The punctuate distribution pattern of yellow fluorescence increase in size and decrease in amount due to the fusion of endosome/lysosome compartments into larger vesicles [248–250]. Both length and width are 160 μm for each picture. Plan-Apochromat 20x/0.8 NA objective lens was used to obtain these images.

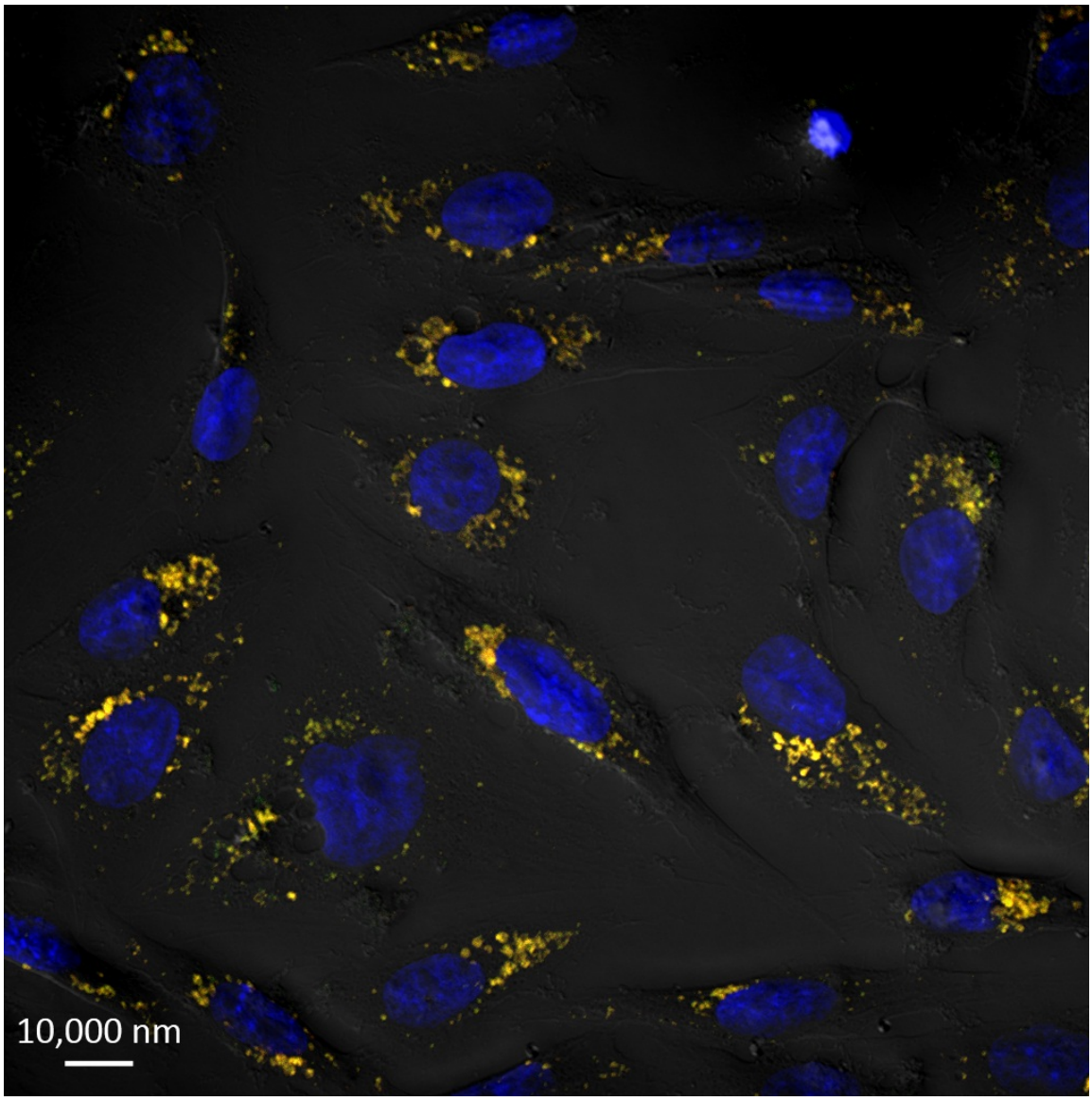

Figure 6.11 Intracellular localization of siRNA in CHO-K1 cells at 3 h after the treatment with STR-H16R8/Cy3-labeled siRNA (red) complexes at R/P 10 with 100 nM of siRNA. Nucleic is stained with DAPI (blue). Endosomes/lysosomes are stained with LysoTracker Green (green). Most of the siRNA is localized in endosome/lysosome and a small amount of siRNA can be found distributing in cytosol (red dots). Plan-Apochromat 40x/0.8 NA objective lens was used to obtain this image.

6.3.7 pH-dependant siRNA release

It has been suggested that the release of siRNA from the internalized complexes is crucial for effective gene silencing, whereby a low intracellular siRNA dissociation would most likely reduce the gene silencing efficiency [251]. On the contrary, a premature extracellular release of siRNA is also undesired. Therefore, siRNA dissociation from the stearylated peptides was investigated in PBS at pH 5.5 and 7.4, mimicking the acidic environment in the endosome/lysosome and the physiological conditions during cell culturing, respectively. Negatively charged heparin was used to represent the endogenous polyanions [252]. For STR-R8 at pH 5.5, siRNA dissociation from the complexes decreased by 15 and 10% in comparison to pH 7.4, at heparin concentrations of 0.02 and 0.05 mg/mL, respectively, while in terms of other stearylated and oligohistidylated oligoarginine, no pronounced change of siRNA release was found when the medium was acidified (Figure 6.12). These results indicated that the acidic environment did not significantly change the release of siRNA from the complexes. In both of the PBS solutions, extended chain lengths of oligohistidine and oligoarginine segments reduced the siRNA release against the heparin competition, which showed a similar order as the siRNA binding capacity of these oligoarginine based molecules (Figure 6.5). Therefore, siRNA dissociation from the internalized complexes would not be an issue in terms of hindering the effective gene silencing. This is because STR-R8 and STR-H8R8, exhibiting higher release of siRNA did not induce effective gene silencing, while STR-HnR8 (n=12, 16 or 20), inducing a higher knockdown efficiency showed a lower siRNA release. On the other hand, less replacement of siRNA by heparin indicated that siRNA could be better protected in the complexes formed with the molecules possessing longer

oligohistidine and oligoarginine chains, presumably preventing siRNA from the degradation in the endosome/lysosome more effectively. However, STR-H8R15, which protected siRNA slightly better than STR-H12R8 (showing a significant knockdown efficiency) did not induce efficient gene silencing. Thus, better protection of siRNA in the complexes, although important, would not be a determining factor to the more efficient gene silencing. However, a certain ratio of histidine/arginine (>1.5) in stearylated peptides is undoubtedly a necessity to ensure the highly efficient intracellular siRNA delivery.

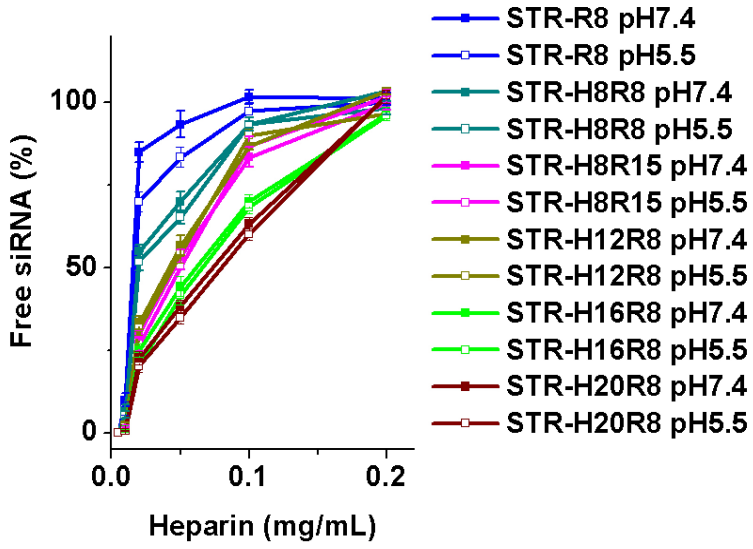

Figure 6.12 pH-dependant siRNA release performed in a serial dilution of heparin in PBS, at pH7.4 or 5.5, respectively. The free siRNA was determined by the RiboGreen method. At pH 5.5, siRNA dissociated from the STR-R8/siRNA complexes decreased slightly, while in terms of the stearylated and oligohistidylated oligoarginine, no significant change of siRNA release was found between pH 7.4 and 5.5.

6.3.8 Endosomal escape mechanism

Chloroquine (CQ) is an endosomolytic agent well known to facilitate the release of entrapped biomolecules by causing the swelling and disruption of endocytic vesicles by osmotic effects [239]. To date, CQ has been widely used to elucidate the uptake mechanism of non-viral nucleic acid delivery systems [253] To confirm that stearylated peptides/siRNA complexes are taken up by an endocytic pathway, gene silencing was carried out in CHO-K1 cells in the presence of CQ at a final concentration of 50 μM. In the case of STR-R8, which induced a high uptake of siRNA but hardly detectable gene silencing, a 13% decrease in mRNA levels was observed when it was simultaneously treated with chloroquine. The effect of CQ was more pronounced however with STR-H8R8 and STR-H16R8, showing a significant increase in gene silencing from 8% to 49% and 45 to 79%, respectively (Figure 6.13a). Therefore, on the one hand, the assay confirmed that the stearylated peptides/siRNA complexes were internalized via endocytosis. On the other hand, such different enhancements with CQ treatment confirmed that the involvement of oligohistidine in STR-R8 could enhance the endosomal escape of siRNA substantially.

All the aforementioned data clearly suggested the important effects of histidine residues on the intracellular trafficking of siRNA. Similar to CQ, the accumulation of histidine residues in endosomes can induce a “proton sponge” effect as well, which will disrupt the endosomal membranes and inevitably result in the release of trapped biologicals. Focusing on STR-H16R8, we used an inhibitor for vacuolar ATPase proton pump, bafilomycin A1 (Baf A1), to reduce the acidification of the endosomes [254,255].

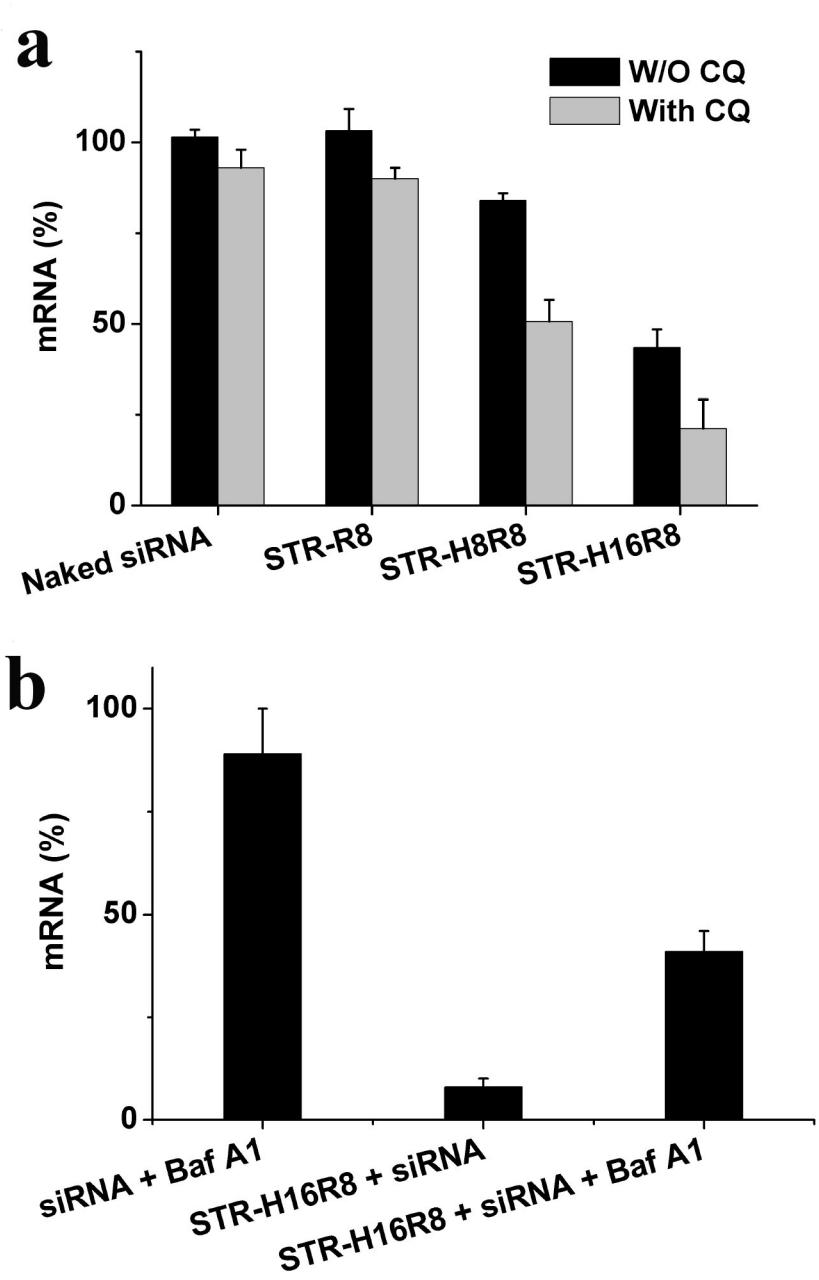

Figure 6.13 The effect of endosomal pathway inhibitors on the silencing efficiency of peptide/siRNA complexes. (a) Effect of an endosomolytic agent, Chloroquine (CQ), on gene silencing of siRNA formulated with STR-R8, STR-H8R8 and STR-H16R8 at R/P 5. CQ improved the mRNA knockdown more pronouncedly for STR-H8R8 and STR-H16R8 than that of STR-R8. (b) Acidification inhibition of endosomes induced by bafilomycin A1 (Baf A1) reduced the knockdown efficiency of STR-H16R8/siRNA complexes at R/P 10 significantly. Both of experiments were conducted in the same manner as gene silencing assay with the siRNA concentration of 100 nM, but with addition of 50 μM CQ or 20 nM Baf A1, respectively, to the wells 3 h after the CHO-K1 cells treated with the complexes.

Naturally, the inhibition of the proton pumps on the endolysosomes should weaken both the "proton-sponge" effect [256] and the pH-dependent endosomal membrane disruption [240]. Figure 6.13b showed that the addition of Baf A1 decreased the gene silencing dramatically. These findings clearly indicated that the endosomal acidification was important to help the release of siRNA formulated in the complexes from endosomes.

The pH-dependent membrane disruption was further investigated by a membrane integrity study using the lactate dehydrogenase (LDH) leakage assay [257]. In terms of all the stearylated peptides, there was no significant pH-dependent promotion of LDH leakage at various concentrations (Figure 6.14), although pH-sensitive membrane disruption was demonstrated with R8 and R15. This suggested that after stearylation or stearylation/oligohistidylation modifications, the pH-sensitive membrane disruption capabilities of the oligoarginine molecules were restrained completely. Moreover, the overall capabilities of membrane disruption were similar among these modified R8 peptides, which were surpassed slightly by STR-H8R15.

The results demonstrated that all these modified stearylated oligoarginines of various concentrations possessed similar membrane disruption capabilities at pH 5.5, 6.3 and 7.4. However, Figure 6.6 revealed that the knockdown efficiency varied remarkably between these oligoarginine derivatives. Thus, we believe that pH sensitive membrane disruption was less likely to be the major endosomal escape pathway induced by these cationic molecules. Based on the comprehensive investigations on the mechanism of endosomal escape, we therefore concluded that the "proton-sponge" effect induced by histidine residues played a predominant role in the escape of siRNA from endosomes to cytosol.

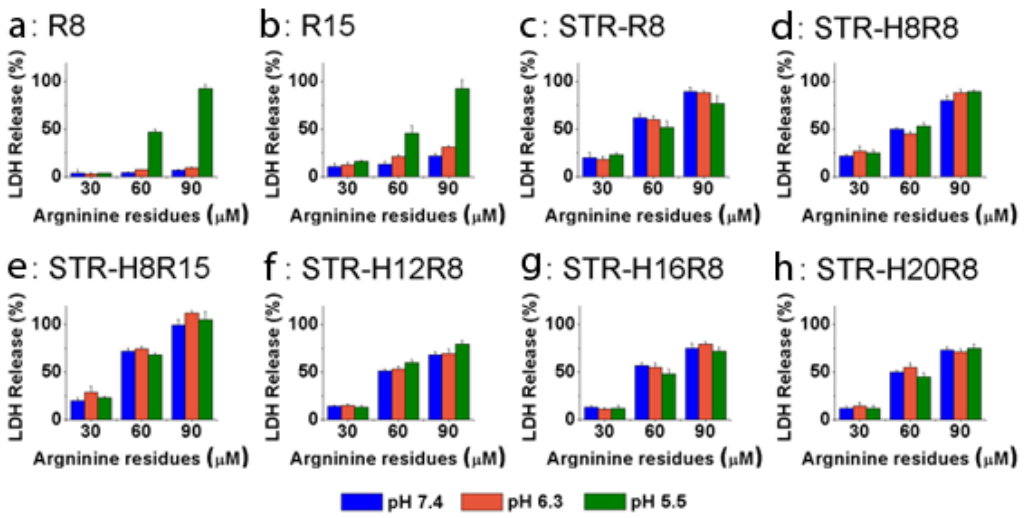

Figure 6.14 Membrane disruption ability of the unmodified and modified oligoarginine in CHO-K1 cells at pH 7.4, 6.3 and 5.5. This was measured by comparing the amount of leaked lactate dehydrogenase (LDH) in the wells with samples to the control well containing the lysis buffer. R8 and R15 showed pH-sensitive membrane disruption, while after stearylation or stearylation/oligohistidylation modifications, the membrane disruption capabilities of STR-R8, STR-H8R8, STR-H12R8, STR-H16R8 and STR-H20R8 are pH-independent and similar. The membrane disruption ability of STR-H8R15 is also not pH-sensitive but induces a slightly higher LDH leakage.

6.4 Conclusions

By fully taking into account the formation of nanoparticles, cellular uptake and intracellular trafficking of siRNA, we have rationally modified oligoarginine with stearic

acid and various oligoarginine in order to deliver siRNA with high efficiency. Furthermore, the relationship between the structures/properties of the oligoarginine based molecules and their biological activities have been investigated in detail. It was found that stearyl moieties could facilitate the formation of small complexes (<200 nm). Extended oligohistidine or oligoarginine segments can further promote the co-assembly of siRNA with these cationic molecules. Increased oligohistidine segments improved the gene silencing, but did not cause the toxicity. Moreover, stearylation modification was necessary to enhance the cellular internalization of siRNA. Most importantly, it was found that improved gene silencing was induced by the stearylated peptides with increased number ratio of histidine/arginine in a peptide sequence. On the contrary, longer oligoarginine segments will induce the toxicity but not enhance the knockdown efficiency. Using these findings, STR-HnR8 (n=16 and 20) were deliberately designed and developed, showing outstanding knockdown efficiency capabilities compared to the most commonly used benchmark delivery systems. Finally, we found that either siRNA release from the complexes or protection of siRNA by the complexes was not a determining factor for highly efficient gene silencing. Also, endosomal escape of siRNA induced by stearylated peptides was not due to pH-dependent membrane disruption, but from "proton-sponge" effect induced by the oligohistidine segments. In summary, we developed a promising platform for the improvement and optimization of CPP-based vectors that can induce highly efficient siRNA delivery. The knowledge generated provides valuable understanding and guidance surrounding the deliberate design and preparation of highly practical CCP-based siRNA delivery systems.

Chapter 7

Co-delivery of hybrid drug nanoparticles and siRNA mediated by a modified cell penetrating peptide for triple synergy to inhibit cancer cell proliferation

---

7.1 Introduction

Combinations of two or more chemotherapeutic agents with different anti-cancer mechanisms have been proved effective in the treatment of many types of cancer. Since cancer is a disease caused by multiple gene mutations [258,259], this combination therapy has advantages by affecting multiple disease pathways. Over the past decade, combinations of conventional chemotherapeutics and small interfering RNA (siRNA) have shown promise with synergistic effects on the treatment of cancer [260,261]. However, co-delivery of anticancer drugs and siRNA is particularly challenging, because of the large differences in the physicochemical properties of the two types of agents. Moreover, uncontrolled agglomerations often lead to the instability of nanoparticles (NPs) in aqueous medium [262]. Therefore, this combination therapy is still in its early discovery stage. To date, only several types of carriers for single drug-siRNA combination have been developed, such as polyplex and lipoplex [263].

Ellipticine (EPT), whose mode of action is based mainly on DNA intercalation and inhibition of topoisomerase II, has exhibited significant antitumor activities [264,265]. 10-Hydroxycamptothecin (HCPT), isolated from Camptotheca acuminata extract, has a broad spectrum of anticancer activities by targeting and inhibiting topoisomerase I [266]. In terms of drug-siRNA combination therapy for cancer treatment, it has been reported that siRNA induced knockdown of the Bcl-2 gene, a key regulator of cell apoptosis [267], could sensitize cancer cells to anticancer drugs [268,269].

Here, by taking all this knowledge into account, we hypothesized that co-delivery of anti-cancer drugs EPT, HCPT and Bcl-2 siRNA will have multiple synergy effect on the treatment of cancer. A novel peptide-based delivery system based on a stearylated and oligohistidylated cell penetrating peptide, stearyl-(histidine)$_{16}$-(arginine)$_8$ (STR-H16R8) was used here as carrier. This peptide was recently developed by us for highly efficient siRNA delivery [270]. In this chapter, at first, carrier-free EPT/HCPT hybrid nanoparticles were prepared by a solvent displacement method [271], as both of the molecules have a poor aqueous solubility [272,273]. Secondly, the NPs were stabilized by surfactant-like and water soluble STR-H16R8 in the aqueous solution. Thirdly, Bcl-2 siRNA was introduced into the drug nanosuspension to form complexes with STR-H16R8. Last, the anti-proliferation effect of this co-delivery system was investigated on cancer cells. We demonstrated that the combination of EPT/HCPT exhibited a synergistic effect on the inhibition of cancer cell proliferation. Furthermore, we found that the cationic stearylated peptide not only improved the stability of nanosuspension, but also significantly enhanced the efficacy of the drugs. Moreover, Bcl-2 siRNA further

increased efficacy of the chemotherapeutics, leading to the triple synergistic effects on suppressing the cancer cell growth.

7.2 Materials and Methods

7.2.1 Materials and reagents

Ellipticine (EPT) (MW, 246.31; >98% purity) was purchased from EMD-Merck (Mississauga, Canada). (S)-10-Hydroxycamptothecin (HCPT) (MW, 364.35; >98% purity) was provided by AdooQ BioScience (Irvine, US). STR-H16R8 was synthesized by Pepscan (Lelystad, The Netherlands). R8 was synthesized by CanPeptide Inc. (Pointe-Claire, Canada). siRNA targeting Bcl-2 oncogene was purchased from Sigma, (Oakville, Canada) with a sense sequence of GUGAAGUCAACAUGCCUGCdTdT and antisense sequence of GCAGGCAUGUUGACUUCACdTdT. The scrambled siRNA from Life Technologies (Carlsbad, USA) was employed as negative control in the experiments.

7.2.2 Cell culture

The non-small lung carcinoma A549 cells (ATCC, Manassas, USA) were cultured in Dulbecco's Modified Eagle Medium-high glucose (DMEM) (Invitrogen, Burlington, Canada) with 10% heat-inactivated FBS. All of the cells were incubated at 37°C in a humidified atmosphere containing 5% CO_2.

7.2.3 Preparation of the nanosuspension

1 mL of 4 mM of EPT and 0.2 mM of HCPT acetone solution was added into 5 mL RNase free water at 40°C under vigorous stirring at 1,000 rpm. 5 min later, 7.5 mL of

RNase free water or STR-H16R8 solution was added into the EPT/HCPT suspension, which was stirred at 200 rpm for 8 hours to remove acetone, the final volume of which was adjusted to 12.5 mL by adding RNase free water. Afterwards, the original EPT/HCPT NP suspension was mixed with RNase free water with the volume ratio of 1: 3, and then mixed with RNase free water or 2 μM siRNA solution, respectively (1:1, v/v). The resulting solutions were incubated for 20 min at room temperature before characterization, determination of drug contents and in vitro release. The EPT/HCPT nanosuspension without STR-H16R8 was subject to lyophilization before observed by Leo-1530 scanning electron microscopy (SEM) (Zeiss, Oberkochen). The nanosuspension was diluted further to 1/10 of the original concentration with Opti-MEM medium (Life Technologies, Carlsbad, USA) before cell treatments with a final concentration of siRNA at 100 nM.

7.2.4 Particle size and zeta potential

The hydrodynamic diameter of the complexes were measured on a Zetasizer Nano ZS (Malvern Instruments, Malvern, UK) equipped with a 4 mW He-Ne laser operating at 633 nm. A quartz microcell (45 μL) with a 3 mm light path was used and the scattered light intensities were collected at an angle of 173°. Zeta potential measurements were also performed on the same machine using clear disposable zeta cells. The zeta potential values were obtained with the multimodal algorithm CONTIN, Dispersion Technology Software 5.0. Three measurements were performed to generate the intensity-based size and zeta potential plot reported herein.

7.2.5 Gene silencing effect of peptide/siRNA complexes

A549 cells (40,000 cells/well) were plated in a 24-well cell culture plate. 24 h later, the medium was removed and washed with PBS. 1.28 μL of Lipofactamine 2000 (Lipo) (Life Technologies, Carlsbad, USA), a commercial transfection reagent, was diluted in 30.72 μL of RNase free water and mixed with 32 μL of Bcl-2 siRNA solution to form complexes with the final concentration of siRNA at 1 μM, which was then diluted in 596 μL of OPTI-MEM medium before transfection. 300 μL of the sample solution containing the lipoplexes of Lipo/siRNA or the complexes of STR-H16R8/siRNA was added to the cells. 3 h later, 300 μL of DMEM with 20% FBS was added. Afterwards, the cells were incubated for 48 hours at 37 °C in a 5% CO_2 atmosphere. The cultures were then washed with PBS. Total RNA was extracted from the cells with TRIzol reagent (Life Technologies, Carlsbad, USA), then treated with chloroform (Sigma, Oakville, Canada) and 2-propanol (Sigma-Aldrich, Oakville, Canada) as recommended by the manufacturer. RNA concentrations were measured by Nanodrop spectrophotometer ND-1000 (Thermo scientific, Ottawa, Canada). All RNAs were reverse transcribed with Bio-Rad iScript cDNA synthesis kit (Bio-Rad, Mississauga, Canada). The cDNA synthesis was primed with a unique blend of oligo (dT) and random primers. The following pairs of primers were used for PCR: 5'-GGTGGGGTCATGTGTGTGG-3' and 5'-CGGTTCAGGTACTCAGTCATCC-3' (Sigma, Oakville, Canada). Here, the housekeeping gene cyclophilin was chosen as an internal control to normalize the Bcl-2 gene. The normalization was performed by the amplification of human cyclophilin with the following primers: 5'-GGTGATCTTTGGTCTCTTCGG-3' and 5'-TAGATGCTCTTTCCTCCTGTG-3' (Sigma, Oakville, Canada). PCR reaction was

performed with Brilliant II Fast SYBR Green QPCR Master Mix (Agilent Technologies, Wilmington, USA) on an Mx3005P™ Real-Time PCR System (Agilent Technologies, Wilmington, USA).

7.2.6 Cytotoxicity assay

A549 cells were plated in to 96-well plates (8,000 cells/well). 24 h later, the medium was removed and washed with PBS. 16 μL of 160 μM of EPT or 8 μM of HCPT DMSO solution was mixed into 48 μL of RNase free water, which were further diluted with 596 μL of OPTI-MEM medium. 60 μL of the sample solution was added to the cells. 3 h later, 60 μL DMEM medium with 20% FBS was added. After incubation for 24 hours, the cultures were washed with PBS. 100 μL of Opti-MEM medium with CCK-8 reagent was then added to each well. Cell viability was assessed by measuring the absorbance at 570 nm with a FLUOstar OPTIMA microplate reader and expressed as the ratio of the cells treated over the nontreated cells (negative control).

7.2.7 Fluorescence-activated cell sorting (FACS)

Cellular uptake of EPT and HCPT was studied using BD FACSCalibur Flow Cytometry (BD Biosciences, Mississauga, Canada). A549 cells (80,000 cells/well) were plated in a 24-well cell culture plate. 24 h later, the medium was removed and washed with PBS. Afterwards, A549 cells were treated with 300 μL of EPT/HCPT NPs, EPT/HCPT NPs/STR-H16R8 or EPT/HCPT NPs/STR-H16R8/BCL-2 siRNA samples in Opti-MEM prepared according to the protocol listed above. Nontreated cells served as a negative control. After 3 h incubation, the culture medium was discarded and cells were washed

with PBS, Trypsin-EDTA was then added to detach the cells from the plate; cells were suspended in 4% PFA solution and collected.

7.3 Results and Discussion

7.3.1 STR-H16R8 could stable EPT/HCPT hybrid nanoparticles in water

In order to develop a nanoparticulate delivery system for intravenous administration, a stable nanoparticle dispersion without agglomeration is prerequisite [262]. In this study, EPT/HCPT hybrid nanoparticles (NPs) prepared in 120 μM of STR-H16R8 showed a stable nanosuspension (Figure 1a, left), while NPs prepared in water sedimentated on the bottom rapidly (Figure 1a, middle). The morphology and structure of the NPs without addition of peptide STR-H16R8 were investigated via SEM, which showed the presence of distinct spherical NPs with an overall diameter of 170 nm and large agglomerations comprising of a number of nanoparticles (Figure 1b).

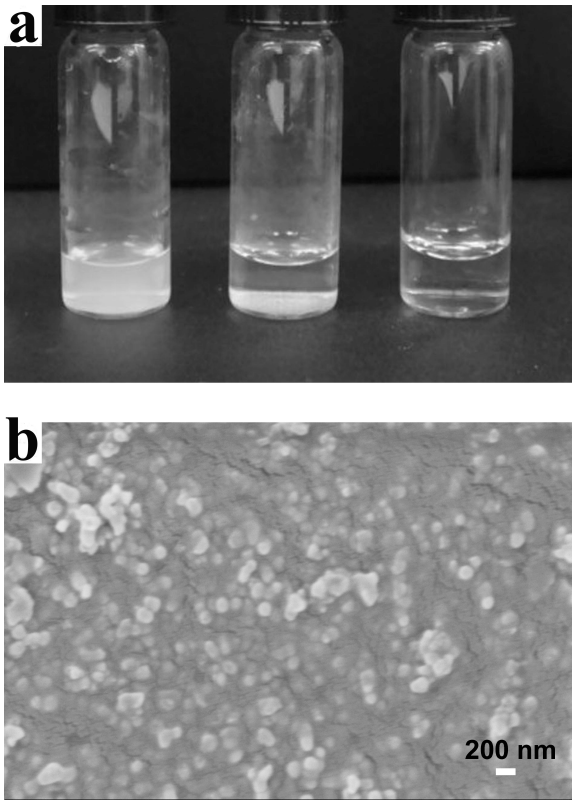

Figure 7.1 a) Photograph of 320 μM of EPT and 16 μM of HCPT hybrid NPs in 120 μM of STR-H16R8 (left) and water (middle) 3 h after preparation. Pure water (right) was used as reference; b) SEM imaging of freeze-dried unstabilized EPT/HCPT NPs.

DLS measurements also showed a > 2 μm diameter of the NPs prepared in water (Figure 7.2a). All these data suggested that the instability of the drug NPs without stabilizer was due to the sedimentation of agglomerations formed by nanoparticles in water. With the addition of 0.6 μM of STR-H16R8, particles sizes were reduced significantly to 770 nm, see Figure 7.2a. When the concentration of STR-H16R8 increased from 3 to 30 μM, the particle sizes decreased further from 331 nm to 195 nm. In 60 μM of the stabilizer, the

particle size was 198 nm, which was almost the same as that in 30 μM, suggesting that the nanoparticles have been stabilized completely, as showed in Figure 7.1a, left. The particle sizes were slightly bigger than that revealed by SEM imaging [274], which could be due to the anchor of STR-H16R8 on the surface of the drug NPs. These results indicated that amphiphilic STR-H16R8 could stabilize EPT/HCPT NPs effectively, leading to a stable nanosuspension with an average particle size of 200 nm. As showed in Figure 7.2b, the zeta potential of drug NPs was -20.4 mV, but increased to 19.2 mV in 0.6 μM of STR-H16R8. The zeta potentials were further increased from 27.1 to 36.8 mV when the concentration of STR-H16R8 altered from 3 to 60 μM. Cationic STR-H16R8 did not aggregate, but freely dissolved in water showing no zeta potential [270]. Therefore, the zeta potential shifting from negative to positive confirmed that cationic STR-H16R8 has anchored on the surface of the NPs. Peptide octaarginine (R8) was also investigated, which failed to stabilize the EPT/HCPT NPs at various concentrations, showing particle sizes of > 2 μm. This proved that it was the hydrophobic interaction between hydrophobic segment of STR-H16R8 and the drugs, rather than the coulombic interaction between cationic oligoarginine and negatively charged surface of the NPs, played a predominant role for improving the stability of the NPs.

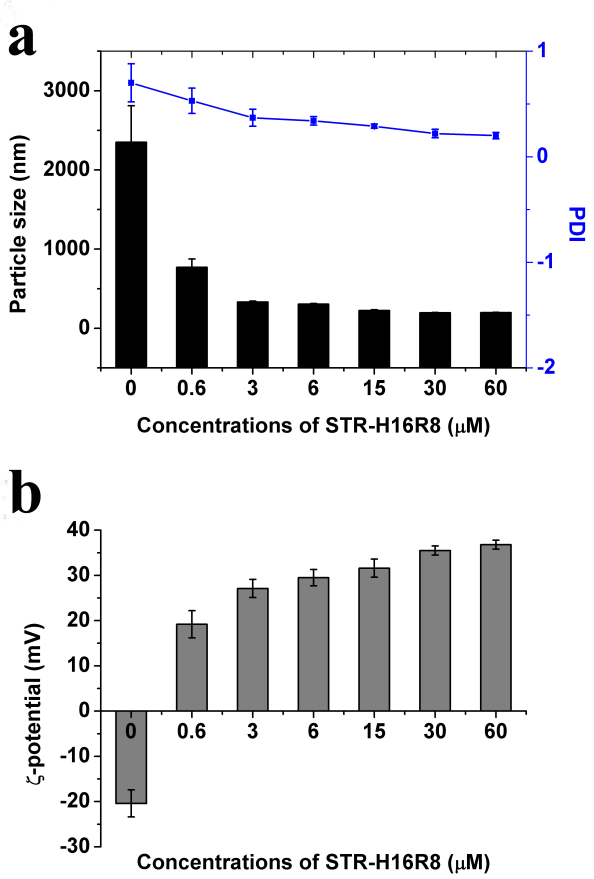

Figure 7.2 (a) Particle size and (b) zeta potential of 40 μM EPT and 2 μM HCPT hybrid NPs in various concentrations of STR-H16R8 solution.

After the addition of 1 μM siRNA solution, the particle sizes and zeta-potential were 121-132 nm and 27-33 mV (Figure 7.3), respectively. These values fell in between that of STR-H16R8/siRNA complexes (75-88 nm and 22-28 mV) [270] and STR-H16R8 stabilized drug NPs (195-331 nm and 27.1-36.8 mV). This suggested that a mixture of peptide/siRNA complexes and stearylated peptide stabilized drug NPs constituted the nanosuspension. More importantly, a particle size of less than 200 nm ensured optimal diffusion through tumor tissues by the enhanced permeation retention effect (EPR) [275].

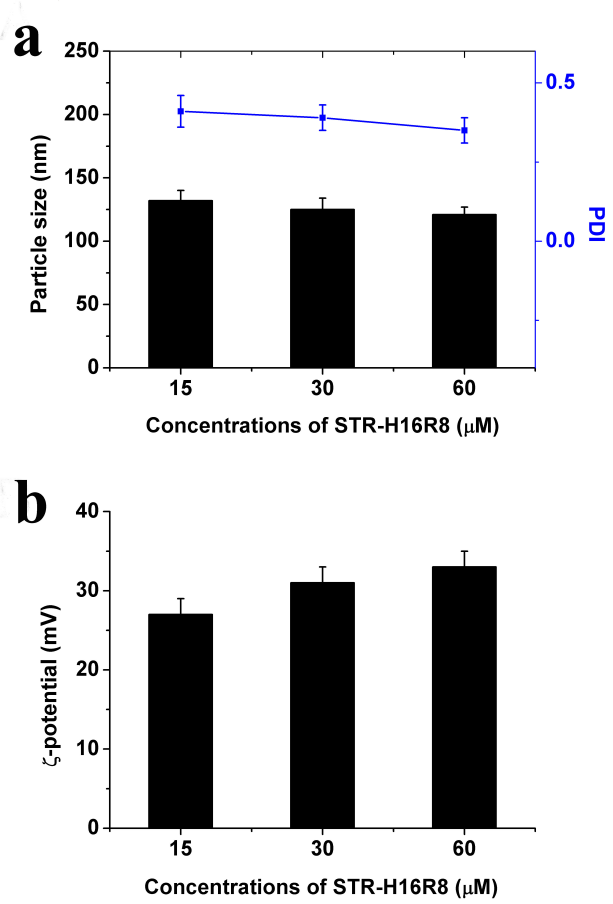

Figure 7.3 (a) Particle size and (b) zeta potential of 40 μM EPT and 2 μM HCPT hybrid NPs and 1 μM of siRNA in various concentrations of STR-H16R8 solution.

7.3.2 Synergistic antitumor effect of EPT/HCPT NPs combined with Bcl-2 siRNA delivered by peptide STR-H16R8

As mentioned above, therapeutic silencing of Bcl-2 gene by specific Bcl-2 siRNA could inhibit tumor growth. Thus, we involved Bcl-2 siRNA in the combination therapy. As in Figure 7.4, at molar ratio (MR) 15 and 30, the STR-H16R8/Bcl-2 siRNA formulations show 33% and 58% lower mRNA levels than that of untreated cells, respectively. At MR

60, STR-H16R8/siRNA induced 86% gene knockdown efficiency. This value was comparable to that of a benchmark, Lipofactamine 2000 (Lipo), which is the most commonly utilized and efficient transfection reagent to introduce siRNA into cells, inducing 83% gene silencing in this assay.

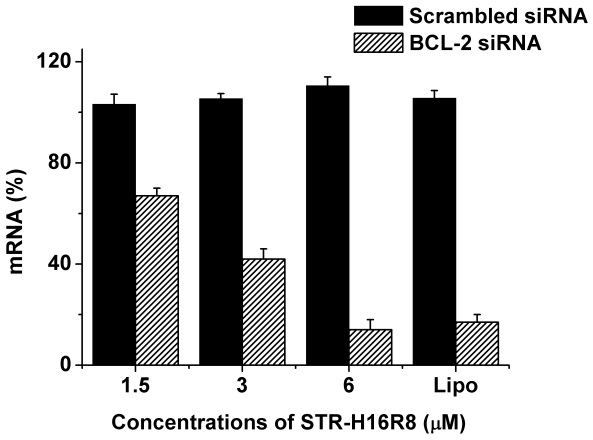

Figure 7.4 Knockdown efficiency of STR-H16R8/Bcl-2 siRNA complexes in A549 cells at molar ratio (MR) of 15, 30 and 60. The corresponding STR-H16R8 concentrations were 1.5, 3 and 6 μM, respectively. siRNA concentration was 100 nM. Lipofactamine 2000 (Lipo) was used as positive control.

Their antitumor cell proliferation ability was evaluated by cytotoxicity assay. The viabilities of A549 cells treated with 1.5, 3 and 6 μM peptide STR-H16R8 only were almost the same as untreated cells, indicating the safety of peptide itself (Figure 7.5a). 1.5, 3 and 6 μM STR-H16R8 formulated with 100 nM of siRNA did not induce any toxicity as well. Cells treated with anti-cancer drug EPT or HCPT only exhibited low cell-killing abilities with > 90% cell viability (Figure 7.5b), while the EPT/HCPT hybrid NPs showed enhanced cytotoxicity resulting in a decreased cell viability of 73%. This suggested a synergistic anticancer effect of DNA intercalator and topoisomerase II

inhibitor, EPT combined with topoisomerase II inhibitor, HCPT. Furthermore, the addition of 1.5, 3 and 6 μM peptide STR-H16R8 solution increased the toxicity of EPT/HCPT NPs significantly, showing cell viabilities of 39%, 28% and 14%, respectively (Figure 7.5c). After 100 nM of Bcl-2 siRNA was involved, the viabilities of A549 cells were further reduced to 29%, 14% and 4%, respectively (Figure7.5c). Taken together, the combination of EPT and HCPT induced a synergistic effect on inhibiting cancer cells growth. With the addition of nontoxic STR-H16R8 and siRNA, a triple synergy was revealed, which improved the efficacy of chemotherapeutics dramatically.

Cellular uptake of EPT and HCPT after the cells were treated with NPs and stabilized NPs was measured by fluorescence activated cell sorting (FACS) in FL-1 channel and FL-2 channel separately. As cell viability was low after treated with the hybrid NPs at STR-H16R8 concentration of more than 1.5 μM, a lower STR-H16R8 concentration of 0.06 and 0.6 μM were used in this assay. As shown in Figure 7.6, the EPT/HCPT NPs only samples showed mean fluorescence intensities of 9.4 and 39.8 for EPT and HCPT, respectively. The addition of 0.06 μM STR-H16R8 significantly increased the mean fluorescence intensity to 15.8 and 72.2 for EPT and HCPT. The intensities were enhanced further with 0.6 μM of STR-H16R8 to 19.7 (EPT) and 78.3 (HCPT), respectively. This increased uptake could be attribute to the change of negatively charged surfaces of drugs to positively charged EPT/HCPT NPs after the addition of STR-H16R8, as positively charged particles have high affinity for the negatively charged outer-membrane leaflet of cancer cells [276].

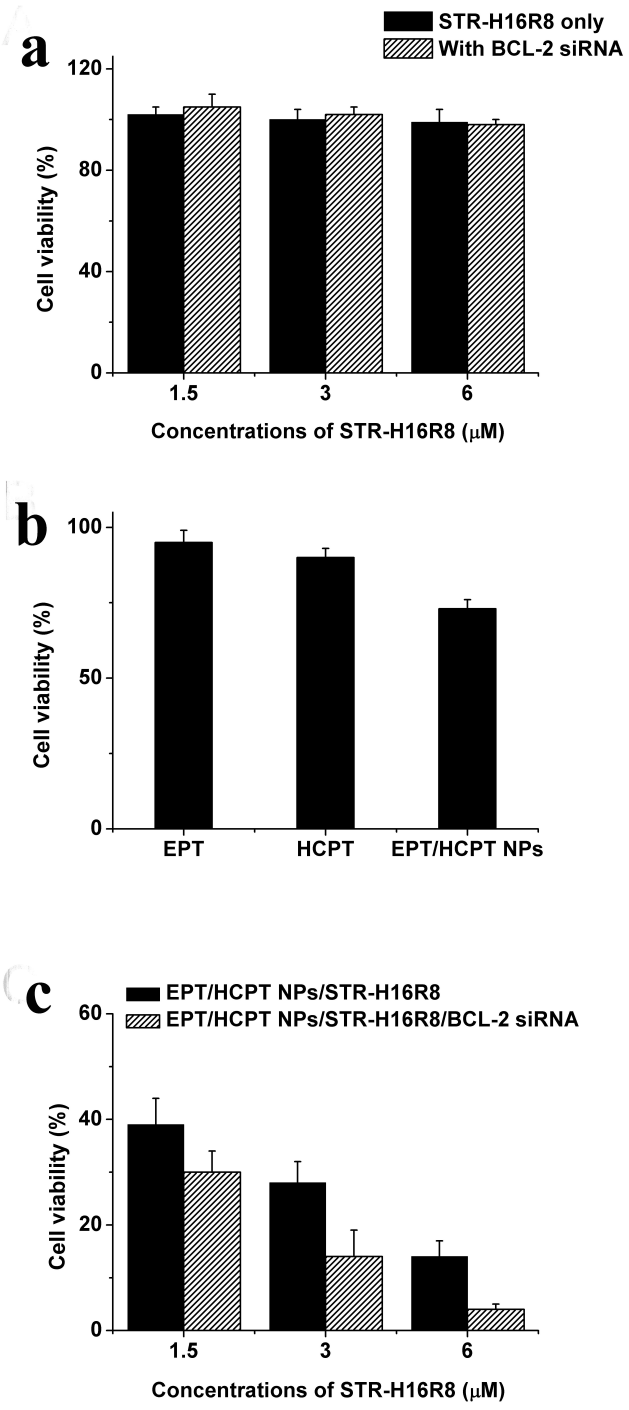

Figure 7.5 Cytotoxicity of (a) STR-H16R8 only and STR-H16R8/Bcl-2 siRNA, (b) EPT only, HCPT only and EPT/HCPT NPs and (c) combination of EPT/HCPT NPs/STR-H16R8 and combination of EPT/HCPT NPs/STR-H16R8/Bcl-2 siRNA on A549 cells. The concentrations of EPT and HCPT were 4 μM and 0.2 μM, respectively. The concentrations of STR-H16R8 were 1.5, 3 and 6 μM for MR 15, 30 and 60, respectively with 100 nM siRNA.

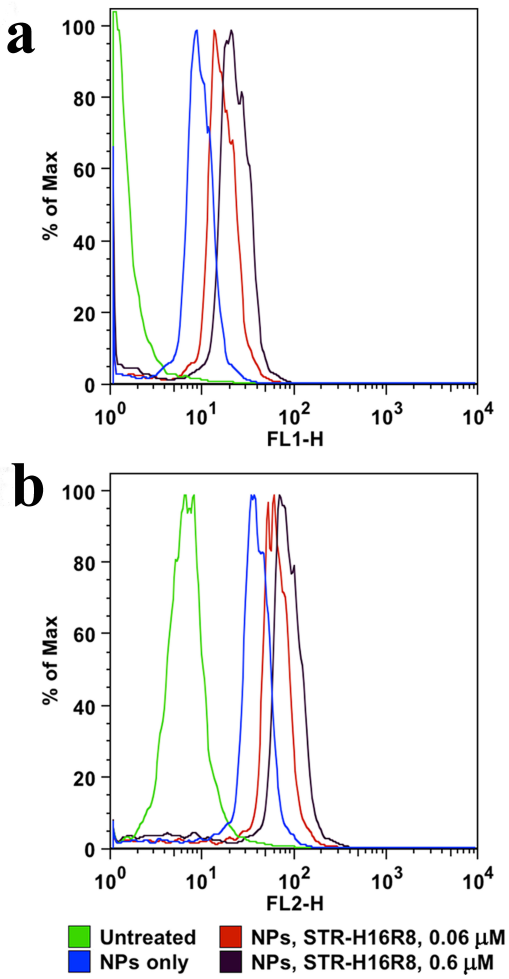

Figure 7.6 Cellular uptake of (a) EPT and (b) HCPT in A549 cells after treatment with bare EPT/HCPT NPs and stabilized NPs with STR-H16R8. The concentrations of EPT and HCPT were 4 μM and 0.2 μM.

7.4 Conclusions

In summary, negatively charged EPT/HCPT hybrid NPs with the particle sizes of 170 nm were prepared, and then further stabilized by surfactant-like and water soluble peptide STR-H16R8 in water. The positively charged surfaces of the stabilized NPs confirmed that cationic STR-H16R8 anchored on the surface of the NPs. We revealed the combination usage of EPT/HCPT exhibited a synergistic effect on the inhibition of cancer cell proliferation, compared to EPT or HCPT alone. Furthermore, the cationic stearylated peptide not only improved the stability of nanosuspension, but also significantly enhanced the efficacy of the drugs due to the increased cellular uptake. Moreover, the addition of Bcl-2 siRNA to the system further increased efficacy of the chemotherapeutics, leading to a triple synergy to suppress the cancer cell growth. In conclusion, a promising co-delivery system for multidrugs and siRNA was developed. We demonstrated its capability for combination therapy by co-delivering EPT, HCPT and siRNA targeting Bcl-2 gene to A549 cancer cells. The fundamental knowledge generated provides valuable understanding and guidance surrounding the combination therapy and design of highly practical co-delivery systems.

Chapter 8

Original Contributions and Recommendations

8.1 Original contributions to research

This thesis presented the potential of peptides as carriers for siRNA delivery both *in vitro* and *in vivo*. We designed several peptide libraries and explored the possibility of these co-assembling, biocompatible peptides for safe and efficient delivery of therapeutic siRNA. The thesis includes the following parts: (i) the discovery and characterization of a co-assembling, amphiphilic peptide C6, which demonstrate high siRNA delivery ability but low gene knockdown efficiency (Chapter 3); (ii) modification of C6 sequences by adding tryptophan residues (Chapter 4) and histidine residues (Chapter 5), both of which improved the gene silencing efficiency significantly; (iii) study of the structure-activity relationship by rationally modifying oligoarginine peptides with oligohistidine and stearyl moieties, providing information for future design of peptide-based delivery vehicles for siRNA (Chapter 6); (iv) exploration of simultaneously delivering anticancer drugs and siRNA into cancer cells to achieve a synergistic therapeutic effect. The original contributions to research are summarized in the following sections.

Peptide C6 family as siRNA delivery carriers *in vitro* and *in vivo*: A model co-assembling, amphiphilic peptide, C6, was found to be able to transport large amounts of siRNA across the cell membrane. Peptide C6 adopted a helical structure upon

coassembling with siRNA. The C6/siRNA coassembly showed a size distribution between 50 and 250 nm, confirmed by dynamic light scattering and atomic force microscopy. Fluorescence microscopy images confirmed the localization of C6/siRNA complexes in the cytoplasm using Cy3-labeled siRNAs. Peptide C6 showed lower toxicity and higher efficiency in cellular uptake of siRNA compared with Lipofectamine 2000. However, the gene silencing efficiency of siRNA delivered by C6 is very low (only 15%), probably due to endosomal entrapment after endocytosis. To avoid lysosomal degradation, siRNAs complexed with the carrier must escape from the endosome into the cytosol, where they can associate with the RISC. Hence, developing peptides that promote endosomal escape is a prerequisite for successful siRNA implementation. Therefore, a peptide library was designed by modifying prototype peptide C6 with endosome-disruptive moiety. C6M1 was obtained by replacing some leucine residues in the sequence with aromatic tryptophan, which is found abundantly in the pore-forming toxins of bacteria. Formed C6M1/siRNA nanoscale complexes are able to deliver siRNA into cells and induce improved gene knockdown (58%) with low toxicity. The increased membrane disruption ability at acidic condition of the peptide with tryptophan residue substitution contributed to the enhanced gene silence efficacy, proved by LDH assay at different pH. Intratumoral injection of the complexes results in a marked reduction of tumor growth through downregulation of antiapoptotic Bcl-2 protein in mice. Different from C6M1, peptides C6M2 to C6M8 were designed by adding pH responsive histidine residues, in order to facilitate the endosomal escape of peptide/siRNA complexes through the “proton sponge effect”. All variations improved the transfection efficiency of C6; several more promising candidates were used for further *in vitro* and *in vivo* evaluation.

The two peptides C6M3 and C6M6 could form stable complexes with siRNA, with a size of around 100 nm. These complexes could be uptaken by cells and showed a punctuate perinuclear distribution after membrane translocation. These peptide/siRNA complexes achieved high transfection efficiency *in vitro* without inducing substantial cytotoxicity. In order to evaluate possible immune side effects of these peptide carriers, biocompatibility studies were conducted in terms of complement activation and cytokine activation. None of the promising peptides induced such activation effects. These data was never reported before for peptide-based siRNA carriers. We further examined the therapeutic potential of this peptide mediated siRNA delivery for cancer treatment by targeting Bcl-2 gene in a mouse tumor model, and demonstrated that tumor growth was inhibited by at least 50%, as a result of the downregulation of Bcl-2 protein.

Primary structure-activity relationship and intracellular trafficking mechanism of peptide/siRNA: oligoarginine peptides, prominent members in CPPs, are rationally modified with oligohistidine and stearyl moieties (STR-) to study the structure-activity relationship of this kind of cell-penetrating peptides. It demonstrated that stearyl groups are necessary to facilitate the formation of nanoscale siRNA complexes. siRNA binding can be promoted further by increasing the chain length of oliogohistidine or oligoarginine segments. Extended oligohistidine segments improve the gene silencing, but do not increase the toxicity. When the ratio of histidine/arginine in a peptide sequence is >1.5, pronounced gene silencing is induced. Following this rule, STR-HnR8 (n=16 and 20) are developed, which showed a high knockdown efficiency (over 90%) rarely reported before. It is found that endosomal escape of siRNA mediated by stearylated and oligohistidylated oligoarginine is only from “proton-sponge” effect, based on data

following the use of chemical inhibitors of endocytic pathways. In addition, the pH dependent membrane disruptive ability does not vary significantly among these peptides.

Co-delivery of anticancer drug nanoparticles and siRNA mediated by STR-H16R8 for triple synergy to inhibit cancer cell proliferation: The effectiveness of combination of two or more chemotherapeutic agents with different mechanisms has been proved in the treatment of cancer. The ability of STR-H16R8 to co-delivery DNA intercalator and topoisomerase II inhibitor, Ellipticine (EPT), topoisomerase I inhibitor, 10-Hydroxycamptothecin (HCPT) and Bcl-2 siRNA into cancer cells were investigated. A solvent displacement method was used to produce the negatively charged EPT/HCPT hybrid nanoparticles (NPs) with a particle size of ca. 170 nm, which exhibited a synergistic effect on the inhibition of cancer cells. The stability of the nanosuspension was improved immensely by the cationic amphiphilic stearylated peptide STR-H16R8, due to the anchor of the peptide on the surface of the NPs through the hydrophobic interaction between hydrophobic segment of STR-H16R8 and the drugs. Moreover, the stabilized NPs showed significantly enhanced efficacy, by reducing the cell viability from 73% to 14%, compared with the bare NPs. The efficacy of the chemotherapeutics was further increased with the addition of Bcl-2 siRNA, leading to the triple synergy to suppress cancer cell growth. This novel multidrugs-siRNA co-delivery platform suggests a new strategy of combination therapy for the treatment of cancer.

8.2 Recommendations

Recommended future work to develop peptide-based nanocarriers for efficient and safe siRNA delivery can be divided into following major parts:

Optimize the peptide/siRNA formulation to further increase transfection efficiency

1. Complete stability studies of peptide/siRNA complexes should be carried out. It is necessary to ascertain that this delivery system can tolerate various physiological conditions during transport to target site in serum. We can consider incorporate polyethylene glycol (PEG) moiety into peptide sequences. PEG is one of the most frequently used polymers for drug delivery with high water solubility, biocompatibility and chain flexibility; it has been introduced to help protect the siRNA by minimizing the interaction with serum proteins in biological fluids. Covalent attachment of PEG to siRNA or its delivery system was found to enhance the circulation time of the complex. Thus, PEG of varying chain lengths can be incorporated in the peptide-siRNA formulation.

2. If any of the tested peptides turns out to be effective at encapsulating, transporting and releasing siRNAs, we can further modify its sequence for cell targeting. Such modifications can be done by one of the following methods: 1) the targeting moiety is attached to one end of the original peptide chain if it is relatively short; 2) the targeting moiety is incorporated into the peptide assemblies by being attached onto the complex surface after the complexation.

3. Since it has been confirmed that our peptide-mediated siRNA delivery is through endocytosis, rather than direct penetration across cell membranes, the specific translocation pathways can be further examined. Chemical inhibitors of endocytosis (sucrose, chlorpromazine, fillipin, nystatin and EIPA) will be used to identify the internalization mechanisms among the three main endocytosis pathways, namely clathrin-dependent, lipid raft/caveolae-mediated and macropinocytosis pathways. Temperature dependence of the uptake will also be studied as an indicator for endocytosis in general. So far, the uptake for all tested peptide-mediated siRNA delivery systems was found to be using endocytosis.

Evaluate therapeutic effect and biocompatibility of peptide/siRNA complexes using intravenous injection *in vivo*:

Preliminary in vivo results have shown that intratumoral injection of Bcl-2 siRNA delivered by C6 family peptides can significantly inhibit the proliferation of tumor cells in a xenograft NSCLC model with nude mice. To explore the possibility of systemic delivery, the complexes of Bcl-2 siRNA with promising peptides with high transfection efficiency and low toxicity in vitro will be administered intravenously. The circulating complexes in the bloodstream will accumulate in the tumor through the enhanced permeability and retention (EPR) effect. The animal model can be established as mentioned in the methods part, by subcutaneous inoculation of 5×10^6 NSCLC A549 cells at the right armpit of six-week-old BALB/c nude mice, or other cell lines can be used. Tumor growth should be monitored on alternating days during treatment and the results

will be compared with those of control groups. After treatments, the animals will be sacrificed; tumor tissue and surrounding skin are excised and put on a microscopy glass slide. Tissue examination for vascularization and angiogenesis will be performed on a microscope. Western blotting can be used to detect knockdown efficiency at the protein level to ascertain whether the Bcl-2 protein level is reduced in the tumor. Note that besides Bcl-2, anti-RRM2, anti-VEGF, anti-HER2, and survivin targeted siRNAs are other extensively used targets. The efficiency of these siRNAs can be assessed on cultured cells first and then choose the best therapeutic siRNA for this and following *in vivo* studies.

Preliminary *in vitro* experiment results have showed the biocompatibility of these peptide/siRNA complexes. To validate safety and biocompatibility of the peptide/siRNA complexes *in vivo*, immune responses and biocompatibility can be examined in mice. After treatments, blood will be collected, liver and kidney will be dissected, collected and frozen stored in -80°C. Blood samples are used to detect liver metabolic biomarkers, bilirubin and alanine aminotransferase (ALT). Plasma cytokines of interleukin (IL) IL1, IL2, IL 6 IL8, and IL18, Tumor necrosis factor alpha (TNFα) can be measured (Multiplex assay). Erythrocyte sedimentation rate (ESR), total and differential white blood cell counts can be performed with flow cytometry. Liver samples are homogenized and hepatic proteins are extracted for alanine aminotransferase (ALT), aspartate aminotransferase (AST), and cytochrome P450 activity analyses. Kidney samples can be processed to assay clusterin and cystatin C for determining renal function.

If the therapeutic efficacy is confirmed by intravenous administration, further biodistribution and pharmacokinetics study can then be carried out.

Appendix

Peptide library for siRNA delivery *

No	Name	Sequence	AA	Design principle
1	C6	RLLRLLLRLWRRLLRLLR	18	These sequences are different derivatives of C6 peptide. W and H amino acids are added at different positions to the sequence to increase the affinity of peptide with membrane and increase endosome escape, respectively. The peptides are synthesized with a cysteamide group at its C-terminus so as to stabilize the carrier/cargo complex and to improve its potency to cross cell membranes. Also the n-term domain was replaced with GLW, which seems to be important in CADY and MPG peptides. The peptides are designed with a stearic acid conjugated to the N-terminal as to increase membrane affinity.
2	C6M	RLWRLWLRLWRRLWRLLR	18	
3	C6M1	RLWRLLWRLWRRLWRLLR	18	
4	C6M2	RLWRLLWHLWRHLWRLLR	18	
5	C6M3	RLWHLLWRLWRRLHRLLR	18	
6	C6M4	HLLRLLLRLWHRLWRLLR	18	
7	C6M5	HLWHLLLRLWRRLLRLLR	18	
8	C6M6	GLWHLLLHLWRRLLRLLR	18	
9	C6M7	GLWHLLLHLWRRHHRHHR	18	
10	C6M8	GLWHLHLHLWRRHHRLLR	18	
11	CADY	GLWRALWRLLRSLWRLLW RA-cysteamide	20	Peptide controls: all there sequences have shown significant gene silencing efficiency
12	MPG-NLS	GALFLGFLGAAGSTMGAW SQPKSKRKV-cysteamide	27	
13	EB1	LIRLWSHLIHIWFQNRRLK WKKK	23	
14	C6-CYSt	RLLRLLLRLWRRLLRLLR-cysteamide	18	C-terminal are modified by Cysteamide group -NH-CH2-CH2-SH which was reported to increase transfection efficiency
15	C6M1-CYSt	RLWRLLWRLWRRLWRLLR -Cysteamide	18	
16	C6M3-CYSt	RLWHLLWRLWRRLHRLLR -Cysteamide	18	

* Peptide Sequence Design and Use Thereof for Peptide-Mediated siRNA Delivery. Patent number: WO2013075244 A1. Inventors: Pu Chen, Mousa Jafari, Wen Xu, Baoling Chen, Ran Pan, Nedra Karunaratne.

17	C6M6-CYSt	GLWHLLLHLWRRLLRLLR-Cysteamide	18	
18	C6-Dr	rLLrLLLrLWrrLLrLLr	18	D form of arginine residue and all amino acids are used in these sequences to evaluate the effect of using two different isomers of arginine and whole sequence on transfection efficiency, stability, and cytotoxicity.
19	C6-D	rllrlllrlwrrllrllr	18	
20	C6M1-Dr	rLWrLLWrLWrrLWrLLr	18	
21	C6M1-D	rlwrllwrlwrrlwrllr	18	
22	C6M3-Dr	rLWHLLWrLWrrLHrLLr	18	
23	C6M3-D	rlwhllwrlwrrlhrllr	18	
24	C6M6-Dr	GLWHLLLHLWrrLLrLLr	18	
25	C6M6-D	glwhlllhlwrrllrllr	18	
26	C1	FQFNFQFNGGGHRRRRRRR	19	C1-family peptides: arginine-Rich domain was replaced with Lysine- rich segment PKKKRKV and PKPKRKV which have shown high nuclear and cytoplasmic localization properties, respectively. The length of self-assembling domain was also changed. H an C amino acids were added to enhance the endosomal scape and siRNA release. In C1M3 the linker GGG was replaced with WSQ.
27	C1M	FQFNFQFNGGGPKKKRKV	18	
28	C1M1	FQFNFQFNGGGPKPKRKV	18	
29	C1M2	FQFNFQFNFQFNGGGPKKKRKV	22	
30	C1M3	FQFNFQFNFQFNWSQPKPKRKV	22	
31	C1M4	FQFNFQFNFQFNGGGPKPKRKV	22	
32	C1M5	FQFNFQFNFQFNGGGCHHRRRRRRHC	26	
33	C1M6	FQFNFQFNFQFNGGGCPKPKRKVC	24	
34	STR-C1	$CH_3(CH_2)_{16}$-GGGPKPKRKV	10+	Stearic acid is used as the hydrophobic domain in a primary amphiphilic structure. The hydrophilic domains are chosen from C1 family peptides.
35	STR-HK	$CH_3(CH_2)_{16}$-HHHPKPKRKV	10+	
36	STR-HKC	$CH_3(CH_2)_{16}$-HHHCPKKKRKVC	12+	

37	E3	RFTFHFRFEFTFHFE	15	E3-family peptides: the hydrophobic amino acids of E3 were replaced with L and W which were reported to have higher affinity with cell membrane.
38	E3M	RLTLHLRLELTLHLE	15	
39	E3M1	RWTWHWRWEWTWHWE	15	
40	A7	HRLRHALAHLLHKLKHLLH ALAHRLRH	27	A7-family peptides: the length of A7 sequence was shorten in A7M and the amino acid K was replaced with R in A7M1
41	A7M	RHALAHLLHKLKHLLHAL AHR	21	
42	A7M1	RHALAHLLHRLRHLLHALA HR	21	
43	MW1	MWKSKIGSWILVRWAMWS KKRPKP	24	These sequences are derived from CPP Bovine PrP MVKSKIGSWILVLFVAMWSDVG LCKKRPKP. The transfection efficiency of Bovine PrP is 48%. Some W and H are added to the sequence to increase the affinity of peptide with membrane and increase endosomal escape.
44	MW2	MWKSHIGSWILVRWAMWS HKRPKP	24	
45	MW3	MWKSKISWILVSKPGLCKK RPKP	23	
46	MW4	MHKSKISWHLVSKPGLCHK RPKP	23	
47	HA2	GLFGAIAGFIENGWEGMID GWYG	23	HA2 has been added to facilitate the endosomal escape for some CPPs, e.g., Penetratin HA2-Penetratin was proved to increase the transfection efficiency of Penetratin.
48	GL1	GLWRAWLWKAFLASNWR RLLRLLR	24	
49	GL2	GLWRASWLKAWLASNWH KKHRLLR	24	
50	GL3	GLWGAWFIEGWEGMIDGR RLLRLLR	23	
51	GL4	GLWRASWLKAFLASNWHK KLHKK	25	
52	HA2-C6	GLFGAIAGFIENGWEGMID GRLLRLLLRLWRRLLRLLR	38	
53	HA2-PK	GLFGAIAGFIENGWEGMID GWYGPKKKRKV	28	
55	CLK	CLKHALAHLAKLRHLLRLL RR	21	

r=D-arginine, h=D-histidine, w=D-tryptophan, g=D-glycine, i=D-leucine
C-terminal cysteamide= NH-CH_2-CH_2-SH Stearic acid modified N-term=$CH_3(CH_2)_{16}$-
Peptides are N-term acetylated, C-term amidated, otherwise mentioned

References

[1] C.W. Schmidt, Therapeutic interference Small RNA molecules act as blockers of disease metabolism, Mod. Drug Discov. (2003) 37–42.

[2] A. Fire, S. Xu, M.K. Montgomery, S.A. Kostas, S.E. Driver, C.C. Mello, Potent and specific genetic interference by double-stranded RNA in Caenorhabditis elegans, Nature. 391 (1998) 806–811.

[3] D. Castanotto, J.J. Rossi, The promises and pitfalls of RNA-interference-based therapeutics, Nature. 457 (2009) 426–33.

[4] S.M. Elbashir, J. Harborth, W. Lendeckel, A. Yalcin, K. Weber, T. Tuschl, Duplexes of 21-nucleotide RNAs mediate RNA interference in cultured mammalian cells, Nature. 411 (2001) 494–498.

[5] G.M. Zou, M.C. Yoder, Application of RNA interference to study stem cell function: current status and future perspectives, Biol. Cell. 97 (2005) 211–219.

[6] K. Okamura, W.J. Chung, J.G. Ruby, H. Guo, D.P. Bartel, E.C. Lai, The Drosophila hairpin RNA pathway generates endogenous short interfering RNAs, Nature. 453 (2008) 803–806.

[7] G. Tang, siRNA and miRNA: an insight into RISCs, Trends Biochem. Sci. 30 (2005) 106–114.

[8] C. Matranga, Y. Tomari, C. Shin, D.P. Bartel, P.D. Zamore, Passenger-strand cleavage facilitates assembly of siRNA into Ago2-containing RNAi enzyme complexes, Cell. 123 (2005) 607–620.

[9] R.I. Gregory, T.P. Chendrimada, N. Cooch, R. Shiekhattar, Human RISC couples microRNA biogenesis and posttranscriptional gene silencing, Cell. 123 (2005) 631–640.

[10] T.P. Chendrimada, R.I. Gregory, E. Kumaraswamy, J. Norman, N. Cooch, K. Nishikura, et al., TRBP recruits the Dicer complex to Ago2 for microRNA processing and gene silencing, Nature. 436 (2005) 740–744.

[11] D. Grimm, Small silencing RNAs: state-of-the-art, Adv. Drug Deliv. Rev. 61 (2009) 672–703.

[12] D. Bumcrot, M. Manoharan, V. Koteliansky, D.W.Y. Sah, RNAi therapeutics: a potential new class of pharmaceutical drugs, Nat. Chem. Biol. 2 (2006) 711–719.

[13] M. Rompf, J.J. Turner, A. Detzer, M. Overhoff, W. Wu, Increased RNAi is related to intracellular release of siRNA via a covalently attached signal peptide, RNA. (2009) 627–636.

[14] Y. Dorsett, T. Tuschl, siRNAs: applications in functional genomics and potential as therapeutics, Nat. Rev. Drug Discov. 3 (2004) 318–329.

[15] S.M. Hammond, A.A. Caudy, G.J. Hannon, Post-transcriptional gene silencing by double-stranded RNA, Nat. Rev. Genet. 2 (2001) 110–119.

[16] I. Melnikova, Wet age-related macular degeneration, Nat. Rev. Drug Discov. 4 (2005) 711–2.

[17] S. Akhtar, I. Benter, Toxicogenomics of non-viral drug delivery systems for RNAi: potential impact on siRNA-mediated gene silencing activity and specificity, Adv. Drug Deliv. Rev. 59 (2007) 164–182.

[18] H. Lage, Potential applications of RNA interference technology in the treatment of cancer, Futur. Oncol. 1 (2005) 103–113.

[19] K. Iwaki, K. Shibata, M. Ohta, Y. Endo, H. Uchida, M. Tominaga, et al., A small interfering RNA targeting proteinase-activated receptor-2 is effective in suppression of tumor growth in a Panc1 xenograft model, Int. J. Cancer. 122 (2008) 658–663.

[20] E. Kawata, E. Ashihara, S. Kimura, K. Takenaka, K. Sato, R. Tanaka, et al., Administration of PLK-1 small interfering RNA with atelocollagen prevents the growth of liver metastases of lung cancer, Mol. Cancer Ther. 7 (2008) 2904–2912.

[21] R.M. Schiffelers, A. Ansari, J. Xu, Q. Zhou, Q. Tang, G. Storm, et al., Cancer siRNA therapy by tumor selective delivery with ligand-targeted sterically stabilized nanoparticle, Nucleic Acids Res. 32 (2004) e149.

[22] D.W. Bartlett, M.E. Davis, Impact of Tumor-Specific Targeting and Dosing Schedule on Tumor Growth Inhibition After Intravenous Administration of siRNA-Containing Nanoparticles, Biotechnology. 99 (2008) 975–985.

[23] K.F. Pirollo, A. Rait, Q. Zhou, S.H. Hwang, J. a Dagata, G. Zon, et al., Materializing the potential of small interfering RNA via a tumor-targeting nanodelivery system, Cancer Res. 67 (2007) 2938–2943.

[24] J.M. Layzer, A.P. Mccaffrey, A.K. Tanner, In vivo activity of nuclease-resistant siRNAs, RNA. 10 (2004) 766–771.

[25] Y. Takahashi, M. Nishikawa, Y. Takakura, Nonviral vector-mediated RNA interference: its gene silencing characteristics and important factors to achieve RNAi-based gene therapy, Adv. Drug Deliv. Rev. 61 (2009) 760–766.

[26] A. Schroeder, C.G. Levins, C. Cortez, R. Langer, D.G. Anderson, Lipid-based nanotherapeutics for siRNA delivery, J. Intern. Med. 267 (2010) 9–21.

[27] D.J. Gary, N. Puri, Y.Y. Won, Polymer-based siRNA delivery: perspectives on the fundamental and phenomenological distinctions from polymer-based DNA delivery, J. Control. Release. 121 (2007) 64–73.

[28] X. Liu, P. Rocchi, L. Peng, Dendrimers as non-viral vectors for siRNA delivery, New J. Chem. 36 (2012) 256–263.

[29] E. Zhao, Z. Zhao, J. Wang, C. Yang, C. Chen, L. Gao, et al., Surface engineering of gold nanoparticles for in vitro siRNA delivery, Nanoscale. 4 (2012) 5102–5109.

[30] Q. Leng, P. Scaria, J. Zhu, N. Ambulos, P. Campbell, a J. Mixson, Highly branched HK peptides are effective carriers of siRNA, J. Gene Med. 7 (2005) 977–986.

[31] C. Lonez, M. Vandenbranden, J.M. Ruysschaert, Cationic liposomal lipids: from gene carriers to cell signaling, Prog. Lipid Res. 47 (2008) 340–347.

[32] Y. Liu, L. Huang, Designer lipids advance systemic siRNA delivery, Mol. Ther. 18 (2010) 669–670.

[33] Y.W. Won, S.M. Yoon, K.M. Lee, Y.H. Kim, Poly(oligo-D-arginine) with internal disulfide linkages as a cytoplasm-sensitive carrier for siRNA delivery, Mol. Ther. 19 (2011) 372–380.

[34] H. Yang, S.Y. Fung, M. Pritzker, P. Chen, Surface-assisted assembly of an ionic-complementary peptide: controllable growth of nanofibers, J. Am. Chem. Soc. 129 (2007) 12200–12210.

[35] D.R. Corey, Chemical modification: the key to clinical application of RNA interference?, J. Clin. Invest. 117 (2007) 3615–3622.

[36] O. Hurko, Understanding the strategic importance of biomarkers for the discovery and early development phases, Drug Discov. World. 7 (2006) 63–74.

[37] L.S. Reddy, V. Sarojamma, V. Ramakrishna, Future of RNAi in Medicine : A Review, World J. Med. Sci. 2 (2007) 1–14.

[38] C. Klein, C.T. Bock, H. Wedemeyer, T. Wüstefeld, S. Locarnini, H.P. Dienes, et al., Inhibition of hepatitis B virus replication in vivo by nucleoside analogues and siRNA, Gastroenterology. 125 (2003) 9–18.

[39] M. Konishi, C.H. Wu, G.Y. Wu, Inhibition of HBV replication by siRNA in a stable HBV-producing cell line, Hepatology. 38 (2003) 842–850.

[40] D. V Morrissey, J.A. Lockridge, L. Shaw, K. Blanchard, K. Jensen, W. Breen, et al., Potent and persistent in vivo anti-HBV activity of chemically modified siRNAs, Nat. Biotechnol. 23 (2005) 1002–1007.

[41] J. Wu, K.M. Nandamuri, Inhibition of hepatitis viral replication by siRNA, Expert Opin. Biol. Ther. 4 (2004) 1649–1659.

[42] C. Klein, C.T. Bock, H. Wedemeyer, T. Wüstefeld, S. Locarnini, H.P. Dienes, et al., Inhibition of hepatitis B virus replication in vivo by nucleoside analogues and siRNA, Gastroenterology. 125 (2003) 9–18.

[43] A.P. McCaffrey, H. Nakai, K. Pandey, Z. Huang, F.H. Salazar, H. Xu, et al., Inhibition of hepatitis B virus in mice by RNA interference, Nat. Biotechnol. 21 (2003) 639–644.

[44] A. Tyagi, F. Ahmed, N. Thakur, A. Sharma, G.P.S. Raghava, M. Kumar, HIVsirDB: A Database of HIV Inhibiting siRNAs, PLoS One. 6 (2011) e25917.

[45] D. Boden, O. Pusch, F. Lee, L. Tucker, B. Ramratnam, Human immunodeficiency virus type 1 escape from RNA interference, J. Virol. 77 (2003) 11531–11535.

[46] X.F. Qin, D.S. An, I.S.Y. Chen, D. Baltimore, Inhibiting HIV-1 infection in human T cells by lentiviral-mediated delivery of small interfering RNA against CCR5, Proc. Natl. Acad. Sci. U. S. A. 100 (2003) 183–188.

[47] P. Kumar, H.S. Ban, S.S. Kim, H. Wu, T. Pearson, D.L. Greiner, et al., T cell-specific siRNA delivery suppresses HIV-1 infection in humanized mice, Cell. 134 (2008) 577–586.

[48] R.M. Surabhi, R.B. Gaynor, RNA interference directed against viral and cellular targets inhibits human immunodeficiency Virus Type 1 replication, J. Virol. 76 (2002) 12963–12973.

[49] M.J. Li, J. Kim, S. Li, J. Zaia, J.K. Yee, J. Anderson, et al., Long-term inhibition of HIV-1 infection in primary hematopoietic cells by lentiviral vector delivery of a triple combination of anti-HIV shRNA, anti-CCR5 ribozyme, and a nucleolar-localizing TAR decoy, Mol. Ther. 12 (2005) 900–909.

[50] S. Prakash, M. Malhotra, V. Rengaswamy, Nonviral siRNA delivery for gene silencing in neurodegenerative diseases, Methods Mol. Biol. 623 (2010) 211–229.

[51] J. Hardy, The genetic causes of neurodegenerative diseases, J. Alzheimer's Dis. 3 (2001) 109–116.

[52] D.C. Rubinsztein, Lessons from animal models of Huntington's disease, Trends Genet. 18 (2002) 202–209.

[53] Y.L. Wang, W. Liu, E. Wada, M. Murata, K. Wada, I. Kanazawa, Clinico-pathological rescue of a model mouse of Huntington's disease by siRNA, Neurosci. Res. 53 (2005) 241–249.

[54] O. Singer, R.A. Marr, E. Rockenstein, L. Crews, N.G. Coufal, F.H. Gage, et al., Targeting BACE1 with siRNAs ameliorates Alzheimer disease neuropathology in a transgenic model, Nat. Neurosci. 8 (2005) 1343–1349.

[55] M.B. Chougule, R.K. Tekade, Current Scene and Prospective Potentials of siRNA in Cancer Therapy, J. Pharmacogenom Pharmacoproteomics. 3 (2012) 3–5.

[56] L. Tedeschi, C. Lande, A. Cecchettini, L. Citti, Hammerhead ribozymes in therapeutic target discovery and validation, Drug Discov. Today. 14 (2009) 776–783.

[57] L.J. Maher, Prospects for the therapeutic use of antigene oligonucleotides., Cancer Invest. 14 (1996) 66–82.

[58] P. Resnier, T. Montier, V. Mathieu, J.P. Benoit, C. Passirani, A review of the current status of siRNA nanomedicines in the treatment of cancer, Biomaterials. 34 (2013) 6429–6443.

[59] A. de Fougerolles, H.P. Vornlocher, J. Maraganore, J. Lieberman, Interfering with disease : a progress report on siRNA-based therapeutics, Nat. Rev. Drug Discov. 6 (2007) 443–453.

[60] A.K. Vaishnaw, J. Gollob, C. Gamba-vitalo, R. Hutabarat, D. Sah, R. Meyers, et al., A status report on RNAi therapeutics Review, Silence. 1 (2010) 1–13.

[61] R. Kanasty, J.R. Dorkin, A. Vegas, D. Anderson, Delivery materials for siRNA therapeutics, Nat. Mater. 12 (2013) 967–977.

[62] Q. Lin, J. Chen, Z. Zhang, G. Zheng, Lipid-based nanoparticles in the systemic delivery of siRNA, Nanomedicine. 9 (2014) 105–120.

[63] F. Liu, Y. Song, D. Liu, Hydrodynamics-based transfection in animals by systemic administration of plasmid DNA, Gene Ther. 6 (1999) 1258–1266.

[64] M.S. Al-Dosari, X. Gao, Nonviral gene delivery: principle, limitations, and recent progress, AAPS J. 11 (2009) 671–681.

[65] A. Jesorka, O. Orwar, Liposomes: Technologies and Analytical Applications, Annu. Rev. Anal. Chem. 1 (2008) 801–832.

[66] J. Adler-Moore, R.T. Proffitt, AmBisome: liposomal formulation, structure, mechanism of action and pre-clinical experience, J. Antimicrob. Chemother. 49 Suppl 1 (2002) 21–30.

[67] Y.K. Oh, T.G. Park, siRNA delivery systems for cancer treatment, Adv. Drug Deliv. Rev. 61 (2009) 850–862.

[68] K. Gao, L. Huang, Nonviral Methods for siRNA Delivery, Mol. Pharm. 6 (2008) 651–658.

[69] H. Lv, S. Zhang, B. Wang, S. Cui, J. Yan, Toxicity of cationic lipids and cationic polymers in gene delivery, J. Control. Release. 114 (2006) 100–9.

[70] I.R. Gilmore, S.P. Fox, A.J. Hollins, M. Sohail, S. Akhtar, The design and exogenous delivery of siRNA for post-transcriptional gene silencing, J. Drug Target. 12 (2004) 315–340.

[71] A. Santel, M. Aleku, O. Keil, J. Endruschat, V. Esche, G. Fisch, et al., A novel siRNA-lipoplex technology for RNA interference in the mouse vascular endothelium, Gene Ther. 13 (2006) 1222–1234.

[72] D.R. Sørensen, M. Leirdal, M. Sioud, Gene Silencing by Systemic Delivery of Synthetic siRNAs in Adult Mice, J. Mol. Biol. 327 (2003) 761–766.

[73] Q. Leng, P. Scaria, J. Zhu, N. Ambulos, P. Campbell, A.J. Mixson, Highly branched HK peptides are effective carriers of siRNA, J. Gene Med. 7 (2005) 977–86.

[74] A. Agarwal, R. Unfer, S.K. Mallapragada, Novel cationic pentablock copolymers as non-viral vectors for gene therapy, J. Control. Release. 103 (2005) 245–258.

[75] H. de Martimprey, C. Vauthier, C. Malvy, P. Couvreur, Polymer nanocarriers for the delivery of small fragments of nucleic acids: oligonucleotides and siRNA, Eur. J. Pharm. Biopharm. 71 (2009) 490–504.

[76] Y. Inoue, R. Kurihara, A. Tsuchida, M. Hasegawa, T. Nagashima, T. Mori, et al., Efficient delivery of siRNA using dendritic poly(L-lysine) for loss-of-function analysis, J. Control. Release. 126 (2008) 59–66.

[77] K.A. Howard, S.R. Paludan, M.A. Behlke, F. Besenbacher, B. Deleuran, J. Kjems, Chitosan/siRNA nanoparticle-mediated TNF-alpha knockdown in peritoneal macrophages for anti-inflammatory treatment in a murine arthritis model, Mol. Ther. 17 (2009) 162–168.

[78] J. Zillies, C. Coester, Evaluating gelatin based nanoparticles as a carrier system for double stranded oligonucleotides, J. Pharm. Pharm. Sci. 7 (2005) 17–21.

[79] Y. Patil, J. Panyam, Polymeric nanoparticles for siRNA delivery and gene silencing, Int. J. Pharm. 367 (2009) 195–203.

[80] A.J. Convertine, D.S.W. Benoit, C.L. Duvall, A.S. Hoffman, P.S. Stayton, Development of a novel endosomolytic diblock copolymer for siRNA delivery., J. Control. Release. 133 (2009) 221–229.

[81] C. Zhu, S. Jung, S. Luo, F. Meng, X. Zhu, T.G. Park, et al., Co-delivery of siRNA and paclitaxel into cancer cells by biodegradable cationic micelles based on PDMAEMA-PCL-PDMAEMA triblock copolymers, Biomaterials. 31 (2010) 2408–16.

[82] B. Urban-Klein, S. Werth, S. Abuharbeid, F. Czubayko, A. Aigner, RNAi-mediated gene-targeting through systemic application of polyethylenimine (PEI)-complexed siRNA in vivo, Gene Ther. 12 (2005) 461–466.

[83] P.H. Tan, L.C. Yang, H.C. Shih, K.C. Lan, J.T. Cheng, Gene knockdown with intrathecal siRNA of NMDA receptor NR2B subunit reduces formalin-induced nociception in the rat, Gene Ther. 12 (2005) 59–66.

[84] M.L. Patil, M. Zhang, O. Taratula, O.B. Garbuzenko, H. He, T. Minko, Internally cationic polyamidoamine PAMAM-OH dendrimers for siRNA delivery: effect of the degree of quaternization and cancer targeting, Biomacromolecules. 10 (2009) 258–266.

[85] A. Joliot, A. Prochiantz, Transduction peptides: from technology to physiology, Nat. Cell Biol. 6 (2004) 189–196.

[86] A. Joliot, A. Prochiantz, Transduction peptides: from technology to physiology, Nat. Cell Biol. 6 (2004) 189–196.

[87] A.D. Frankel, C.O. Pabo, Cellular Uptake of the Tat Protein from Human lmmunodeficiency Virus, Cell. 55 (1988) 1189–1193.

[88] M. Green, P.M. Loewenstein, Autonomous functional domains of chemically synthesized human immunodeficiency virus tat trans-activator protein, Cell. 55 (1988) 1179–1188.

[89] A. Joliot, C. Pernelle, H. Deagostini-Bazin, A. Prochiantz, Antennapedia homeobox peptide regulates neural morphogenesis, Proc. Natl. Acad. Sci. U. S. A. 88 (1991) 1864–1868.

[90] M. Zorko, U. Langel, Cell-penetrating peptides: mechanism and kinetics of cargo delivery, Adv. Drug Deliv. Rev. 57 (2005) 529–545.

[91] L.N. Patel, J.L. Zaro, W.C. Shen, Cell penetrating peptides: intracellular pathways and pharmaceutical perspectives, Pharm. Res. 24 (2007) 1977–1992.

[92] S.D. Laufer, T. Restle, Peptide-mediated cellular delivery of oligonucleotide-based therapeutics in vitro: quantitative evaluation of overall efficacy employing easy to handle reporter systems, Curr. Pharm. Des. 14 (2008) 3637–55.

[93] J. Wang, Z. Lu, M.G. Wientjes, J.L.-S. Au, Delivery of siRNA Therapeutics: Barriers and Carriers, AAPS J. 12 (2010) 492–503.

[94] F. Simeoni, M.C. Morris, F. Heitz, G. Divita, Insight into the mechanism of the peptide-based gene delivery system MPG: implications for delivery of siRNA into mammalian cells, Nucleic Acids Res. 31 (2003) 2717–2724.

[95] S. Veldhoen, S.D. Laufer, A. Trampe, T. Restle, Cellular delivery of small interfering RNA by a non-covalently attached cell-penetrating peptide: quantitative analysis of uptake and biological effect, Nucleic Acids Res. 34 (2006) 6561–6573.

[96] E. Gros, S. Deshayes, M.C. Morris, G. Aldrian-Herrada, J. Depollier, F. Heitz, et al., A non-covalent peptide-based strategy for protein and peptide nucleic acid transduction, Biochim. Biophys. Acta. 1758 (2006) 384–93.

[97] M.C. Morris, L. Chaloin, M. Choob, J. Archdeacon, F. Heitz, G. Divita, Combination of a new generation of PNAs with a peptide-based carrier enables efficient targeting of cell cycle progression, Gene Ther. 11 (2004) 757–764.

[98] T. Endoh, T. Ohtsuki, Cellular siRNA delivery using cell-penetrating peptides modified for endosomal escape, Adv. Drug Deliv. Rev. 61 (2009) 704–709.

[99] M. Jafari, P. Chen, Peptide mediated siRNA delivery, Curr. Top. Med. Chem. 9 (2009) 1088–97.

[100] R. Fischer, M. Fotin-Mleczek, H. Hufnagel, R. Brock, Break on through to the other side-biophysics and cell biology shed light on cell-penetrating peptides, Chembiochem. 6 (2005) 2126–2142.

[101] E. Vives, Present and future of cell-penetrating peptide mediated delivery systems: “is the Trojan horse too wild to go only to Troy?,” J. Control. Release. 109 (2005) 77–85.

[102] J.J. Schwartz, S. Zhang, Peptide-mediated cellular delivery, Curr. Opin. Mol. Ther. 2 (2000) 162–7.

[103] K.M. Stewart, K.L. Horton, S.O. Kelley, Cell-penetrating peptides as delivery vehicles for biology and medicine, Org. Biomol. Chem. 6 (2008) 2242–2255.

[104] S. Veldhoen, S.D. Laufer, T. Restle, Recent developments in peptide-based nucleic acid delivery, Int. J. Mol. Sci. 9 (2008) 1276–1320.

[105] M. Tyagi, M. Rusnati, M. Presta, M. Giacca, Internalization of HIV-1 tat requires cell surface heparan sulfate proteoglycans, J. Biol. Chem. 276 (2001) 3254–3261.

[106] M. Rusnati, D. Coltrini, P. Oreste, G. Zoppetti, A. Albini, D. Noonan, et al., Interaction of HIV-1 Tat protein with heparin. Role of the backbone structure, sulfation, and size, J. Biol. Chem. 272 (1997) 11313–11320.

[107] M. Rusnati, G. Tulipano, D. Spillmann, E. Tanghetti, P. Oreste, G. Zoppetti, et al., Multiple interactions of HIV-I Tat protein with size-defined heparin oligosaccharides, J. Biol. Chem. 274 (1999) 28198–28205.

[108] D. Derossi, S. Calvet, A. Trembleau, A. Brunissen, G. Chassaing, A. Prochiantz, Cell internalization of the third helix of the Antennapedia homeodomain is receptor-independent, J. Biol. Chem. 271 (1996) 18188–18193.

[109] S. Deshayes, A. Heitz, M.C. Morris, P. Charnet, G. Divita, F. Heitz, Insight into the mechanism of internalization of the cell-penetrating carrier peptide Pep-1 through conformational analysis, Biochemistry. 43 (2004) 1449–1457.

[110] T. Niidome, K. Takaji, M. Urakawa, N. Ohmori, A. Wada, T. Hirayama, et al., Chain length of cationic alpha-helical peptide sufficient for gene delivery into cells, Bioconjug. Chem. 10 (1999) 773–780.

[111] G. Tunnemann, G. Ter-avetisyan, R.M. Martin, M. Stockl, A. Herrmann, M.C. Cardoso, Live-cell analysis of cell penetration ability and toxicity of oligo-arginines, J. Pept. Sci. 14 (2008) 469–476.

[112] A. Fittipaldi, A. Ferrari, M. Zoppé, C. Arcangeli, V. Pellegrini, F. Beltram, et al., Cell membrane lipid rafts mediate caveolar endocytosis of HIV-1 Tat fusion proteins, J. Biol. Chem. 278 (2003) 34141–3419.

[113] J.S. Wadia, R. V Stan, S.F. Dowdy, Transducible TAT-HA fusogenic peptide enhances escape of TAT-fusion proteins after lipid raft macropinocytosis, Nat. Med. 10 (2004) 310–315.

[114] F. Duchardt, M. Fotin-Mleczek, H. Schwarz, R. Fischer, R. Brock, A comprehensive model for the cellular uptake of cationic cell-penetrating peptides, Traffic. 8 (2007) 848–866.

[115] M. Pooga, M. Hällbrink, M. Zorko, U. Langel, Cell penetration by transportan, FASEB J. 12 (1998) 67–77.

[116] S. Deshayes, S. Gerbal-Chaloin, M.C. Morris, G. Aldrian-Herrada, P. Charnet, G. Divita, et al., On the mechanism of non-endosomial peptide-mediated cellular delivery of nucleic acids, Biochim. Biophys. Acta. 1667 (2004) 141–147.

[117] M.C. Morris, P. Vidal, L. Chaloin, F. Heitz, G. Divita, A new peptide vector for efficient delivery of oligonucleotides into mammalian cells, Nucleic Acids Res. 25 (1997) 2730–2736.

[118] S.D. Conner, S.L. Schmid, Regulated portals of entry into the cell, Nature. 422 (2003) 37–44.

[119] R. Fischer, M. Fotin-Mleczek, H. Hufnagel, R. Brock, Break on through to the other side-biophysics and cell biology shed light on cell-penetrating peptides, Chembiochem. 6 (2005) 2126–2142.

[120] M.M. Verbeek, I. Otte-Holler, J.A.M. Fransen, R.M.W. de Waal, Accumulation of the Amyloid- Precursor Protein in Multivesicular Body-like Organelles, J. Histochem. Cytochem. 50 (2002) 681–690.

[121] A.K. Varkouhi, M. Scholte, G. Storm, H.J. Haisma, Endosomal escape pathways for delivery of biologicals, J. Control. Release. 151 (2011) 220–228.

[122] Y. Xu, F.C. Szoka, Mechanism of DNA release from cationic liposome/DNA complexes used in cell transfection, Biochemistry. 35 (1996) 5616–5623.

[123] I.M. Hafez, N. Maurer, P.R. Cullis, On the mechanism whereby cationic lipids promote intracellular delivery of polynucleic acids, Gene Ther. 8 (2001) 1188–1196.

[124] T. Endoh, M. Sisido, T. Ohtsuki, Cellular siRNA delivery mediated by a cell-permeant RNA-binding protein and photoinduced RNA interference, Bioconjug. Chem. 19 (2008) 1017–1024.

[125] P.A. Shaw, I.R. Catchpole, C.A. Goddard, W.H. Colledge, Comparison of protein transduction domains in mediating cell delivery of a secreted CRE protein, Biochemistry. 47 (2008) 1157–1166.

[126] M.E. Martin, kevin G. Rice, Peptide-guided gene delivery, AAPS J. 9 (2007) E18–29.

[127] H. Michiue, K. Tomizawa, F.Y. Wei, M. Matsushita, Y.F. Lu, T. Ichikawa, et al., The NH2 terminus of influenza virus hemagglutinin-2 subunit peptides enhances the antitumor potency of polyarginine-mediated p53 protein transduction, J. Biol. Chem. 280 (2005) 8285–8289.

[128] S. Abes, D. Williams, P. Prevot, A. Thierry, M.J. Gait, B. Lebleu, Endosome trapping limits the efficiency of splicing correction by PNA-oligolysine conjugates, J. Control. Release. 110 (2006) 595–604.

[129] P. Lundberg, S. El-Andaloussi, T. Sütlü, H. Johansson, U. Langel, Delivery of short interfering RNA using endosomolytic cell-penetrating peptides, FASEB J. 21 (2007) 2664–2671.

[130] K. Berg, P.K. Selbo, L. Prasmickaite, T.E. Tjelle, K. Sandvig, J. Moan, et al., Photochemical Internalization : A Novel Technology for Delivery of Macromolecules into Cytosol, Cancer Res. 59 (1999) 1180–1183.

[131] J.R. Maiolo, E.A. Ottinger, M. Ferrer, Specific redistribution of cell-penetrating peptides from endosomes to the cytoplasm and nucleus upon laser illumination, J. Am. Chem. Soc. 126 (2004) 15376–15377.

[132] M. Matsushita, H. Noguchi, Y.F. Lu, K. Tomizawa, H. Michiue, S.-T. Li, et al., Photo-acceleration of protein release from endosome in the protein transduction system, FEBS Lett. 572 (2004) 221–226.

[133] T. Endoh, M. Sisido, T. Ohtsuki, Cellular siRNA delivery mediated by a cell-permeant RNA-binding protein and photoinduced RNA interference, Bioconjug. Chem. 19 (2008) 1017–1024.

[134] S. Oliveira, M.M. Fretz, A. Høgset, G. Storm, R.M. Schiffelers, Photochemical internalization enhances silencing of epidermal growth factor receptor through improved endosomal escape of siRNA, Biochim. Biophys. Acta. 1768 (2007) 1211–1217.

[135] M. Dominska, D.M. Dykxhoorn, Breaking down the barriers: siRNA delivery and endosome escape, J. Cell Sci. 123 (2010) 1183–1189.

[136] S. Tiwari, M. Gupta, S.P. Vyas, Nanocarrier Mediated Cytosolic Delivery of Drug, DNA and Proteins, Proc. Natl. Acad. Sci. India Sect. B Biol. Sci. 82 (2012) 127–150.

[137] S.L. Lo, S. Wang, An endosomolytic Tat peptide produced by incorporation of histidine and cysteine residues as a nonviral vector for DNA transfection, Biomaterials. 29 (2008) 2408–2414.

[138] P. Midoux, M. Monsigny, Efficient gene transfer by histidylated polylysine/pDNA complexes, Bioconjug. Chem. 10 (1999) 406–411.

[139] A. Kichler, C. Leborgne, J. März, O. Danos, B. Bechinger, Histidine-rich amphipathic peptide antibiotics promote efficient delivery of DNA into mammalian cells, Proc. Natl. Acad. Sci. U. S. A. 100 (2003) 1564–1568.

[140] C.D. Novina, P.A. Sharp, The RNAi revolution, Nature. 430 (2004) 161–164.

[141] K.A. Whitehead, R. Langer, D.G. Anderson, Knocking down barriers: advances in siRNA delivery, Nat. Rev. Drug Discov. 8 (2009) 129–138.

[142] P. Chen, H. Yang, S. Fung, Amino acid pairing-based self assembling peptides and methods, US Pat. WO/2009/026729. (2009).

[143] P. Chen, M. Jafari, J.X. Jiang, S.-Y. Fung, H. Yang, Peptide sequences and peptide mediated siRNA delivery, Pat. No. WO/2011/020188. filed Augu (2011).

[144] L. Crombez, A. Charnet, M.C. Morris, G. Aldrian-Herrada, F. Heitz, G. Divita, A non-covalent peptide-based strategy for siRNA delivery, Biochem. Soc. Trans. 35 (2007) 44–46.

[145] I. Nakase, A. Tadokoro, N. Kawabata, T. Takeuchi, H. Katoh, K. Hiramoto, et al., Interaction of arginine-rich peptides with membrane-associated proteoglycans is crucial for induction of actin organization and macropinocytosis, Biochemistry. 46 (2007) 492–501.

[146] S. Futaki, T. Suzuki, W. Ohashi, T. Yagami, S. Tanaka, K. Ueda, et al., Arginine-rich peptides: An abundant source of membrane-permeable peptides having potential as carriers for intracellular protein delivery, J. Biol. Chem. 276 (2001) 5836–5840.

[147] P.Y. Chou, G.D. Fasman, Structural and functional role of leucine residues in proteins, J. Mol. Biol. 74 (1973) 263–281.

[148] U. Langel, Handbook of Cell-Penetrating Peptides, 2nd Editio, CRC Press, Boca Raton, 2006.

[149] H. Maeda, J. Wu, T. Sawa, Y. Matsumura, K. Hori, Tumor vascular permeability and the EPR effect in macromolecular therapeutics: A review, J. Control. Release. 65 (2000) 271–284.

[150] M. Jafari, W. Xu, S. Naahidi, B. Chen, P. Chen, A new amphipathic, amino-acid-pairing (AAP) peptide as siRNA delivery carrier: physicochemical characterization and in vitro uptake, J. Phys. Chem. B. 116 (2012) 13183–13191.

[151] C.W. Schmidt, Small RNA molecules act as blockers of disease metabolism., Mod. Drug Discov. (2003) 37–42.

[152] S. Trabulo, A.L. Cardoso, M. Mano, M.C.P. de Lima, Cell-Penetrating Peptides—Mechanisms of Cellular Uptake and Generation of Delivery Systems, Pharmaceuticals. 3 (2010) 961–993.

[153] Y. Chiu, A. Ali, C. Chu, H. Cao, T.M. Rana, Visualizing a Correlation between siRNA Localization , Cellular Uptake , and RNAi in Living Cells, 11 (2004) 1165–1175.

[154] D. Derossi, a H. Joliot, G. Chassaing, A. Prochiantz, The third helix of the Antennapedia homeodomain translocates through biological membranes., J. Biol. Chem. 269 (1994) 10444–10450.

[155] K. Rittner, A. Benavente, A. Bompard Sorlet, F. Heitz, G. Divita, R. Brasseur, et al., New basic membrane-destabilizing peptides for plasmid-based gene delivery in vitro and in vivo, Mol. Ther. J. Am. Soc. Gene Ther. 5 (2002) 104–114.

[156] M. Jafari, W. Xu, S. Naahidi, B. Chen, P. Chen, A new amphipathic, amino-acid-pairing (AAP) peptide as siRNA delivery carrier: physicochemical characterization and in vitro uptake., J. Phys. Chem. B. 116 (2012) 13183–91.

[157] D. Peer, J. Lieberman, Special delivery: targeted therapy with small RNAs, Gene Ther. 18 (2011) 1–7.

[158] P.Y. Chou, G.D. Fasman, Structural and Functional Role of Leucine Residues in Proteins, J.Mol. Biol. (1973) 263–281.

[159] S.J. Tilley, H.R. Saibil, The mechanism of pore formation by bacterial toxins., Curr. Opin. Struct. Biol. 16 (2006) 230–236.

[160] S.M. Raja, S.S. Rawat, A. Chattopadhyay, a K. Lala, Localization and environment of tryptophans in soluble and membrane-bound states of a pore-forming toxin from Staphylococcus aureus., Biophys. J. 76 (1999) 1469–1479.

[161] S.R. Dennison, J. Wallace, F. Harris, D.A. Phoenix, Amphiphilic alpha-helical antimicrobial peptides and their structure/function relationships, Protein Pept. Lett. 12 (2005) 31–39.

[162] N. Wiradharma, U. Khoe, C.A. Hauser, S.V. Seow, S. Zhang, Y.Y. Yang, Synthetic cationic amphiphilic α-helical peptides as antimicrobial agents, Biomaterials. 32 (2011) 2204–2212.

[163] Z. Shi, C.A. Olson, A.J. Bell, N.R. Kallenbach, Stabilization of alpha-Helix Structure by Polar Side- Chain Interactions : Complex Salt Bridges , Cation – π Interactions , and C – H . . . OH-Bonds, Biopolymers. 60 (2001) 366–380.

[164] C. Alemän, Effect of the environment and role of the pi-pi stacking interactions in the stabilization of the 3(10)-helix conformation in dehydroalanine oligopeptides., Int. J. Pept. Protein Res. 46 (1995) 408–418.

[165] Malvern Instruments Ltd, Zeta potential - An introduction in 30 minutes (KB000734), Www.malvern.com. (n.d.).

[166] J. Reiman, V. Oberle, I.S. Zuhorn, D. Hoekstra, Size-dependent internalization of particles via the pathways of clathrin- and caveolae-mediated endocytosis, Biochem. J. 377 (2004) 159–169.

[167] S.M. Moghimi, B. Bonnemain, Subcutaneous and intravenous delivery of diagnostic agents to the lymphatic system: applications in lymphoscintigraphy and indirect lymphography, Adv. Drug Deliv. Rev. 37 (1999) 295–312.

[168] R.I. Mahato, Biomaterials for Delivery and Targeting of Proteins and Nucleic Acids, CRC Press, Boca Raton, 2004.

[169] S.Y. Berezhna, L. Supekova, F. Supek, P.G. Schultz, A. a Deniz, siRNA in human cells selectively localizes to target RNA sites., Proc. Natl. Acad. Sci. U. S. A. 103 (2006) 7682–7687.

[170] J.P. Richard, K. Melikov, E. Vives, C. Ramos, B. Verbeure, M.J. Gait, et al., Cell-penetrating peptides. A reevaluation of the mechanism of cellular uptake., J. Biol. Chem. 278 (2003) 585–590.

[171] K. Miyata, M. Oba, M. Nakanishi, S. Fukushima, Y. Yamasaki, H. Koyama, et al., Polyplexes from poly(aspartamide) bearing 1,2-diaminoethane side chains induce pH-selective, endosomal membrane destabilization with amplified transfection and negligible cytotoxicity., J. Am. Chem. Soc. 130 (2008) 16287–16294.

[172] A. Sorkin, M. Von Zastrow, Signal transduction and endocytosis: close encounters of many kinds, Nat. Rev. Mol. Cell Biol. 3 (2002) 600–614.

[173] K.A. Browne, E. Blink, V.R. Sutton, C.J. Froelich, D.A. Jans, A. Joseph, et al., Cytosolic Delivery of Granzyme B by Bacterial Toxins : Evidence that Endosomal Disruption , in Addition to Transmembrane Pore Formation , Is an Important Function of Perforin Cytosolic Delivery of Granzyme B by Bacterial Toxins : Evidence that Endosomal D, Mol. Cell. Biol. 19 (1999) 8604–8615.

[174] J. Oehlke, A. Scheller, B. Wiesner, E. Krause, M. Beyermann, E. Klauschenz, et al., Cellular uptake of an alpha-helical amphipathic model peptide with the potential to deliver polar compounds into the cell interior non-endocytically, Biochim Biophys Acta. 1414 (1998) 127–139.

[175] Z. Liang, Y. Yoon, J. Votaw, M.M. Goodman, L. Williams, Silencing of CXCR4 Blocks Breast Cancer Metastasis Silencing of CXCR4 Blocks Breast Cancer Metastasis, Cancer Res. (2005) 967–971.

[176] M. Ocker, D. Neureiter, M. Lueders, S. Zopf, M. Ganslmayer, E.G. Hahn, et al., Variants of bcl-2 specific siRNA for silencing antiapoptotic bcl-2 in pancreatic cancer, Gut. 54 (2005) 1298–1308.

[177] J. Yano, K. Hirabayashi, S.-I. Nakagawa, T. Yamaguchi, M. Nogawa, I. Kashimori, et al., Antitumor activity of small interfering RNA/cationic liposome complex in mouse models of cancer., Clin. Cancer Res. 10 (2004) 7721–6.

[178] M.H. Kang, C.P. Reynolds, Bcl-2 inhibitors: targeting mitochondrial apoptotic pathways in cancer therapy, Clin. Cancer Res. 15 (2009) 1126–1132.

[179] E. Bernstein, A.A. Caudy, S.M. Hammond, G.J. Hannon, Role for a bidentate ribonuclease in the initiation step of RNA interference, Nature. 409 (2001) 363–366.

[180] M. Ferrari, Vectoring siRNA therapeutics into the clinic.pdf, Nat. Rev. Clin. Oncol. 7 (2010) 485–486.

[181] P.K. Kaiser, R.C.A. Symons, S.M. Shah, E.J. Quinlan, H. Tabandeh, D. V Do, et al., RNAi-based treatment for neovascular age-related macular degeneration by Sirna-027, Am. J. Ophthalmol. 150 (2010) 33–39.e2.

[182] J.M. Jacque, K. Triques, M. Stevenson, Modulation of HIV-1 replication by RNA interference, Nature. 418 (2002) 435–438.

[183] J.J. Turner, S.W. Jones, S.A. Moschos, M.A. Lindsay, M.J. Gait, MALDI-TOF mass spectral analysis of siRNA degradation in serum confirms an RNAse A-like activity, Mol. Biosyst. 3 (2007) 43–50.

[184] Y.C. Tseng, S. Mozumdar, L. Huang, Lipid-based systemic delivery of siRNA, Adv. Drug Deliv. Rev. 61 (2009) 721–731.

[185] S.J.H. Soenen, A.R. Brisson, M. De Cuyper, Addressing the problem of cationic lipid-mediated toxicity: the magnetoliposome model, Biomaterials. 30 (2009) 3691–701.

[186] M.C. Filion, N.C. Phillips, Toxicity and immunomodulatory activity of liposomal vectors formulated with cationic lipids toward immune effector cells, Biochim. Biophys. Acta. 1329 (1997) 345–56.

[187] O.M. Merkel, R. Urbanics, P. Bedocs, Z. Rozsnyay, L. Rosivall, M. Toth, et al., In vitro and in vivo complement activation and related anaphylactic effects associated with polyethylenimine and polyethylenimine-graft-poly(ethylene glycol) block copolymers., Biomaterials. 32 (2011) 4936–42.

[188] S. Fawell, J. Seery, Y. Daikh, C. Moore, L.L. Chen, B. Pepinsky, et al., Tat-mediated delivery of heterologous proteins into cells, Proc. Natl. Acad. Sci. U. S. A. 91 (1994) 664–668.

[189] G. Ruan, A. Agrawal, A.I. Marcus, S. Nie, Imaging and tracking of tat peptide-conjugated quantum dots in living cells: new insights into nanoparticle uptake, intracellular transport, and vesicle shedding, J. Am. Chem. Soc. 129 (2007) 14759–66.

[190] F. Said Hassane, a F. Saleh, R. Abes, M.J. Gait, B. Lebleu, Cell penetrating peptides: overview and applications to the delivery of oligonucleotides., Cell. Mol. Life Sci. 67 (2010) 715–26.

[191] A. Muratovska, M.R. Eccles, Conjugate for efficient delivery of short interfering RNA (siRNA) into mammalian cells, FEBS Lett. 558 (2004) 63–68.

[192] L. Crombez, G. Aldrian-Herrada, K. Konate, Q.N. Nguyen, G.K. McMaster, R. Brasseur, et al., A new potent secondary amphipathic cell-penetrating peptide for siRNA delivery into mammalian cells., Mol. Ther. 17 (2009) 95–103.

[193] A. Erazo-Oliveras, N. Muthukrishnan, R. Baker, T.Y. Wang, J.P. Pellois, Improving the Endosomal Escape of Cell-Penetrating Peptides and Their Cargos: Strategies and Challenges, Pharmaceuticals. 5 (2012) 1177–1209.

[194] W. Xu, M. Jafari, F. Yuan, P. Ran, C. Baoling, D. Yong, et al., In vitro and in vivo therapeutic siRNA delivery induced by a tryptophan-rich endosomolytic peptide, Submitt. to J. Mater. Chem. B. (n.d.).

[195] P. Midoux, C. Pichon, J.J. Yaouanc, P.A. Jaffrès, Chemical vectors for gene delivery: a current review on polymers, peptides and lipids containing histidine or imidazole as nucleic acids carriers, Br. J. Pharmacol. 157 (2009) 166–178.

[196] L. Crombez, G. Aldrian Herrada, K. Konate, Q.N. Nguyen, G.K. McMaster, R. Brasseur, et al., A new potent secondary amphipathic cell-penetrating peptide for siRNA delivery into mammalian cells, Mol. Ther. 17 (2009) 95–103.

[197] P.E.G. Thorén, D. Persson, P. Isakson, M. Goksör, A. Onfelt, B. Nordén, Uptake of analogs of penetratin, Tat(48-60) and oligoarginine in live cells, Biochem. Biophys. Res. Commun. 307 (2003) 100–107.

[198] D.A. Steinhauer, S.A. Wharton, J.J. Skehel, D.C. Wiley, Studies of the membrane fusion activities of fusion peptide mutants of influenza virus hemagglutinin, J. Virol. 69 (1995) 6643–6651.

[199] A. Kichler, C. Leborgne, J. März, O. Danos, B. Bechinger, Histidine-rich amphipathic peptide antibiotics promote efficient delivery of DNA into mammalian cells, Proc. Natl. Acad. Sci. U. S. A. 100 (2003) 1564–1568.

[200] L.J. Jones, S.T. Yue, C.Y. Cheung, V.L. Singer, RNA quantitation by fluorescence-based solution assay: RiboGreen reagent characterization, Anal. Biochem. 265 (1998) 368–74.

[201] S. Deshayes, K. Konate, A. Rydström, L. Crombez, C. Godefroy, P.-E. Milhiet, et al., Self-assembling peptide-based nanoparticles for siRNA delivery in primary cell lines., Small. 8 (2012) 2184–8.

[202] Zeta Potential of colloids in Water and Waste water. ASTM Standard D, 4187-82, American Society for Testing and Materials, West Conshohocken, PA, USA, 1985.

[203] C. Pichon, C. Gonçalves, P. Midoux, Histidine-rich peptides and polymers for nucleic acids delivery, Adv. Drug Deliv. Rev. 53 (2001) 75–94.

[204] K. Chang, Y. Higuchi, S. Kawakami, F. Yamashita, M. Hashida, Efficient gene transfection by histidine-modified chitosan through enhancement of endosomal escape, Bioconjug. Chem. 21 (2010) 1087–1095.

[205] P. Midoux, C. Pichon, J.J. Yaouanc, P.A. Jaffrès, Chemical vectors for gene delivery: a current review on polymers, peptides and lipids containing histidine or imidazole as nucleic acids carriers, Br. J. Pharmacol. 157 (2009) 166–178.

[206] Q. Leng, A.J. Mixson, Modified branched peptides with a histidine-rich tail enhance in vitro gene transfection, Nucleic Acids Res. 33 (2005) e40.

[207] M. Stevenson, V. Ramos Perez, S. Singh, M. Soliman, J.A. Preece, S.S. Briggs, et al., Delivery of siRNA mediated by histidine-containing reducible polycations, J. Control. Release. 130 (2008) 46–56.

[208] M. Harboe, T.E. Mollnes, The alternative complement pathway revisited, J. Cell. Mol. Med. 12 (2008) 1074–1084.

[209] Y. Tsujimoto, L. Finger, J. Yunis, P. Nowell, C. Croce, Cloning of the chromosome breakpoint of neoplastic B cells with the t(14;18) chromosome translocation, Science . 226 (1984) 1097–1099.

[210] R.J. Youle, A. Strasser, The BCL-2 protein family: opposing activities that mediate cell death, Nat. Rev. Mol. Cell Biol. 9 (2008) 47–59.

[211] K.W. Yip, J.C. Reed, Bcl-2 family proteins and cancer, Oncogene. 27 (2008) 6398–6406.

[212] B.N. Fahy, M.G. Schlieman, M.M. Mortenson, S. Virudachalam, R.J. Bold, Targeting BCL-2 overexpression in various human malignancies through NF-kappaB inhibition by the proteasome inhibitor bortezomib, Cancer Chemother. Pharmacol. 56 (2005) 46–54.

[213] W.J. Placzek, J. Wei, S. Kitada, D. Zhai, J.C. Reed, M. Pellecchia, A survey of the anti-apoptotic Bcl-2 subfamily expression in cancer types provides a platform to predict the efficacy of Bcl-2 antagonists in cancer therapy, Cell Death Dis. 1 (2010) e40.

[214] G. Sithanandam, L.W. Fornwald, J.R. Fields, N.L. Morris, L.M. Anderson, Anti-tumor efficacy of naked siRNAs for ERBB3 or AKT2 against lung adenocarcinoma cell xenografts, Int. J. Cancer. 130 (2012) 251–258.

[215] A. Morin, C. Gallou Kabani, J.R.R. Mathieu, F. Cabon, Systemic delivery and quantification of unformulated interfering RNAs in vivo, Curr. Top. Med. Chem. 9 (2009) 1117–1129.

[216] H. Shen, T. Sun, M. Ferrari, Nanovector delivery of siRNA for cancer therapy, Cancer Gene Ther. 19 (2012) 367–373.

[217] G.R. Devi, siRNA-based approaches in cancer therapy, Cancer Gene Ther. 13 (2006) 819–829.

[218] S.D. Laufer, A. Detzer, G. Sczakiel, T. Restle, Selected Strategies for the Delivery of siRNA In Vitro and In Vivo, in: V.A. Erdmann, J. Barciszewski (Eds.), RNA Technol. Their Appl., Springer, Berlin, Heidelberg, 2010: p. p 29–58.

[219] C.R. Allerson, N. Sioufi, R. Jarres, T.P. Prakash, N. Naik, A. Berdeja, et al., Fully 2 ′-Modified Oligonucleotide Duplexes with Improved in Vitro Unmodified Small Interfering RNA, J. Med. Chem. 48 (2005) 901–904.

[220] M. Dominska, D.M. Dykxhoorn, Breaking down the barriers: siRNA delivery and endosome escape, J. Cell Sci. 123 (2010) 1183–9.

[221] E. Check, Gene therapy put on hold as third child develops cancer, Nature. 433 (2005) 561.

[222] S. Hacein-Bey-Abina, C. Von Kalle, M. Schmidt, M. McCormack, N. Wulffraat, P. Leboulch, et al., LMO2-associated clonal T cell proliferation in two patients after gene therapy for SCID-X1, Science. 302 (2003) 415–419.

[223] M.A. Kay, State-of-the-art gene-based therapies: the road ahead, Nat. Rev. Genet. 12 (2011) 316–28.

[224] G.R. Rettig, M.A. Behlke, Progress toward in vivo use of siRNAs-II, Mol. Ther. 20 (2012) 483–512.

[225] C. Alabi, A. Vegas, D. Anderson, Attacking the genome: emerging siRNA nanocarriers from concept to clinic, Curr. Opin. Pharmacol. 12 (2012) 427–433.

[226] P. Kesharwani, V. Gajbhiye, N.K. Jain, A review of nanocarriers for the delivery of small interfering RNA, Biomaterials. 33 (2012) 7138–7150.

[227] J. Zhou, K.T. Shum, J.C. Burnett, J.J. Rossi, Nanoparticle-Based Delivery of RNAi Therapeutics: Progress and Challenges, Pharmaceuticals. 6 (2013) 85–107.

[228] H. Lv, S. Zhang, B. Wang, S. Cui, J. Yan, Toxicity of cationic lipids and cationic polymers in gene delivery, J. Control. Release. 114 (2006) 100–109.

[229] S.J.H. Soenen, A.R. Brisson, M. De Cuyper, Addressing the problem of cationic lipid-mediated toxicity: the magnetoliposome model, Biomaterials. 30 (2009) 3691–3701.

[230] S. Akhtar, I. Benter, Toxicogenomics of non-viral drug delivery systems for RNAi: potential impact on siRNA-mediated gene silencing activity and specificity, Adv. Drug Deliv. Rev. 59 (2007) 164–182.

[231] B. Ballarín González, K.A. Howard, Polycation-based nanoparticle delivery of RNAi therapeutics: adverse effects and solutions, Adv. Drug Deliv. Rev. 64 (2012) 1717–1729.

[232] K.M. Wagstaff, D.A. Jans, Protein Transduction: Cell Penetrating Peptides and Their Therapeutic Applications, Curr. Med. Chem. 13 (2006) 1371–1387.

[233] M. Lindgren, Ü. Langel, Classes and prediction of cell-penetrating peptides, Methods Mol. Biol. 683 (2011) 3–19.

[234] J. Hoyer, I. Neundorf, Peptide vectors for the nonviral delivery of nucleic acids, Acc. Chem. Res. 45 (2012) 1048–1056.

[235] T. Lehto, K. Kurrikoff, Ü. Langel, Cell-penetrating peptides for the delivery of nucleic acids, Expert Opin. Drug Deliv. 9 (2012) 823–836.

[236] A.H. van Asbeck, A. Beyerle, H. McNeill, P.H.M. Bovee-Geurts, S. Lindberg, W.P.R. Verdurmen, et al., Molecular parameters of siRNA--cell penetrating peptide nanocomplexes for efficient cellular delivery, ACS Nano. 7 (2013) 3797–3807.

[237] S. EL Andaloussi, T. Lehto, I. Mäger, K. Rosenthal-Aizman, I.I. Oprea, O.E. Simonson, et al., Design of a peptide-based vector, PepFect6, for efficient delivery of siRNA in cell culture and systemically in vivo, Nucleic Acids Res. 39 (2011) 3972–3987.

[238] P. Midoux, C. Pichon, J.J. Yaouanc, P.A. Jaffrès, Chemical vectors for gene delivery: a current review on polymers, peptides and lipids containing histidine or imidazole as nucleic acids carriers, Br. J. Pharmacol. 157 (2009) 166–178.

[239] I.A. Khalil, K. Kogure, H. Akita, H. Harashima, Uptake Pathways and Subsequent Intracellular Trafficking in Nonviral Gene Delivery, Pharmacol. Rev. 58 (2006) 32–45.

[240] W. Li, F. Nicol, F.C. Szoka, GALA: a designed synthetic pH-responsive amphipathic peptide with applications in drug and gene delivery, Adv. Drug Deliv. Rev. 56 (2004) 967–985.

[241] K.K. Hou, H. Pan, L. Ratner, P.H. Schlesinger, S.A. Wickline, Mechanisms of Nanoparticle-Mediated siRNA Transfection by Melittin-Derived Peptides, ACS Nano. 7 (2013) 8605–8615.

[242] J.E. Summerton, Endo-Porter: a novel reagent for safe, effective delivery of substances into cells, Ann. N. Y. Acad. Sci. 1058 (2005) 62–75.

[243] Z.X. Zhao, S.Y. Gao, J.C. Wang, C.J. Chen, E.Y. Zhao, W.J. Hou, et al., Self-assembly nanomicelles based on cationic mPEG-PLA-b-Polyarginine(R15) triblock copolymer for siRNA delivery, Biomaterials. 33 (2012) 6793–9807.

[244] E. Gonçalves, E. Kitas, J. Seelig, Binding of oligoarginine to membrane lipids and heparan sulfate: structural and thermodynamic characterization of a cell-penetrating peptide, Biochemistry. 44 (2005) 2692–702.

[245] D.J. Mitchell, L. Steinman, D.T. Kim, C.G. Fathman, J.B. Rothbard, Polyarginine enters cells more efficiently than other polycationic homopolymers, J. Pept. Res. 56 (2000) 318–325.

[246] Y. Nakamura, K. Kogure, S. Futaki, H. Harashima, Octaarginine-modified multifunctional envelope-type nano device for siRNA, J. Control. Release. 119 (2007) 360–367.

[247] H. Maeda, Tumor-Selective Delivery of Macromolecular Drugs via the EPR Effect : Background and Future Prospects, Bioconjug. Chem. 21 (2010) 797–802.

[248] J. Rink, E. Ghigo, Y. Kalaidzidis, M. Zerial, Rab conversion as a mechanism of progression from early to late endosomes, Cell. 122 (2005) 735–749.

[249] C.E. Futter, A. Pearse, L.J. Hewlett, C.R. Hopkins, Multivesicular endosomes containing internalized EGF-EGF receptor complexes mature and then fuse directly with lysosomes, J. Cell Biol. 132 (1996) 1011–1023.

[250] J.P. Luzio, B.A. Rous, N.A. Bright, P.R. Pryor, B.M. Mullock, R.C. Piper, Lysosome-endosome fusion and lysosome biogenesis, J. Cell Sci. 113 (2000) 1515–1524.

[251] J.C. Geoghegan, B.L. Gilmore, B.L. Davidson, Gene Silencing Mediated by siRNA-binding Fusion Proteins Is Attenuated by Double-stranded RNA-binding Domain Structure, Mol. Ther. Acids. 1 (2012) 1–9.

[252] O. Zelphati, Y. Wang, S. Kitada, J.C. Reed, P.L. Felgner, J. Corbeil, Intracellular delivery of proteins with a new lipid-mediated delivery system, J. Biol. Chem. 276 (2001) 35103–35110.

[253] W. Liang, J. Lam, Endosomal escape pathways for non-viral nucleic acid delivery systems, in: B. Ceresa (Ed.), Mol. Regul. Endocytosis, InTech, Rijeka, 2012: p. p 429–456.

[254] E.J. Bowman, A. Siebers, K. Altendorf, Bafilomycins: a class of inhibitors of membrane ATPases from microorganisms, animal cells, and plant cells., Proc. Natl. Acad. Sci. U. S. A. 85 (1988) 7972–7976.

[255] B.P. Crider, X.S. Xie, D.K. Stone, Bafilomycin Inhibits Proton Flow through the H+ Channel of Vacuolar Proton Pumps, J. Biol. Chem. 269 (1994) 17379–17381.

[256] Y. Yue, F. Jin, R. Deng, J. Cai, Z. Dai, M.C.M. Lin, et al., Revisit complexation between DNA and polyethylenimine--effect of length of free polycationic chains on gene transfection, J. Control. Release. 152 (2011) 143–151.

[257] K. Miyata, M. Oba, M. Nakanishi, S. Fukushima, Y. Yamasaki, H. Koyama, et al., Polyplexes from poly(aspartamide) bearing 1,2-diaminoethane side chains induce pH-selective, endosomal membrane destabilization with amplified transfection and negligible cytotoxicity, J. Am. Chem. Soc. 130 (2008) 16287–16294.

[258] D. Hanahan, R.A. Weinberg, The Hallmarks of Cancer, Cell. 100 (2000) 57–70.

[259] D. Miles, G. von Minckwitz, A.D. Seidman, Combination versus sequential single-agent therapy in metastatic breast cancer, Oncologist. 7 Suppl 6 (2002) 13–19.

[260] M. Izquierdo, Short interfering RNAs as a tool for cancer gene therapy, Cancer Gene Ther. 12 (2005) 217–227.

[261] H. Shen, T. Sun, M. Ferrari, Nanovector delivery of siRNA for cancer therapy, Cancer Gene Ther. 19 (2012) 367–373.

[262] A. Besheer, J. Vogel, D. Glanz, J. Kressler, T. Groth, K. Mader, Characterization of PLGA Nanospheres Stabilized with Amphiphilic Polymers : Hydrophobically Modified Hydroxyethyl Starch vs Pluronics, Mol. Pharm. 6 (2009) 407–415.

[263] J. Li, Y. Wang, Y. Zhu, D. Oupický, Recent advances in delivery of drug-nucleic acid combinations for cancer treatment, J. Control. Release. 172 (2013) 589–600.

[264] C. Auclair, Multimodal action of antitumor agents on DNA: the ellipticine series, Arch. Biochem. Biophys. 259 (1987) 1–14.

[265] N.C. Garbett, D.E. Graves, Extending nature's leads: the anticancer agent ellipticine, Curr. Med. Chem. Anticancer. Agents. 4 (2004) 149–172.

[266] Y.H. Ling, B.S. Andersson, J.A. Nelson, DNA topoisomerase I as a site of action for 10-hydroxycamptothecin in human promyelocytic leukemia cells, Cancer Biochem. Biophys. 11 (1990) 23–30.

[267] J.M. Adams, S. Cory, The Bcl-2 protein family: arbiters of cell survival, Science (80-.). 281 (1998) 1322–1326.

[268] C.W. Beh, W.Y. Seow, Y. Wang, Y. Zhang, Z.Y. Ong, P.L.R. Ee, et al., Efficient delivery of Bcl-2-targeted siRNA using cationic polymer nanoparticles: downregulating mRNA expression level and sensitizing cancer cells to anticancer drug, Biomacromolecules. 10 (2009) 41–48.

[269] C. Zheng, M. Zheng, P. Gong, J. Deng, H. Yi, P. Zhang, et al., Polypeptide cationic micelles mediated co-delivery of docetaxel and siRNA for synergistic tumor therapy, Biomaterials. 34 (2013) 3431–3438.

[270] D. Chu, W. Xu, R. Pan, Y. Ding, P. Chen, Rational modification of cell penetrating peptides for highly efficient siRNA delivery- structure-activity relationship and mechanism of intracellular trafficking of siRNA (submitted to nat. comm.), (n.d.).

[271] M. Beck-Broichsitter, E. Rytting, T. Lebhardt, X. Wang, T. Kissel, Preparation of nanoparticles by solvent displacement for drug delivery: a shift in the "ouzo region" upon drug loading, Eur. J. Pharm. Sci. 41 (2010) 244–253.

[272] S. Kunadharaju, M. Savva, Thermodynamic Studies of 10-Hydroxy-camptothecin in Aqueous Solutions, J. Chem. Eng. Data. 55 (2010) 103–112.

[273] S. Lu, H. Wang, Y. Sheng, M. Liu, P. Chen, Molecular binding of self-assembling peptide EAK16-II with anticancer agent EPT and its implication in cancer cell inhibition, J. Control. Release. 160 (2012) 33–40.

[274] W. Li, Y. Yang, C. Wang, Z. Liu, X. Zhang, F. An, et al., Carrier-free, functionalized drug nanoparticles for targeted drug delivery, Chem. Commun. 48 (2012) 8120–8122.

[275] H. Maeda, Tumor-selective delivery of macromolecular drugs via the EPR effect: background and future prospects, Bioconjug. Chem. 21 (2010) 797–802.

[276] J.S. Mader, D.W. Hoskin, Cationic antimicrobial peptides as novel cytotoxic agents for cancer treatment, Expert Opin. Investig. Drugs. 15 (2006) 933–946.